EARLY PLIOCENE EVOLUTION OF COCCOLITHOPHORES IN THE CARIBBEAN SEA: TAXONOMY, BIOSTRATIGRAPHY, PALEOECOLOGY AND PALEOCEANOGRAPHY

Daniela Crudeli

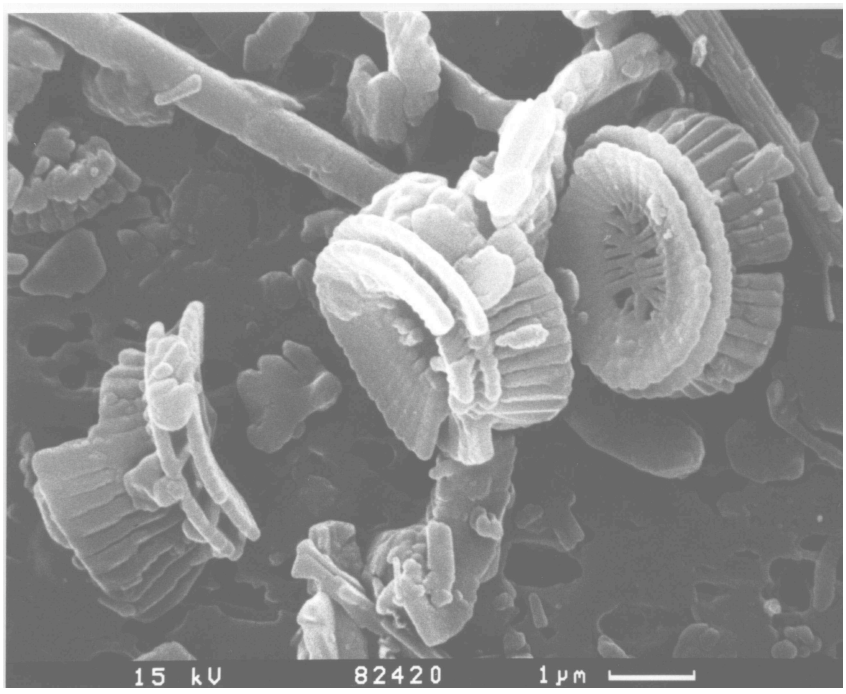

Dissertation zur Erlangung des Doktorgades der
Mathemathisch-Naturwissenschaftlichen Fakultät der
Christian-Albrechts-Universität zu Kiel

vorgelegt von
Daniela Crudeli

Kiel, 2005

EARLY PLIOCENE EVOLUTION OF COCCOLITHOPHORES IN THE CARIBBEAN SEA: TAXONOMY, BIOSTRATIGRAPHY, PALEOECOLOGY AND PALEOCEANOGRAPHY

Evolution von Coccolithophoriden während des frühen Pliozäns in der Karibik: Taxonomie, Biostratigraphie, Paläoökologie und Paläozeanographie

Dissertation
zur Erlangung des Doktorgrades
der Mathematisch-Naturwissenschaflichen Fakultät
der Christian-Albrechts-Universität
zu Kiel
vorgelegt von

Daniela Crudeli

Kiel
2005

Referentin: Prof. Dr. Priska Schäfer

Koreferentin: Dr. Mara Weinelt

Tag der Disputation: 04-07-2005

Zum Druck genehmigt, Kiel, den: 27-06-2006

Der Dekan
Gez. J. Grotemeyer

Abstract

The early Pliocene was a period of significant turnover among reticulofenestrid coccolithophores (Young, 1989) including the first consistent occurrence (FCO) of small *Gephyrocapsa* and the first occurrence (FO) of *Pseudoemiliania.* These bioevents have been widely recognised by light microscopy (LM), and precede by a few hundred thousand years the last occurrence of other important Neogene calcareous nannofossils (Perch-Nielsen, 1985; Young, 1998). The evolutionary development of these coccolithophores in relation to environmental and paleoceanographic changes is, however, poorly understood (Bown et al., 2004). In order to get an insight into the tempi and modes of their evolutionary radiation, we conducted a high-resolution scanning electron microscopy (SEM) study of calcareous nannofossils from cores from the South Caribbean Sea (ODP Hole 1000A) which include the FCO of small *Gephyrocapsa* (Kameo and Sato, 2000). The interval on which the thesis focuses corresponds to 4.5-3.8 Ma (Steph et al., in revision), an interval where the gradual shoaling of the Isthmus of Panama led to significant changes in the surface water circulation patterns and hydrography in the Caribbean Sea (Haug et al., 2001).

The investigated sediments are exceptionally well-preserved and contain a number of previously undescribed morphotypes. Several new, very small to small (<3µm, 3-5µm) reticulofenestrid species - *Reticulofenestra calicis* n. sp., *R. alis* n. sp., *R. pujosiae* n. sp. and *R. premoliae* n. sp. - were recognised from these sediments and accurately described. These new species proved to be key-species for the reconstruction of the phylogeny of *Gephyrocapsa theyeri*, arguably the first evolved species of the *Gephyrocapsa* plexus. The FO of the species could be defined and dated at 4.45Ma by high-resolution stable isotope stratigraphy (Steph et al., in revision). The evolutionary development of *Gephyrocapsa*, from the FO of *G. theyeri* on has been investigated in detail by SEM observations and high-resolution morphometry. Five new *Gephyrocapsa* species were recognised and described - *G. drieveri* n. sp., *G. samtlebenii* n. sp., *G. bollmannii* n. sp., *G. matsuokae* n. sp. and *G. jerkovicii* n. sp. and, *G.* sp. cf. *theyeri,* are present. The occurrence of the new species is traced in the cores. A pattern of initial radiation among the plexus is recognised which is followed by successive speciation events. The detailed study of the evolutionary origin of the group provides a perspective for the investigation of their radiation in the Quaternary. The hitherto unrecognised biodiversity of coccolithophores indicates that the early Pliocene reticulofenestrid turnover is more complex than previously thought and provides a new insight into the evolution of the group. The here presented high-resolution taxonomic study shows, that the complexity recently discovered by molecular genetics among planktonic organisms can also be traced in the fossil record.

The abundance of the deep dwelling species *Florispharea profunda,* a species not considered in previous studies of the cores (Kameo and Sato, 2000), is quantified by SEM. The relative abundance of *F. profunda*, a proxy for surface water productivity (Kinkel et al., 2000), provided significant information for understanding the "anomalous" high sea surface temperature obtained by Mg/Ca-ratios in planktic foraminifera.

Kurzfassung

Das frühe Pliozän war eine Periode mit signifikanten Umwälzungen innerhalb der reticulofenestriden Coccolithophoriden (Young 1989), welche das erste konsistente Auftreten von *Gephyrocapsa* und das erste Auftreten von *Pseudoemiliania* beinhaltet. Diese Evolutionsereignisse sind in einer Reihe lichtmikroskopischer Studien erkannt worden, und erfolgten demnach einige hundert tausend Jahre vor dem letzten Auftreten anderer wichtiger kalkiger Nannofossilien des Neogens (Perch-Nielsen, 1985; Young, 1998). Die evolutive Entwicklung dieser Coccolithophoren und ihre Abhängigkeit von Veränderungen der Umwelt und der Paläozeanographie ist jedoch nach wie vor wenig verstanden (Bown et al., 2004). Um ein besseres Verständnis von der Geschwindigkeit und den Mechanismen der evolutiven Radiation von Coccolithophoriden zu erlangen, wurde eine hochauflösende Raster-Elektronen-Mikroskopie –Studie an Nannofossilien in Sedimentkernen aus der südlichen Karibik (ODP Bohrloch 1000A), durchgeführt die das erste Auftreten von *Gephyrocapsa* (Kameo and Sato, 2000) beinhalten. Der Zeitraum, auf den sich diese Dissertation konzentriert, entspricht 4.5 bis 3.8 Millionen Jahre vor heute, ein Intervall, in dem die graduelle Schließung des Isthmus von Panama zu signifikanten Veränderungen in der Oberflächenwasserzirkulation und Hydrographie in der Karibik geführt haben (Haug et al., 2001).
Die untersuchten Sedimente sind außergewöhnlich gut erhalten und beinhalten eine Reihe von bisher unbeschriebenen Morphotypen. In diesen Sedimenten wurde eine Anzahl neuer, sehr kleiner bis kleiner (<3µm bis 3.5µm) reticulofenestriden Arten - *Reticulofenestra calicis* n. sp., *R. alis* n. sp., *R. pujosiae* n. sp. and *R. premoliae* n. sp. - beobachtet und detailliert beschrieben. Diese neuen Arten erwiesen sich als Schlüsselarten für die Rekonstruktion der Phylogenie von *Gephyrocapsa theyeri*, welche als erste Art der Gattung *Gephyrocapsa* entstand. Das erste Auftreten dieser Art konnte definiert werden und mittels hochauflösenden stabilen Isotopenstratigraphie auf 4.45 Millionen Jahre datiert werden (Steph et al., in revision). Die Evolution von *Gephyrocapsa,* beginnend mit dem ersten Auftreten von *G. theyeri*, wurde durch detaillierte und ausführliche Beobachtungen im Raster-Elektronen-Mikroskop und hochauflösende Morphometrie erforscht. Fünf neue Arten von *Gephyrocapsa* wurden erkannt und beschrieben - *G. drieveri* n. sp., *G. samtlebenii* n. sp., *G. bollmannii* n. sp., *G. matsuokae* n. sp. und *G. jerkovicii* n. sp., sowie *G.* sp. cf. *theyeri*. In den Kernen aus der Karibik konnte das Vorkommen der neuen Arten genau bestimmt werden. Dabei ist ein Muster einer initalen Radiation unter den Arten und nachfolgender Faunenneubildung erkennbar. Die genaue Untersuchung des evolutiven Usprungs der Gruppe liefert einen Ausblick auf weitere Untersuchungen ihrer Radiation im Quartär. Die bisherige unbekannte Artenvielfalt der Coccolithophoriden zeigt, dass der im frühen Pliozän stattgefundene Artenumschwung viel komplexer war als bisher angenommen wurde, und neue Erkenntnis zur Evolution dieser Gruppe liefert. Die hier durchgeführten, hochauflösenden taxonomischen Untersuchungen zeigen, dass die in letzter Zeit mit Hilfe molekularer Genetik entdeckte Komplexität planktischenr Organismengruppen auch in fossilen Proben zurückverfolgt werden kann.
Die Häufiggkeit der tieflebenden Coccolithophoride? *Florisphaera profunda*, einer Art, die in vorangegangen Studien der Kerne nicht erfasst wurde, ist im Raster-Elektronen-Mikroskop quantifiziert wurden. Die relative Häufigkeit von *F. profunda*, als „Proxy“ für die Produktivitätsrekonstruktion (Kinkel et al., 2000), lieferte maßgebliche Informationen zum Verständnis der „unnormal“ hohen Oberflächenwassertemperaturen, die zuvor mit Hilfe von Mg/Ca-Verhaältnissen in planktischen Foraminiferen rekronstruiert worden waren..

Contents

CHAPTER 1

CHAPTER 1

1. Introduction

Coccolithophores are a major group of photosynthetic pelagic unicellular algae, producing an exoskeleton of minute calcium carbonate plates called coccoliths. They occur in abundance and contribute a major part of pelagic primary production. Moreover, they have additional feedback effects on the climate-ocean system through their strong influence on the global biogeochemical cycles of carbon-carbonate and sulphur (Honjo, 1976; Westbroek et al., 1993; Westbroek et al., 1994). The distribution of modern coccolithophores and their biodiversity is closely correlated with climatic and oceanographic zones (Brand, 1994; Winter et al., 1994). Coccolithophores have an exceptional fossil record, likely being the most stratigraphically complete of any fossil groups (Bown et al., 2004). This provides a record of the relationship and interaction between environment and biological complexity-diversity through time.

An enormous and fascinating literature exists centred on the open question - *why is nature divided into discrete groups- species, rather than forming an organic continuum?* Nonetheless the origin of biodiversity is still an unresolved problem as admitted by the architect of the "Modern Evolutionary Synthesis" (Ernst Mayr, 1904-2005). Changes in biodiversity of coccolithophores, and hence their evolutionary development, appears to follow major global change in the Earth´s system (Bown et al., 2004). There have been, however, very few detailed studies of coccolithophore evolution (e.g. Raffi et al., 1998; Knappertsbusch, 2000, and Young et al., 1994 for review) and major insights come from long-term paleo-biodiversity estimates (Bown et al., 2004 and references therein).

In 2001, the DFG Research Unit "Impact of Gateways on Oceanic Circulation, Climate and Evolution" at Kiel University started to address questions on the rule of the closure of major oceanic gateways and related changes in circulation patterns and hydrography on coccolithophore evolution. This thesis has been accomplished within the subproject "Impact of Gateways on Evolution of coccolithophores – a morphometric approach".

Within this frame, this thesis has been initiated to study the impact of the closure of the Central America Seaway (CAS) on coccolithophores evolution over the Pliocene. During preliminary low-resolution screening by scanning electron microscope (SEM) and light microscope (LM) of samples from the chosen site in the Caribbean (ODP Hole 1000A), we noted that most samples were exceptionally well-preserved and contained a range of undescribed reticulofenestids (Young, 1989). The reticulofenestrid group includes a wide range of phylogenetically related coccolithophores species belonging to *Reticulofenestra*, *Pseudoemiliania, Gephyrocapsa* and *Emiliania*. Therefore, it was necessary to revise and improve the existing taxonomy of this group of coccolithophores in the Pliocene. Consequently, this thesis is basically a taxonomic thesis and it focuses on species-level coccolithophore evolution. The results of this thesis provide a solid calibration base and a framework for future research on the tempo, modes and causes of evolution in coccolithophores.

1.1. Aim of the study and strategy

This thesis focuses on coccoliths, in particular reticulofenestrid coccoliths (Young, 1989). These dominate nannofossil assemblages since the Eocene (Young, 1989; Young, 1998) and form a substantial component of the modern phytoplankton biomass (Okada and McIntyre, 1977). The targeted time interval covers the early Pliocene in the Caribbean Sea, which is characterised by a

major turnover among reticulofenestrids as well as pronounced changes in the surface water circulation patterns associated with the early closing history of the Isthmus of Panama (Steph et al., in revision; Groeneveld et al., submitted).

1.1.1. The objectives of this thesis are:

1 – to describe the biodiversity among the very small to small (<3µm to 3-5µm) reticulofenestrid coccoliths by applying accurate SEM observations

2 – to produce, for the first time, a high-resolution record of size variations among the small *Gephyrocapsa* coccoliths

3 – to determine the species-level composition of the small *Reticulofenestra* and *Gephyrocapsa* populations

4 – to investigate, at high-resolution the composition of the total nannoflora

1.1.2. Strategy

Different strategies have been employed to get significant data on several aspects on coccolithophores evolution.

Selection of the time interval and of the coccolithophores group

The closure of the low-latitude Panama Gateway led to significant changes in the surface water circulation and warm-pool formation in the Caribbean Sea, the equatorial Pacific and the Indian Ocean (Haug and Tiedemann, 1998; Haug et al., 2001; Molnar and Cane, 2002). Basic insights into the impact of the closure of the Isthmus of Panama on oceanic circulation and climate has been provided by the Kiel paleoceanographic research group (Haug and Tiedemann, 1998; Haug et al., 2001). Profound changes in paleoceanography were documented close to 4.2 Ma based on stable oxygen isotope measurements in planktonic foraminifera from the Caribbean and eastern equatorial Pacific (Haug et al., 2001). Accordingly, a time interval in the early Pliocene from 4.5 to 3.8 Ma was chosen, showing the first influence of the closure history of the Isthmus on surface water circulation in the Caribbean and eastern equatorial Pacific (Haug and Tiedemann, 1998; Haug et al., 2001).

High-resolution stable isotope data from planktonic foraminifera were used to reconstruct an orbitally tuned time scale for ODP Site 1000 with a resolution of 3 ky (Steph et al., in revision). These data showed that the shoaling of the Isthmus of Panama led to an increase in surface water salinity at about 4.3 Ma, due to reduced inflow of low salinity waters from the Pacific. The same samples used for the oxygen isotope record were investigated within this thesis to document the evolutionary history of coccolithophores and their potential relationship to environmental changes in the Caribbean Sea.

The time interval roughly coincides with several known diversification events and floral turnover among coccolithophores mainly documented by LM biostratigraphic studies (first occurrence and last occurrence). The LM first consistent occurrence (FCO) of coccoliths of the genus *Gephyrocapsa* and the first occurrence (FO) of *Pseudoemiliania* are widely documented to fall within this time interval (Young, 1998; Kameo and Sato, 2000; Okada, 2000; Marino and Flores, 2002). However, previous studies on this major evolutionary event among coccolithophores were not carried out at high resolution and without taxonomic detail and could therefore not resolve the tempi and modes of biological evolution either to what extent biological and environmental events were related. The

evolutionary development of coccolithophores in relation to the significant climatic changes which have characterised the last 5 million years are thus poorly understood. This is mainly due to the fact that coccoliths studies are mainly carried out by LM which cannot resolve the species-level identity of forms. In particular, reticulofenestrids are mainly LM size-defined groups (e.g. Backman, 1980). From the well documented almost synchronous LM first occurrence and last occurrence of coccoliths of biostratigraphy, sympatric speciation appears the main evolutionary mode.

The main focus was on the radiation of the reticulofenestrids in the early Pliocene. We focused our attention on the evolutionary development of reticulofenetrids, leading to the origin of the genus *Gephyrocapsa* from the genus *Reticulofenestra*, a group of coccolithophores to which, the modern *Emiliania huxleyi* is phylogenetically related. This was previously inferred by morphological and structural similarity of their coccoliths (Young et al., 1999 and references therein) but has been recently demonstrated by molecular genetic studies. These have shown that *E. huxleyi*, the most abundant modern reticulofenestrid coccolithophores species and the subject of intensive studies (Westbroek et al., 1994 and references therein), recently diverged from the *Gephyrocapsa* clade (Sáez et al., 2004). The early divergence of *E. huxleyi* was already supported by stratophenetic data that documented the synchronous occurrence of *E. huxleyi* at 270kyr (Thierstein et al., 1977).

Previous authors have qualitatively observed a time-progressive size increase, from < 2 μm to 3.5 μm after the FCO, of small *Gephyrocapsa* (e.g. Okada, 2000) but no detailed morphometric studies were carried out to date and the reasons for the observed size increase in the early Pliocene are unknown. Few species have been described from the Pliocene, jet suggested significant biodiversity.

Material

In order to obtain insights of the influences of changes in circulation patterns and hydrography related to the closure of the CAS, two ODP Sites, Site 1000A (Leg 165, South Caribbean Sea) and Site 1241 (Leg 202, Eastern Equatorial Pacific) were selected (Fig. 1) for this study. In the course of the study it became clear that the microevolutionary history of *Gephyrocapsa* in the two sites was very similar, therefore, the better preserved assemblages from the Caribbean Site were focussed on. Data from the Pacific cores will be presented in successive manuscripts.

Site 1000A was chosen because of its shallowest depth (916m) providing good preservation of primary assemblages. Preliminary observations by LM and SEM indicate that samples recovered at Site 1000A are exceptionally well preserved, similar to the type of sediments referred to as Nannofossil-Lagerstätten (Bown, 1993). Biodiversity estimations are particularly biased by preservation (Young et al., in press) and it has been shown that the number of species can be much higher in this type of sediments (Crudeli and Young, 2003). In parallel, a high-resolution age model of these cores was developed (Steph et al., in revision).

A short overview of the site location and material is given here.

<u>ODP Site 1000 (Caribbean)</u>

Locations and quality of sample material.

Site 1000 is located within the Pedro Channel on the Northern Nicaraguan Rise, 265 km west of Jamaica (water depth, 916 m) (Sigurdsson et al., 1997; Fig. 1).

The Pliocene sediments are a mixture of calcareous ooze and bank-derived neritic carbonates with a minor component of terrigenous sediments. Due to the shallow water depth of the site, the preservation of foraminifers and coccoliths is excellent. Carbonate contents of the sediment range between 77 and 93 wt-% (Sigurdsson et al., 1997). Aragonite (mostly in form of fine, platform-derived needles) is observed across the interval from cores 1000A-15H to 1000A-7H. The high aragonite contents (up to 60 %, Groeneveld et al., submitted), increase the diagenetic potential of the sediment, as aragonite can be dissolved and recrystallised after burial. Variable carbonate overgrowth on coccoliths was recognised in selected intervals of the analysed cores. The depth interval from 138.45 mbsf to 118.25 mbsf, (1000A–16H-2 to 1000A–14H-1) corresponding to the time interval from 4.5 – 3.8 Ma was selected for this study. The high-resolution stratigraphy developed by Steph et al. (in revision) yielded a temporal resolution generally better than 3 ky.

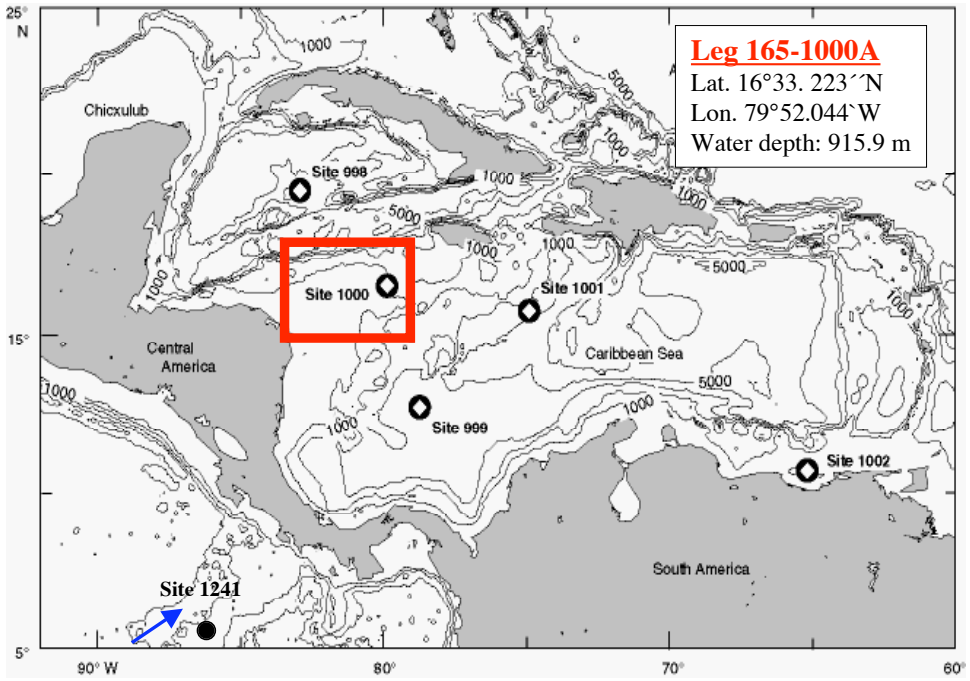

Fig. 1. Map of the tropical East Pacific and the Caribbean, showing the location of the ODP Site 1000 analysed in this thesis. The location of Site 1241 is also shown.

Methods

For paleoceanographic, paleoenvironmental, and biostratigraphic studies based on calcareous nannofossils, light microscope (LM) is an unique research instrument. The vast majority of forms are easily recognised at species level by LM, and can be rapidly counted. However for a number of forms, this seems not to be sufficient. For example, the recent molecular genetic studies indicate that *Calcidiscus leptoporus* is composed by various cryptic species that can partially overlap in size and are differentiated by subtle details in the central area structure (Sáez et al., 2003) which are not easily observable by LM.

Previous studies by LM of these sediments indicated the presence of numerous small reticulofenestrids (Kameo and Bralower, 2000; Kameo and Sato, 2000). This was confirmed by our preliminary observations by LM and scanning electron microscope (SEM). A micropaleontologic

study by LM would have resulted in underestimation of this component of the assemblages, either in term of abundance and biodiversity.

Reticulofenestra, *Dictyococcithes*, *Pseudoemiliania*, *Gephyrocapsa* and *Emiliania* belong to the family Noelaerhabdaceae (Romein, 1979; Young, 1989; Young, 1998). These coccoliths have similar basic structure and rim morphology and are termed reticulofenestrids (Young, 1989; Young et al., 1997) (Fig. 2). Reticulofenestrid coccoliths dominate the assemblage from the Eocene to the recent. Generic attribution is based on morphological characters as presence of - 1 slits between elements of the distal shield (*Pseudoemiliania* Gartner, 1969), - 2 bridge that span the central area (*Gephyrocapsa* Kamptner, 1943), – 3 few slits or no slits between elements of the distal shield and absence of the previous structures (*Reticulofenestra* Hay, Mohler and Wade, 1966), and - 4 slits between all distal shield, and some proximal shield, elements (*Emiliania,* Hay and Mohler, 1967). *Dictyococcites* (Black, 1967) differs from *Reticulofenestra* by a closed central area. Variation is, however, continuous and the validity of the genus is questionable (e.g. Young, 1990)

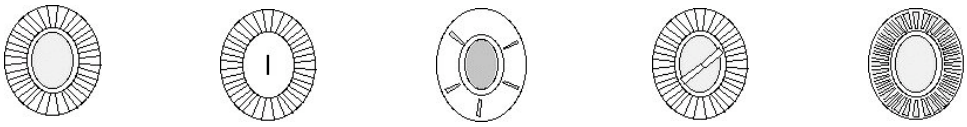

Reticulofenestra ***Dictyococcithes*** ***Pseudoemiliania*** ***Gephyrocapsa*** ***Emiliania***

Fig. 2. Generic distinctions. The five genera *Reticulofenestra, Dictyococcithes, Pseudoemiliania*, *Gephyrocapsa* and *Emiliania* have identical basic structure. *Reticulofenestra* has the typical morphology, *Dictyococcithes* is differentiated by a closed central area, *Pseudoemiliania* by presence of slits between elements of the distal shield, *Gephyrocapsa* has a bridge over the central area, *Emiliania* has slits between elements of the distal and proximal shield. Figures from INA www.nhm.ac.uk/hosted_sites/ina/.

Species are discriminated on the base of presence/absence of peculiar structures (e.g. ornamentation), coccoliths size, number of slits. These characters are often subtle and thus not detectable by LM. Consequentially, specimens are often counted and classified by LM using an informal nomenclature (see fig. 3). Since calcareous nannofossil studies have historically been carried out by LM, available data on reticulofenestrids are represented by fossil records of informal groups rather then of valid species.

Small *Gephyrocapsa* is a LM taxonomic group and includes coccoliths that are differentiated from other similar forms of similar size by the presence of a birefringent bar spanning the coccolith central area. Only few studies have investigated the species-level variation of the Pliocene *Gephyrocapsa* (e.g. Samtleben, 1978; Samtleben, 1980). Since the major objective of the thesis was to decipher the evolutionary history of these coccolithophores during the closure of the Isthmus of Panama, the work has been carried out by SEM. We conducted a study on the species-level variation of the Pliocene small reticulofenestrids and of small specimens of *Gephyrocapsa* whose phenetic variability and diversity is extremely poorly known. Among the small reticulofenestrids group we recognised and described four new species (Chapter 2 and Chapter 3) whereas among the small Gephyrocapsa up to 5 new species (Chapter 4) were discovered. We showed an higher biodiversity among the calcareous nannoflora which has fundamental implication for paleoecological and paleoceanographic applications and evolutionary studies.

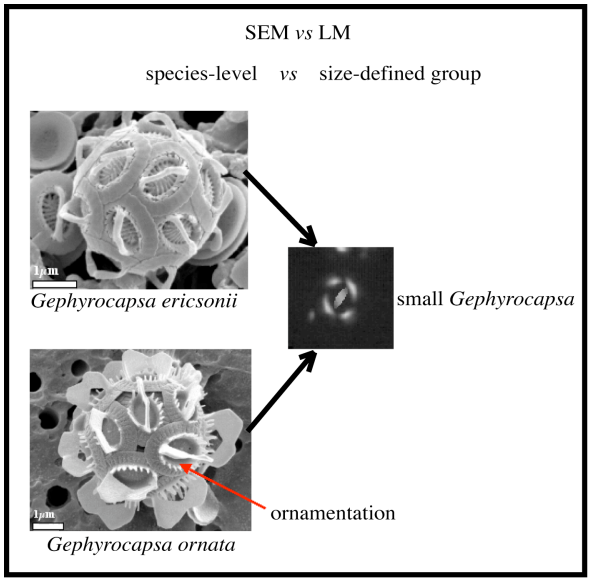

Fig. 3. Coccoliths of *Gephyrocapsa ericsonii* and *G. ornata,* two modern species, are very similar in size. *G. ornata* differs from *G. ericsonii* by the presence of ornamentations around the central area which are only visible under the SEM. Under the LM, the coccoliths of two species appear identical and, during analyses, these will be grouped together under the informal name small *Gephyrocapsa*. SEM images are from INA www.nhm.ac.uk/hosted_sites/ina/.

Although Kameo and Sato (2000) quantified the nannoflora from several Caribbean and Pacific Sites (including those presented in this thesis) providing valuable information on environmental variations on either side of the Isthmus of Panama, *Florisphaera profunda* was not quantified thus leaving out an important component of the coccolithophore assemblage. In contrast, this species could be quantified in this thesis. These data provided information on primary productivity variation during the Pliocene key time-interval of the closure of the Panama Isthmus (Chapter 5)

The composition of calcareous nannofossil assemblages was initialy quantified by SEM in terms of relative abundance (%). However, in order to retrieve more information on paleofluxes and coccolithophore ecology, absolute abundances, calculated in concentration per gram of sediment (number of specimens/g) and accumulation rate (number of specimens/cm^2/ky) are given as well.

Details on sample preparation and quantification methods are included in Chapter 4.

1.2. Outline of this thesis

Results of this thesis are presented in Chapters that correspond to manuscripts that are published or will be submitted for publication in peer reviewed scientific journals. In addition, the manuscript by Groeneveld et al. (submitted), in which the author of this thesis is co-author, is included.

Chapter 1.3. includes an introduction to coccolithophores.

Chapters 2, 3, 4 and 5 contain the manuscripts. A summary of their content is reported in the following.

Chapter 2 - *Reticulofenestra calicis* n. sp., an unusual small reticulofenestrid coccolith from the Lower Pliocene of the South Caribbean Sea
Crudeli, D. and Kinkel, H.
Micropaleontology, 50, 4, 369-379, 2004.

Chapter 2 includes a research paper published in Micropalaeontology, 2004.

In this manuscript, a new very small to small coccolith observed from cores from ODP Hole 1000A (early Pliocene) is described by SEM and LM. The species is unusual in being characterised by extension of the outer tube elements, a structural-morphological variation not previoulsy described in reticulofenestrids. The species documents a previously unknown biodiversity among this group of coccolithophores. It demonstrates how limited the present knowledge on coccolithophore biodiversity may be, which has various implications for coccolithophores paleo-diversity estimation and for the understanding of their evolution. This paper underlines the importance of high-resolution SEM studies and of the preservation of samples, an issue recently discussed by Young et al. (in press) concerning the discrepancy between the amazing biodiversity of modern coccolithophores and the "poverty" of that recorded in the fossil record.
R. calicis n. sp. is similar to modern *Emiliania huxleyi* var. *corona* and to *Reticulofenestra maceria* and its occurrence provides a link for the understanding of the evolutionary development of these modern coccolithophores. Moreover, it is particularly significant since it occurs close to the FCO of small *Gephyrocapsa.* The fossil record of this species is presented in Chapter 3 where, the possible phylogeny is discussed. The FO has been dated by high-resolution isotope stratigraphy (Steph et al., in revision) and its occurrence, as well as its relative short stratigraphic range make it an ideal biostratigraphic marker for fine subdivision of the *R. pseudoumbilicus* Zone. Furthermore, the comparison of its stratigraphic range from different locations will provide valuable insights to synchronous or diachronous evolutionary events and principal modes of plankton dispersal.

Chapter 3 - *Reticulofenestra alis* sp. nov., *R. pujosiae* sp. nov. and *R. premoliae* sp. nov., key-species in the reconstruction of the phylogeny of *Gephyrocapsa theyeri* and *R. calicis* (Coccolithophore, early Pliocene, South Caribbean Sea)
Crudeli, D., Young, J.R. and Kinkel, H.

Chapter 3 includes a research paper that will be submitted, after revision, to Journal of Micropalaeontology.

Three very small phylogenetically related reticulofenestrids are described (ODP Hole 1000A, early Pliocene). The implications related to evolution are similar to that provided by *R. calicis*. As example, the new species demonstrate hidden biodiversity which has implication for evolutionary studies. Recognition of these specie in other locations will be of significance in better constrain the extent of coccolithophores dispersal. The fossil record of *R. calicis* is documented in this work. In addition, a single small *Gephyrocapsa* species occurs in association with these species. This first *Gephyrocapsa* is extremely similar to *G. theyeri* that was described by Pujos (1987) from the late Miocene of the Eastern Equatorial Pacific. However, in our study it appeared to have a definite first occurrence within the early Pliocene. To clarify the age relations of this taxon, we re-analysed the topotype material (the samples from which the type of the species has been described) of *G. theyeri.* Our examination of the material indicates an early Pliocene rather than late Miocene age of the samples and the presence of *G. theyeri* could not be confirmed. These observations support our inference that *G. theyeri* is restricted to the Pliocene. We also discuss the reliability of previous reports by LM and SEM of *Gephyrocapsa* coccoliths from the Miocene with the intention to stimulate discussion and perhaps re-examination of Miocene samples. This would provide a significantly clearer picture of the evolutionary history of this important group of coccolithophores. The recognition of the three new species is particularly significant since it allowed for the first time, on a species-level base, to infer phylogenetic relation of *Gephyrocapsa* and to discuss the phylogeny of *R. calicis*.

Chapter 4 - Behind the increase in size of small *Gephyrocapsa*: the earliest adaptive radiation of the the populations (early Pliocene, South Caribbean Sea)
Crudeli, D., Young, J.R. and Kinkel, H.

Chapter 4 includes a research paper that will be submitted, after revision, to Marine Micropalaeontology.

After having established the specific composition of the earliest *Gephyrocapsa* population (*G. theyeri*, Chapter 3), in this research paper we focus on the species-level variation and evolutionary development of the genus. From thousands of size measurements by high-resolution SEM we provide a detailed record of size variation of the population, not available before. This, coupled with extensive documentation of morphological variation of forms by numerous micrographs and video-prints allow us to consistently identify a number of new *Gephyrocapsa* species and to semi-quantitatively trace their occurrence in the cores (Hole 1000A, 15H-7 to 14H-1). These results allow us to discuss aspects of species-level evolution of coccolithophores. Surprisingly, the pattern of size variation is closely similar to that recorded by low-resolution morphometry in the Quaternary (Samtleben, 1980; Matsuoka & Okada 1990; Matsuoka and Fujioka, 1992). The results of this work support that the Quaternary cycles of size variation of the *Gephyrocapsa* plexus are evolutionary. This was already predicted by the authors, but, given lack of species-level determination, the presence of mixed

populations, and possibly also including long ranging forms, could not be conclusive. Possible causes for the cyclic in size variation are discussed.
In the light of the results on *Gephyrocapsa* evolution, we discuss the extent to which the species provide evidence of very fast evolution among reticulofenestrid coccolithophores.

Chapter 5 - The Pliocene Mg/Ca SST increase in the Caribbean: Western Atlantic Warm Pool formation, salinity influence or diagenetic overprint?
Groeneveld, J., Nürnberg, D., Steph, S., Tiedemann, R., Reichart, G.J, Reuning, L. and **Crudeli, D.**

Chapter 5 includes a research paper by Groeneveld et al. submitted to Geochemistry, Geophysics, Geosystems.

In chapter 5, the influence of salinity and/or diagenesis on the Mg/Ca ratios in planktic foraminifers in the Pliocene in the Caribbean Sea (Hole 1000A) are discussed. Mg/Ca ratios are a relatively new proxy for estimating past sea-surface temperatures, which could, in combination with paired stable oxygen isotope measurements, enable precise reconstructions of the surface water properties where these organisms live. These reconstructions represent an important approach to decipher the paleoceanographic history of the investigated area.
However, Mg/Ca ratios of foraminiferal shells are highly sensitive to diagenesis. Within this study we observed diagenetic overgrowth of foraminiferal shells, which resulted from the dissolution of aragonite and reprecipitation as calcite. Apparently there is a good correlation and a cyclic behaviour of aragonite dissolution and precipitation and Mg/Ca ratios in foraminifera shells in ODP Site 1000. However, it was unclear what caused this cyclicity, but we could show by using the relative abundance of the deep dwelling coccolithophore *Florisphaera profunda* as an indicator for productivity, that most likely this cyclic pattern was caused by changes in the flux of organic matter to the seafloor and its subsequent impact on the diagenetic behaviour of aragonite. Apparently high values of *F. profunda*, indicative for lower productivity, are correlated to higher aragonite contents in the underlying sediments and low Mg/Ca ratios in foraminiferal shells. On the other hand low values of *F. profunda*, indicating higher productivity, are characterised by low aragonite contents and increased Mg/Ca ratios in foraminiferal shells. Thus the paleoproductivity reconstructions based on the coccolith assemblages provide a conclusive explanation for the observed diagenetic pattern.
The specific paleoenvironmental-paleoceanographic implications of *F. profunda* will be discussed in a successive paper.

Chapter 6 includes a summary of the results of this thesis and conclusions.
In order to understand the rule of the paleoenvironmental-paleoceanographic changes related to the closure of the CAS on the evolutionary radiation of *Gephyrocapsa* coccolithophores, the pattern of microevolution, *Gephyrocapsa* and *F. profunda* paleofluxes obtained during this thesis are compared with abiotic proxies profiles obtained from the same cores (Hole 1000A) by S. Steph and J. Groeneveld and co-workers. The comparison is presented as a very draft for a co-authored publication.

In this chapter, data obtained during this thesis (not included in the thesis) from a co-eval stratigraphic interval (Site 1241) from the Eastern Equatorial Pacific (Tiedemann et al., submitted), are compared with results from Caribbean Site 1000A.

Chapter 7 provides a summary of the publications

Appendix A-(1-15) includes morphometric data of *Gephyrocapsa* coccoliths from the investigated cores (Hole 1000A) (Chapter 4).

Appendix B-(1-3) includes the frequency distribution of the length of *Gephyrocapsa* coccoliths from the investigated cores (Hole 1000A) (Chapter 4).

- The references cited are reported for each Chapter.
- e.g. (Crudeli et al., in prep. 3) cited in the manuscripts in preparation for submission (Chapter 3 and 4) corresponds to the manuscript included in Chapter 3.

- All data that were generated by the author within the framework of this thesis are available or will be available (after publication of the manuscripts) at the PANGAEA database.

1.3. Coccolithophores

1.3.1. Biodiversity

Recent molecular genetic studies have shown that many coccolithophores conventionally regarded as single species are in fact monophyletic assemblages of sibling species, typically with subtle morphological differences (Sáez et al., 2003; Fig. 4). These studies of molecular phylogeny of coccolithophores are limited to a few key species (Sáez et al., 2003). However, the consistent finding of cryptic or pseudo-cryptic species in other pelagic protists suggests that the pattern is widespread in the pelagic domain (de Vargas et al., 1999; Norris and de Vargas, 2000; de Vargas et al., 2004).
Within a phenotype commonly described as a single species (e.g. *Helicosphaera carteri*), more genetically distinct species have been recognised which often differ by subtle variations in the morphology of their coccoliths (Sáez et al., 2003; Fig. 4).

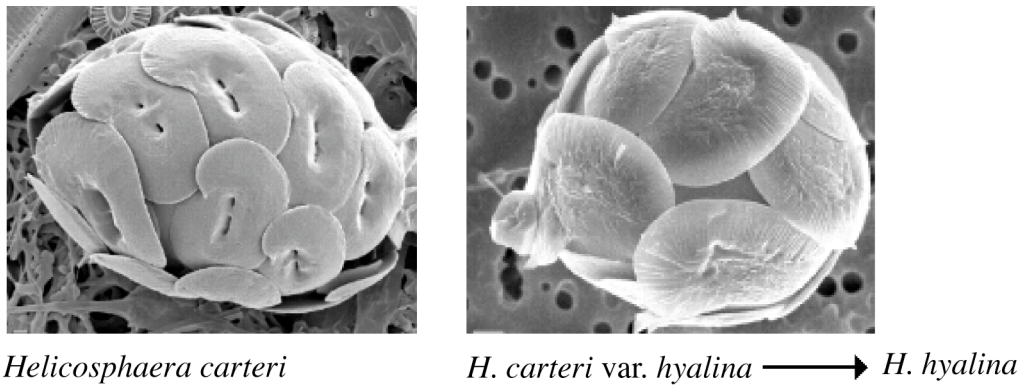

Fig. 4. SEM images of *Helicosphaera carteri* and *H. hyalina. H. hyalina* was previously recognised as a variety of *H. carteri.* The scale bar (white) indicates 1µm. SEM images from INA www.nhm.ac.uk/hosted_sites/ina.

Therefore, in contrast to morphospecies with a considered cosmopolitan distribution, the ocean may be inhabited by sibling species, which possibly evolved peculiar distinct ecological affinities with adaptation to different allopatric spatio-temporal ranges (de Vargas et al., 2004). Subtle morphological variation confirms in many cases genetic differentiation. On the contrary, cryptic speciation is also possible. *Syracosphaera pulchra* and *Coronosphaera mediterranea* have been widely recognised as well defined single species. Nonetheless, recent studies from *combination coccospheres* (Geisen et al., 2002) and culture studies suggest that they include more than one species, but these are only recognisable in the haploid holococcolith producing phase. There is no obvious evidence for morphological difference in the diploid heterococcolith producing phase (Geisen et al., 2002; Geisen et al., 2004). In addition, more then one discrete coccolith can be produced by single extant coccolithophore species and this suggests that polymorphism almost certainly also occurred in fossil species (Young et al., 2003; Young et al., in press). As a result of recent research, it is predicted that the number of modern species will increase from the actual estimates of 200 species (Young et al., 2003) to up to 500 species (Young et al., in press).

1.3.2. Evolutionary model in planktonic organisms

An intriguing result of recent research on biodiversity is that in many cases the molecular clock estimates suggest that the pseudo-cryptic sibling species have deep divergences close to the origin of the broader morphotypes (Sáez et al., 2003).

These findings allowed to introduce the concept of super-species (assemblage of allopatric species of monophyletic origin often with distinct morphological differences) for the evolution of planktonic organisms (de Vargas et al., 2004, Fig. 5). Two end-member models of evolution within a super-species were proposed; speciation associated with a flurry of genotypic variation without comparable morphological differentiation (Fig. 5, B) or morphological diversification associated with genotypic differentiation (Fig. 5, A). In the latter case, the model of planktonic organisms evolution suggests that the speciation event occurs after the phenotype of the mother species has stabilised into an adaptive, optimal peak and when the super-species increases its ecological range.

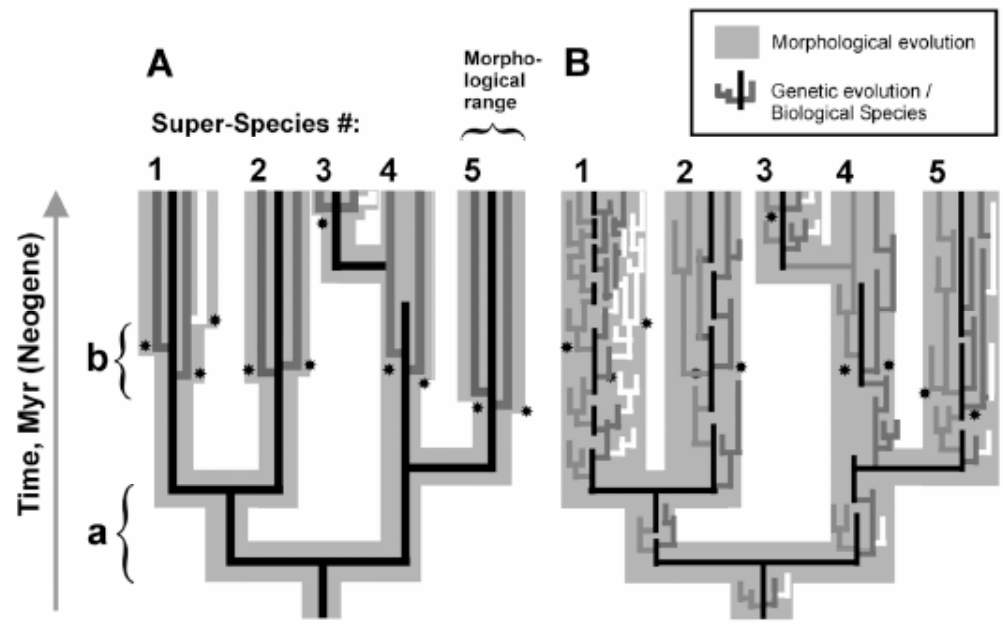

Fig. 5. Two hypothetical models of evolution among marine planktonic protists developed from results of molecular genetic (foraminifers or coccolithophores) (after de Vargas et al., 2004).

In the fossil record, the level of variation now recognised as indicative of pseudo-cryptic speciation is detectable, but has rarely been documented at the level of detail we now realize is necessary to test such evolutionary hypotheses (de Vargas et al., 2004 for synthesis). There are few detailed studies on species-level evolution of coccolithophores from the geological archive, which are of significance to test the evolutionary hypothesis and to enlarge the knowledge on the tempo, mode and mechanisms of morphological evolution and speciation among this group of primary producers. An objective of the current study was to investigate whether fine morphological differentiation patterns could be observed occurring continuously within a closely studied group.

1.3.3. Phylogeny of the reticulofenestrids – state of the art

Phylogenetic relations among reticulofenestrids have been inferred on the base of LM and SEM observations of coccoliths morphology and structure (eg. Young, 1989). Successive high-resolution SEM works have showed that reticulofenestrids consistently have the same microstructure, a character that further constrains the phylogeny of the group (Young and Bown, 1991; Young et al., 1992; Young et al., 1999).

As previously discussed, reticulofenestrids are basically LM size-defined groups. As such, it is recommended to always report the LM taxonomic concept adopted during analyses (Young, 1998). Commonly used and widely accepted LM species names are *Reticulofenestra haqii* and *R. minuta* for Miocene reticulofenestrids 3-5 μm and < 3 μm in size, respectively, and *R. minutula* for Pliocene forms (3-5 μm). Forms with few slits between elements of the distal shield and sub-circular specimens with numerous slits are referred to *Pseudoemiliania ovata* and *P. lacunosa*, respectively. *Gephyrocapsa* specimens 3-5 μm and < 3 μm in size, are informally named small *Gephyrocapsa* and large *Gephyrocapsa*, respectively. Due to the dominance of LM studies, the phylogeny of the reticulofenestrids is essentially a genus-level phylogeny (Fig. 6). From the stem genus *Reticulofenestra*, in the Pliocene, *Pseudoemiliania* and *Gephyrocapsa* evolved. *Emiliania* has been considered to have diverged from *Pseudoemiliania* in the Pleistocene (Thierstein et al., 1977). However, recent molecular genetic studies suggest that *Emiliania* evolved from the *Gephyrocapsa* clade (Sáez et al., 2004).

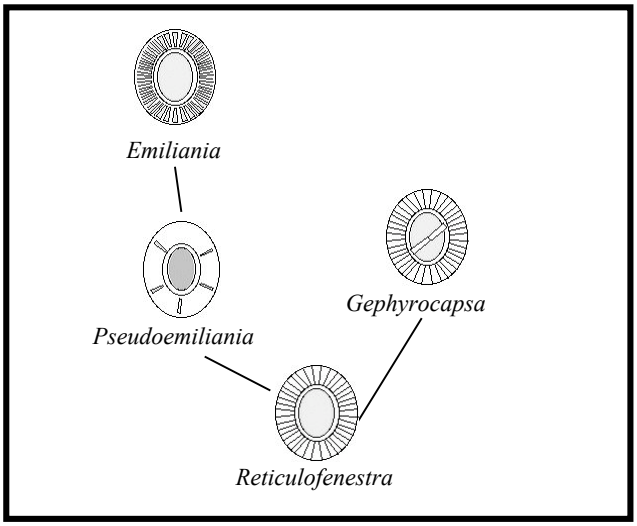

Fig. 6. Genus-level phylogeny of reticulofenestrids: *Reticulofenestra*, *Pseudoemiliania, Gephyrocapsa* and *Emiliania* (redrawn from Driever, 1988).

The evolutionary history of this group of coccoliths is mainly reconstructed on the base of stratophenetic and LM biostratigraphic data. The LM first consistent occurrence (FCO) of small *Gephyrocapsa* and the first occurrence (FO) of *Pseudoemiliania* fall within the early Pliocene (eg. Young, 1998; Kameo and Sato, 2000). These events coincide with the disappearance of selected *Reticulofenestra* species. Occurrence data from literature and morphological continuity among these coccoliths allowed Young (1998) to suggest possible phyletic relations among Neogene reticulofenestrid coccoliths (Fig. 7).

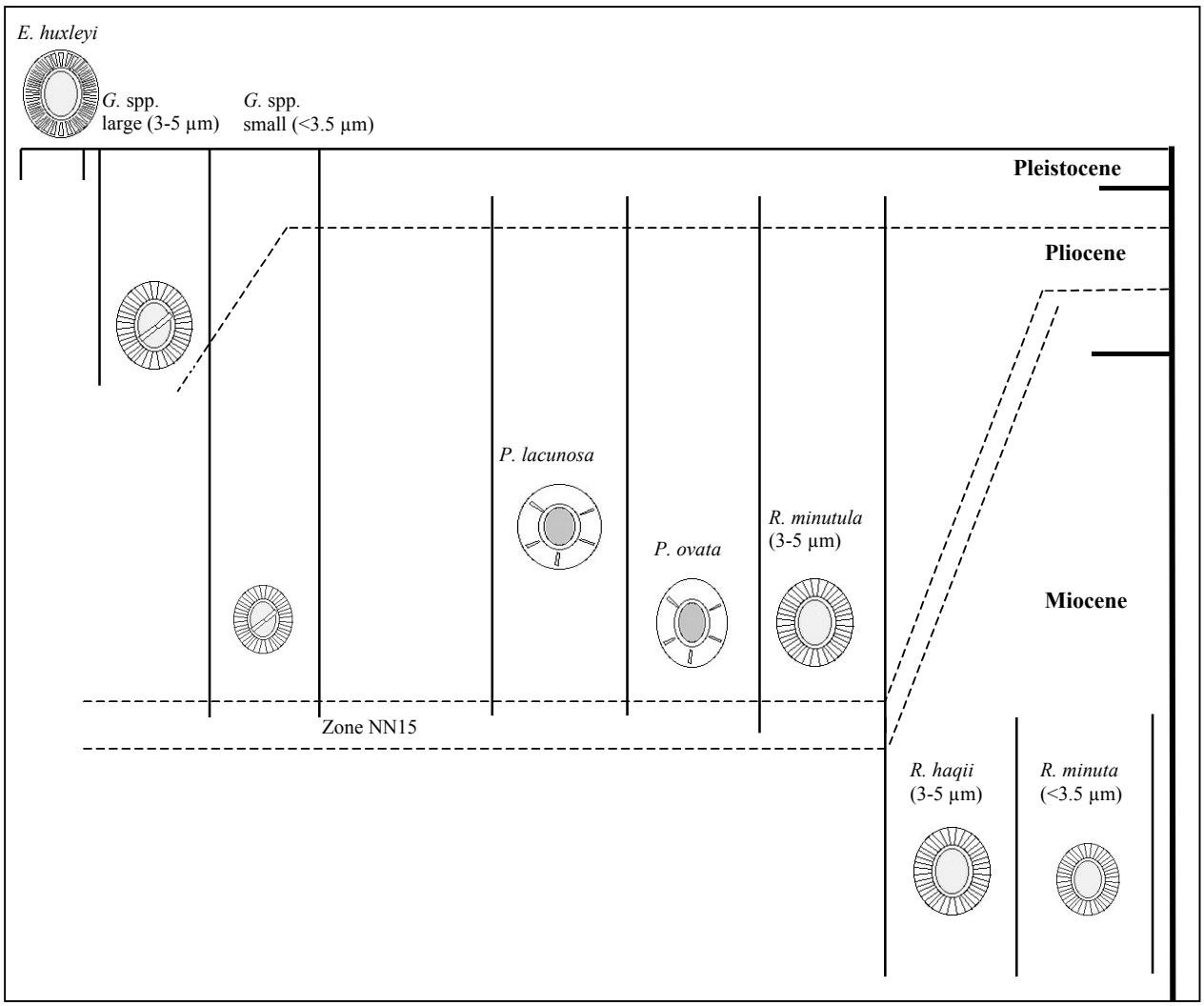

Fig 7. Stratigraphic distribution of Neogene reticulofenestrid coccoliths. The range of species is indicated by solid bars. Close spacing of range-bars indicates likely evolutionary relationship and, when adjacent, indicate intergradational morphotypes (redrawn from Young, 1998).

Young (1990) conducted a low-resolution LM morphometric study on size variation of Neogene reticulofenestrids without applying taxonomic concepts to the group. The author documented similar size variation patterns from different oceanic settings. Climate effects on a genetically unchanged population or evolutionary changes without climate effect have been suggested as possible causes for variation (Young, 1990). Successively, the author combined accepted LM taxonomic concepts of forms and available occurrence data to the size variation pattern and developed basic models for its taxonomic interpretation (Fig. 8).

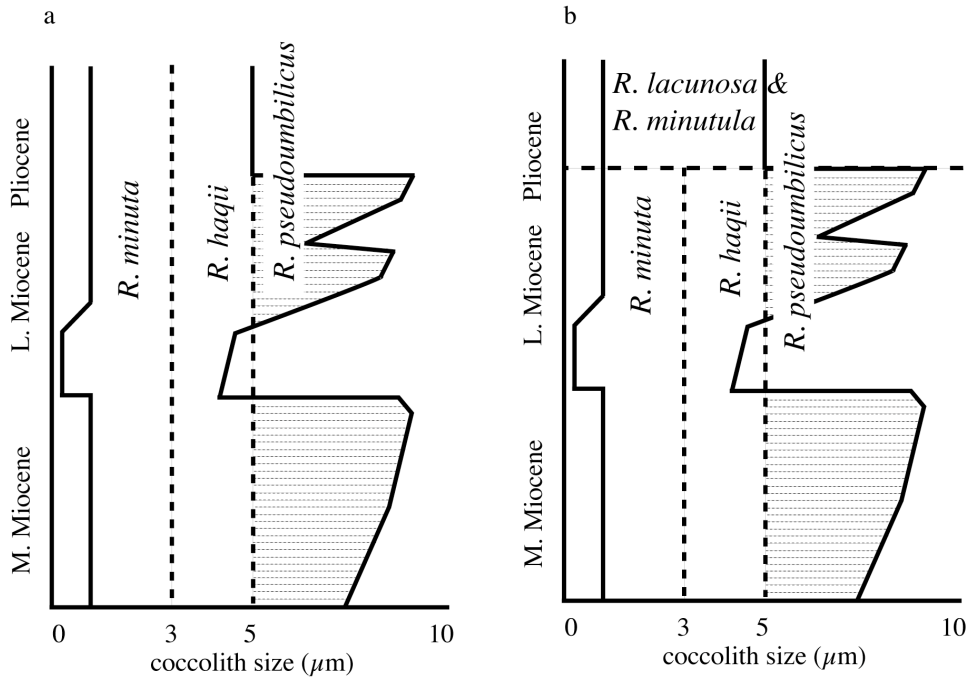

Fig. 8. Taxonomic interpretation of Neogene reticulofenestrid size variation (after Young, 1990).
a – LM morphological subdivision based on coccolith size.
b – Proposed evolutionary scheme. The lineages are separated in the early Pliocene. In addition to the last occurrence of the large *R. pseudoumbilicus*, size variation is accompanied here with morphological-structural variability of forms. As example, *Pseudoemiliania lacunosa*, with slits between elements of the distal shield appear.

1.3.4. Fossil record and environmental changes

The fossil record of calcareous nannofossils probably tracks changes in the global character of the Earth´s system (Bown et al., 2004). Recently, a compilation of changes in diversity of the Mesozoic and Cenozoic calcareous nannoflora was developed, which shows a good correlation between changes in the diversity of assemblages and major environmental changes (Bown et al., 2004; Fig. 9).

The earliest coccolithophore populations are of Norian age (Late Triassic), restricted to low latitudes and consist of very small forms (2µm). Only one of these survived the Triassic-Jurassic boundary. Subsequently, coccolithophores diversified again and became dominant forms in the Jurassic to Cretaceous marine realms (Bown, 1998; Bown and Cooper, 1998; Bown et al., 1992). The diversity of coccolithophores increased throughout the Mesozoic, reaching a maximum close to the Cretaceous/Tertiary (K/T) boundary (Fig. 9). After the K/T boundary crisis, coccolithophore diversity recovered in the Palaeogene, followed by major fluctuations which might have been driven by global environmental changes. In particular, there is a diversity loss in the past ca 5 Ma, approximately coinciding with the climatic deterioration in the Late Neogene which culminated in the Northern Hemisphere Glaciation in the Pliocene. The Pliocene diversity decline is due to the extinction of *Sphenolithus, Discoaster*, many *Scyphosphaera* species and *R. pseudoumbilicus*, which dominated primary productivity throughout the Neogene. So far, the radiation of a few eutrophic forms, *Pseudoemiliania* and *Gephyrocapsa* has been documented Yet, the results of this thesis indicate that these biodiversity estimates need to be revised.

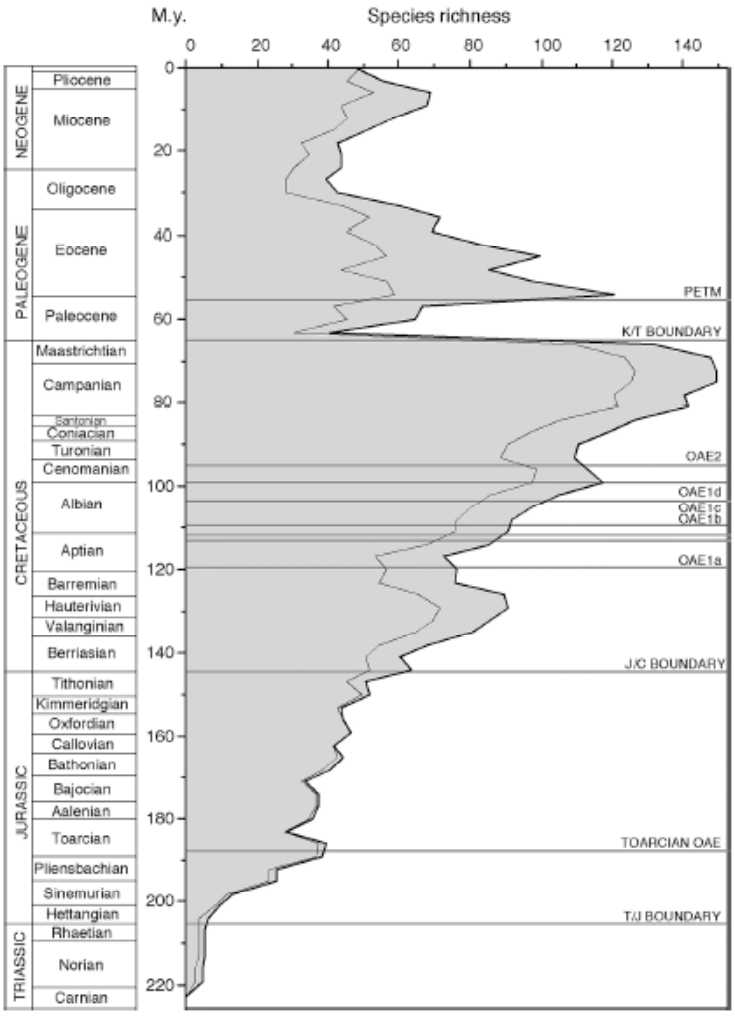

Fig. 9. Species richness of coccolithophores (light line) and all the nannoflora as reconstructed by application of the palaeontological species data to the deep–sea geological record (after Bown et al., 2004). OAE, oceanic anoxic event, PETM, Paleocene/Eocene thermal maximum.

1.3.5. Coccolithophores ecology and biogeography

Coccolithophores live in the photic zone where light levels allow photosynthesis. Many factors control the geographical and vertical distribution of coccolithophores. These include light, salinity and temperature profiles, water mass characteristics such as nutrient content and ocean currents (Winter et al., 1994; Brand, 1994).

Coccolithophores constitute the most significant phytoplankton group in stable and relatively low nutrient domains where they often display an amazing biodiversity (Jordan and Winter, 2000; Winter et al., 2002; Young et al., 2003). Selected species such as *E. huxleyi* and *Gephyrocapsa* have an r-adaptation, responding with increased growth rates to enhanced nutrient levels. *E. huxleyi* is very sensitive to increases in nutrient contents and can produce huge blooms (Winter et al., 1994; Nanninga and Tyrrel, 1996). In the oligotrophic domains, peaks in abundance of *E. huxleyi* are responsible for the seasonal coccolithophore production during winter wind-driven breakdown of stratification (Knappertsbusch, 1993; Ziveri et al., 2000). In highly eutrophic and instable systems

such as upwelling areas, monospecific assemblages are often dominant and the productivity of coccolithophores is enhanced. In contrast, in oligotrophic and stable domains, coccolithophore production is low and the population is much more diverse.

Stable oceanic domains, such as the Subtropical Zone, characterized by a stratified water column (McIntyre and Be, 1967), are often characterized by a depth separation of coccolithophore communities (Winter et al., 1994). Most coccolithophores live in the upper and middle photic zone. A typical lower photic zone form is *F. profunda*, an *incertae sedis* floriform species (Jordan and Kleijne, 1994; Young, 1994) typical of low latitude regions with a depth range of about 100-150 m (Okada and Honjo, 1973; Okada and McIntyre, 1977). The relative abundance of *F. profunda* in surface-sediments is high in oligotrophic areas and decreases with increasing productivity of surface waters (e.g. Beaufort et al. 1997). This primarily results from the adaptation of *F. profunda* to the light limited but nutrient rich lower photic zone, and the relative abundance is driven by the amount of coccolithophores that grow in the upper photic zone due to the availability of nutrients (Kinkel et al. 2000, Fig. 10). Therefore, changes in the abundance of the deep dwelling species have successfully been used for paleo-reconstructions of coccolithophores, as well as overall primary productivity (Molfino and McIntyre, 1990a; Molfino and McIntyre, 1990b; Beaufort et al., 1997; Kinkel et al., 2000; Thomson et al., 2004).

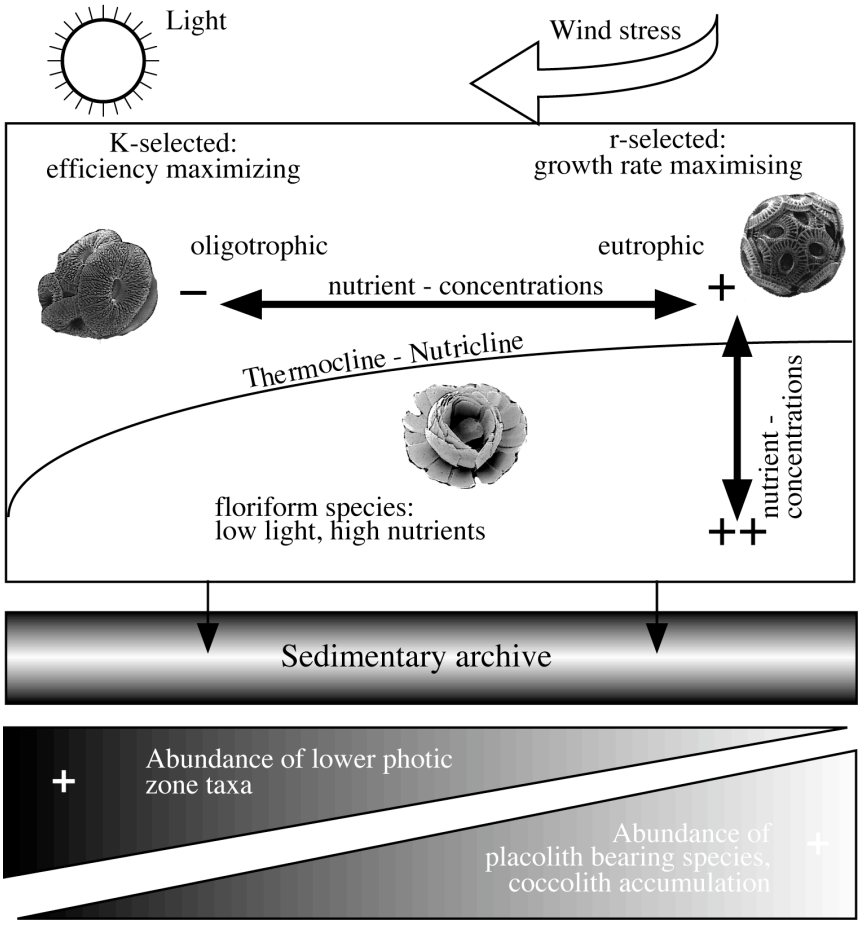

Fig. 10. Model of the coccolithophore response to changing surface water nutrient conditions (after Kinkel et al., 2000).

1.3.6. Coccolithophores biology – reproduction and life cycle

Coccolithophores are marine flagellates, microalgae belonging to the Phylum Haptophyta Hibberd, 1972 ex Cavalier-Smith, 1986, division Prymnesiophyceae Hibberd, 1976.

Recent studies, particularly within the CODENET project (Coccolithophorid Evolutionary Biodiversity and Ecology Network) resulted in the definitive documentation of complex life-cycles as a fundamental feature of coccolithophore ecology and biology (Thierstein and Young, 2004). Coccolithophores have a haplo-diplontic life cycle, with the haploid and diploid phases being independently capable of photosynthesis and asexual binary reproduction (mitosis), previously documented only in a very few forms (Parke and Adams, 1960).

The life cycle phases are characterised by distinct biomineralisation modes. They produce heterococcoliths (diploid) and holococcoliths (haploid), or occasionally nannoliths (Geisen et al., 2002; Houdan et al., 2004; Noël et al., 2004). *Emiliania* and the coastal *Pleurochrysis* calcify only in the diploid phase. *Emiliania* produces coccolith-bearing cells (C-cells) and non-coccolith-bearing cells (naked, N-cells and scale-bearing, S-cells) during their life cycles (Houdan et al, 2004). Molecular genetic works (e.g., Sáez et al., 2004) show that the basal coccolithophore clade (family Noelaerhabdaceae) includes *Emiliania* and *Gephyrocapsa* that only calcify in the diploid phase. It has been suggested that calcification in coccolithophores evolved first in the diploid phase and has been successively transferred into the haploid phase (Young and Henriksen, 2003).

1.3.7. Biomineralization

Coccoliths are minute, morphologically elaborate, scales of calcium carbonate covering the cell in single or multiple layers, the so-called coccospheres. Two main morphologically-structurally different types of coccoliths, heterococcoliths and holococcoliths, can be distinguished, which are produced by distinct biomineralization modes. Heterococcoliths are formed of a radial array of interlocked crystal-units of variable architecture and size and are formed intracellularly (Westbroek et al., 1989; Young et al., 1992). Holococcoliths are commonly smaller and are formed from minute (<0.1 μm) identical non-interlocked euhedral crystallites (Young et al., 1992; Young et al., 1999) and their formation most likely occurs extracellularly (Rowson et al., 1986).

Information on holococcolith biomineralization is scarce because forms are extremely small in size (<2 μm) and culture observations are limited. Most Information is available on heterococcoliths Heterococcolith biomineralization is a complex process even though it occurs in unicellular organisms (Young and Henriksen, 2003). As shown by cytological studies on *Pleurochrysis carterae*, the formation of coccoliths occurs in a vesicle derived from the Golgi body and starts with the formation of an organic scale. The vesicle is modified and contains dense particles called coccolithosomes. Nucleation occurs around the rim of the precursor organic base-plate scale. Growth proceeds upwards and outwards and gives rise to the complete coccolith. Biomineralization has been extensively studied in *Emiliania,* which can be easily cultured under controlled laboratory conditions. With respect to *Pleurochrysis*, the mode of coccolith formation in *Emiliania* is different in detail but the general pattern is very similar. Nucleation gives rise to a ring of simple crystals (proto-coccolith ring) with alternate c-axis orientations, sub-vertical (V unit) and sub-radial (R unit) c-axis orientations (Young et al., 1992). Growth proceeds outwards forming the distal and proximal shield elements and inwards producing the central area structure (Young, 1989; Westbroek, et al., 1989; Young and Bown, 1991;

Didymus et al., 1994; Davis et al., 1995; Young et al., 1992; Young et al., 1999). The pattern of regular alternation of V and R crystals is known as the V/R model of nucleation and represents a valuable instrument in inferring homology between pats of coccoliths and so phylogenetic relations of forms (Young and Bown, 1991; Young et al., 1992; Young and Bown, 1997).
As a result of interaction between inorganic and organic systems during growth, the simple calcite crystals are heavily modified as compared to the regular inorganic form. The final shape of coccoliths is thus the result of a biologically controlled biomineralization process within the vesicle (Young and Henriksen, 2003). The biochemistry of *P. carterae* has been studied in detail and it has shown the importance of complex acid polysaccharides in the regulation of the shape of the produced biomineral and this has led to the suggestion that similar complexes are responsible for controlling mineralogy and crystal growth in different coccoliths (Young and Henriksen, 2003 and references therein).

1.3.8. Function of coccoliths

The function of coccoliths is still under discussion. Possibly they have been adapted to exploit a range of different functions (Young, 1994). One of the most likely functions is protection of the delicate cell-membrane from the immediate environment, bacterial attacks, and mechanical damage. It was shown that coccolithophores can be grazed upon by a wide range of copepods, salps and other zooplankton with no distinction between e.g. coccoliths-bearing cell of *E. huxleyi* or naked cell or size. However, size and calcification may still be adaptive for lowering ingestion by other organisms, since it was shown that grazing pressure was most efficient on diatoms than on *E. huxleyi* cells (Nejstgaard et al., 1996). Moreover, coccoliths may perform an important role in nutrient uptake. Coccoliths may also be able to regulate reflection of light away from the cell or refraction of light into the cell as a function of the preferred depth of the zone where they proliferate. Finally, calcification and photosynthesis may be closely coupled and thus production of carbon dioxide during calcification, which is used during photosynthesis, may be of energetic advantage.

1.3.9. Taxonomy

The classification of coccolithophores began with the work of Murray and Blackman (1898) in the North Atlantic and of Lohmann (1902) in the Mediterranean. The successive works of Kamptner (1928, 1941, 1943) and Deflandre (1952) enlarged the knowledge of diversity among the group. Pioneer workers generally subdivided forms on the base of general shape. The advent of Transmission Electron Microscopy (TEM) in the 1950s and of Scanning Electron Microscopy (SEM) in the 1960s and the start of the Deep Sea Drilling Project (DSDP) led to a growing interest in coccoliths (Deflandre and Fert, 1954). Fine morphological differences between forms started to be observed with the contemporary development of descriptive taxonomic nomenclature (Braarud et al., 1955).
The SEM and TEM allowed detailed recognition of morphological variation among forms on which coccolithophores taxonomy is based. The potential of the fossil record of calcareous nannofossils as a stratigraphic tool for oil companies, biostratigraphic and paleoenvironmental studies resulted in detailed SEM and light microscopy taxonomic works (e.g. Bukry, 1973a; Bukry, 1973b). In recent years, the interest of nannofossil workers was mainly focused on LM biostratigraphy and paleoceanographic applications, with electron microscopy rarely being used for assemblage studies in pre-Quaternary sediments. Sometimes, however, it is difficult to correlate between species defined by

LM and SEM (e.g. Black, 1968). This is particularly true for the reticulofenestrids. By LM these are mainly size-defined groups (Backman, 1980). Many synthesis papers are available, but these in are particular focus on family and generic classification of calcareous nannofossils (Tappan, 1980; Perch-Nielsen, 1985). Recent taxonomic studies on living coccolithophores focused on specific geographic areas (Winter et al., 1978; Winter et al., 1979; Okada and Honjo, 1973; Okada and Honjo, 1975; Okada and McIntyre, 1977; Okada and McIntyre, 1979) or on selected species (Heimdal and Gaarder, 1980). Although the small size of coccoliths resulted in a general delay of taxonomic studies with respect to much larger marine protists like foraminifera, the research over the last 50 years resulted in a very detailed knowledge of the morphological diversity of coccolithophores (Bown, 1998; Bown et al., 2004). The discovery of cryptic species, the evidence for life cycles discussed above and polymorphism made it necessary to revise the taxonomy of modern coccolithophores (Young et al., 2003). Nonetheless, the results from modern assemblages have implications concerning different aspects of the study of fossil coccoliths. At the same time, the results of recent molecular genetic studies, culture and water samples studies strongly supports the efforts of micropaleontologists in finely subdividing species so that a very consistent concept of species (morphospecies) is actually available for most groups.

References

Backman, J. 1980. Miocene-Pliocene nannofossils and sedimentation rates in the Hatton-Rockall Basin, NE Atlantic Ocean. Stockholm Contributions in Geology, 36, 1-91.

Beaufort, L., Lancelot, Y., Camberlin, P., Cayre, O., Vincent, E., Bassinot, F. and Labeyrie, L. 1997. Insolation cycles as a major control of equatorial Indian Ocean primary production. Science, 278, 1451-1454.

Billard, C. 1994. Life cycles. In: Green, J.C. and Leadbeater, B.S.C. (Eds.), The Haptophyte Algae. The Systematics Association Special Volume 51. Clarendon Press, Oxford, 167-186.

Black, M. 1968. Taxonomic problems in the study of coccoliths. Paleontology, 11, 5, 793-813.

Bown, P.R. 1993. New holococcoliths from the Toarcian - Aalenian (Jurassic) of northern Germany. Senckenbergiana Lethaea, 73, 2, 407-419.

Bown, P.R. 1998. Triassic. In: Bown, P.R. (Ed.)., Calcareous Nannofossil Biostratigraphy. Kluwer Academic Publishers, Dordrecht, Boston, London, 29-32.

Bown, P.R. and Cooper, M.K.E. 1998. Jurassic. In: Bown, P.R. (Ed.), Calcareous Nannofossil Biostratigraphy. Kluwer Academic Publishers, Dordrecht, Boston, London, 34-54.

Bown, P.R., Burnett, J.A. and Gallagher, L.T. 1992. Calcareous nannoplankton evolution. Memorie di Scienze Geologiche, 43, 1-17.

Bown, P.R., Lees. J.A. and Young, J.R. 2004. Calcareous nannoplankton evolution and diversity through time. In: Thierstein, H.R. and Young, J.R. (Eds.), Coccolithophores - From molecular processes to global impact. Springer, 481-508.

Braarud, T., Deflandre, G., Halldal, P. and Kamptner, E. 1955. Terminology, nomenclature, and systematics of the Coccolithophoridae. Micropaleontology, 1, 2, 157-159.

Brand, L.E. 1994. Physiological ecology of marine cocoolithophores. In: Winter, A. and Siesser, W.G., Coccolithophores. Cambridge University Press, 39-49.

Bukry, D. 1973a. Low-latitude coccolith biostratigraphic zonation. Initial Reports of the Deep Sea Drilling Project 15, U.S. Govt. Printing Office, Washington , 685-703.

Bukry, D. 1973b. Coccolith stratigraphy, eastern equatorial Pacific, Leg 16, Deep Sea Drilling Project. Initial Reports of the Deep Sea Drilling Project 16, U.S. Govt. Printing Office, Washington, 653-711.

Crudeli, D. and Young, J.R. 2003. SEM-LM study of holococcoliths preserved in eastern Mediterranean sediments (Holocene/late Pleistocene). Journal of Nannoplankton Research, 25, 39-50.

Davis, S.A., Young, J.R. and Mann, S. 1995. Electron microcopy studies of shield elements of *Emiliania huxleyi* coccoliths. Botanica Marina, 38, 493-497.

Deflandre, G. 1952. Classe des Coccolithophoridés. (Coccolithophoridae Lohmann, 1902). Traite de Zoologie 1. Ed. by: P.P. Grassé. Masson. Paris: 439-470.

Deflandre, G. and Fert, C. 1954. Observations sur les Coccolithophoridés actuels et fossiles en microscopie ordinaire et électronique. Annales de Paléontologie, 40, 115-176.

Didymus, J.M., Young, J.R. and Mann, S. 1994. Constuction and morphogenesis of the chiral ultrastructure of coccoliths from the marine alga *Emiliania huxleyi*. Proceedings of the Royal Society of London, 258, 237-245.

Driever, B.W.M. 1988. Calcareous nannofossils biostratigraphy and paleoenvironmental interpretation of the Mediterranean Pliocene. Utrecht Micropaleontological Bulletins 36, 1-245.

Geisen, M., Billard, C., Broerse, A.T.C., Cros, L., Probert, I. and Young, J.R. 2002. Life-cycle associations involving pairs of holococcolithophorid species: intraspecific variation or cryptic speciation? European Journal of Phycology, 37, 531-550.

Geisen, M., Young, J.R., Probert, I., Sáez, A.G., Baumann, K.-H., Bollmann, J., Cros, L., Devargas, C., Medlin, L.K. and Sprengel, C. 2004. Species level variation in coccolithophores. In: Thierstein, H.R., Young, J.R. (Eds.), Coccolithophores - From molecular processes to global impact. Springer, 327-366.

Groeneveld, J., Nürnberg, D., Steph, S., Tiedemann, R., Reichart, G.J., Reuning, L., Crudeli, D., (submitted). Increasing Mg/Ca SSTs for the Pliocene Caribbean: Western Atlantic Warm Pool formation, salinity influence or diagenetical overprint? Geochem. Geophys. Geosyst.

Haug, G.H. and Tiedemann, R., 1998. Effect of the formation of the Isthmus of Panama on Atlantic Ocean thermohaline circulation. Nature, 393, 673-676.

Haug, G.H., Tiedemann, R., Zahn, R. and Ravelo, A.C. 2001. Role of Panama uplift on oceanic freshwater balnce. Geology, 29, 207-210.

Heimdal, B.R. and Gaarder, K.R. 1980. Coccolithophorids from the northern part of the eastern central Atlantic. I. Holococcolithophorids. "Meteor" Forschungs-Ergebnisse. Reihe D, 32, 1-14.

Honjo, S. 1976. Coccoliths: production, transportation and sedimentation. Marine Micropaleontology, 1, 65-79.

Houdan, A., Billard, C., Marie, D., Not, F. Sáez, A.G, Young, J.R. and Probert, I. 2004. Holococcolithophore-heterococcolithophore (Haptophyta) life cycles: flow cytometric analysis of relative ploidy levels. Systematics and Biodiversity, 4, 453-465.

Jordan, R.W. and Kleijne, A. 1994. A classification system for living coccolithophores. In: Winter, A. and Siesser, W.G. (Eds.), Coccolithophores. Cambridge University Press, Cambridge, 83-105.

Jordan, R.W. and Winter, A. 2000. Assemblages of coccolithophorids and other living microplankton off the coast of Puerto Rico during January-May 1995. Marine Micropaleontology, 39, 113-130.

Kameo, K. and Bralower, T.J. 2000. Neogene calcareous nannofossil biostratigraphy of Sites 998, 999, and 1000, Caribbean Sea. Proceedings of the Ocean Drilling Program, Scientific Results 165, 3-17.

Kameo, K. and Sato, T. 2000. Biogeography of Neogene calcareous nannofossils in the Caribbean and the eastern equatorial Pacific-floral response to the emergence of the Isthmus of Panama. Marine Micropaleontology, 39, 201-218.

Kamptner, E. 1928. Über das System und die Phylogenie der Kalkflagellaten. Archiv für Protistenkunde, 58, 173-184.

Kamptner, E. 1941. Die Coccolithineen der Südwestküste von Istrien. Naturhistorisches Museum in Wien, Annalen, 51, 54-149.

Kamptner, E. 1943. Zur Revision der Coccolithineen-Spezies *Pontosphaera huxleyi* Lohmann. Akademie der Wissenschaften in Wien, Anzeiger, 80, 11, 43-49.

Kinkel, H., Baumann, K.-H., Cepek, M. 2000. Coccolithophores in the equatorial Atlantic Ocean: response to seasonal and Late Quaternary surface water variability. Marine Micropaleontology, 39, 87-112.

Knappertsbusch, M. 1993. Geographic distribution of living and Holocene coccolithophores in the Mediterranean Sea. Marine Micropaleontology, 21, 219-247.

Knappertsbusch, M.W. 2000. Morphologic evolution of the coccolithophorid *Calcidiscus leptoporus* from the early Miocene to recent. Journal of Palaeontology, 74, 712-730.

Lohmann, H. 1902. Die Coccolithophoridae, eine Monographie der Coccolithen bildenden Flagellaten, zugleich ein Beitrag zur Kenntnis des Mittelmeerauftriebs. Archiv für Protistenkunde I, 89-165.

Marino, M. and Flores, J.A., 2002. Miocene to Pliocene calcareous nannofossil biostratigraphy at ODP Leg 177 Sites 1088 and 1090. Mar. Micropaleontol. 45, 291-307.

McIntyre, A. and Be, A.W.H. 1967. Modern coccolithophidae of the Atlantic Ocean – I. Placoliths and cyrtoliths. Deep-Sea Research, 14, 561-597.

Molfino, B. and McIntyre, A. 1990a. Precessional forcing of nutricline dynamics in the Equatorial Atlantic. Science, 249, 766-769.

Molfino, B. and McIntyre, A. 1990b. Nutricline variation in the Equatorial Atlantic coincident with the Younger Dryas. Paleoceanography, 5, 997-1008.

Molnar, P. and Cane, M.A. 2002. El Nino's tropical climate and teleconnections as a blueprint for pre-Ice Age climates. Paleoceanography, 17, 2, 1-11, 10.1029/2001PA000663.

Murray, G. and Blackman, V.H. 1898. On the nature of the coccospheres and rhabdospheres. Philosophical Transactions of the Royal Society of London, 190B, 427-441.

Nanninga, H.J. and Tyrrell, T. 1996. The importance of light for the formation of algal blooms by *Emiliana huxleyi*. Marine Ecology Progress Series, 136, 195-203.

Nejstgaard, J.C., Gismervik, I. and Solberg, P.T. 1996. Feeding and reproduction by *Calanus finmarchicus*, and microzooplankton grazing during mesocosms blooms of diatoms and the coccolithophores *Emiliania huxleyi*. Marine Ecology Progress Series, 147, 197-217.

Noël, M.-H., Kawachi, M. and Inouye, I. 2004. Induced dimorphic life cycle of a Coccolithophorid, *Calyptrosphaera sphaeroidea* (Prymnesiophyceae, Haptophyta). Journal of Phycology, 40, 1, 112-129.

Norris, R.D. and de Vargas, C. 2000. Evolution all at sea. Nature, 405, 23-24.

Okada, H., 2000. Neogene and Quaternary calcareous nannofossils from the Blake Ridge, Sites 994, 995, and 997. Proceedings of the Ocean Drilling Program, Scientific Results 164, 331-345.

Okada, H. and Honjo, S. 1973. The distribution of oceanic coccolithophorids in the Pacific. Deep Sea Research, 20, 3, 355-374.

Okada, H. and Honjo, S. 1975. Distribution of Coccolithophores in Marginal Seas along the Western Pacific Ocean and in the Red Sea. Marine Biology, 31, 271-285.

Okada, H. and McIntyre, A. 1977. Modern coccolithophores of the Pacific and North Atlantic Oceans. Micropaleontology, 23, 1, 1-55.

Okada, H. and McIntyre, A. 1979. Seasonal distribution of modern coccolithophores in the Western North Atlantic Ocean. Marine Biology, 54, 319-328.

Parke, M. and Adams, I. 1960. The motile *Crystallolithus hyalinus* (Gaardner and Markali) and non-motile phase in the live history of *Coccolithus pelagicus* (Wallich) Schiller. Journal of the Marine Biological Association of the United Kingdom, 39, 263-274.

Perch-Nielsen, K. 1985. Cenozoic calcareous nannofossils. In: Bolli, H.M., Saunders, J.B. and Perch-Nielsen, K. (Eds.), Plankton Stratigraphy. Cambridge University Press, Cambridge, 427-555.

Raffi, I., Backman, J., and Rio, D., 1998. Evolutionary trends of tropical calcareous nannofossils in the late Neogene. Marine Micropaleontology, 35, 17-41.

Romein A.J.T. 1979. Lineages in Early Paleogene calcareous nannoplankton. Utrecht Micropalaeontological Bulletins, 22, 1-231.

Rowson, J.D., Leadbeater, B.S.C. and Green, J.C. 1986. Calcium carbonate deposition in the motile (*Crystallolithus*) phase of *Coccolithus pelagicus* (Prymnesiophyceae). British Phycological Journal, 21, 359-370.

Sáez, A.G., Probert, I., Geisen, M., Quinn, P., Young, J.R. and Medlin, L.K. 2003. Pseudo-cryptic speciation in coccolithophores. Proceedings of the National Academy of Sciences of the United States of America, 100, 12, 7163-7168.

Sáez, A.G., Probert, I., Young, J.R. and Medlin, L.K. 2004. A review of the phylogeny of the Haptophyta. In: Thierstein, H.R. and Young, J.R. (Eds.), Coccolithophores - From molecular processes to global impact. Springer, 251-270.

Samtleben, C. 1978. Pliocene-Pleistocene coccolith assemblages from the Sierra Leone Rise – Site 366, Leg 41. Initial Reports of the Deep Sea Drilling Project 41, U.S. Govt. Printing Office, Washington, 913-931.

Samtleben, C. 1980. Die Evolution der Coccolithophoriden-Gattung *Gephyrocapsa* nach Befunden im Atlantik. Paläontologische Zeitschrift, 54, 1/2, 91-127.

Sigurdsson, H., Leckie, R.M., Acton, G.D. et al. 1997. Proc. ODP Initial Reports, 165.

Steph, S., Tiedemann, R., Groeneveld, J., Nürnberg, D., Reuning, R. and Haug, G. (in revision). Changes in Caribbean surface hydrography during the Pliocene shoaling of the Central American Seaway. Paleoceanography.

Tappan, H. 1980. Haptophyta, coccolithophores, and other calcareous nannoplankton. *In* The Paleobiology of Plant Protists, Freeman W.H. and Company, San Francisco, 678-803.

Thierstein, H.R. and Young, J.R. 2004. Coccolithophores - From molecular processes to global impact. Springer.

Thierstein, H.R., Geitzenauer, K.R., Molfino, B. and Shackleton, N.J. 1977. Global synchroneity of late Quaternary coccolith datum levels; validation by oxygen isotopes. Geology 5, 4000-4004.

Thomson, J., Crudeli, D., de Lange, G.J., Slomp, C.P., Erba, E., Corselli, C. and Calvert, S.E. 2004. *Florisphaera profunda* and the origin and diagenesis of carbonate phases in eastern Mediterranean sapropel units. Paleoceanography, 19, 3, PA3003, 10.1029/2003PA000976.

de Vargas, C., Norris, R.D., Zaninetti, L., Gibb, S.W. and Pawlowski, J. 1999. Molecular evidence for cryptic speciation in planktonic foraminifera and their relation to oceanic provinces. Proceedings of National Academy of Sciences of the United States of America, 96, 2864-2868.

de Vargas, C., Sáez, A.G., Medlin, L.K. and Thierstein, H.R. 2004. Super-species in the calcareous plankton. In: Thierstein, H.R. and Young, J.R. (Eds.). Coccolithophores - From Molecular Processes to Global Impact. Springer, 271-298.

Westbroek, P., Young, J.R. and Linschooten, K. 1989. Coccolith production (Biomineralization) in the marine alga *Emiliania huxleyi*. Journal of Protozoology, 36, 4, 368-373.

Westbroek, P., Brown, C.W., van Bleijswijk, J., Brownlee, C., Brummer, G.J., Conte, M., Egge, J., Fernandez, E., Jordan, R., Knappertsbusch, M., Stefels, J., Veldhuis, M., van der Wal, P. and Young, J.R. 1993. A model system approach to biological climate forcing. The example of *Emiliania huxleyi*. Global and Planetary Change, 8, 27-46.

Westbroek, P., van Hinte, J.E., Veldhuis, M., Brummer, G.-J., Brownlee, C., Grenn, J.C., Harris, R., and Riddervold Heimdal, B. 1994. *Emiliania huxleyi* as a key to biosphere-geosphere interactions. In: Green, J.C. and Leadbeater, B.S.C. (Eds.), The Haptophyte Algae. The Systematics Association Special Volume 51. Clarendon Press, Oxford, 320-334.

Winter, A., Reiss, Z. and Luz, B. 1978. Living *Gephyrocapsa protohuxleyi* McIntyre in the Gulf of Elat (Aqaba). Marine Micropaleontology, 3, 295-298.

Winter, A., Reiss, Z. and Luz, B. 1979. Distribution of living coccolithophore assemblages in the Gulf of Elat (Aqaba). Marine Micropaleontology, 4, 197-223.

Winter, A., Jordan, R.W. and Roth, P.H. 1994. Biogeography of living coccolithophores in ocean water. In: Winter, A. and Siesser, W.G. (Eds.), Coccolithophores. Cambridge University Press, Cambridge, 171-177.

Winter, A., Rost, B., Hilbrecht, H. and Elbrächter, M. 2002. Vertical and horizontal distribution of coccolithophores in the Caribbean Sea. Geo-Marine Letters, 22, 3, 150-161.

Young, J.R. 1989. Observations on heterococcolith rim structure and its relationship to developmental processes. In: Crux J.A. and van Heck S.E. (Eds.), Nannofossils and their Applications. Ellis Horwood, Chichester, 1-20.

Young, J.R. 1990. Size variation of Neogene *Reticulofenestra* coccoliths from Indian Ocean DSDP cores. Journal of Micropaleontology, 9, 71-85.

Young, J.R. 1994. Functions of coccoliths. In: Winter, A. and Siesser, W.G. (Eds), Coccolithophores. Cambridge University Press, Cambridge, 63-82.

Young, J.R. 1998. Neogene. In: Bown, P.R., (Ed)., Calcareous Nannofossil Biostratigraphy. Kluwer Academic Publishers, 225-265.

Young, J.R. and Bown, P.R. 1991. An ontogenetic sequence of coccoliths from the Late Jurassic Kimmeridge clay of England. Paleontology, 34, 4, 843-850.

Young, J.R. and Bown, P.R. 1997. Cenozoic calcareous nannoplankton classification. Journal of Nannoplankton Research, 19, 36-47.

Young, J.R. and Henriksen, K. 2003. Biomineralization within vesicles: the calcite of coccoliths. In: Dove, P.M., de Yoreo, J.J. and Weiner, S. (Eds.), Biomineralization. Reviews in Mineralogy and Geochemistry, 54, 189-215.

Young, J.R., Didymus, J.M., Bown, P.R., Prins, B. and Mann, S. 1992. Crystal assembly and phylogenetic evolution in heterococcoliths. *Nature*, 356, 516-518.

Young, J.R., Bown, P.R. and Burnett, A. 1994. Palaeontological perspectives. In: Green, J.C. and Leadbeater, B.S.C. (Eds.), The Haptophyte Algae. The Systematics Association Special Volume 51. Clarendon Press, Oxford, 379-392.

Young, J.R., Bergen, J.A., Bown, P.R., Burnett, J.A., Fiorentino, A., Jordan, R.W., Kleijne, A., van Niel, B.E., Romein, A.J.T. and von Salis, K. 1997. Guidelines for coccolith and calcareous nannofossil terminology. Palaeontology, 40, 875-912.

Young, J.R., Davis, S.A., Bown, P.R. and Mann, S. 1999. Coccolith ultrastructure and biomineralization. Journal of Structural Biology, 126, 195-215.

Young, J.R., Geisen, M., Cros, L., Kleijne, A., Sprengel, C., Probert, I. and Østergaard, J. 2003. A guide to extant coccolithophore taxonomy. Journal of Nannoplankton Research, Special Issue 1, 1-125.

Young, J.R., Geisen, M. and Probert, I. (in press). A review of selected aspects of coccolithophore biology with implications for palaeobiodiversity estimation. Micropaleontology.

Ziveri, P., Rutten, A., de Lange, G.J., Thomson, J. and Corselli, C. 2000. Present-day coccolith fluxes recorded in central eastern Mediterranean sediment traps and surface sediments. Palaeogeography, Palaeoclimatology, Palaeoecology, 158, 175-195.

CHAPTER 2

Reticulofenestra calicis n. sp., an unusual small reticulofenestrid coccolith from the Lower Pliocene of the South Caribbean Sea

Daniela Crudeli and Hanno Kinkel

Institute for Geosciences, Christian-Albrechts-Universität Kiel, Ludewig-Meyn-Str. 10, 24118 Kiel, Germany

Micropaleontology, 50, 4, 369-379, 2004

Reticulofenestra calicis n. sp., an unusual small reticulofenestrid coccolith from the Lower Pliocene of the South Caribbean Sea

Daniela Crudeli and Hanno Kinkel
Institute for Geosciences, Christian-Albrechts-Universität Kiel, Ludewig-Meyn-Str. 10, 24118 Kiel, Germany
email: dc@gpi.uni-kiel.de

ABSTRACT: A new, very small to small (2.4 to 4.6µm) reticulofenestrid coccolith, *Reticulofenestra calicis* n. sp., is described by scanning electron and light microscopy from the Lower Pliocene (Zone CN11 of Okada and Bukry 1980) of the South Caribbean Sea. The coccolith shows typical reticulofenestrid distal and proximal shields but the distal shield is surmounted by a cup-shaped structure formed from extensions of the inner and outer tube elements. A new genus is not introduced, although this structure is peculiar for reticulofenestrids. We base generic attribution on the distal shield morphology. The species occasionally has few slits between the distal shield elements. Attribution to the genera *Reticulofenestra* instead of *Pseudoemiliania* is discussed in detail.

R. calicis n. sp. is structurally similar to the modern *Emiliania huxleyi* var. *corona* and to *Reticulofenestra maceria.*

R. calicis n. sp., readily recognized under the light microscope in side view, has a short stratigraphic range. If the species proves not to be under strong ecological control, it will constitute a new biostratigraphic marker for subdivision of the *R. pseudoumbilicus* Zone.

INTRODUCTION

Coccoliths of the family Noelaerhabdaceae Jerkovic 1970 emend. Young and Bown 1997b are dominant forms among Late Eocene through Quaternary calcareous nannofossil assemblages (Perch-Nielsen 1985). Important modern genera include *Emiliania* Hay and Mohler in Hay et al. 1967 and *Gephyrocapsa* Kamptner 1943 (e.g., Okada and McIntyre 1977). They constitute a structurally homogeneous and phylogenetically related group (Romein 1979, Backman 1980, Perch-Nielsen 1985, Young 1989, Young et al. 1992, Young 1998). The stem genus, *Reticulofenestra* Hay, Mohler and Wade 1966 emend. Gallagher 1989 most likely evolved from *Toweius* Hay and Mohler 1967 in the early Eocene through a progressive modification of the coccolith ultrastructure (Romein 1979, Young et al. 1992). Coccoliths of this family are structurally similar and termed reticulofenestrids (Young 1989, Young et al. 1997).

The Pliocene reticulofenestrid group has been studied in detail by Backman (1980) from DSDP Atlantic cores and by Driever (1988) from Mediterranean land sections. In particular, Backman (1980) proposed the distinction of very small to small (<3µm, 3-5µm, Young et al. 1997) reticulofenestrids by LM (light microscope) and these concepts are successfully applied in both biostratigraphic and paleoceanographic studies with slight modifications (e.g., Kameo and Sato 2000, Okada 2000, Marino and Flores 2002). Detailed studies on size variability of Pliocene reticulofenestrids have been conducted by Young (1990, Indian Ocean and Red Sea), Takayama (1993, Equatorial Pacific), Kameo and Takayama (1999, North Atlantic) and Kameo and Bralower (2000, Caribbean Sea).

Light microscopy studies often prohibit the observation of fine scale morphological variability of very small to small forms.

In the course of a high resolution quantitative SEM (scanning electron microscope) analysis of calcareous nannofossils from the Lower Pliocene of the South Caribbean Sea we have observed a previously undescribed very small to small reticulofenestrid species. We describe it formally here, discuss its generic affiliation and potential stratigraphic usefulness.

Reticulofenestrids

Morphological and structural aspects of Late Eocene to Recent species of the Noelaerhabdaceae have been reviewed by Young (1989) who introduced the term reticulofenestrids for these coccoliths. These constitute of 6 cycles of elements, the distal and proximal shield, the inner and outer tube with opposite imbrication (anticlockwise and clockwise, respectively), the central area structures and the cover plate which, in Neogene forms, is substituted by a rising collar around the central area. The discrete elements composing those cycles are formed by a crystal unit with approximately radial c-axis, the so called R-unit (Young 1989, Young et al. 1992). Investigation on *Emiliania huxleyi* (Lohmann 1902) Hay and Mohler in Hay et al. 1967 ultrastructure revealed the presence of a vestigial unit with approximately vertical c-axis, V-unit (Young et al. 1992, Young et al. 1999).

MATERIALS AND METHODS

The species described in this work has been observed from the Lower Pliocene from cores of the South Caribbean Basin (ODP Leg 165, Site 1000A, latitude 16°33.223'N longitude 79°52.044'W, 916m water depth) (Sigurdsson, Leckie, Acton et al. 1997). The interval investigated is composed of homogeneous, moderately bioturbated light grey and grey foraminiferal bearing nannofossil ooze (Sigurdsson, Leckie, Acton et al. 1997).

Samples for SEM study have been prepared following the method of Andruleit (1996). An amount of 0.1g of dry sediment was diluted with carbonate-saturated tap water and the solution divided with a rotary splitter device. A final solution with 0.001g of sediment was filtered with a low-pressure vacuum

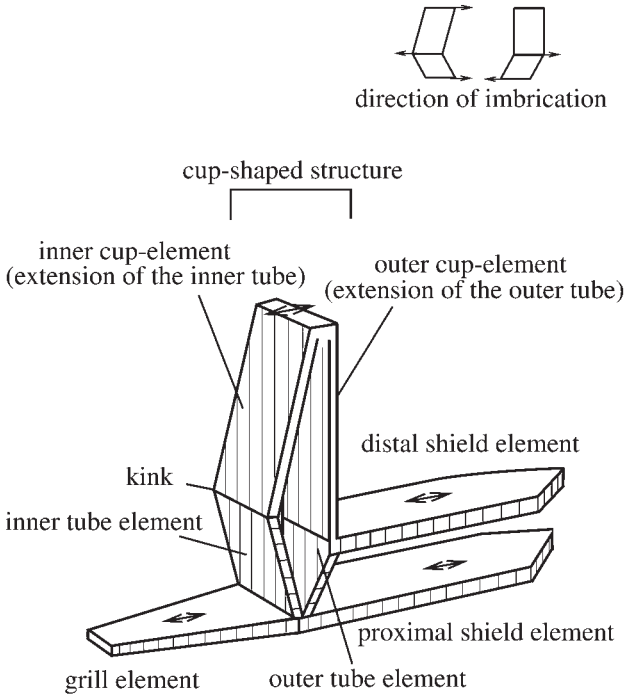

TEXT-FIGURE 1
Reticulofenestra calicis n. sp., schematic drawing of a segment showing the main discrete elements. The drawing is adapted from Young (1989, his fig. 1.6).
Up to the level of the distal shield the inner tube is anticlockwise imbricate (pl. 2, fig. 3). Up to this level the outer tube is clockwise imbricate. Clockwise imbrication of the outer tube is commonly visible on broken or etched reticulofenestrids (e.g., Young 1989, Young et al. 1992). The inner tube changes direction of imbrication (kink) and extends upward (pl. 2, fig. 3) (inner cup-element). From the outside, no kink is visible. A cycle of vertically oriented elements is visible (pl.1, figs. 3, 5). This indicates that the outer tube element changes direction of growth at the level of the distal shield and extends upward. The sketch on the upper right side of the panel shows the imbrication direction of the inner and outer tube elements and of the inner and outer cup-elements. The small arrows indicate the radial c-axis of the R-unit (Young et al. 1992). For simplification, the V-unit is omitted.

pump onto a polycarbonate-membrane filter (pore size, 0.40µm; diameter, 50mm). Species inventory was conducted at a magnification of 6.000x using a CamScan 44. Detailed morphological observation of the new species required magnification of 20.000x.

The size range given here is based on numerous measurements at 20.000x magnification from samples at about 10cm resolution encompassing the entire stratigraphic distribution of the species. Details on measurements are given in the follow, the number of specimens measured per sample are given in brackets. The length and width range of the species is based on 101 measurements (1 to 9 specimens). A cup-shaped structure, described thereafter, often obscured the outer part of the rim. For description purposes, the size has been additionally measured on broken and/or etched forms and in proximal view. 134 specimens were measured in this view (1-10 specimens). The length and width of the cup-shaped structure is based on 401 measurements in distal view (4 to 20 specimens). On 337 specimens in side view we measured the height, from the distal shield level, of the cup-shaped (1 to 20 specimens). On the same specimens, in this view, we measured the length of the structure. These values correspond or do not to the maximum length of the cup-shaped structure in distal view due to the difficulty in evaluating true side view orientation. The cup-shaped structure is weakly flaring, its length roughly approximates the length of the distal shield.

The stratigraphic distribution of the species was determined by high resolution SEM quantitative analyses of the calcareous nannoflora from the 138.45mbsf to118.25 mbsf sedimentary interval (Crudeli et al. in prep.) coupled with extensive SEM examination of samples close to the boundary intervals of the occurrence.

For light microscoscopy, a Leitz Orthoplan polarizing microscope was used at 1000x magnification. Smear slides were prepared following standard preparation techniques and using Norland Optical Adhesive. The LM images illustrated in plate 3 were acquired using a Wild MPS 52 connected photo camera.

The description of the species is based on the nomenclature of Young et al. (1997).

Details of the specimens illustrated in plates 1-3 are given in figure captions.

The samples on which this study is based are stored in the ODP Microfossil Reference Centre in Basel (see plate captions for details).

SYSTEMATICS

The higher systematic position of the species follows Young and Bown (1997a, b) and Young et al. (2003).

Kingdom CHROMISTA Cavalier-Smith 1981
Division (Phylum) HAPTOPHYTA Hibberd 1972 ex Cavalier-Smith 1986
Class PRYMNESIOPHYCEAE Hibberd 1976
Subclass PRYMNESIOPHYCIDAE Cavalier-Smith 1986
Order ISOCHRYSIDALES Pascher 1910 emend. Edvardsen and Eikrem 2000 in Edvardsen et al. 2000
Family NOELAERHABDACEAE Jerkovic 1970 emend. Young and Bown 1997b
Genus *Reticulofenestra* Hay, Mohler and Wade 1966 emend. Gallagher 1989 = Genus *Apertaperta* Hay, Mohler and Wade 1966.
Type species *Reticulofenestra caucasica* Hay, Mohler and Wade 1966

Reticulofenestra calicis Crudeli and Kinkel **n. sp.**
Plate 1; plate 2, figures 1-5

Etymology: from Latin *calix, calicis* (masculine noun) = cup, referring to the cup-shaped structure surrounding the central area

Holotype: plate 2, figure 1

Type locality: South Caribbean Sea, ODP Hole 1000A (16°33.223´N 79°52.044´W)

Type level: ODP Sample 1000A-15H-4, 95-97cm (132.25mbsf)

Paratypes: plate 1; plate 2, figures 2-5

Depository: ODP Microfossil Reference Center, Basel

Stratigraphic range: Lower Pliocene, *R. pseudoumbilicus* Zone, Zone CN11 of Okada and Bukry (1980)

SCANNING ELECTRON MICROSCOPE EXAMINATION

Diagnosis

Very small to small reticulofenestrid coccolith (2.4 to 4.6µm) with a cup-shaped structure surmounting the distal shield and surrounding the central area. The cup-shaped structure consists of an inner and an outer cycle of elements (inner cup-element and outer cup-element cycle). The inner cup-elements are clockwise imbricate and are continuous with the inner tube elements that are anticlockwise imbricate till the level of the distal shield. The outer cup-elements extend vertically. In distal view the cup-shaped structure totally obscures the outer part of the coccolith rim, more rarely, the outer 0.1 to 0.5µm of the rim width are visible.

Description

Shields and central area

The coccoliths of this species are constituted by two broadly to normally elliptical shields convex distally and concave proximally with a slightly outward sloping rim (pl. 1, figs. 3-6, pl. 2, figs. 3, 5). The length of the distal shield ranges from 2.4-4.6µm (average 3.2µm) that is slightly larger than the proximal shield (pl. 1, figs. 3-6). The width of the coccoliths varies between 1.9-4.0µm (average 2.5µm). The distal and proximal shields are formed from approximately 30-45 elements, with weak sinistral obliquity. The distal shield elements can be closely spaced (pl. 2, figs. 1) or separated by a few, relatively narrow and irregularly spaced slits (pl. 2, figs. 2, 4). Qualitative observations indicate that specimens of *R. calicis* n. sp. without slits are more common. The central area is wide (pl. 1, figs. 1-2, pl. 2, fig. 2) and is characterized by a grill composed of thin bars that are conjunct with the proximal shield elements (pl. 1, fig. 3). Often, bars end inwards with a small protrusion (pl. 1, fig. 1, pl. 2, fig. 1).

Cup-shaped structure

Structure, morphology, remarks

A schematic drawing of the cup-shaped structure described and interpreted thereafter is presented in text-figure 1. The sketch is adapted from Young (1989, his fig. 1.6). A single segment is represented here.

From the inside, the inner tube elements are anticlockwise imbricate till approximately the level of the distal shield, the inner cup-elements show clockwise imbrication (pl. 2, figs. 3-4). A kink just above the distal shield level marks the difference in growth direction of the inner tube and inner cup-elements (pl. 2, figs. 3-4). From the outside, cup-elements simply grow vertically, they do not show imbrication, and the kink is not visible (pl. 1, figs. 3, 5-6). This suggests that the outer cup-elements are composed by the extension of the outer tube elements. The shields of *R. calicis* n. sp. show the typical reticulofenestrid morphology and structure and imply that the outer tube elements have clockwise imbrication.

The cup-shaped structure is thus composed by extension of the inner and outer tube elements that have changed growth direction at the level of the distal shield.

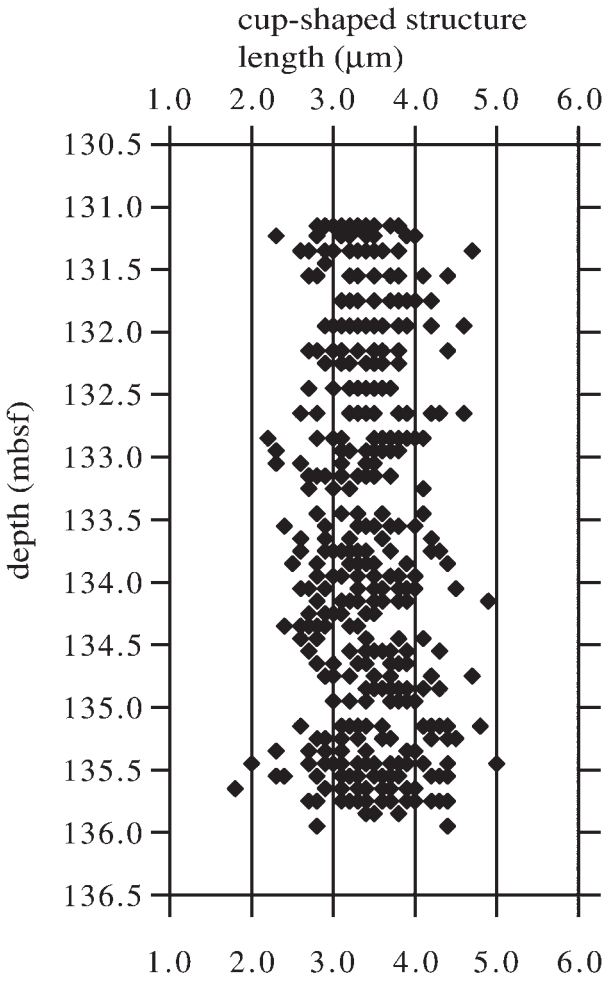

TEXT-FIGURE 2
Reticulofenestra calicis n. sp., length of the cup-shaped structure measured in distal view by SEM. The LM image of *R. calicis* n. sp. reflects the size of the cup-shaped structure which roughly approximate the size of the coccolith.

The opposite imbrication of the inner and outer tube elements inhibits their fusion under condition of diagenetic secondary calcification (Young 1989). The absence of imbrication of the outer cup-elements likely has favored fusion between the inner and outer cup-elements. The fusion of the cup-elements is visible in side view on broken coccoliths (pl. 2, fig. 3).

The terminations of the cup-elements appear broadly enlarged outwards, likely in relation to elements fusion (pl. 1, figs. 1-2, pl. 2, fig. 2).

Etching and/or breakage occurs close to the level at which the tube elements change imbrication (pl. 2, fig. 2). The level represents a structural weakness. Etching and/or breakage also occurs just above this level which is possibly due to structural weakness of the cup-element (pl. 2, fig. 2). The outer cup-elements usually show regular crystal faces, occasionally crystal faces appear more irregular in proximity to the distal shield (pl. 1, figs. 3, 5). The irregular surface possibly corresponds to the previous structural weakness.

The length and width of the cup-shaped structure range from 1.8-5.0µm and 1.4-4.2µm (text-figs. 2-3), respectively resulting in a broad to narrow elliptical shape.

In most cases, the cup-shaped structure obscures the outer part of the rim (pl. 1, fig. 1, pl. 2, fig. 2). Occasionally, the cup-shaped structure is weakly smaller than the rim (pl. 1, fig. 2). The cup-elements are enlarged upward, show equal height and are inclined outwards at low but variable angle (15°-35°) with respect to vertical direction (pl. 1, figs. 5-6, pl. 2, fig. 3). The number of cup-elements range from 32-46. In reticulofenestrids, the number of elements composing the different cycles is identical (Young 1989). This is related to biomineralization mechanisms (e.g., Young 1989, Young et al. 1999). On the same specimens we occasionally counted a larger number of cup-elements (1 to 5) with respect to distal shield elements. This is explained by difficulties of counting, in distal view, shield elements of specimens with cup-shaped structure very weakly smaller than the rim.

The height of the cup-shaped structure ranges from 0.7-3.5µm (average 1.4µm). The plot of the height and length of the structure measured in side view shows that the height is not directly related to coccolith size (text-fig. 3).

LIGHT MICROSCOPE EXAMINATION

Description and remarks

In side view and under CN (crossed nicols) the species has a sub-polygonal profile. The outer parts are birefringent whereas the central part shows no birefringence (pl. 3, figs. 1-3). The coccolith shows identical extinction pattern at 45° to the nicols. This indicates that the cycles have optical continuity with sub-radial crystallographic c-axes (text-fig. 1).

The species is often not entirely observable in true side view but variably tilted with respect to the horizontal plain, or broken (pl. 3, figs. 4-5). During routine work the coccolith could be misidentified as a fragment of a different species.

In distal view and CN the coccolith appears as a small bright elliptical ring with defined outer margins and having a wide central area (pl. 3, figs. 6-7). Using deep focusing in CN and transmitted light, the cup-shaped structure is identifiable by the irregularity of its profile. The species shows radial extinction.

The bright part of the coccolith in distal view is due to the cup-shaped structure, which is relatively high and thick. Since the structure is flaring, the central area of the species is wider when compared to other small reticulofenestrids.

BIOSTRATIGRAPHIC POSITION

R. calicis n. sp. is rare to common at OPD Site 165-1000A in the interval from Sample 15H-7, 15-17cm (135.95mbsf) where it is rare to Sample 15H-3, 135-137cm (131.15mbsf). This sample interval belongs to Zone CN11 of Okada and Bukry (1980) (Kameo and Bralower 2000) (4.335 MA-4.200 Ma, Steph et al., submitted). A few broken species of *R. calicis* n. sp. are observed in a few samples just above the 131.15mbsf level.

DISCUSSION ON TAXONOMY

Family attribution

The relationship between the LM extinction pattern in CN and reticulofenestrid structure has been discussed at length (Romein 1979, Driever 1988, Young 1989, Young et al. 1996). The CN study indicates that the cycles of *R. calicis* n. sp. have optical continuity with sub-radial crystallographic c-axes (e.g. pl. 3, figs. 1-3). This ultrastructure is typical for reticulofenestrids (Young 1989, Young and Bown 1991, Young et al. 1992) and allows to refer the coccolith to the family Noelaerhabdaceae.

Generic attribution

The composite cup-shaped structure is undescribed in reticulofenestrids, the extension of the outer tube elements represents a novelty. *R. calicis* n. sp. could have been used in emendation of a new genus of the Noelaerhabdaceae.

Coccoliths in which few inner tube elements are modified to form a bridge spanning the central area are included in *Gephyrocapsa.* The morphology of the bridge varies and represents a basic feature in definition of species (e.g., Pirini Radrizzani and Valleri 1977, Samtleben 1980, Lohman and Ellis, 1981). The modern *Gephyrocapsa ornata* Heimdal 1973 is characterized by a bridge formed from two thin plates and by a ring of low tooth-like protrusions continuing with the central tube. In this species, both the inner tube elements forming the tooth-like protrusions and those forming the bridge can show very different directions of growth even on a single coccosphere (Young, written communication, 2003). In species of *Gephyrocapsa*, growth occurs preferentially inward and commonly few inner tube elements are modified, which makes a major difference compared to *R. calicis* n. sp.

The genus of the Noelaerhabdaceae, *Bekelithella* Bona and Gal 1985 described from the Paratethys (Late Miocene, Pannonian) includes coccoliths with a crown surrounding the central area. *Bekelithella*, as the Paratethys genus *Noelaerhabdus* Jerkovic 1970 are endemic (Young 1998).

R. calicis n. sp. has a typical reticulofenestrid rim. This represents a useful base for generic attribution. *R. calicis* n. sp., may or may not have a few slits between elements of the distal shield (pl. 2, figs. 2 and 1, respectively). Presence or absence of slits between elements of the distal shield is generic character of *Pseudoemiliania* Gartner 1969 and *Reticulofenestra*, respectively. Among Pliocene small reticulofenestrids there is a continuous variation from elliptical forms with a variable number of slits to elliptical forms without slits to sub-circular forms with many slits (McIntyre et al. 1967, Samtleben 1978, Young 1989, Young 1990, pers. observations) which have prompted discussion about the validity of separating such forms into different genera (Samtleben 1978, Young 1989, Young 1990). In particular, Young (1990) argued that the variability observed in the small Pliocene reticulofenestrids could represent an example of an "allometric relationship between coccolith size and morphology within a single species". In his emended taxonomic scheme, Young (1990) therefore included specimens with "lacunosa" morphology in the genus *Reticulofenestra.*

The fact that specimens of *R. calicis* n. sp. with or without slits are present in the same samples and throughout the same stratigraphic interval suggests that they represent a single species characterized by intraspecific variation. Whereas for recent reticulofenestrids, e.g. *E. huxleyi* and *G. oceanica* Kamptner 1943 an ample intraspecific variability is established (e.g. Young and Westbroek 1991, Bollman 1997), it is not yet clear how much intraspecific variability occurs within the Pliocene reticulofenestrids. On the other hand, the fact that small placoliths with or without slits can develop a similar structure around the central area supports the suggestion by previous au-

thors (Samtleben 1978, Young 1989, Young 1990) regarding affiliation of closely similar forms to due different genera.

Similarity with other medium size reticulofenestrids

Medium size reticulofenestrid coccoliths with a protruding collar were observed by Driever (1988) from the Mediterranean Pliocene (his pl. 2, figs. 7-8). Similar forms were observed by us within the interval of occurrence of *R. calicis* n. sp. (pl. 2, fig. 6). Driever (1988) referred the coccolith to *R. pseudoumbilicus* (Gartner 1967) Gartner 1969 small specimens. Given absence of formal description of such coccoliths, in this work we adopted the nomenclature by Driever (1988). The species (Driever 1988, his pl. 2, figs. 7-8, this work, pl. 2, fig. 6) has bars joining along a median suture as in the original description of Gartner (1967).

In these coccoliths, the collar is composed by extension of inner tube elements that show anticlockwise imbrication, occasionally, the upper part of very few elements shows a kink that suggests a change of imbrication (pl. 2, fig. 6). The kink occurs well above the distal shield (pl. 2, fig. 6) and not at the distal shield level as in *R. calicis* n. sp. In addition, *R. calicis* n. sp. has a narrower rim so that, in distal view, the outer part of the rim is not or only slightly visible.

R. pseudoumbilicus is mainly a size defined group. Forms >7µm are of biostratigraphic significance (e.g., Young 1998 and references therein). *R. pseudoumbilicus* small specimens demonstrate phenetic variability among the medium size reticulofenestrid coccoliths. The phylogeny of *R. calicis* n. sp. is discussed in a separate manuscript (Crudeli et al., in prep.).

Structural similarity with recent reticulofenestrid coccolithophores

The tendency in elevation of the inner tube elements is characteristic of a few modern species. In these forms, the inner tube elements do not change direction of imbrication and the extension of the outer cycle elements is not described.

In *Emiliania huxleyi* var. *corona* (Okada and McIntyre 1977) Jordan and Young 1990 the inner tube elements variably extend upwards above the level of the distal shield forming a crown around the central area. According to the original description of *E. huxleyi* var. *corona* the wall only occasionally surrounds the central area at uniform height whereas in the species described here, the cup-shaped structure is continuous around the central area.

Also *Rericulofenestra maceria* (Okada and McIntyre 1977) Young et al. 2003, originally assigned to *Umbilicosphaera* Lohmann 1902, has a crown around the central area with more conspicuous elements along the long axis and depressed elements along the short axis. *R. maceria* has been observed from the North Atlantic (Pleistocene) by Martini (1993) (*Emiliania coronata,* pro syn.) who noted that elements were depressed at two sides diagonally oriented to the long axis of the coccoliths.

PALEOECOLOGY – EVOLUTION

There are no indications that endemism occurs among calcareous nannoplankton in the studied interval in the Caribbean Sea (Gartner et al. 1983/84, Garner et al. 1987, Kameo and Sato 2000, Kameo and Bralower 2000). The Caribbean had open connections to the Atlantic and Pacific Oceans during the Pliocene, since the Isthmus of Panama was not yet closed (e.g., Haug et al. 2001), during the occurrence of *R. calicis* n. sp.

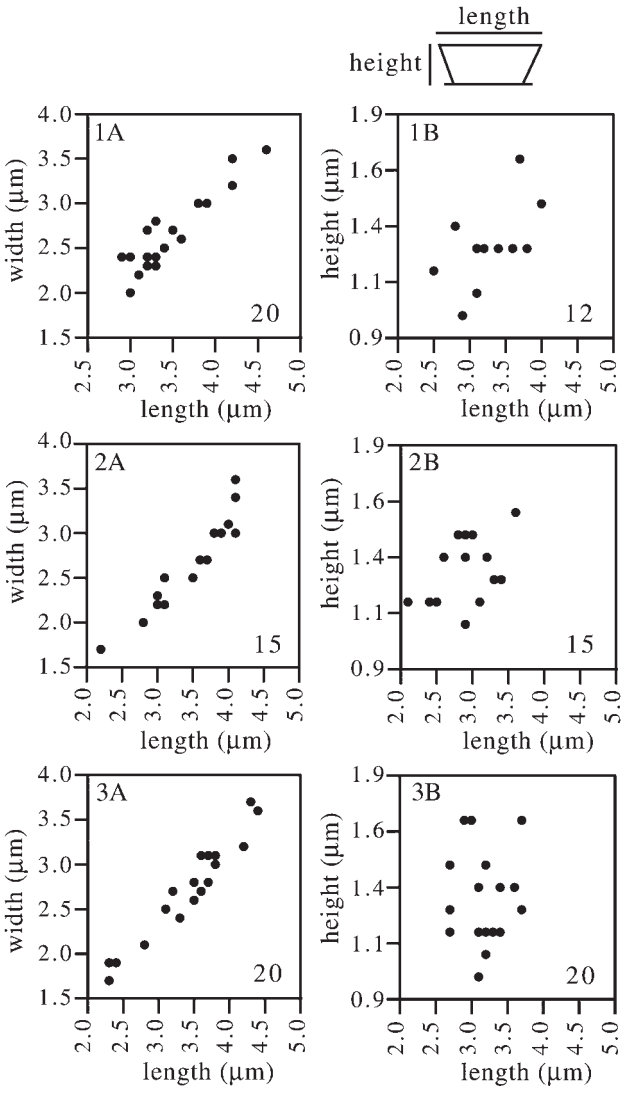

TEXT-FIGURE 3
Morphological variability of *Reticulofenestra calicis* n. sp. whitin the same sample. Tree samples are selected from its stratigraphic range. A - plots of the length versus width of the cup-shaped structure measured in distal view by SEM. B - plots of the length versus height of the cup-shaped structure measured in side view. The number on the low right side of each panel refers to the number of specimens measured. 1– Sample 1000A 15H-4, 65-67cm (131.95mbsf), 2- Sample 1000A 15H-5, 5-7cm (132.85mbsf) 3- Sample 1000A 15H-6, 125-127cm (135.55 nmbsf).

Endemism tends to occur in semi-enclosed basins. Moreover, *R. calicis* n. sp. occurs in samples from the Eastern Equatorial Pacific (Crudeli et al., in prep.), which had very different paleoceanographic and ecologic boundary conditions.

Young (1989), describing coccolith biomineralization, discussed the possibility that processes such as the cup-shaped structure discussed here are formed by modification of the single crystal unit in a final phase of its development, thus unrelated with the basic coccolithogenesis process, and are likely a result of ecological adaptation. The fact that the tube elements in *R. calicis* n. sp. extend and change direction of imbrication upwards is in agreement with this suggestion.

The occurrence of *R. calicis* n. sp. is almost coeval with the FCO of small *Gephyrocapsa* in the site studied and both events follow the FO of *Pseudoemiliania*. Other small reticulofenestrids show variable extension of the tube elements during the critical time interval (Crudeli et al. in prep.). This points towards a general diversification and evolutionary changes among reticulofenestrids during this period. The short range of *R. calicis* n. sp. (5m) indicates that this coccolith was not as successful as the species of *Gephyrocapsa* and *Pseudoemiliania* which became dominant elements of nannofossil assemblages shortly after their appearance (Gartner et al. 1983/84, Garner et al. 1987, Okada 2000, Kameo and Sato 2000, Marino and Flores 2002).

A new biostratigraphic marker?

The *R. pseudoumbilicus* Zone was introduced by Gartner (1969) from subtropical western Atlantic cores and defined as the interval from the LO of *Amaurolithus tricorniculatus* and the LO of *R. pseudoumbilicus*. The Zone was incorporated in the Standard Neogene Calcareous Nannofossil Zonation as Zone NN15 (Martini and Worsley 1970, Martini 1971) that correlates with the CN11 Zone of Okada and Bukry (1980).

The beginning of the *Discoaster asymmetricus* acme is of biostratigraphic significance for subdivision of Zone CN11 (Bukry 1973, Bukry 1975, Okada and Bukry 1980). The event is not always identifiable or the marker species is absent (e.g., Gartner et al. 1983/84, Garner et al. 1987, Sato et al. 1991, Takayama, 1993, Gartner and Shyu 1996). In addition, *D. asymmetricus* is often difficult to distinguish from other similar forms (Perch-Nielsen 1985). In the Caribbean Basin, Kameo and Bralower (2000) recognized the FCO of *D. asymmetricus* in Hole 998A but not in Hole 1000A and in Hole 999A.

R. calicis n. sp. has a short stratigraphic range (4.335 Ma-4.200 Ma) within the *R. pseudoumbilicus* Zone. The age range was achieved by orbital tuning of high resolution stable oxygen and carbon isotope records of planktic foraminifera (Steph et al., submitted).

If *R. calicis* n. sp. proves not to be strictly ecologically controlled it could represent a new biostratigraphic marker for subdivision of the *R. pseudoumbilicus* Zone.

CONCLUSIONS

A new distinctive reticulofenestrid coccolith, *R. calicis* n. sp., has been described from the Lower Pliocene of the South Caribbean Sea. The species is distinguishable from other reticulofenestrids of similar size because of a composite flaring structure surrounding the central area, the cup-shaped structure. This is composed by an inner and an outer cycle of elements (inner and outer cup-element) continuous with the inner and outer tube elements. The outer cup-element cycle represents a structural novelty in reticulofenestrids.

R. calicis n. sp., shows a high phenotypic variability within the Lower Pliocene small reticulofenestrids. This was not previously recorded.

This new species indicates that the evolution of *Gephyrocapsa* and *Pseudoemiliania* is associated with the rise of other species and thus more complex than previously thought.

The short stratigraphic range of *R. calicis* n. sp., makes it a potential new biostratigraphic marker for subdividing the *R. pseudoumbilicus* Zone.

ACKNOWLEDGMENTS

We thank Ute Schuldt and Beate Bader for SEM assistance; Jeremy R. Young for discussion on structure of the species and on its relations with other reticulofenestrids, and for sending us unpublished micrographs of reticulofenestrids; Michael Knap-

PLATE 1

Figures 1-6, SEMs of *Reticulofenestra calicis* n. sp. in distal, proximal and side view.
The plate illustrates the size variability of the species. For each illustration in plates 1-2, the type of the species, ODP Sample, micrograph, negative, magnification and code of the SEM stub are given.

1 Distal view of a coccolith with preserved grill, the rim is obscured by the cup-shaped structure. Scale bar, 1µm. Paratype, Sample 1000A-15H-5, 5-7cm (132.85mbsf), 83097, 5262-31, 20.000x.

2 Distal view of a coccolith, the rim is partially visible. Scale bar, 1µm. Paratype, Sample 1000A-15H-4, 85-87cm (132.15mbsf), 83104, 5263-3, 20.000x.

3 Proximal view of a coccolith slightly inclined downwards on the right side with respect to the horizontal plain. The grill elements are conjunct with the proximal shield elements. Note the well developed crystal face of the outer cup-elements and the irregularity of their surface close to the distal shield. Scale bar, 1µm. Paratype, Sample 1000A-15H-5, 75-77cm (133.55 mbsf), 82430, 5241-22, 20.000x.

4 Proximal view of a coccolith showing the slightly different sizes of the proximal and distal shield. Scale bar, 1µm. Paratype, Sample 1000A-15H-5, 5-7cm (132.85mbsf), 83096, 5262-30, 20.000x.

5 Side view of a coccolith showing outer cup-elements extending vertically upward. The arrow indicates outer cup-elements with irregular crystal faces. Scale bar, 300nm. Paratype, Sample 1000A-15H-6, 95-97cm (135.25mbsf), 83116, 5263-15, 28.500x.

6 Side view of a coccolith showing that outer cup-elements extend upward vertically. Scale bar, 1µm. Paratype, Sample 1000A-15H-6 , 95-97cm (135.25mbsf), 83001, 5260-6, 20.000x.

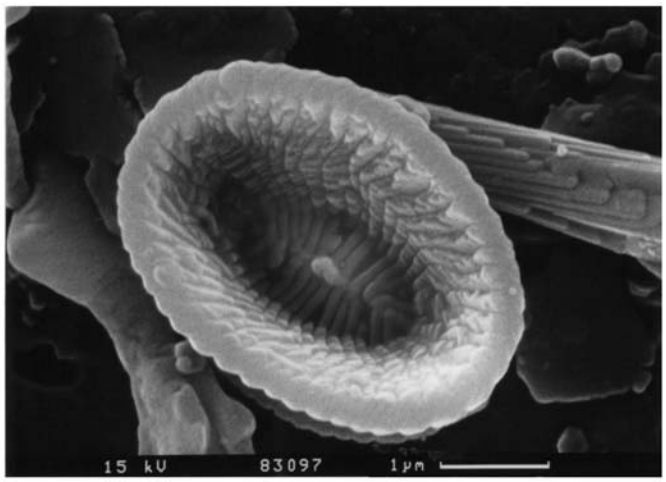
15 kV 83097 1µm

1


15 kV 83104 1µm

2

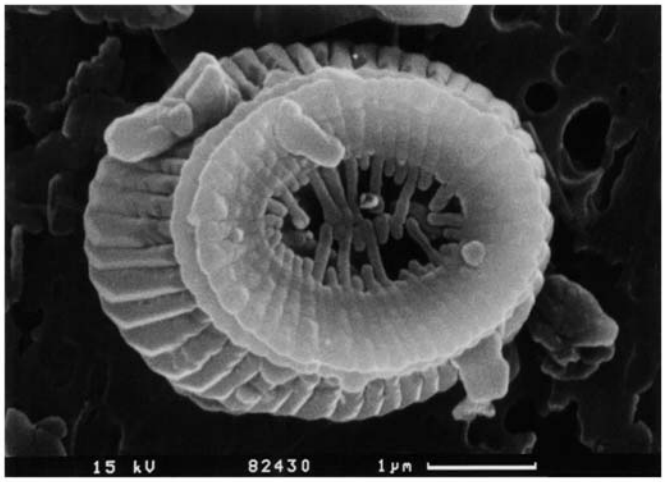
15 kV 82430 1µm

3

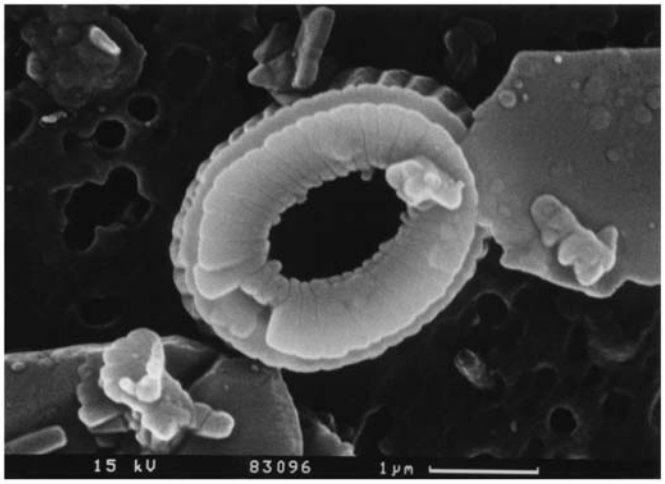
15 kV 83096 1µm

4

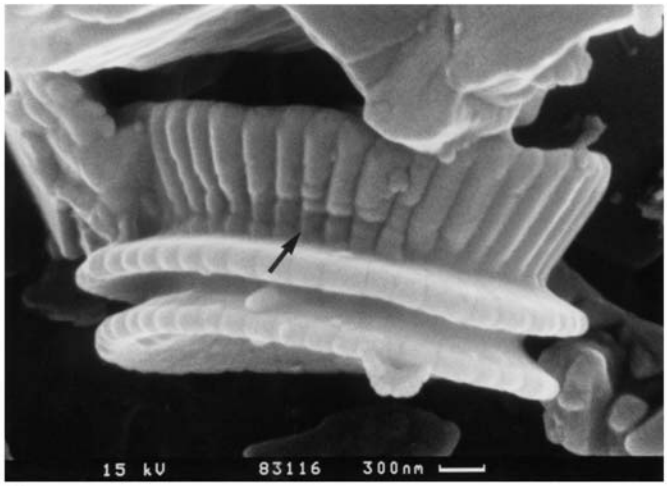
15 kV 83116 300nm

5

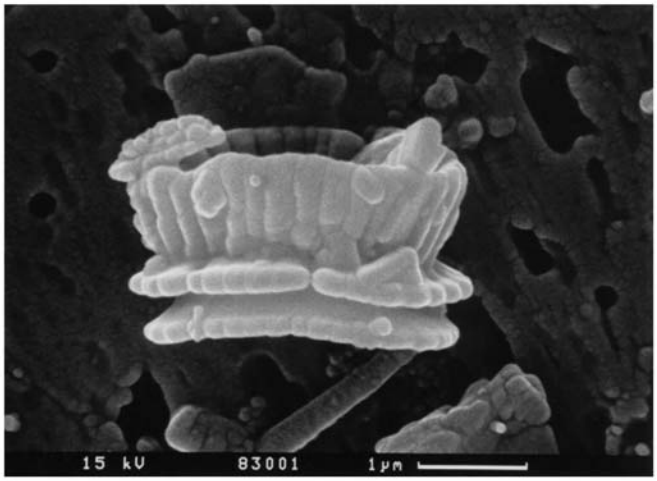
15 kV 83001 1µm

6

pertsbusch and Jeremy R. Young for their helpful suggestions in pre-reviewing the manuscript. Discussions with Priska Schäfer greatly increased the quality of the initial manuscript. We warmly thank two anonymous reviewers for useful comments that improved the final script. This research used samples provided by the Ocean Drilling Program (ODP). ODP is sponsored by the U.S. National Science Foundation (NSF) and participating countries under management of Joint Oceanographic Institutions (JOI), Inc. Funding for this research was provided by Deutsche Forschungsgemeinschaft (DFG) Gateways Research Unit, Kiel University. This work represents a partial fulfilment of the requirements for the degree of Doctor of Natural Sciences at the University of Kiel for D. Crudeli.

REFERENCES

ANDRULEIT, H., 1996. A filtration technique for quantitative studies of coccoliths. *Micropaleontology*, 42(4): 403-406.

BACKMAN, J., 1980. Miocene-Pliocene nannofossil and sedimentation rates in the Hatton-Rockall Basin, NE Atlantic Ocean. *Acta Universitatis Stockholmiensis, Stockholm Contributions in Geology,* 36(1): 1-91.

BOLLMANN, J., 1997. Morphology and biogeographgy of *Gephyrocapsa* coccoliths in Holocene sediments. *Marine Micropaleontology,* 29: 319-350.

BUKRY, D., 1973. Low-latitude coccolith biostratigraphic zonation. *Initial Reports of the Deep Sea Drilling Project,* 15: 685-703.

———, 1975. Coccolith and silicoflagellate stratigraphy, Northwestern Pacific Ocean. *Initial Reports of the Deep Sea Drilling Project,* 32: 677-701.

DRIEVER, B.W.M., 1988. Calcareous nannofossils biostratigraphy and paleoenvironmental interpretation of the Mediterranean Pliocene. *Utrecht Micropalaeontological Bulletins,* 36: 1-245.

GARTNER, S., 1967. Calcareous nannofossils from Neogene of Trinidad, Jamaica, and Gulf of Mexico. The University of Kansas. *Paleontological Contributions,* 29: 1-7.

———, 1969. Correlation of Neogene planktonic foraminifera and calcareous nannofossil zones. *Transactions of the Gulf Coast Association of Geological Societies,* 19: 585-599.

GARTNER, S. and SHYU, J.-P., 1996. Aspects of calcareous nannofossil biostratigraphy and abundance in the Pliocene and Late Miocene of site 905. *Proceedings of the Ocean Drilling Program, Scientific Results,* 150: 53-62.

GARTNER, S., CHEN, M.P. and STANTON, R.J., 1983/84. Late Neogene nannofossils biostratigraphy and paleoceanography of the Northeastern Gulf of Mexico and adjacent areas. *Marine Micropaleontology,* 8: 17-50.

GARTNER, S., CHOW, J. and STANTON Jr., R.J., 1987. Late Neogene paleoceanography of the Eastern Caribbean, the Gulf of Mexico, and the eastern equatorial Pacific. *Marine Micropaleontology,* 12: 255-304.

HAUG, G.H., TIEDEMANN, R., ZAHN, R. and RAVELO, C.R., 2001. Role of Panama uplift on oceanic freshwater balance. *Geological Society of America,* 29(3): 207-210.

KAMEO, K. and TAKAYAMA, T., 1999. Biostratigraphic significance of sequential size variations of the calcareous nannofossil genus *Reticulofenestra* in the Upper Pliocene of the North Atlantic. *Marine Micropaleontology,* 37: 41-52.

KAMEO, K. and BRALOWER, T.J., 2000. Neogene calcareous nannofossil biostratigraphy of Sites 998, 999, and 1000, Caribbean Sea. *Proceedings of the Ocean Drilling Program, Scientific Results,* 165: 3-17.

KAMEO, K. and SATO, T., 2000. Biogeography of Neogene calcareous nannofossils in the Caribbean and the eastern equatorial Pacific-flo-

---

PLATE 2

Figures 1-5, SEMs of *Reticulofenestra calicis* n. sp. showing morphological and structural details.
Fig. 6, SEM of *Reticulofenestra pseudoumbilicus* small specimen (*sensu* Driever 1988).

1 Distal-oblique view of a coccolith with closely spaced distal shield elements 30° SEM tilt. Scale bar, 1µm. Holotype, Sample 1000A-15H-4, 95-97cm (132.25 mbsf), 83142, 5264-6, 20.000x.

2 Distal view of a coccolith with partially etched/broken cup-shaped structure. Etching and/or breakage occurs close to the level at which the inner tube elements change imbrication (right side), and above this level (left side). Few slits between elements of the distal shield are present. Scale bar, 1µm. Paratype, Sample 1000A-15H-5, 95-97cm (133.75mbsf), 82421, 5241-13, 20.000x.

3 Side view of a broken coccolith. The inner tube elements are sinistrally imbricate till the level of the distal shield (kink) whereas their upward extension (inner cup-elements) are dextrally imbricate. Scale bar, 1µm. Paratype, Sample 1000A-15H-6, 95-97cm (135.25mbsf), 83109, 5263-8, 20.000x.

4 Oblique-distal view of a broken coccolith. Note the kink close to the level of the distal shield. Few slits are present between elements of the distal shield. Scale bar, 1µm. Paratype, Sample 1000A-15H-5, 95-97cm (133.75mbsf), 82426, 5241-18, 18.000x.

5 View of three *R. calicis* n. sp. specimens in side (lower left side) and oblique-proximal view (centre and upper right side) Sample 1000A-15H-5, 95-97cm (133.75mbsf), 82420, 5241-12, 11.000x.

6 Distal view of *R. pseudoumbilicus* small specimens (*sensu* Driever, 1988). The collar elements are anticlockwise imbricate. The upward terminations of two elements of the collar (upper-right side of the image) show slightly different imbrication. The central area elements join along a median suture. Sample 1000A-15H-6, 115-117cm (135.45mbsf), 82827, 5254-16, 16.000x.


15 kV 83142 1µm

1

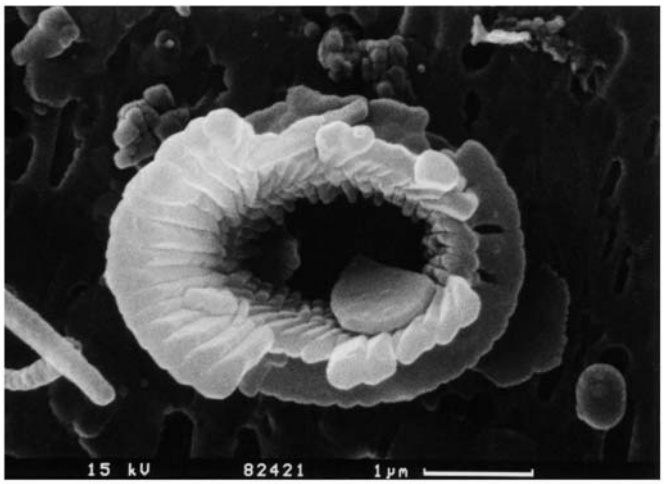
15 kV 82421 1µm

2

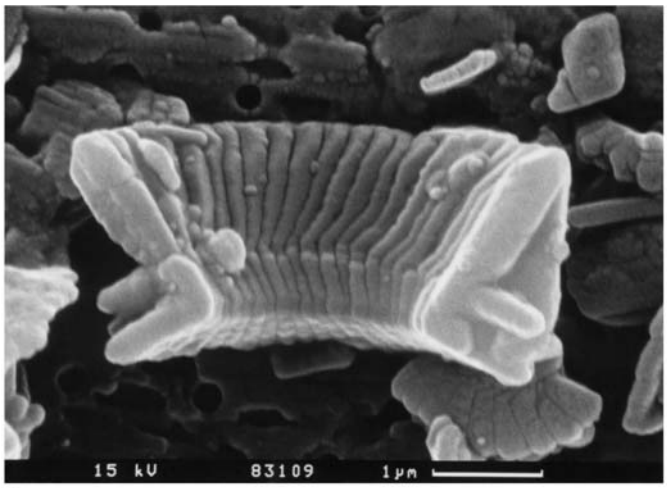
15 kV 83109 1µm

3

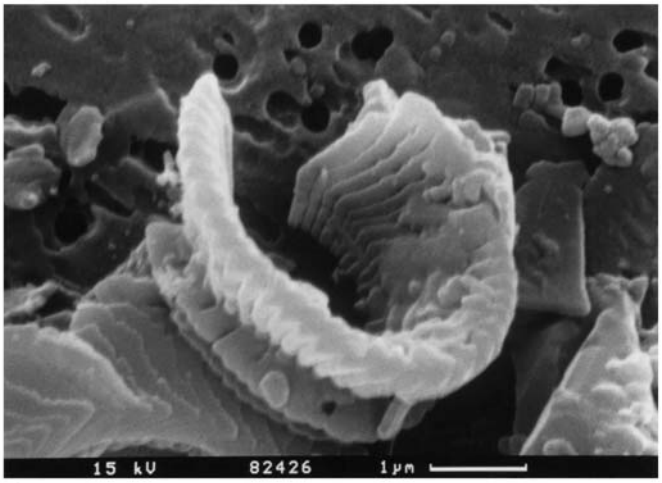
15 kV 82426 1µm

4

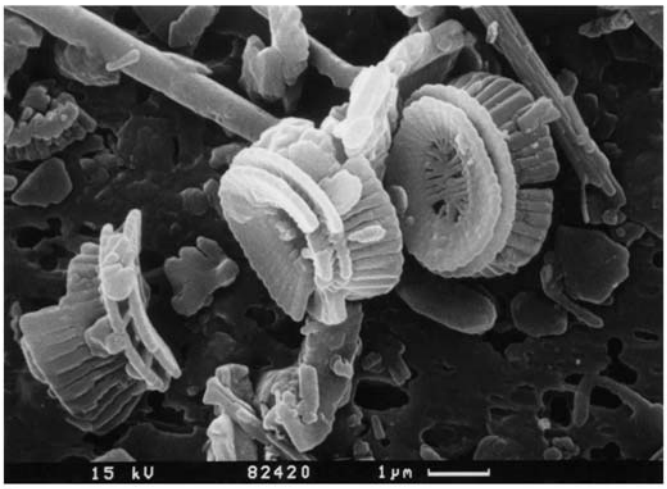
15 kV 82420 1µm

5

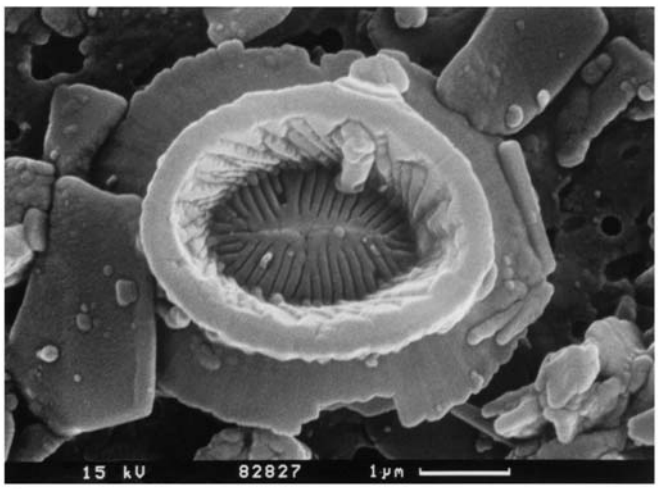
15 kV 82827 1µm

6

ral response to the emergence of the Isthmus of Panama. *Marine Micropaleontology,* 39: 201-218.

LOHMAN, W.H. and ELLIS, C.H., 1981. A new species and new fossil occurrences of calcareous nannoplankton in Eastern Mediterranean. *Journal of Paleontology,* 55(2): 389-394.

MARINO, M. and FLORES, J.A., 2002. Miocene to Pliocene calcareous nannofossil biostratigraphy at ODP Leg 177 Sites 1088 and 1090. *Marine Micropaleontology,* 45: 291-307.

MARTINI, E., 1971. Standard Tertiary and Quaternary calcareous nannoplankton zonation. In: Farinacci, A., Ed., Proceedings of the Second Planktonic Conference, Roma 1970. *Edizioni Tecnoscienza,* Roma, 2: 739-785.

———, 1993. *Emiliania coronata*, a new calcareous nannoplankton species from the North Atlantic Pleistocene. *Zitteliana*, 20: 87-92.

MARTINI, E. and WORSLEY, T., 1970. Standard Neogene calcareous nannoplankton zonation. *Nature*, 225: 189-290.

MCINTYRE, A., BÉ, A.W.H. and PREIKSTAS, R., 1967. Coccoliths and the Pliocene-Pleistocene boundary. *Progress in Oceanography,* 3: 3-25.

OKADA, H., 2000. Neogene and Quaternary Calcareous Nannofossils from the Blake Ridge, Sites 994, 995, and 997. *Proceedings of the Ocean Drilling Program, Scientific Results,* 164: 331-341.

OKADA, H. and MCINTYRE, A., 1977. Modern coccolithophores of the Pacific and North Atlantic Oceans. *Micropaleontology*, 23(1): 1-55.

OKADA, H. and BUKRY, D., 1980. Supplementary modification and introduction of code numbers to the low-latitude biostratigraphic zonation (Bukry, 1973; 1975). *Marine Micropaleontology,* 5: 321-325.

PERCH-NIELSEN, K., 1985. Cenozoic calcareous nannofossils. In: Bolli, H.M., Saunders, J.B. and Perch-Nielsen, K., Eds., *Plankton Stratigraphy.* Cambridge University Press, p. 427-554.

PIRINI RADRIZZANI, C. and VALLERI, G., 1977. New data on calcareous nannofossils from the Pliocene of the Tyrrhenian basin Site 132 DSDP, Leg 13. *Rivista Italiana di Paleontologia,* 83(4): 897-924.

ROMEIN, A.J.T., 1979. Lineages in Early Paleogene calcareous nannoplankton. *Utrecht Micropalaeontological Bulletins,* 22: 1-231.

SAMTLEBEN, C., 1978. Pliocene-Pleistocene coccolith assemblages from the Sierra Leone Rise - Site 366, Leg 41. *Initial Reports of the Deep Sea Drilling Project*, 41, Supplement to Volume 38, 39, 40 and 41: 913-931. Washinigton, DC: US Government Printing Office.

SAMTLEBEN, C., 1980. Die Evolution der Coccolithophoriden-Gattung *Gephyrocapsa* nach Befunden im Atlantik. *Paläontologische Zeitschrift,* 54(1/2): 91-127.

SATO, T., KAMEO, K., TAKAYAMA, T., 1991. Coccolith biostratigraphy of the Arabian Sea. *Proceedings of the Ocean Drilling Program, Scientific Results,* 117: 37-54.

SIGURDSSON, H. LECKIE, R.M., ACTON, G.D. et al., 1997. *Proceedings of the Ocean Drilling Program, Initial Reports,* 165: 231-289.

STEPH, S., TIEDEMANN, R., GROENEVELD, J., NURNBERG, D., REUNING, L., HAUG, G. (submitted). Changes in Caribbean surface hydrography during the Pliocene shoaling of the Central American Seaway. *Paleoceanography.*

TAKAYAMA, T., 1993. Notes on Neogene calcareous nannofossil biostratigraphy of the Ontong Java Plateau and size variations of *Reticulofenestra* coccoliths. *Proceedings of the Ocean Drilling Program, Scientific Results,* 130: 179-229.

YOUNG, J.R., 1989. Observations on heterococcolith rim structure and its relationship to developmental processes. In: Crux J. and van Heck S. E., Eds, *Nannofossils and their biostratigraphic applications.* Chichester: Ellis Horwood Limited, p. 1-20.

———, 1990. Size variation of Neogene *Reticulofenestra* coccoliths from Indian Ocean DSDP cores. *Journal of Micropaleontology,* 9: 71-85.

———, 1998. Neogene nannofossils. In: Bown, P.R., Ed*., Calcareous Nannofossil Biostratigraphy.* British Micropalaeontology Society Publications Series, Cambridge: Kluwer Academic Publisher, p. 225-265.

YOUNG, J.R. and WESTBROEK, P., 1991. Genotypic variation in the coccolithophorid species *Emiliania huxleyi*. *Marine Micropaleontology,* 18: 5-23.

YOUNG, J.R. and BOWN, P.R., 1991. An ontogenic sequence of coccoliths from the Late Jurassic Kimmeridge Clay of England. *Paleontology*, 34(4): 843-850.

———, 1997a. Higher classification of calcareous nannoplankton. *Journal of Nannoplankton Research,* 19: 15-20.

———, 1997b. Cenozoic calcareous nannoplankton classification. *Journal of Nannoplankton Research,* 19: 36-47.

YOUNG, J.R., DIDYMUS, J.M., BOWN, P.R., PRINS, B. and MANN, S., 1992. Crystal assembly and phylogenetic evolution in heterococcoliths. *Nature*, 356: 516-518.

YOUNG, J.R., KUCERA, M. and CHUNG, H.-W., 1996. Automated biometrics on captured light microscope images of coccolith of *E. huxleyi*. In: Moguilevsky, A. and Whatley, R., Eds., *Microfossils and Oceanic Environments.* University of Wales, Aberystwyth Press, p. 261-280.

YOUNG, J.R., BERGEN, J.A., BOWN, P.R., BURNETT, J.A., FIORENTINO, A., JORDAN, R.W., KLEIJNE, A., van NIEL, B.E., ROMEIN, A.J.T. and von SALIS, K., 1997. Guidelines for coccolith and calcareous nannofossil terminology. *Palaeontology*, 40: 875-912.

YOUNG, J.R., DAVIS, S.A., BOWN, P.R., MANN, S., 1999. Coccolith ultrastructure and biomineralisation. *Journal of Structural Biology,* 12: 195-215.

YOUNG, J.R., GEISEN, M., CROS, L., KLEIJNE, A., SPRENGEL, C. PROBERT, I. and ØSTERGAARD, J.B., 2003. A guide to extant coccolithophore taxonomy. *Journal of Nannoplankton Research,* Special Issue 1: 1-123.

Manuscript received December 21, 2003
Manuscript accepted August 3, 2004

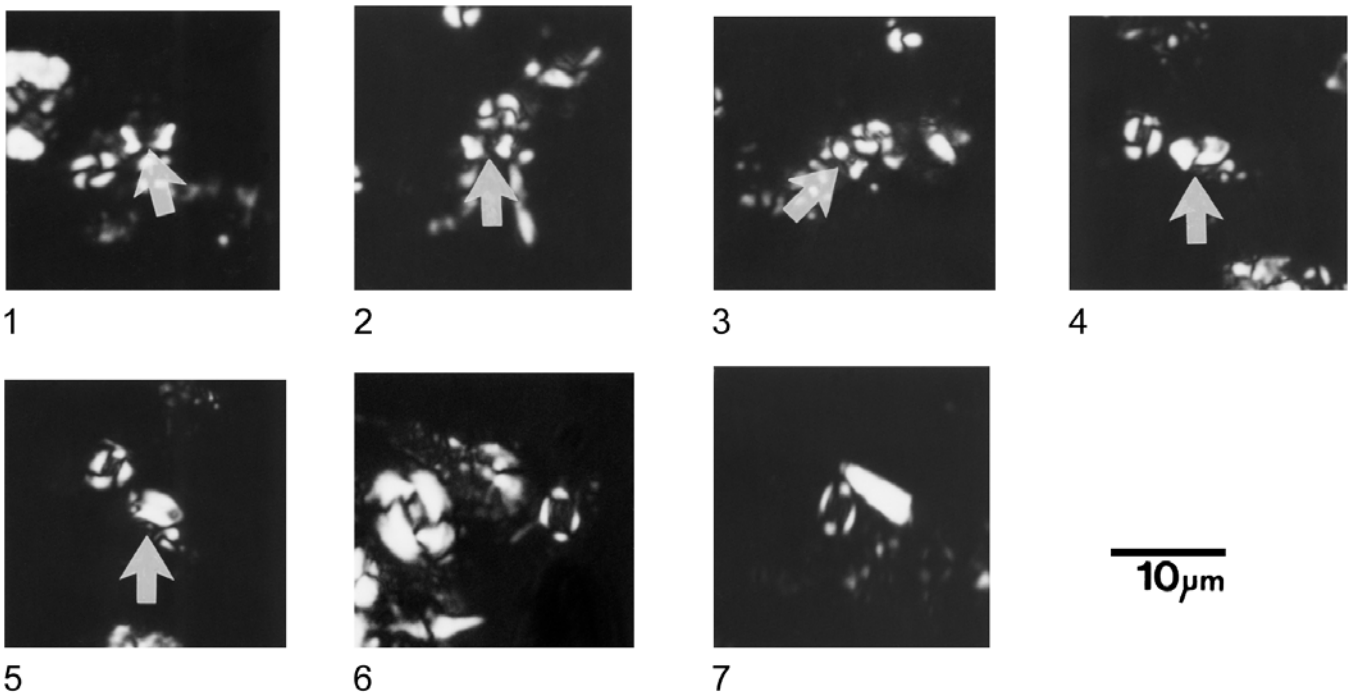

PLATE 3

Figures 1-7, LM images of *Reticulofenestra calicis* n. sp., CN. The black bar indicates the scale, the arrows indicate the specimens. For each illustration, the code of the ODP Sample is given.

1 Side view, parallel to the nicols. Note the sub-polygonal profile of the form. The outer parts of the coccolith are birefringent whereas the central part is not birefringent. Sample 1000A-15H-6, 105-107cm (135.35mbsf).

2 Side view, parallel to the nicols. The specimen is slightly larger then that in fig. 1, same plate. Sample 1000A-15H-5, 65-67cm (133.45mbsf).

3 View of the specimen illustrated in figure 2, at 30° to the nicols. At 45° to the nicols, the specimen shows similar profile (not illustrated). Sample 1000A-15H-5, 65-67cm (133.45mbsf).

4 View of a specimen tilted of about 45° from true side view. Sample 1000A-15H-5, 65-67cm (133.45mbsf).

5 View of the specimen illustrated in figure 4, at 30° to the nicols. Note the concomitant extinction of elements. Sample 1000A-15H-5, 65-67cm (133.45 mbsf).

6 Distal view, parallel to the nicols. Sample 1000A-15H-6, 105-107cm (135.35mbsf).

7 Distal view, at 5° to the nicols. Sample 1000A-15H-6, 105-107cm (135.35mbsf).

CHAPTER 3

Reticulofenestra alis n. sp., *R. pujosiae* n. sp. and *R. premoliae* n. sp., key-species in the reconstruction of the phylogeny of *Gephyrocapsa theyeri* and *R. calicis* (Coccolithophore, early Pliocene, South Caribbean).

Daniela Crudeli[1], Jeremy R. Young[2], and Hanno Kinkel[1]

[1]Institute for Geosciences, Christian-Albrechts-Universität Kiel, Ludewig-Meyn-Str. 10, 24118 Kiel, Germany

[2]Palaeontology Dept., Cromwell Road, The Natural History Museum, London SW7 5BD, UK

Manuscript to be submitted to Journal of Micropalaeontology

CHAPTER 3

Reticulofenestra alis n. sp., *R. pujosiae* n. sp. and *R. premoliae* n. sp., key-species in the reconstruction of the phylogeny of *Gephyrocapsa theyeri* and *R. calicis* (Coccolithophore, early Pliocene, South Caribbean)

DANIELA CRUDELI[1], JEREMY R. YOUNG[2] & HANNO KINKEL[1]

1Institute for Geosciences, Christian-Albrechts-Universität Kiel, Ludewig-Meyn-Str. 10, 24118 Kiel, Germany.

2Palaeontology Dept., Cromwell Road, The Natural History Museum, London SW7 5BD, UK.

ABSTRACT - Three new very small phylogenetically related reticulofenestrids, *Reticulofenestra alis* n. sp., *R. pujosiae* n. sp., and *R. premoliae* n. sp. are described from cores from the South Caribbean Basin (ODP Hole 1000A, early Pliocene). *R. alis* n. sp. and *R. premoliae* n. sp. include different morphotypes, we discuss the consistency of attribution to a single species.

We analyse in detail *Gephyrocapsa* specimens close to the SEM FCO of small *Gephyrocapsa.* The population is composed of *G. theyeri,* a species described from the late Miocene of the Eastern Equatorial Pacific. Re-examination of topotype material indicates an early Pliocene rather then late Miocene age of the samples but presence of the species could not be confirmed. The age of the holotype of *G. theyeri* is thus unknown. At Site 1000, *G. theyeri* has a FO at 137.15 mbsf (4.45 Ma). The species is probably phylogenetically related to *R. alis* n. sp. and *R. pujosiae* n. sp. as suggested by morphological-structural continuity. We document the fossil record of *R. calicis*, a species described from the same sediment sections. *R. calicis* has phylogenetic relationship with *R. alis* n. sp. and *R. premoliae* n. sp.

The new species are quantified in terms of absolute abundances and compared to small *Gephyrocapsa* and *R. calicis*. The new species, present in the older samples analysed in this study, indicate that significant diversification among reticulofenestrids occurred prior to 4.5 Ma. *G. theyeri* and *R. calicis* occur geologically synchronous based on an orbital tuned time scale suggesting that a common evolutionary forcing may be responsible for species-level evolution among reticulofenestrids.

INTRODUCTION

Coccolithophores are an important group of photosynthetic pelagic unicellular algae (Haptophyta, Edvardsen *et al.*, 2000) whose exoskeleton is composed of minute calcium carbonate plates of variable shape and architecture, coccoliths. Since the initial works on systematic and distribution and the pioneer studies by transmission and scanning electron microscope (TEM, SEM) on coccolithophores (Lohmann, 1902; Deflandre & Fert, 1954), a vast number of studies concerning various aspects of this group have been carried out and resulted in detailed knowledge of their species-level diversity. Most studies, however, have been based on light microscopy (LM) and part of the coccolithophores biodiversity may thus have been missed (Young *et al.*, 1994; Young *et al.*, 2005).

Emiliania huxleyi, *Gephyrocapsa* and *Reticulofenestra* are among the most common and abundant coccolithophores in present oceans (Okada & McIntyre, 1977). Most of the species produce coccoliths that are very small to small in size (<3 µm and 3-5 µm, Young *et al.*, 1997) showing a very wide range of morphological variability and many species and varieties are described (Young *et al.*, 2003). By contrast, the fossil record of very small to small reticulofenestrids (Young, 1989; Young *et al.*, 1997) is conventionally represented as limited to a set of species with very long geological ranges. For example, *R. minuta* is conventionally used for *Reticulofenestra* specimens less than 3 µm long from the late Oligocene to the Pliocene.

We have recently conducted a high-resolution quantitative SEM study of calcareous nannofossils from exceptionally well-preserved early Pliocene sediments (ODP Hole 1000A, South Caribbean Sea). The studied interval, 4.5-3.8 Ma, was recognised as a period of significant turnover in the reticulofenestrids including the LM FCO of small *Gephyrocapsa* and the FO of *Pseudoemiliania* (Kameo & Sato, 2000). We have previously described one new very small to small reticulofenestrid species (Crudeli & Kinkel, 2004) *R. calicis,* characterised by a significant structural variation of the coccoliths with respect to that of typical reticulofenestrids (Young, 1989) and suggesting that the early Pliocene reticulofenestrid turnover is more complex than previously recognised. From the same sediment sections, we have now recognised three further new reticulofenestrid species. In this work, we describe these species and discuss their phylogeny. In addition, we document the fossil record of *R. calicis* and discuss its possible phylogenetic relationship to the newly recognised species.

The types of the new species (SEM stubs and accompanying sub-samples of the topotype material) are deposited at the Department of Palaeontology, The Natural History Museum, London.

Reticulofenestrid radiation in the early Pliocene

In the early Pliocene, reticulofenestrids underwent significant diversification. *Pseudoemiliania* first occurred in the fossil record followed slightly later by the FCO of small *Gephyrocaps*a. These bioevents have been widely recognised by LM, and precede by a few hundred thousand years the LO of large (>7 µm) *R. pseudoumbilicus* and of other important Neogene nannofossils (Perch-Nielsen, 1985; Young, 1998). They also represent one of the major Neogene biotic turnovers among reticulofenestrids (Bown *et al.*, 2004; Gibbs *et al.*, 2005).

Nonetheless, the early evolutionary history of *Gephyrocapsa*, a very complex genus of modern diversity and phytoplankton biomass (Okada & McIntyre, 1977; Bollmann, 1997) is not well constrained in terms of the timing or species level diversity. Whereas the FO of *Pseudoemiliania* is a well constrained bioevent, the LM FO of *Gephyrocapsa* has still to be established. The first consistent and global occurrence of small *Gephyrocapsa* is widely documented within Zone NN15 of Martini, 1971 (Subzone Cn11b of Okada & Bukry, 1980) (Hay & Beaudry, 1973; Rio, 1982; Driever, 1988; Sato *et al.*, 1991; Kameo & Sato, 2000; Marino & Flores, 2002). However, e.g. Okada (2000) reported the FO of *Gephyrocapsa* in Zone NN13 (CN11a) from the Blake Ridge Nose area in the northwestern Atlantic and Driever (1988) observed small specimens in Zone NN12-13 from Mediterranean land sections. Moreover, other publications documented small *Gephyrocapsa* within the Miocene (Jiang & Gartner, 1984; Pujos, 1987; Gartner & Shyu, 1996; Triantaphyllou, 2000).

There are few SEM studies and SEM documentation of the diversity of the early Pliocene population. Pirini Radrizzani & Valleri (1977) documented *Gephyrocapsa* specimens from the *R*.

pseudoumbilicus Zone NN15 (Tyrrhenian Basin, DSDP Leg 13, Site 132) observing the dominance of very small forms (<2 µm, their *Gephyrocapsa* sp. and *G. aperta* group) and the sporadic presence of larger forms (their *G. caribbeanica*). Samtleben (1980) conducted a detailed morphometric study of *Gephyrocapsa* from the early Pliocene of the Atlantic (DSDP Leg 41, Site 366A cores 7-5 and 7-4) and described *G.* sp. 1 as the ancestral species of the plexus. *G.* sp. 1 was successively considered a synonym of *G. theyeri* by Pujos (1987) who described the species from the Miocene of the Pacific. Bonci & Pirini Radrizzani (1992) and Triantaphyllou (2000) also documented *Gephyrocapsa* specimens by SEM from the Miocene of Mediterranean land sections.
No detailed taxonomic studies of *Gephyrocapsa* specimens close to their LM FCO have been carried out to date. In this work, we conduct detailed SEM examinations on *Gephyrocapsa* specimens occurring close to the LM (Kameo & Sato, 2000) and SEM (this work) FCO of small *Gephyrocapsa* in order to define the taxonomy and phylogeny of that population.

MATERIALS

The species are observed from the early Pliocene (Zone CN11 of Okada & Bukry 1980, Kameo & Bralower 2000) from a core from the South Caribbean Basin (ODP Leg 165, Hole 1000A, latitude 16°33.223´N longitude 79°52.044´W, 916m water depth) (Sigurdsson *et al.*, 1997). The age model of the cores is based on orbitally tuned high-resolution stable isotope stratigraphy (Steph *et al.*, in revision).

METHODS

Sample preparation and quantitative analyses

Two-hundred and three samples at 10 cm intervals (138.45 mbsf to 118.25 mbsf) were analysed for calcareous nannofossils composition (this work; Crudeli *et al.*, in preparation). Sample preparation was based on the filtration method of Andruleit (1996) with slight modifications. These are described in Crudeli & Kinkel (2004) and details are reported in Crudeli *et al.* (in preparation 4). The concentration of calcareous nannofossils (number of specimens per gram of dry sediments) (e.g. Andruleit, 1996) was quantified by SEM (CamScan 44) at 6000× magnification. In order to constrain the range of *Gephyrocapsa* specimens, 10 samples below the SEM FCO depth (~ 1 m) were re-analysed screening a much wider (about four time) area of the SEM stub-filter. SEM magnification of 6000× was used along a transect of fixed length across the stub and the presence of specimens evaluated. A further qualitative check of the presence of specimens was carried out.

Taxonomic study

Morphological observations of the new species were conducted by SEM at 20000×. The distal shield length and width, the central-area width, rim width, and number of distal shield elements of each species-morphotype is based on measurements of 7 to 65 specimens at 20000× from one or, when specimens rare, two closely spaced samples. The nomenclature of Young *et al.* (1997) is adopted in this description. Additional descriptive terms used here are: transverse pole, position along the side intersecting the coccolith short axis and longitudinal pole, position along the end intersecting the coccolith long axis.

Remarks on quantification and taxonomy

The concentration of the new species and of *Gephyrocapsa* coccoliths refers to specimens in distal view, and side view where recognisable. Tilted forms with spines, in which the morphology of the distal shield was not visible, were assigned to *R. premoliae* n. sp. type 1. During routine quantification, a slight increase in size of forms with one or two arch-shaped structures, for which an informal taxonomic nomenclature was applied, was qualitatively observed and a set of length and width measurements on that population was subsequently carried out.

SYSTEMATIC DESCRIPTIONS

Kingdom **Chromista** Cavalier-Smith, 1981

Phylum **Haptophyta** Hibberd, 1972 ex Cavalier-Smith, 1986

Class **Prymnesiophyceae** Hibberd, 1976

Subclass **Prymnesiophycidae** Cavalier-Smith, 1986

Order **Isochrysidales** Pascher, 1910 emend. Edvardsen & Eikrem, 2000 in Edvardsen *et al.,* 2000

Family **Noelaerhabdaceae** Jerkovic, 1970 emend. Young & Bown, 1997b

Genus ***Reticulofenestra*** Hay, Mohler & Wade, 1966 emend. Gallagher, 1989

= Genus *Apertapetra* Hay *et al.,* 1966

Reticulofenestra alis n. sp. Crudeli & Young

(Pl. 1, figs 1-15, Pl. 2, figs 1-5).

Derivation of name. From Latin*, ales, alis* (masculine noun) (= wing), referring to the arch-shaped structure, similar to a wing.

Diagnosis. Very small placolith with shields of similar size, narrow rim, wide central-area with no central-area structure and with one or two distal arch-shaped structures along the side.

Holotype. SEM micrograph 83323, (Pl. 1, fig. 1).

Paratypes. SEM micrographs 82675, 83159, 82666, 84171, 82964, 83321, 84166, 83319, 82702, 83005, 86594, 83264, 86124, 83313, 83164, 86568, 81929, 81930, 85452 (Pl. 1, figs 2-15, Pl. 2, figs 1-5).

Type Material. ODP Sample 1000A-16H-1, 5-7 cm (136.35 mbsf).

Type locality and horizon. South Caribbean Sea, ODP Hole 1000A (16°33.223´N 79°52.044´W), early Pliocene, *R. pseudoumbilicus* Zone, Zone CN11 of Okada & Bukry (1980).

Description

R. alis n. sp. shows phenetic variability and various morphotypes are recognised. The range of variation of *R. alis* n. sp. is based on different morphotypes (153 specimens) described in the following. Morphological details of the morphotypes and the number of morphotype-specimens

measured per sample are reported in appendix. The species is constituted of two broadly to narrowly elliptical (1.1-1.6, 1.3 average) slightly convex shields of very similar dimensions. The coccolith length is 1.5-2.4 µm (1.9 µm average) and the width is 1.2-2.0 µm (1.5 µm average). The central-area is usually wide but in *R. alis* n. sp. type 3, it is from wide to narrow. The central-area has no structures and the rim is narrow. The distal shield is formed by 20-34 elements that are usually closely spaced, occasionally very weakly slitted. These elements are of similar shape and length. Very rarely, their terminations show incipient hammer-like morphology. Due to the narrow rim and to the arch/es, which does not allow complete observation of the distal shield morphology, the obliquity is not consistently visible. The inner tube elements are either weakly anticlockwise imbricated, or not imbricated. Along one or both sides of the coccolith, these elements, and the corresponding outer tube elements, extend above the distal shield level and give rise to an arch-shaped structure. Usually, the inner tube elements not forming the arch extend to or weakly above the level of the distal shield. Occasionally, from the base of the arch and/or from the upward termination of the inner tube elements, on the distal shield elements, a few overgrowth occurs.

Morphotypes. *R. alis* n. sp. includes five morphotypes. *R. alis* n. sp. type 1 (Pl. 1, figs 1-5) has an arch that develops along one side of the distal shield. On the opposite side, the inner tube elements extend to or weakly above the distal shield level. A few specimens occur in which these elements extend weakly below this level. These are among the forms with very narrow rim, so the variation may be due to preservation. *R. alis* n. sp. type 2 (Pl. 1, figs 7-10) differs from *R. alis* n. sp. type 1 because two arches develop along the side of the coccolith and, very occasionally, are connected along one end (Pl. 1, fig. 10). The rim morphology is identical to that of type 1. *R. alis* n. sp. type 3 (Pl. 2, figs 1-5) differs from type 1 and type 2 because of the morphology-structure of the arch, as described below. The central-area of *R. alis* n. sp. type 3 is from narrow to wide and, occasionally, shows an irregularly elliptical profile. Within the interval of its maximum concentration (Fig. 3), the morphotype frequently shows weak slitting of the distal shield elements. In *R. alis* n. sp. type 3, the tube elements close to the longitudinal poles appear to extend weakly below the distal shield level. However, the SEM resolution and small size of the specimens do not allow consistent assessment of such qualitative observation. Except for this, the rim morphology is very similar to the previous types. *R. alis* n. sp. type 4 and *R. alis* sp. nov type 5 have slightly wider rims and, commonly, are slightly larger in size with respect to the previous types. They are characterised by one arch or two arches along the sides respectively (Pl. 1, figs 11-12 and Pl. 1, figs 13-15, respectively). More commonly, in these types, the inner tube elements that do not form the arch extend weakly above the distal shield level. Few specimens having a grill formed by calcified bars enlarged inward or partially preserved thin bars were observed (Pl. 1, fig. 11). Due to the still narrow rim, the obliquity of the distal shield is not consistently visible.

Arch-shaped structure

The arch-shaped structure of *R. alis* n. sp. is formed by variable extension and fusion of the inner and outer tube elements, showing variations in the orientation with respect to the vertical direction and in its development along the side as described in the following.

Structure. The arch-shaped structure is schematised in figure 1 with references to plate 1, figures 2-3. The discrete portions of the inner tube elements above the distal shield level are termed inner arch-elements whereas the elements visible from the outside are called outer arch-elements. From the inside, the inner tube elements are anticlockwise imbricated till the level of the distal shield. From the longitudinal pole, these progressively extend upward above this level maintaining the same imbrication (Pl. 1, fig. 2; Fig. 1a, anticlockwise, a-inner arch-element) and change imbrication variably upward (Fig. 1a, clockwise, c-inner arch-element) in correspondence of a kink. The outer arch-elements do not have imbrication and extend vertically (Pl. 1, fig. 3; Fig. 1a). From the outside, the kink is not visible. This suggests that the outer arch-elements represent the extension of the outer tube elements. This also occurs in *R. calicis* (Crudeli & Kinkel, 2004).

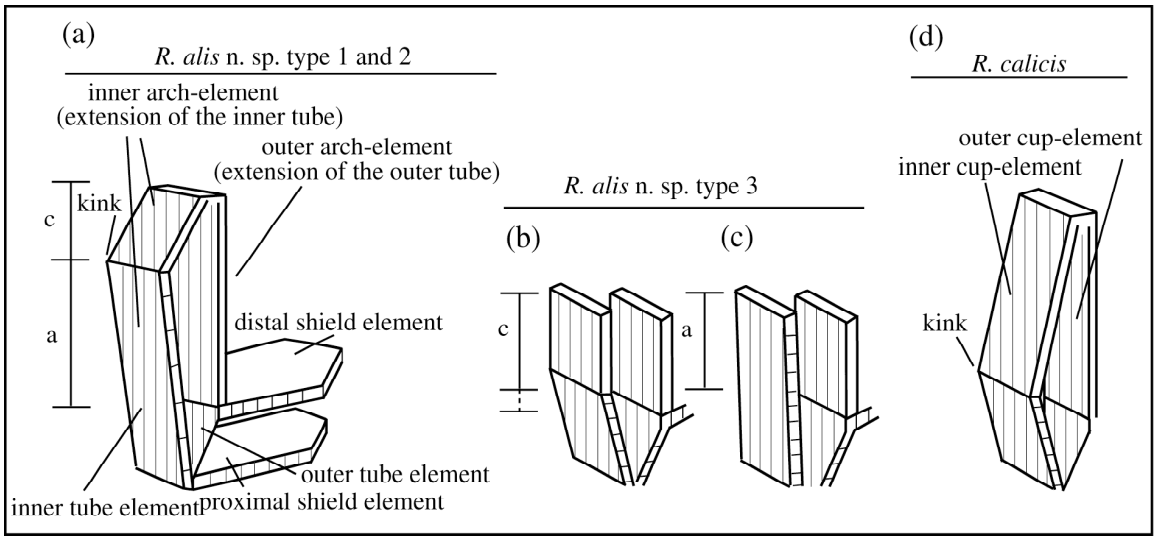

Fig. 1. Schematic drawing of a segment of *Reticulofenestra alis* n. sp. (a-c) compared with that of *R. calicis* (d) modified from Crudeli & Kinkel (2004). Up to the level of the distal shield, the drawings are from Young (1989).
(a) The scheme is valid for *R. alis* n. sp. type 1 and 2, type 4 and 5. Up to the level of the distal shield the inner and outer tube elements are respectively anticlockwise and clockwise imbricate (Young, 1989). Above this level, the inner tube element extends upward maintaining the same imbrication (anticlockwise, a-inner arch-element), it changes imbrication upward (clockwise, c-inner arch-element) (Pl. 1, fig. 2) in correspondence of a kink. The outer arch-element extends upward vertically (Pl. 1, fig. 3).
(b-c) Two structural variations of the arch-shaped structure of *R. alis* n. sp. type 3. The outer arch-element is represented, although it may be absent. See text for discussion.
(b) The extension is composed by the c-inner arch-element that has no or extremely weak imbrication whereas the a-inner arch-element is absent. The inner tube changes imbrication at or just below the distal shield level.
(c) The extension is composed by the a-inner arch-element that has no or extremely weak imbrication, whereas the c-inner arch-element is absent.
(d) The inner tube element of *R. calicis* changes imbrication (kink) close to the distal shield level. From the outside, the kink is not visible since the outer tube changes imbrication at the distal shield level and extends vertically.

Morphology. The c-inner arch-elements are enlarged upward and show sub-polygonal shape (Pl. 1, fig. 2). From the distal shield level, the outer arch-elements are vertical whereas they are variably enlarged upward and often show well-developed crystal faces (Pl. 1, fig. 3). From the outside, these

faces develop from about the level, which, from the inside, corresponds to the kink. Thus, they may be simply the outer crystal faces of the c-inner arch-elements. This would suggest that the outer tube elements do not entirely form the outer arch-elements. The degree of imbrication of the a- and c-inner arch-elements varies from low to moderate. The maximum extension of the arch ranges between ≈0.5-1.5 μm and is reached by the elements close to or at the transversal pole. Only very few specimens depart from this. Here, on one side, few (1-3) tube elements close to the longitudinal pole show incipient extension (Pl. 1, fig. 6). The arch commonly extends inward (Pl. 1, figs 4-5) or vertically (Pl. 1, figs 1-2), rarely slightly outward. It shows morphological variability in the development along one side. This commences from the longitudinal poles or variably just before or just after these resulting in variable longitudinal and/or transversal asymmetry of the coccolith (Fig. 2). On the same *R. alis* n. sp. type 2, type 3 and type 5 specimens, the arch is symmetric or shows different development on opposite side (Pl. 1, fig. 9).

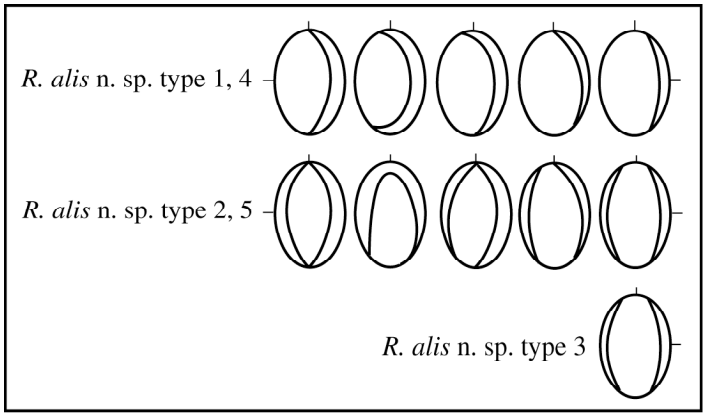

Fig. 2. *R. alis* n. sp., asymmetric coccolith, schematic drawing (distal view) showing the variation in the development, along the central-area, of the tube elements that give rise to the arch/es.

Morphological-structural variation - *R. alis* n. sp. type 3. In *R. alis* n. sp. type 3, in distal view, a variable number of discrete elements (2-7) close to and at the transverse pole extend outwards at low angle above the distal shield level and show very weak anticlockwise imbrication to no imbrication. These have regular sub-polygonal shape. The degree of calcification of these elements and their inward extension varies and can cause partial closure of the central-area. From the outside, elements extend vertically (Pl. 2, figs 3-4). From the inside, we observed a kink on few tilted forms. We interpret the morphology of *R. alis* n. sp. type 3 extensions by comparison with the structure described above. The element visible in distal view may be formed by the c-inner arch-element (Fig. 1b). In this case, the a-inner arch-element is absent and a change in imbrication (kink) occurs at or somewhere below the distal shield level. Alternatively, the extension is the a-inner arch-element which lacks the upper part (c-inner arch-element) (Fig. 1c). The absence of visually detectable imbrication of the extended elements agrees with the fact that the inner tube elements of *R. alis* n. sp. are extremely weak or not imbricate. By comparison with the arch-shaped structure described above, a contribution of the outer tube elements is possible. The morphology described before, makes a transition to low extensions of elements at both the transversal poles (Pl. 2, fig. 5).

Comparison with the cup-shaped structure of *R. calicis.* The cup-shaped structure of *R. calicis* is composed by an inner cycle of elements (inner cup-element) clockwise imbricate and an outer cycle of elements (outer cup-element) vertically oriented continuous with the inner and outer tube elements, respectively (Fig. 1d). The cycles result from their upward extension and fusion associated with a change in imbrication close to the distal shield level. In *R. alis* n. sp., from the inside and from the longitudinal pole, the inner tube elements extend upwards and progressively change imbrication (Fig. 1a-c) whereas the elements at the longitudinal pole do not extend. In *R. alis* n. sp., no cycles are formed and the coccolith show structural asymmetry. The outer cup-element cycle of *R. calicis* is entirely formed by the upward extension of the outer tube elements. In *R. alis* n. sp., as discussed, they possibly constitute only the lower portion of the outer arch-elements.

Differential diagnosis. *R. alis* n. sp. is similar in size and number of elements to *R. minuta* Roth 1970, the arch/es distinguish the species. *R. alis* n. sp. differs from *R. calicis* because of the discontinuity of the extended elements and in not having a grill.

Discussion of variation

The presence of one or two arches, their morphological-structural variation (*R. alis* n. sp. type 3), the slightly wider rim and size of the coccoliths (*R. alis* n. sp. type 4 and type 5) may or may not be of taxonomic significance. We discuss how these characters represent phenetic variation among a single species. Alternative possibilities are discussed.

Arch-shaped structure. We initially focus on *R. alis* n. sp. type 1. The arch of *R. alis* sp. nov type 1 could represent phenetic variation among a species that also produces unornamented coccoliths. *E. huxleyi* includes various unornamented coccoliths, likely produced by separate genotypes (Young *et al.,* 2003 and references therein). The ornate variety, *E. huxleyi* var. *corona* (Okada & McIntyre, 1977) Jordan & Young 1990 is likely also a separate genotype (Young & Westbroek, 1991) and suggests the taxonomic significance of the arch. The inner tube elements of modern *E. huxleyi* var. *corona* and *R. maceria* (Okada & McIntyre, 1977) Young *et al.,* 2003 give rise to a crown surrounding the central-area that differs in upward extension and development around the central-area. These modern species, indicate that the inner tube can be variably developed around the central-area and suggests caution in considering the presence of one or two arches on otherwise similar coccoliths, of taxonomic importance. The tooth-like protrusions of modern *G. ornata* Heimdal, 1973 may show variability in direction of extension, even on a single coccosphere and suggest eco-plasticity of the protrusions. Similarly, the discontinuity of the crown (*E. huxleyi* var. *corona* and *R. maceria*) is indicative of plasticity. A similar variation is expressed by the arch of *R. alis* n. sp. type 1. In addition, *R. alis* n. sp. type 1 and type 2 are similar in size, rim morphology and central-area. The arch that develops along one side in type 1 shows similar morphological variation to the two arches that develop in type 2. Moreover, *R. alis* n. sp. type 1 and type 2, have similar stratigraphic distributions (Fig. 3), as subsequently do type 4 and type 5, which further suggests that they were formed by a single coccolithophore species.

The inner tube elements that extend above the distal shield appear plastic morphologies. It is thus likely that the variation of the arch-shaped structure on *R. alis* n. sp. type 3 is related to plasticity

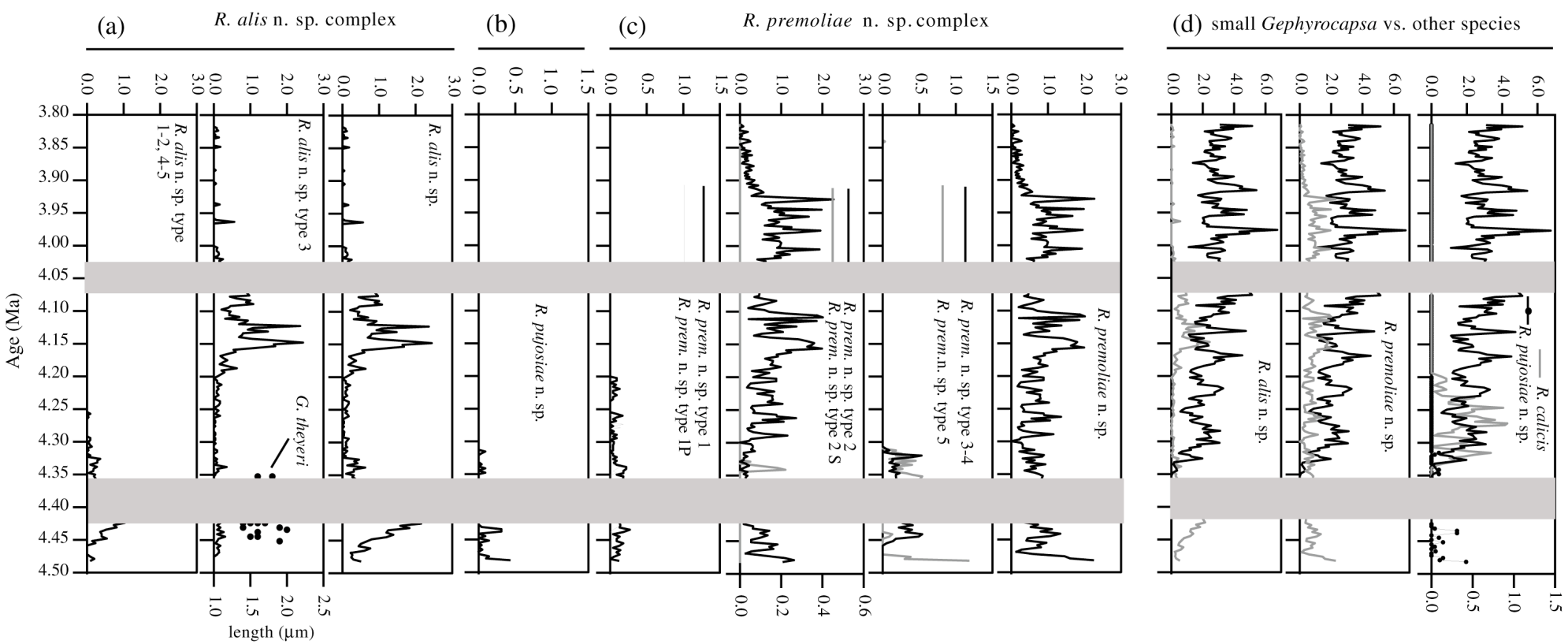

Fig. 3. Absolute abundance (no.x10^9g-1) of *R. alis* n. sp., *R. pujosiae* n. sp., *R. premoliae* n. sp. and *R. calicis* and comparison with the concentration of small *Gephyrocapsa*; (a) from the left side, *R. alis* n. sp. type 1-2, 4-5, *R. alis* n. sp. type 3 and *R. alis* n. sp.; (b) *R. pujosiae* n. sp.; (c) from the left side, *R. premoliae* n. sp. type 1 and *R. premoliae* n. sp. type 2 with more pronounced tube extensions (P), *R. premoliae* n. sp. type 2 and *R. premoliae* n. sp. type 2 with weakly slitted distal shield elements (S), *R. premoliae* n. sp. type 3 and *R. premoliae* n. sp. type 4, and *R. premoliae* n. sp. type 5; (d) concentration of *R. alis* n. sp., *R. premoliae* n. sp. *R. pujosiae* n. sp. and *R. calicis* compared with that of small *Gephyrocapsa*.

species-morphotypes	n. specimens	ODP Sample	maximum length (µm)	minimum length (µm)	average length (µm)	maximum width (µm)	minimum width (µm)	average width (µm)	maximum ellipticity	minimum ellipticity	average ellipticity	CA maximum width (µm)	CA minimum width (µm)	CA average width (µm)	rim maximum width (µm)	rim minimum width (µm)	rim average width (µm)	n. DS elements	slitting	CA structures	structure/extension	inner tube extension	outer tube extension
R. alis n. sp. type 1	35	16H-1, 5-7cm	2.1	1.3	1.7	1.7	1.1	1.4	1.4	1.1	1.3	0.7	0.5	0.6	0.5	0.2	0.3	24-32	no	no	1 arch	p	p
R. alis n. sp. type 2	16, 18	16H-1, 75-77cm -16H-1, 5-7cm	2.3	1.5	1.9	1.9	1.2	1.5	1.5	1.1	1.3	0.9	0.5	0.7	0.5	0.3	0.4	24-32	no	no	2 arches	p	p
R. alis n. sp. type 3	15, 30	15H-7, 25-27cm -15H-2, 125-127cm	2.3	1.3	1.8	2.0	1.0	1.3	1.6	1.2	1.4	0.8	0.3	0.5	0.6	0.3	0.4	20-32	vo	no	2 arches	p	p
R. alis n. sp. type 5	21, 13*	16H-1, 5-7cm	2.8	1.7	2.2	2.3	1.3	1.8	1.4	1.1	1.2	1.3	0.5	0.8	0.6	0.3	0.5	22-34	no	vo	2 arches	p	p
R. alis n. sp.	148		2.8	1.3	1.9	2.3	1.0	1.5	1.6	1.1	1.3	1.3	0.3	0.7	0.6	0.2	0.4	20-34				p	p
R. pujosiae n. sp.	45	16H-2, 25-27cm	3.0	1.4	2.2	2.3	1.1	1.8	1.4	1.1	1.2	1.0	0.3	0.6	0.7	0.3	0.6	22-38	vo	no	low extension NE-SW	p	no
R. premoliae n. sp. type 1	20*		3.1	1.1	2.1	2.4	1.8	2.1	1.3	1.2	1.2							24-38	vo	grill	2 spines E-W	p	no
R. premoliae n. sp.. type 2	60, 5*	15H-4, 5-7cm	3.2	1.8	2.5	2.7	1.5	2.1	1.4	1.1	1.2	1.1	0.4	0.7	0.8	0.3	0.7	24-38	vo	grill	incipient extension E-W	p	no
R. premoliae n. sp. type 3	*7**		2.6	1.7	2.2	2.1	1.4	1.8	1.3	1.1	1.2							24-34	p	grill	2 spines E-W	p	no
R. premoliae n. sp. type 4	32, 2*	16H-2, 25-27cm	2.6	1.6	2.2	2.2	1.1	1.7	1.5	1.1	1.3	1.0	0.5	0.7	0.6	0.3	0.4	22-34	p	grill	incipient extension E-W	p	no
R. premoliae n. sp.	126		2.9	1.6	2.3	2.4	1.5	1.9	1.4	1.1	1.2							22-38					

Table 1. Morphological-structural characters of *R. alis* n. sp. and *R. premoliae* n. sp. and morphotypes and of *R. pujosiae* n. sp. CA, central area, DS, distal shield, no, absent, vo, very occasional, p, present. The table reports the number of morphotypes-specimens on which the description is based and the ODP sample/s from which these are described. The symbol * indicates that the specimens are observed from other samples. Five specimens of *R. premoliae* n. sp. type 4 subject of detailed morphometry show identical size variation to *R. premoliae* n. sp. type 5. This is further confirmed by low resolution morphometry on randomly observed specimens, which are omitted in the table.

rather than being of taxonomic significance. *R. alis* n. sp. type 1 and type 2 are common in the lower interval investigated where *R. alis* n. sp. type 3 is rare (Fig. 3). In contrast, type 3 increases in concentration in correspondence to significant palaeoceanographic and palaeoecological changes at Site 1000 (Steph *et al.*, in revision and Crudeli *et al.*, in preparation, respectively). So, it is expected that the species adopted the morphology in order to survive under newly occurring palaeoecological conditions. This morphotype may, however, represent a separate species. The different distribution discussed above may similarly be due to the fact that *R. alis* n. sp. type 3 is a different species with different ecology. The arch of *R. alis* n. sp. type 3 very commonly develops symmetrically or asymmetrically on the sides. No specimens with a single arch are observed neither from the interval where the type is rare or more common (Fig. 3). This is a different pattern from the co-occurrence of *R. alis* n. sp. type 1 and 2 and *R. alis* n. sp. type 4 and 5 (Fig. 3). Among the modern *E. huxleyi*, the type with inner tube elements developing below the distal shield level, possibly represents a separate genotype. In *R. alis* n. sp. type 3 specimens, the tube elements that do not form the low arches appear to extend weakly below to the distal shield level. However, the SEM resolution and small size of the specimens do not allow complete observation of this variation. Nonetheless, this subtle difference could simply be related to the structural variation of the arch-shape structure itself. Moreover, the role of dissolution on very small tube elements it is not clear.

Size and central-area structure. Length measurements of *R. alis* n. sp. in the 137.75-135.65-mbsf interval (4.47-4.32 Ma, ≈150 kyr) show an increase in size of this population (Fig. 4a). Examination of *R. alis* n. sp. type 1 and type 2 and *R. alis* n. sp. type 4 and type 5 from the same sample (136.35 mbsf) show that large size (*R. alis* n. sp. type 5) corresponds to a roughly proportional increase in the number of elements, central-area width and rim width (Fig. 4b), and suggests that the types belong to a single species. *R. alis* n. sp. type 4 and type 5 are thus probably the result of an anagenetic microevolutionary increase in size of *R. alis* n. sp. The fact that size increase occurs synchronously in both forms with one arch (types 1 and 4) and two arches (types 2 and 5) further supports the inference that the variation in number of arches is intraspecific.

The occasional occurrence of *R. alis* type 4 and type 5 specimens with central-area structures may suggest that the absence of the latter in most specimens is due to preservation. During coccolithogenesis, central-area structures develop contemporary to other discrete elements (Young, 1989; Young & Westbroek, 1991; Young *et al.*, 1992; Young *et al.*, 1999). So, if central-area structures are present, this would suggest that type 4 and type 5 belong to a different species. However, heavy preservation effects are unlikely since e.g. delicate spines are often preserved. The arch is likely a generally robust morphology since it results from fusion of elements. So, its preservation can not be used as a proxy for dissolution. Moreover, no *R. alis* n. sp. type 1-3 specimens with a developed central structure were observed despite hundreds of specimens being observed by coccolith biomineralization mode. Among these, the tube elements show the most variation (Young, 1989). They can extend symmetrically inward closing the central-area which may represent (eco)phenotypic character of species or be of taxonomic significance (e.g. Young, 1989; Young & Westbroek, 1991; Beaufort & Heussner, 2001; Young *et al*., 2003). The tube elements can also extend symmetrically below the distal shield level in which case, with the co-occurrence of other variation, they are possibly indicative of genetic differentiation, as in *E. huxleyi* species. Young (1989)

discussed in particular the variation of the inner tube elements above the distal shield level shown by *Gephyrocapsa* and *Noelaerhabdus* species. In *Gephyrocapsa* and *Noelaerhabdus,* the inner tube elements are selectively modified above this level, and the pattern departs from the model of uniform growth of elements around the central-area (Young, 1989). In *Gephyrocapsa* and *Noelaerhabdus*, few elements above the distal shield are modified. In e.g. *R. alis* n. sp. 1, commonly, more than five elements are modified. Increased morphological variation may suggest a much more ecological complexity of this small reticulofenestrid species.

Molecular genetic studies and morphological observation on modern coccolithophores have recently shown that morphological differences, often subtle, between otherwise very similar coccoliths of extant coccolithophores distinguish among biological sister species (Geisen *et al.,* 2002; Sáez *et al.,* 2003). The coccolith morphology of cryptic species appears to have been stable from their evolution suggesting a strong pressure from environment acting on coccolith morphology (Sáez *et al.,* 2003). Heterococcoliths are formed intracellularly and then pushed outwards. Coccolithogenesis occurs within the cell vesicle derived from the Golgi body and appears associated with complex acid polysaccharides that play a rule in the regulation of the shape of biomineral formed (Young & Henriksen, 2003 and references therein). Despite an allowed degree of variation, most of the tested coccolithophores produce identical coccoliths reflecting an identical biomineralization mode.

E. huxleyi var. *corona* and *R. maceria* depart from this pattern but also from the model of uniform growth of elements in reticulofenestrids (Young, 1989; Young *et al.,* 1999). A single coccosphere produces coccoliths in which the inner tube elements, above the shield level, extend variably and selectively around the central-area and, contemporary, other coccoliths that show similar variation but differ in pattern in detail. A similar pattern is shown by *R. alis* n. sp. (Fig. 2). Formation of morphologically different coccoliths by a single coccolithophore, e.g. *E. huxleyi* var. *corona* suggests that the vesicle variably operate. Since the functioning of the vesicle is directly driven by the biology of the cell, it is expected that the forms posses very distinct autoecology.

Reticulofenestra pujosiae n. sp. Crudeli & Young
(Pl. 2, figs 6-11)

Derivation of name. Dedicated to Annick Pujos, who described *G. theyeri.*

Diagnosis. Very small to small placolith with narrow rim, moderately wide central-area with no central-area structure and with low distal extensions of a few inner tube elements in NE-SW position.

Holotype. SEM micrograph 85444 (Pl. 2, fig. 11).

Paratypes. SEM micrographs 85443, 85960, 84335, 84550, 85962, (Pl. 2, figs 6-10).

Type Material. ODP Sample 1000A-16H-2, 25-27 cm (138.45 mbsf).

Type locality and horizon. South Caribbean Sea, ODP Hole 1000A (16°33.223´N 79°52.044´W), early Pliocene, *R. pseudoumbilicus* Zone, Zone CN11 of Okada & Bukry (1980).

Description and dimensions. The species is very small in size (1.4-3 µm, 2.2 µm average), normally to broadly elliptical (1.1-1.4). A few larger specimens, 4.0 µm long and 3.0 µm wide occur. The central-area is wide and lacks central-area structures. In the smallest coccoliths, the central-area can be narrow. The distal shield is composed of 22 to 38 commonly closed elements. Usually, the distal shield elements are of similar length (Pl. 2, figs 8, 12), occasionally those in NE (SW) or rarely in NE and SW positions are weakly shorter (Pl. 2, figs 9-11). The inner tube elements extend to the distal shield level, a variable number of inner tube elements (1-7) in NE-SW position show low extensions above this level. Very occasionally, only the inner tube elements in NE (SW) position extend. The elements commonly extend from just after the longitudinal pole (1-2 elements after) or variably after (3-5 elements after). In the smaller forms, commonly, only 1-3 inner tube elements extend. In the larger coccoliths, the low inner tube extensions frequently give rise to an arch-like morphology. On the same specimen, the number of low inner tube extensions in one position (e.g. NE) can be different from that on the opposite side.

Differential diagnosis. The low inner tube elements extensions in NE-SW position, distinguish the species from *R. minuta* and *R. alis* n. sp.

Discussion on variation

Incipient extensions above the distal shield level shown by coccoliths of *R. premoliae* n. sp., are probably due to dissolution or breakage of spines (see discussion below). By contrast, the low extensions shown by coccoliths of *R. pujosiae* n. sp. are probably not due to dissolution of a spine structure since no coccoliths have been observed in these sediments with a spine structure in these positions. *G. theyeri* is extremely rare (Fig. 3) and has a narrow rim, so it is unlikely that the low extensions of the species are the result of a dissolved bridge. The species shows variation in size, however, increase in size corresponds to a roughly similar increase in central-area width and number of elements and there is not significant variation in rim. Therefore, it is likely that the variation is simply related to size (Young, 1989). Hence, there are no indications from morphometry, of the presence of more than one species. The smallest forms are likely due to preservation since their central-area size is similar to other specimens (compare Pl. 2, fig. 7 and fig. 9).

Reticulofenestra premoliae n. sp. Crudeli & Young
(Pl. 3, figs 1-15)

Derivation of name. Dedicated to Isabella Premoli Silva, micropalaeontologist.

Diagnosis. Very small placolith with shields of similar size, wide central-area, narrow rim with distal spines close and at or at the transversal pole and central-area grill.

Holotype. SEM micrograph 82557 (Pl. 3, fig. 1).

Paratypes. SEM micrographs 82663, 83122, 83144, 81949, 83140, 81866, 86591, 83112, 84174, 84564, 84336, 85439, 83266, 84334 (Pl. 3, figs 2-15).

Type material. ODP Sample 1000A-15H-4, 5-7 cm (131.35 mbsf).

Type locality and horizon. South Caribbean Sea, ODP Hole 1000A (16°33.223´N 79°52.044´W), early Pliocene, *R. pseudoumbilicus* Zone, Zone CN11 of Okada & Bukry (1980).

Description and dimensions. *R. premoliae* n. sp. type 1 and type 2 show similar size and identical rim morphology, which is described below. They differ in the extension of the inner tube elements above the distal shield. In *R. premoliae* n. sp. type 1 (Pl. 3, figs 1-5), the inner tube elements close to and/or at the transverse poles extend above the distal shield level and give rise to spines (1-5) which height range between 1-1.5 µm. Spines are commonly sub-vertical at the lower part and are enlarged upwards just above the distal shield level showing a sub-polygonal shape, occasionally they are massive. On the same specimens, spines are commonly similar in shape. Tooth-like protrusions around the central-area occur very occasionally (Pl. 3, fig. 3). In *R. premoliae* n. sp. type 2 (Pl. 3, figs 6-7), spines are substituted by low extensions of the inner tube elements in identical position. Since the spines are delicate structures, *R. premoliae* n. sp. type 2 is likely to be a preservational artefact of *R. premoliae* n. sp. type 1. Rare specimens with spines on only one side and a low extension or absence on the opposite side may be similarly due to preservation. Coccoliths with upward development of extension intermediate between *R. premoliae* n. sp. type 1 and type 2 are more common in samples where *R. premoliae* n. sp. type 1 is consistently present (Fig. 3). This, in addition to similarity in rim, supports the inference that the *R. premoliae* n. sp. type 2 morphology is due to preservation. When otherwise necessary, we refer to these types as *R. premoliae* n. sp. type 1-2.

R. premoliae n. sp. type 1-2 is very small in size and is constituted by two slightly convex shields of similar size (Tab. 1). The morphology of the rim described hereafter is mainly based on observations of *R. premoliae* n. sp. type 2 specimens since type 1 specimens are much rarer. The distal shield is formed by 24-38 closely spaced elements. Commonly, the elements are of similar shape, occasionally, a few elements (1-2) in variable position along the central-area are thinner. On the same specimens, few distal shield elements (1-3) are thinner at the base (i.e. close to the respective tube element) and have incipient hammer-like morphology that results in a weak slitting of adjacent elements (few specimens observed). The rim is narrow, the central-area is wide and usually spanned by a grill formed by thin bars continuous with the proximal shield elements that meet along a median suture. The terminations of the bars at the suture are variably thickened resulting in a variably prominent median ridge. These often have a hammer-like morphology. Bars are occasionally heavily enlarged inwards resulting in an almost closed central-area.

The inner tube elements are commonly weakly anticlockwise imbricate, occasionally they are not imbricate. Commonly they all extend slightly above the distal shield level, occasionally only a few elements extend just at this level which is, at least in part, certainly due to preservation. Due to the narrow rim the obliquity of the distal shield is not consistently observable.

Among *R. premoliae* n. sp. type 2, two morphotypes (A and B) are easily qualitatively distinguishable from the same sample (Pl. 3, fig. 5). *R. premoliae* n. sp. type 2A is larger, composed of more distal shield elements and has a wide central-area. *R. premoliae* n. sp. type 2B is smaller, composed of fewer distal shield elements and has a narrower central-area. Intermediate forms occur. There is good

relation between size, central-area width, number of elements and the rim does not vary too much, which suggests that it is possible that these are separate species.

R. premoliae n. sp. shows variation in rim morphology, with some specimens showing slitting between the elements and these show, variably, hammer-like terminations. Two morphotypes showing this rim morphology are recognised. *R. premoliae* n. sp. type 3 (Pl. 3, figs 8-10) possesses spines in transversal position, and *R. premoliae* n. sp. type 4 (Pl. 3, figs 11-15) lacks spines but does have low extensions of inner tube elements in this position. *R. premoliae* n. sp. type 4 is likely a preservation artefact of type 3 and we refer to these as *R. premoliae* n. sp. type 3-4. The description of the rim is based on *R. premoliae* n. sp. type 4 but similar variations occur in *R. premoliae* n. sp. type 3. In type 3 and 4, the morphology of the central-area structure is identical to that of type 1 and 2. The proximal shield is formed by closely spaced elements of similar shape and size, without slits between them. The number of elements is identical to that of the distal shield. All the proximal shield elements have terminations dextrally oriented or a variable number have straight termination.

The distal shield is of similar size, variably smaller or slightly larger than the proximal shield. This observation is based on the comparison between the length of distal shield elements with hammer-like termination and the size of the proximal shield visible because of the different outward development of the other distal shield elements.

The distal shield elements show a similar, generally weak, degree of slitting around the central-area or the elements along the sides are less to no slitted, those at the end/s are clearly slitted. Specimens with less slitted elements at one end and variably slitted elements on the opposite end also occur. The slitted elements show hammer-like morphology, those not slitted show incipient hammer-like or rounded morphology. Rarely, all the distal shield elements are of roughly similar length and all have moderately developed to incipient hammer-like termination. More commonly, the elements at the end are longer than those along the side that can be also very short. Regardless to the different length of the distal shield elements and number of hammer-like termination, the hammer-like terminations have symmetric hammer-head to asymmetric-dextral hammer-head. Here, the hammer-heads are clearly continuous with the element and, when well formed appear as discrete elements. Overgrowth can result in a similar shape but in this material there is only slight overgrowth. Commonly, the inner tube elements all extend to the distal shield level, although occasionally a variable number extend below it, which may be due to preservation of these small elements. The inner tube elements are very weakly anticlockwise imbricated. In most specimens they are not imbricated.

A fifth morphotype within *R. premoliae* n. sp. is distinguished by small size, narrow rims and rounded terminations of all the distal shield elements. Typically the distal shield elements at the sides are shorter, less or non-slitted, and the inner tube elements appear to extend weakly below the distal shield level (*R. premoliae* n. sp. type 5, Pl. 3, fig. 15). *R. premoliae* n. sp. type 5 shows morphological continuity with *R. premoliae* n. sp. type 3-4 but, from the same sample, the types are distinguishable. It is possible that type 5 represents simply specimens in which the shields have been dissolved leaving only the tube.

Differential diagnosis. The spines of *R. premoliae* n. sp. distinguish the species from *R. minuta*, *R. alis* n. sp. and *R. pujosiae* n. sp. *R. premoliae* n. sp. differs from *Gephyrocapsa duoalatus* (Martini, 1980) Martini, 1993 because the spines are not conjunct distally. *R. premoliae* n. sp. differs from

Noelaerhabdus species because these are larger (commonly >3 μm, up to 6 μm in size), the number of distal shield elements is commonly higher, the spine is single and develops on only one side, is >2 μm height up to 12 μm, this has variable aberrant morphology including bifurcation (Jerkovic, 1970; Bona & Gal, 1985; Marunteanu, 1997).

Discussion on variation

R. premoliae n. sp. type 1-2 and *R. premoliae* n. sp. type 3-4 are very close in size, have similar central-area structure, and have distal spines (or low extensions) whose shape, number and position is identical. They show various differences in rim morphology. This mainly concerns the degree of slitting between the distal shield elements, the morphology of their outward terminations, and subtle variation in imbrication of the distal shield elements. Among the same species, in addition to intraspecific variation, rim morphology may be influenced by several other factors (Young & Westbroek, 1991; Young, 1994a).

Intraspecific variation. Varying degrees of slitting are shown within well-recognised modern species. The modern e.g. *G. ericsonii* and *G. ornata* may have slits between distal shield elements, slitted shield elements to closely spaced elements with variable hammer-like terminations (e.g. McIntyre & Bé, 1967; Winter *et al.*, 1978; Young *et al.*, 2003). So, hammer-like termination and slitting vs. absence is likely, as also showed by the previous species and *R. calicis* (Crudeli & Kinkel, 2004), intraspecific.

Dissolution. The variability of the morphology of the terminations of the distal shield elements, their different length, and the variable extension of the inner tube with respect to the distal shield level may be due to dissolution. In particular, the fact that the elements at the side have more commonly rounded terminations and are shorter is possibly related to the lower ellipticity of the coccoliths at these positions (Young, 1989). In contrast, the elements close to the end are much more robust as in *E. huxleyi.* Preservation of delicate spines on these specimens and presence of other delicate species (Crudeli *et al.*, in preparation) suggest minor effects of dissolution. In addition, very short elements at the side with incipient hammer like termination occur, therefore only part of the observed morphological variability may be due to dissolution.

Malformation. Teratological malformation (Young *et al.*, 1997) is not a likely primary cause of rim variation. Malformation has been widely documented on *E. huxleyi* coccoliths. This results in variable length of the distal shield elements and irregular shape of the hammer-head and of the inner tube elements (e.g. Young, 1994b). Comparison with illustrations of malformed *E. huxleyi* specimens (e.g. Young & Westbroek, 1991; their Plate I, figs 6-7; Young, 1994b, his figs 4D-E, G-H; Batvik *et al.*, 1997, their Figs. 2B-D) suggests different causes for the rim variation of *R. premoliae* type 3-4. Coccoliths of the same species from a single sample show a different degree of malformation (compare figs 4E and 4G of Young, 1994b). By contrast, only the type of variation described above is displayed by the specimens observed here. Generally, malformed and normally formed coccoliths of the same species co-occur (Young & Westbroek, 1991; Young, 1994b; Batvik *et al.*, 1997) and, when

malformation occurs, it occurs also in other species (Okada & Honjo, 1975; Kleijne, 1990). In this material, other coccoliths, e.g. *Helicosphaera* are normally formed.

Degree of calcification. In *E. huxleyi*, variation in the degree of calcification influences the slitting of the proximal shield elements, the width of the inner tube elements, and the thickness of the distal shield elements (Young, 1994b). A decrease in the degree of calcification could explain the slitting of the distal shield elements vs. closely spaced elements as the occasional lower extension of the inner tube elements. The importance of the degree in calcification in variation is supported by the occurrence of rare specimens with most distal shield elements clearly slitted with variable terminations and few elements (3-5) closely spaced of similar length (Pl. 3, fig. 8). As for dissolution, it is difficult to reconcile under calcification with the presence of highly calcified spines on the same specimen. It is possible that the spines were of significant ecological importance for the species, and therefore, under ecological stress, the form used energy to form these morphologies resulting in under-calcified distal shield elements. Under-calcification would have been expected to affect the proximal shield elements, but these appear to be normally formed.

Different species – evolutionary control? *R. premoliae* n. sp. type 1-2 and *R. premoliae* n. sp. type 3-4 show differences in rim morphology. Among these, the most evident is the absence and presence of slits, respectively. As discussed above, dissolution and under calcification are difficult to reconcile with presence of highly calcified spines on the same specimens. Since also malformation appears an unlikely cause of rim variation, the alternative explanation is that *R. premoliae* n. sp. type 1-2 and type 3-4 are separate species. *R. premoliae* n. sp. type 1-2 and *R. premoliae* n. sp. type 3-4 show different abundance in the same interval (Fig. 3). This pattern is in agreement with the presence of two separate species with differential ecology.
In the same samples, there is a subtle transition between *R. premoliae* n. sp. type 5 and *R. alis* n. sp. type 3. As discussed, *R. premoliae* n. sp. type 5 may be due to dissolution, however, in few specimens spines are preserved, a fact that suggests that this morphology may be primary. Hence, the similarity between *R. premoliae* n. sp. type 5 and *R. alis* n. sp. type 3 may suggest that *R. premoliae* n. sp. type 3-4 is phylogenetically related to *R. alis* n. sp. rather than to *R. premoliae* n. sp. (type 1-2) and would support that the *R. premoliae* n. sp. types belong to two different species. Nonetheless, if *R. premoliae* n. sp. type 3-5 represents a separate species, this species shows ample morphological variation that as discussed above, is not easily related to dissolution, malformation or under calcification. The alternative possibility is that the rim variation is due to evolutionary control.

Morphology based phylogeny
The three new species are characterised by variable extension of the tube elements above the distal shield and are roughly similar in size and rim morphology suggesting a close phylogenetic relation. The lineage possibly evolved from *R. minuta* (Fig. 5), a species described from the lower Oligocene (Roth 1970). The presence vs. absence of central-area structures suggests that the couple *R. alis* n. sp. and *R. pujosiae* n. sp. and the couple *R. calicis* and *R. premoliae* n. sp. represent separate lineages (Fig. 5a). The latter species show a similar central-area structure to those of *R. pseudoumbilicus* small specimens *sensu* Driever (1988) (Crudeli & Kinkel, 2004), and suggest affinity. On the other hand, *R.*

pseudoumbilicus small specimen *sensu* Driever (1988) show a protruding collar formed by extension of inner tube elements and this variation occurs in the species described here. So, despite the larger size, these may represent a suitable common ancestor of the species. As discussed, *R. premoliae* n. sp. type 3-4 may be a different species from *R. premoliae* n. sp. type 1-2, but if so they are certainly very closely related. The subtle transition of *R. premoliae* n. sp. type 5 with *R. alis* n. sp. type 3 suggests affinity with the *R. alis* n. sp. lineage (Fig. 5b).

Generic affiliation of the new species

Noelaerhabdus, *Bekelithella* Bona & Gal 1985 and *Gephyrocapsa* Kamptner 1943 include forms characterised by variable extension of the inner tube above the distal shield level. However, the genera *Noelaerhabdus* and *Bekelithella* have only been recorded from the Miocene of the Paratethyan area and appear to be endemic to that region (Young, 1998 and references therein). As discussed, the new species are probably phylogenetically related. Also, *G. theyeri* is probably phylogenetically related to *R. alis* n. sp. and *R. pujosiae* n. sp. Therefore, *Gephyrocapsa* could be an appropriate genus. However, *Gephyrocapsa* has an important LM significance (e.g. Rio, 1982; Perch-Nielsen, 1985) and affiliation of forms without bridge to *Gephyrocapsa* would not be convenient. *Reticulofenestra* is certainly a strongly paraphyletic taxon and possibly polyphyletic taxa, thus not ideal in a meaningful classification of forms (Young *et al.*, 2003). However, *Reticulofenestra*, defined by absence of peculiar features is the most neutral genus. We thus follow Young (1990) who assigned coccoliths with *Pseudoemiliania* morphology to *Reticulofenestra* and Crudeli & Kinkel (2004) who assigned the morphologically-structurally variable *R. calicis* to *Reticulofenestra*.

The extension of the outer tube elements of *R. calicis* represents a structural novelty for reticulofenestrids (Crudeli & Kinkel, 2004). The authors envisaged the possibility of introduction of a new genus for reticulofenestrids with outer tube extension. *R. alis* n. sp. show moderate extension of the outer tube elements which is however rather clear in *R. alis* n. sp. type 3**.** Nonetheless, the forms are clearly reticulofenestrids. The trait supports the monophyletic origin of species.

Palaeoecology

The modern non-ornate *E. huxleyi* species, which probably include various genotypes (Young & Westbroek, 1991; Medlin *et al.,* 1996; Young *et al.,* 2003), dominate assemblages in most ocean. By contrast, specimens of *E. huxleyi* var. *corona* are much less common (Jordan *et al.*, 2000 and references therein) and often occur in phosphate depleted water (Cortés *et al.*, 2001). *G. ornata* is also a rare small modern coccolithophore distributed in low latitude oceans (Hagino *et al.,* 2000; Takahashi & Okada, 2000). The extremely rare modern coccolithophores with high not connected elements, referred to as ?*Gephyrocapsa,* may represent malformation of various species (Young *et al.*, 2003). It is interesting to note that these forms are observed from various oligotrophic domains (Mediterranean and Red Sea, oligotrophic gyre of the eastern central Atlantic and Pacific, Young *et al.,* 2003 and references therein). There is not much known about the palaeoecology of *Noelaerhabdus* and *Bekelithella* species described from the intercontinental Paratethys bioprovince. However, it is expected that these ornamented endemic reticulofenestrids have evolved functional morphologies in response to the peculiar palaeoecological conditions which also resulted in proliferation of a vast amount of various endemic organisms here (e.g. Gulyas, 2001 and references

therein). It appears thus likely that the ornamented reticulofenestrids are in an intermediate position in the range of the ecological adaptive strategies recognised in coccolithophores (Young, 1994b). It is likely that the species described here, as *R. calicis*, had a more K-selected ecological adaptation. This appears very consistent with the model of variation of the tube elements above the distal shield as a significant functional morphology.

OCCURRENCE AND PHYLOGENY OF *R. CALICIS*

R. calicis occurs soon after the SEM FCO of *G. theyeri* (Fig. 3). The similarity in central-area structure of *R. calicis* and *R. premoliae* n. sp. suggests a phylogenetic relation. *R. calicis* is characterised by extension of the outer tube elements, a variation characteristic of *R. alis* n. sp. and suggests affinity. The few observed *R. alis.* n. sp. specimens with central-area structure may thus represent transitional forms to *R. calicis.* This is ambiguous and there is the possibility that *R. calicis* includes more than one species. This would not be unexpected since the strong ecological affinity of the extension may have been equally developed on different species.

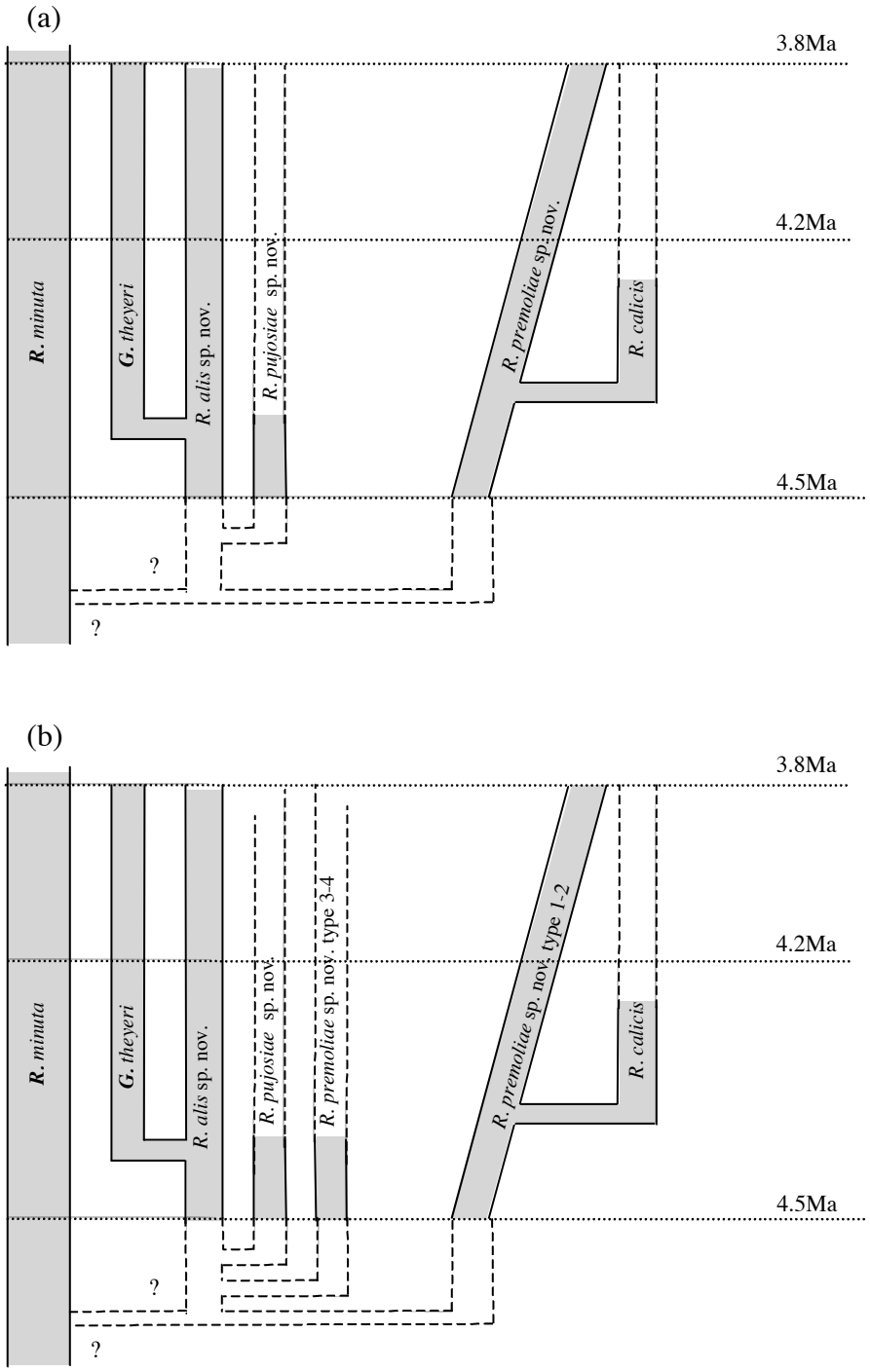

Fig. 5. (a) Phylogeny of *R. alis* n. sp., *R. pujosiae* n. sp., *R. premoliae* n. sp., *G. theyeri* and *R. calicis*; (b) alternative phylogeny if *R. premoliae* n. sp. type 3-4 are different species from *R. premoliae* n. sp. type 1-2.

OCCURRENCE AND PHYLOGENY OF *G. THEYERI*

Occurrence of *G. theyeri* at Site 1000A

The first, extremely rare *Gephyrocapsa* specimens, identical to the holotype of *G. theyeri* Pujos (1987), occur in our material at 137.15 mbsf (Sample 16H-1, 85-87 cm, 4.45 Ma). Despite extensive

SEM observations no specimens were found from 138.45 mbsf to 137.15 mbsf (Tab. 2). In standard counting, *G. theyeri* occurs in samples at 136.43 mbsf (Sample 15H-7, 63-65 cm, 4.35 Ma) (0.04x109 specimens g-1, Fig. 3). This is termed the FCO of the species. Above 136.43 mbsf, *G. theyeri* is very rare, so it is unlikely that specimens below this depth are reworked. From 136.43 mbsf till few meters upward, the *Gephyrocapsa* population is composed entirely of *G. theyeri,* further upward, other *Gephyrocapsa* species occur (Crudeli *et al.*, in preparation 4).

Core	Type	Section	Top	Bottom	Depth (mbsf)	Age (Ma)	(1) n. *G. theyeri* specimen	(2) n. *G. theyeri* specimen
15	H	0	5	7	136.43	4.3527	3	1
16	H	1	5	7	136.35	4.4240	0	6
16	H	1	15	17	136.45	4.4273	0	0
16	H	1	25	27	136.55	4.4309	1	1
16	H	1	35	37	136.65	4.4342	0	1
16	H	1	45	47	136.75	4.4378	0	1
16	H	1	55	57	136.85	4.4411	0	0
16	H	1	65	67	136.95	4.4448	0	2
16	H	1	75	77	137.05	4.4480	0	0
16	H	1	85	87	137.15	4.4517	0	1
16	H	1	95	97	137.25	4.4550	0	0
16	H	1	105	107	137.35	4.4586	0	0
16	H	1	115	117	137.45	4.4619	0	0
16	H	1	125	127	137.55	4.4655	0	0
16	H	1	135	137	137.65	4.4688	0	0
16	H	1	145	147	137.75	4.4721	0	0
16	H	2	5	7	138.25	4.4757	0	0
16	H	2	15	17	138.35	4.4790	0	0
16	H	2	25	27	138.45	4.4816	0	0

Table 2. ODP Hole 1000A. (1) Number of *G. theyeri* specimens observed during screening of a wider area of the SEM stub-filter from 10 samples below the SEM FCO depth of the species (136.43-137.15 mbsf (2) number of *G. theyeri* specimens observed during further qualitative observations. The age of samples is from Steph *et al.* (in revision).

Re-examination of the topotype material of *G. theyeri* Pujos (1987)

Our earliest common *Gephyrocapsa* specimens are extremely similar to the holotype of *G. theyeri* Pujos (1987), which was illustrated by SEM from the late Miocene Sample 572A-15-3, 0.1 cm (Leg 85, Eastern Equatorial Pacific). Pujos (1987), working almost exclusively by LM, reported *G. theyeri* as being abundant in the late Miocene at Site 572 and ranging down to the middle Miocene (zone NN4) (average relative abundance, ~20%) whereas other Pacific Sites contained no *G. theyeri* specimens in this time interval. These occurrences appeared highly anomalous in comparison to our data, which suggest a clear FO of the morphotype within the early Pliocene (Zone NN15, 137.15

mbsf, 4.45 Ma). A possible explanation of the anomaly is that the sample dating was wrong since there is evidence of slumping in the core and diatom data (Baldauf *et al.*, 1985) suggested a Pliocene age for the type interval. Therefore, we requested topotype samples from the DSDP in order to both check the age of the sample and confirm the abundance of the morphotype.

Sample age (LM). The holotype sample contains abundant but poorly preserved nannofossils, along with common diatoms. *Discoasters* are common but extensive searching revealed only two possible *D. quinqueramus* specimens (<0.1% of the total discoaster assemblage). The sample contains common *D. brouweri*, *D. surculus*, *S. abies*, and *R. pseudoumbilicus* >7 μm, so are clearly late Miocene - early Pliocene in age (NN11-15). *Discoaster* cf. *altus* and *Calcidiscus tropicus* with grill are both common suggesting an early Pliocene rather than late Miocene age (Young, 1998).

***Gephyrocapsa* presence (LM and SEM).** In LM, in the topotype samples, we did observe small reticulofenestrids which might be interpreted as having a bridge. In the SEM, however, we did not find any *Gephyrocapsa* specimens despite extensive searching. This raises the question whether sample confusion occurred and the holotype *G. theyeri* specimen actually came from another sample. In this case the age of the type specimen would have to be regarded as unknown.

FO of *G. theyeri*

The holotype of *G. theyeri* is morphologically identical to our specimens. The age of the type sample is ambiguous but from diatom data is most likely early Pliocene. However, since we could not confirm the presence of *G. theyeri* in the type sample it is possible that it was described from another early Pliocene sample. Therefore, *G. theyeri,* at Site 1000A, has the FO at sample 137.15 mbsf (4.45 Ma). Examination of micrographs of *G*. sp. 1 (Samtleben, 1980, his Pl. 12, figs 23-27), all from sample DSDP 41, 366A-7-5, 63-65 cm, indicates that only a few *G. theyeri* specimens, morphologically similar to the earliest specimens from Site 1000A are imaged, while the others are more similar to morphotypes that occur later at this site (Crudeli *et al*., in preparation 4). Re-examination of micrographs of Pirini Radrizzani & Valleri (1977) indicates that *G. theyeri* is present in the early Pliocene of the Tyrrhenian Sea (their Pl. 62, figs 6-8). Other morphotypes co-occur and may suggest that the FO of *G. theyeri* would be recorded in older sediments here. Hence, clear evidence exists that *G. theyeri* occurs in early Pliocene sediments from the Caribbean, Mediterranean and Pacific and so probably was globally distributed at low latitudes.

Phylogeny from morphology

G. theyeri specimens are similar in size, central-area and rim morphology to *R. alis* n. sp. and to the smaller specimens of *R. pujosiae* n. sp. In particular, the shape of the c-inner arch-elements of *R. alis* n. sp. are similar to the elements forming the bridge of *G. theyeri.* The c-inner arch-elements of *R. alis* n. sp. show clockwise imbrication, a geometric aspect related to the NE-SW direction of the bridge of *G. theyeri*. These morphological similarities suggest that *G. theyeri* and *R. alis* n. sp. are closely related.

***Gephyrocapsa* from the Miocene**

Whilst it is generally agreed that the first readily identifiable *Gephyrocapsa* specimens occur in the Pliocene there have been several records of *Gephyrocapsa* from the Miocene. As discussed above re-examination of the material worked on by Pujos (1987), who was a highly experienced nannofossil palaeontologist, shows that for these very small specimens SEM examination is necessary to confirm LM identifications of possible *Gephyrocapsa* specimens.

Gephyrocapsa specimens were illustrated by SEM by Bonci & Pirini-Radrizzani (1992) from a Messinian spongolithic level underlain by a Tortonian marly succession at the upper part of the S. Agata Fossili Formation, Italy. The specimen (Bonci & Pirini-Radrizzani, 1992, their Pl. 1, fig. 7) shows a low bridge with not clear offset and attribution to *Gephyrocapsa* may be arbitrary. *Gephyrocapsa* specimens were documented by LM and SEM by Triantaphyllou (2000) from Miocene diatomites (Metochia Formation, Gavdos Island, Greece) correlated with the Tripoli Formation (Hilgen *et al.*, 1995) (7.00-5.98 Ma, Hilgen & Krijgsman, 1999). The single specimen illustrated by SEM in proximal view (her Pl. I, fig. 13) is 3.8 µm in size and shows a bridge with NE-SW orientation that is very unlikely for *Gephyrocapsa* (Young, 1989). Jiang & Gartner (1984) reported small *Gephyrocapsa* in the middle and late Miocene (South Atlantic), but this record was not supported by SEM observations. Specimens were observed only at the shallowest (526A) out of the five close sites (Leg 74 Sites 525 to 529) analysed. Since reticulofenestrids have broad ecological adaptation, this single report appears anomalous unless the deeper sites are affected by strong dissolution. In these cores, sedimentation is partially disturbed, particularly in the middle late Miocene to Pliocene sections (Fütterer, 1984) and preservation of calcareous nannofossils is generally moderate to good. However, in the Miocene sections preservation of *Discoasters* is poor (Jiang & Gartner, 1984), so misidentification of forms can not be ruled out.

EVOLUTIONARY IMPLICATIONS

Time and place of diversification of the new species

We did not observe the species described in this work, or *Pseudoemiliania* coccoliths, during the SEM survey of the *G. theyeri* type material, that as discussed, is likely early Pliocene in age from LM. The absence could be due to unfavourable palaeoecological conditions at Site 572A or the species evolved later. Few ecologically restricted coccolithophores have been reported so far (e.g. Jerkovic, 1970), and endemism is not common in pelagic organisms such as coccolithophores. The lack of previous records of the species described here could be due to methods of study (LM vs. SEM), assemblage preservation or sampling resolution. At the relatively shallow and carbonate-saturated Site 1000A preservation of samples is exceptional supported by preserved delicate grill of very small reticulofenestrids, exceptionally preserved *Sphenolithus* and holococcoliths (our unpubl. data; Roth & Thierstein, 1972; Thierstein, 1980) and preserved delicate spines (Pl. 3). The composition of the nannoflora (Crudeli *et al.*, in preparation) and the biodiversity of reticulofenestrids (this work) suggest ecological complexity of the surface water at Caribbean Site 1000A. With respect to the oceanic setting, the palaeoecological-palaeoenvironmental conditions may have favoured high biodiversity in the Caribbean Sea and increased the change of observation of the species that are expected to have a global distribution at low latitude.

Adaptive radiation of *G. theyeri* and *R. calicis*

G. theyeri is a morphotype consistently recognised by SEM in these sediments and, comparison with modern species, suggests that *G. theyeri* likely represents a genuine species. The FO of *G. theyeri* lags the FCO by ~100kyr. The delay is roughly similar to that of the evolution of e.g. *E. huxleyi.* The first appearance and acme of *E. huxleyi* are separated by about 200kyr (Thierstein *et al.*, 1977; Berggren *et al.*, 1980). The microevolutionary study of the genus *Eiffellithus* (Watkins & Bergen, 2003) and of other calcareous nannofossils (Raffi *et al.*, 1998) show comparable time lags between FO and dominance. The increase of the species after its FO at Site 1000A indicates progressive adaptation and fitness and suggests that an optimal phenotype was developed by selection. From the Caribbean and the Eastern Equatorial Pacific, Kameo & Sato (2000) recorded by LM the FCO of small *Gephyrocapsa* at about 4.37 Ma. At site 1000A, the FCO occurrence of *G. theyeri* is very nearly synchronous. Nonetheless, the distribution of *G. theyeri* is clearly global as is indicated by previous SEM documentation discussed above.

Evolutionary forcing may be multiple and is still to be understood. *G. theyeri* and *R. calicis* show roughly opposite concentrations which suggests adaptation to separate ecological niches (Fig. 4). The two phylogenetically related species evolved almost synchronously and suggest a common triggering mechanism for these speciation events. It may be suggested that the significant palaeoceanographic changes occurring during the closure of the Panama Gateway (e.g. Steph *et al.*, in revision) had a significant impact on the diversification of the reticulofenestrids.

The Pliocene speciation events among the *Gephyrocapsa* group (Samtleben, 1980) or the diversification in the Quaternary, and the Pleistocene evolution of *E. huxleyi* (Thierstein *et al.*, 1977) testify a continuous pattern of diversification among reticulofenestrids. Although it is not clear if the disappearance of *R. calicis* is due to palaeoecology, it may suggest very fast evolution.

ACKNOWLEDGEMENTS

This research used samples provided by the Ocean Drilling Program. The ODP is sponsored by the U.S. National Science Foundation (NSF) and participating countries under management of Joint Oceanographic Institutions (JOI), Inc. Funding for this research was provided by Deutsche Forschungsgemeinschaft (DFG) Gateways Research Unit (Impact of Gateways on ocean circulation, climate, and evolution), Kiel University. U. Schuldt and B. Bader and C. Jones are warmly thanked for SEM assistance at Kiel University and at the NHM, London, respectively. We are grateful to E. Erba for help in literature searching and to Priska Schäfer and M. Weinelt for helpful comments.

This work represents part of the Doctor of Natural Sciences thesis at the University of Kiel of D.C.

REFERENCES

Andruleit, H. 1996. A filtration technique for quantitative studies of coccoliths. *Micropaleontology,* **42**(4): 403-406.

Baldauf, J.G. 1985. A high resolution late Miocene-Pliocene Diatom biostratigraphy for the Eastern Equatorial Pacific. *In:* Mayer, L., Theyer, F. *et al.* (Eds), *Initial Reports of the Deep Sea Drilling Project,* **85**. US Government Printing Office, Washington, 457-475.

Batvik, H., Heimdal, B.R., Fagerbakke, K.M. & Green, J.C. 1997. Effects of unbalanced nutrient regime on coccolith morphology and size in *Emiliania huxleyi* (Prymnesiophyceae). *European Journal of Phycology,* **32**: 155-165.

Beaufort, L. & Heussner, S. 2001. Seasonal dynamics of calcareous nannoplankton on a West European continental margin: The Bay of Biscay. *Marine Micropaleontology,* **43**: 27-55.

Berggren, W.A., Burckle, L.H., Cita, M.B., Cooke, H.B.S., Funnell, B.M., Gartner, S., Hays, J.D., Kennett, J.P., Opdyke, N.D., Pastouret, L., Shackleton, N.J. & Takayanagi, Y. 1980. Towards a Quaternary time scale. *Quaternary Research,* **13**: 277-302.

Bollmann, J. 1997. Morphology and biogeography of *Gephyrocapsa* coccoliths in Holocene sediments. *Marine Micropaleontology,* **29**: 319-350.

Bona, J. & Gal, M. 1985. Kalkiges Nannoplankton im Pannonien Ungarns. *In:* Papp, A., Jambor, A. & Steininger, F. (Eds), *Chronostratigraphie und Neostratotypen, Miocan der Zentralen Paratethys, M6 Pannonien.* Veda SAV, Bratislava, 482-515.

Bonci, M.C. & Pirini Radrizzani, C. 1992. Presence of small *Gephyrocapsae* in Late Miocene diatomaceous levels (S. Agata Fossili Formation, Serraville Scrivia, Alessandria, Italy). *Memorie di Scienze Geologiche, Padova,* **43**: 351-355.

Bown, P.R., Lees. J.A. & Young, J.R. 2004. Calcareous nannoplankton evolution and diversity through time. *In:* Thierstein, H.R. & Young, J.R. (Eds), *Coccolithophores - From molecular processes to global impact.* Springer, 481-506.

Cortés, M.Y., Bollmann, J. & Thierstein, H.R. 2001. Coccolithophore ecology at the HOT station ALOHA, Hawaii. *Deep Sea Research II,* **48**: 1957-1981.

Crudeli, D. & Kinkel, H. 2004. *Reticulofenestra calicis* n. sp., an unusual small reticulofenestrid coccolith from the Lower Pliocene of the South Caribbean Sea. *Micropaleontology,* **50**(4): 369-379.

Deflandre, G. & Fert, C. 1954. Observations sur les Coccolithophoridés actuels et fossiles en microscopie ordinaire et électronique. *Annales de Paléontologie,* **40**: 115-176.

Driever, B.W.M. 1988. Calcareous nannofossils biostratigraphy and paleoenvironmental interpretation of the Mediterranean Pliocene. *Utrecht Micropaleontological Bulletins,* **36**: 1-245.

Edvardsen B. Eikrem, W., Grenn, J.C., Andersen, R.A., Moon-van der Staay, S.Y. & Medlin, L.K. 2000. Phylogenetic reconstructions of the Haptophyta inferred from 18S ribosomal DNA sequences and available morphological data. *Phycologia,* **39**(1): 19-35.

Fütterer, D.K. 1984. Bioturbation and trace fossils in deep sea sediments of the Walvis Ridge, Southeastern Atlantic, Leg 74. *In:* Moore, T.C., Jr., Rabinowitz, P.D. *et al.* (Eds), *Initial Reports of the Deep Sea Drilling Project*, **74**. US Government Printing Office, Washington, 543-555.

Gartner, S. & Shyu, J.-P. 1996. Aspects of calcareous nannofossil biostratigraphy and abundance in the Pliocene and late Miocene of site 905. *In:* Mountain, G.S., Miller, K.G., Blum, P., Poag, C.W. & Twichell, D.C. (Eds), *Proceedings of the Ocean Drilling Program, Scientific Results,* **150**. College Station, TX (Ocean Drilling Program), 53-62.

Geisen, M., Billard, C., Broerse, A.T.C., Cros, L., Probert, I. and Young, J.R. 2002. Life-cycle associations involving pairs of holococcolithophorid species: intraspecific variation or cryptic speciation? European *Journal of Phycology*, **37**: 531-550.

Gibbs, S.J., Young, J.R., Bralower, T.J. & Shackleton, N.J. 2005. Nannofossil evolutionary events in the mid-Pliocene: an assessment of the degree of synchrony in the extinctions of *Reticulofenestra pseudoumbilicus* and *Sphenolithus abies*. *Palaeogeography Palaeoclimatology, Palaeoecology,* **217**: 155-172.

Gulyas, Jr.S. 2001. The palaeogeography of Lake Pannon during deposition of the Congeria rhomboidea beds. *Geologia Croatica,* **54**(1): 15-26.

Hagino, K., Okada, M., & Matsuoka, H. 2000. Spatial dynamics of coccolithophores assemblages in the Equatorial Western-Central Pacific Ocean. *Marine Micropaleontology,* **39**: 53-72.

Hay, W.W. & Beaudry, F.M. 1973. Calcareous nannofossils - Leg 15 Deep Sea Drilling Project. *In:* Edgar, N.T., Saunders, J.B. *et al.* (Eds), *Initial Reports of the Deep Sea Drilling Project,* **15**. US Government Printing Office, Washington, 625-683.

Heimdal, B.R. 1973. Two new taxa of recent coccolithophorids. *"Meteor" Forschungsergebnisse, Reihe D,* Biologie (13): 70-75.

Hilgen, F.J. & Krijgsman, W. 1999. Cyclostratigraphy and astrochronology of the Tripoli diatomite formation (pre-evaporite Messinian, Sicily, Italy). *Terra Nova,* **11**: 16-22.

Hilgen, F.J., Krijgsman, W., Langereis, C.G., Lourens, L.J., Santarelli, A. & Zachariasse, W.J. 1995. Extending the astronomical (polarity) time scale into the Miocene. *Earth and Planetary Science Letters,* **136**: 495-510.

Jerkovic, M.L. 1970. *Noëlaerhabdus* nov. gen. type d'une nouvelle famille de Coccolithophoridés fossiles: Noëlaerhabdus du Miocêne supérieur de Yougoslavie. *Comptes Rendus (Hebdomadaires des Séances) de l'Académie des Sciences de Paris, Série D,* **270**: 468-470.

Jiang, M.-J. & Gartner, S. 1984. Neogene and Quaternary calcareous nannofossil biostratigraphy of the Walvis Ridge. *In:* Moore, T.C., Jr., Rabinowitz, P.D. *et al.* (Eds), *Initial Reports of the Deep Sea Drilling Project,* **74**. US Government Printing Office, Washington, 561-595.

Jordan, R.W., Broerse, A.T.C., Hagino, K., Kinkel, H., Sprengel, C., Takahashi, K. & Young, J.R. 2000. Taxon lists for studies of modern nannoplankton. *Marine Micropaleontology,* **39**: 309-314.

Kameo, K. & Bralower, T.J. 2000. Neogene calcareous nannofossil biostratigraphy of Sites 998, 999, and 1000, Caribbean Sea. *In:* Leckie, R.M., Sigurdsson, H., Acton, G.D. & Draper, G. (Eds), *Proceedings of the Ocean Drilling Program, Scientific Results,* **165**. College Station, TX (Ocean Drilling Program), 3-17.

Kameo, K. & Sato, T. 2000. Biogeography of Neogene calcareous nannofossils in the Caribbean and the eastern equatorial Pacific-floral response to the emergence of the Isthmus of Panama. *Marine Micropaleontology,* **39**: 201-218.

Kamptner, E. 1943. Zur Revision der Coccolithineen-Spezies *Pontosphaera huxleyi* Lohm. Akademie der Wissenschaften in Wien, Anzeiger, 80, 11, 43-49.

Kleijne, A. 1990. Distribution and malformation of extant calcareous nannoplankton in the Indonesian Seas. *Marine Micropaleontology,* **16**: 293-316.

Lohmann, H. 1902. Die Coccolithophoridae, eine Monographie der Coccolithen bildenden Flagellaten, zugleich ein Beitrag zur Kenntnis des Mittelmeerauftriebs. *Archiv für Protistenkunde I*: 89-165.

Marino, M. & Flores, J.A. 2002. Miocene to Pliocene calcareous nannofossil biostratigraphy at ODP Leg 177 Sites 1088 and 1090. *Marine Micropaleontology,* **45**: 291-307.

Martini, E. 1971. Standard Tertiary and Quaternary calcareous nannoplankton zonation. *In:* Farinacci, A. (Ed.), *Proceeding of the II Planktonic Conference, Roma 1970.* Edizioni Tecnoscienza, Roma, 738-785.

Martini, E. 1980. Oligocene to recent calcareous nannoplankton from the Philippine Sea. *In:* Kroenke, L., Scott, R. *et al.* (Eds), *Initial Reports of the Deep Sea Drilling Project,* **59**. US Government Printing Office, Washington, 547-565.

Martini, E. 1993. *Emiliania coronata*, a new calcareous nannoplankton species from the North Atlantic Pleistocene. *Zitteliana,* **20**: 87-92.

Marunteanu, M. 1997. Evolution line of the endemic genus *Noelaerhabdus* (Pannonian; Pannonian Basin). *Acta Palaeontologica Romaniae,* **1**: 96-102.

Medlin, L.K., Barker, G.L.A., Campbell, L., Green, J.C., Hayes, P.K., Marie, D., Wrieden, S. & Vaulot, D. 1996. Genetic characterisation of *Emiliania huxleyi* (Haptophyta). *Journal of Marine Systems,* **9**: 13-32.

McIntyre, A. & Be, A.W.H. 1967. Modern coccolithophidae of the Atlantic Ocean – I. Placoliths and cyrtoliths. *Deep-Sea Research*, **14**:561-597.

Okada, H. 2000. Neogene and Quaternary Calcareous Nannofossils from the Blake Ridge, Sites 994, 995, and 997. *In:* Paull, C.K., Matsumoto, R., Fallace, P.J. & Dillon, W.P. (Eds), *Proceedings of the Ocean Drilling Program, Scientific Results,* **164**. College Station, TX (Ocean Drilling Program), 331-341.

Okada, H. & Honjo, S. 1975. Distribution of Coccolithophores in Marginal Seas along the Western Pacific Ocean and in the Red Sea. *Marine Biology,* **31**: 271-285.

Okada, H. & McIntyre, A. 1977. Modern coccolithophores of the Pacific and North Atlantic Oceans. *Micropaleontology,* **23**(1): 1-55.

Okada, H. & Bukry, D. 1980. Supplementary modification and introduction of code numbers to the low-latitude coccolith biostratigraphic zonation (Bukry, 1973; 1975). *Marine Micropaleontology,* **5**: 321-325.

Perch-Nielsen, K. 1985. Cenozoic calcareous nannofossils. *In:* Bolli, H.M., Saunders, J.B. & Perch-Nielsen, K. (Eds), *Plankton Stratigraphy*. Cambridge University Press, Cambridge, 427-554.

Pirini Radrizzani, C. & Valleri, G. 1977. New data on calcareous nannofossils from the Pliocene of the Tyrrhenian basin Site 132 DSDP, Leg 13. *Rivista Italiana di Paleontologia e Stratigrafia,* **83**(4): 897-924.

Pujos, A. 1987. Late Eocene to Pleistocene medium-sized and small-sized "Reticulofenestrids". *In:* Stradner, H. & Perch-Nielsen, K. (Eds), *Proceeding of the International Nannoplankton Association Meeting, Vienna 1985. Abhandlungen der Geologischen Bundesanstalt,* **39**: 239-277.

Raffi, I., Backman, J. & Rio, D. 1998. Evolutionary trends of tropical calcareous nannofossils in the late Neogene. *Marine Micropaleontology,* **35**: 17-41.

Rio, D. 1982. The fossil distribution of coccolithophore genus *Gephyrocapsa* Kamptner and related Plio-Pleistocene chronostratigraphic problems. *In:* Prell, W.L., Gardner, J.V. *et al.* (Eds), *Initial Reports of the Deep Sea Drilling Project,* **68**. US Government Printing Office, Washington, 325-343.

Roth, P.H. 1970. Oligocene calcareous nannoplankton biostratigraphy. *Eclogae Geologicae Helvetiae,* **63**: 799-881.

Roth, P.H. & Thierstein, H. 1972. Calcareous nannoplankton: Leg 14 of the Deep Sea Drilling Project. *In:* Hayes, D.E., Pimm, A.C. *et al.* (Eds), *Initial Reports of the Deep Sea Drilling Project,* **14**. US Government Printing Office, Washington, 421-485.

Sáez, A.G., Probert, I., Geisen, M., Quinn, P., Young, J.R. and Medlin, L.K. 2003. Pseudo-cryptic speciation in coccolithophores. *Proceedings of the National Academy of Sciences of the United States of America,* 100, **12**: 7163-7168.

Sato, T., Kameo, K., & Takayama, T. 1991. Coccolith biostratigraphy of the Arabian Sea. *In:* Prell, W.L., Niitsuma, N. *et al.* (Eds), *Proceedings of the Ocean Drilling Program, Scientific Results,* **117**. College Station, TX (Ocean Drilling Program), 37-54.

Samtleben, C. 1980. Die Evolution der Coccolithophoriden-Gattung *Gephyrocapsa* nach Befunden im Atlantik. *Paläontologische Zeitschrift,* **54**(1/2): 91-127.

Sigurdsson, H., Leckie, R.M., Acton, G.D. *et al.* 1997. *Proceedings of the Ocean Drilling Program, Initial Reports,* **165**. College Station, TX (Ocean Drilling Program).

Steph, S., Tiedemann, R., Groenevel, J., Nürnberg, D., Reuning, R. & Haug, G. in revision. Changes in Caribbean surface hydrography during the Pliocene shoaling of the Central American Seaway. *Paleoceanography*.

Takahashi, K., & Okada, H. 2000. The paleoceanography for the last 30,000 years in the southeastern Indian Ocean by means of calcareous nannofossils. *Marine Micropaleontology,* **40**: 83-103.

Thierstein, H.R. 1980. Selective dissolution of late Cretaceous and earliest Tertiary calcareous nannofossils: experimental evidence. *Cretaceous Research,* **2**: 165-176.

Thierstein, H.R., Geitzenauer, K.R., Molfino, B. & Shackleton, N.J. 1977. Global synchroneity of late Quaternary coccolith datum levels; validation by oxygen isotopes. *Geology,* **5**: 4000-4004.

Triantaphyllou, M. 2000. Short note on the occurrence of small *Gephyrocapsa* species and birefringent ceratoliths in Messinian diatomites (Gavdos Island, Southern Greece). *Journal of Nannoplankton Research,* **22**(1): 37-40.

Watkins, D.K. & Bergen, J.A. 2003. Late Albian adaptive radiation in the calcareous nannofossil genus *Eiffellithus*. *Micropaleontology,* **49**(3): 231-252.

Winter, A., Reiss, Z. & Luz, B. 1978. Living *Gephyrocapsa protohuxleyi* McIntyre in the Gulf of Elat (Aqaba). *Marine Micropaleontology,* 3: 295-298.

Young, J.R. 1989. Observations on heterococcolith rim structure and its relationship to developmental processes. *In:* Crux, J. & van Heck, S.E. (Eds), *Nannofossils and their applications. Proceeding Second International Nannoplankton Association Symposium, London 1987.* Ellis Horwood Limited, Chichester, 1-20.

Young, J.R. 1990. Size variation of Neogene *Reticulofenestra* coccoliths from Indian Ocean DSDP cores. *Journal of Micropalaeontology,* **9**(1): 71-86.

Young, J.R. 1994a. Variation in *Emiliania huxleyi* cocccolith morphology in samples from the norwegian Ehux experiment, 1992. *Sarsia,* **79**: 417-425.

Young, J.R. 1994b. Functions of coccoliths. *In:* Winter, A. & Siesser, W.G. (Eds), *Coccolithophores.* Cambridge University Press, Cambridge, 63-82.

Young, J.R. 1998. Neogene nannofossils. *In:* Bown, P.R. (Ed), *Calcareous Nannofossil Biostratigraphy.* Kluwer Academic Publisher, Cambridge, 225-265.

Young, J.R. & Westbroek, P. 1991. Genotypic variation in the coccolithophorid species *Emiliania huxleyi*. *Marine Micropaleontology,* **18**: 5-23.

Young, J.R. & Bown, P.R. 1997. Cenozoic calcareous nannoplankton classification. *Journal of Nannoplankton Research,* **19**: 36-47.

Young, J.R. & Henriksen, K. 2003. Biomineralization within vesicles: the calcite of coccoliths. *In:* Dove, P.M., J. De Yoreo, J. & Weiner, S. (Eds), *Reviews in Mineralogy and Geochemistry 54,* 189-215.

Young, J.R., Didymus, J.M., Bown, P.R., Prins, B. & Mann, S. 1992. Crystal assembly and phylogenetic evolution in heterococcoliths. *Nature*, **356**: 516-518.

Young, J.R., Bown, P.R. & Burnett, A. 1994. Palaeontological perspectives. *In:* Green, J.C. & Leadbeater, B.S.C. (Eds), *The Haptophyte Algae.* Clarendon Press, Oxford, 379-392.

Young, J.R., Bergen, J.A., Bown, P.R., Burnett, J.A., Fiorentino, A., Jordan, R.W., Kleijne, A., van Niel, B.E., Romein, A.J.T. & von Salis, K. 1997. Guidelines for coccolith and calcareous nannofossil terminology. *Palaeontology,* **40**: 875-912.

Young, J.R., Davis, S.A., Bown, P.R. & Mann, S. 1999. Coccolith ultrastructure and biomineralisation. *Journal of Structural Biology,* **126**: 195-215.

Young, J.R., Geisen, M., Cros, L., Kleijne, A., Sprengel, C., Probert, J. & Østergaard, J. 2003. A guide to extant coccolithophore taxonomy. *Journal of Nannoplankton Research,* **1**: 1-125.

Young, J.R., Geisen, M. & Probert, J. in press. A review of selected aspects of coccolithophore biology with implications for palaeobiodiversity estimation. *Micropaleontology*.

Explanation of Plate 1. New very small reticulofenestrids from the early Pliocene of the Caribbean Sea**.** For each illustration, the ODP Sample, micrograph code, SEM magnification and scale bar are given.

fig. 1. *Reticulofenestra alis* n. sp. type 1, distal view, holotype, 16H-1, 5-7 cm (136.35 mbsf), 83323, 20000×, 1 µm.

fig. 2. *R. alis* n. sp. type 1, distal-oblique view. View of the arch-shaped structure from the inside. This extends vertically. The inner tube elements, from the longitudinal pole progressively extend upward and maintain anticlockwise imbrication, they change imbrication in correspondence of a kink, paratype, 16H-1, 75-77cm (137.05 mbsf), 82675, 20000×, 1 µm.

fig. 3. *R. alis* n. sp. type 1, distal-oblique view. View of the arch-shaped structure from the outside. From the distal shield level, the outer arch-elements extend vertically, are enlarged upwards showing sub-polygonal crystal face, SEM tilt 30°, paratype, 16H-1, 5-7 cm (136.35 mbsf), 83159, 20000×, 1 µm.

fig. 4. *R. alis* n. sp. type 1, distal-oblique view. The arch extends slightly inward. Note the crystal faces of the terminations of the arch-elements, paratype, 16H-1, 75-77 cm (137.05 mbsf), 82666, 20000×, 1 µm.

fig. 5. *R. alis* n. sp. type 1, distal-oblique view. The arch extends inward and commences slightly before the longitudinal pole (lower side). The upward terminations of the arch-elements show well developed crystal faces. Note a few overgrowth on the distal shield (lower end on the coccolith), paratype, 15H-0, 5-7 cm (136.43 mbsf), 84171, 34000×, 300nm.

fig. 6. *R. alis* n. sp., distal view. One arch develops along one side whereas on the opposite side three inner tube elements show low extension, note the upward vertical orientation of the outer arch-elements (right side of the form), paratype, 16H-1, 135-137 cm (137.65 mbsf), 82964, 25000×, 1 µm.

fig. 7. *R. alis* n. sp. type 2, distal-oblique view. Two arches develop along the coccolith sides. The inner tube elements close to the longitudinal poles, do not extend, SEM tilt 26°, paratype, 16H-1, 5-7 cm (136.35 mbsf), 83321, 20000×, 1 µm.

fig. 8. *R. alis* n. sp. type 2, side view. The outer arch-elements extend vertically and are enlarged upward, a few overgrowth occurs on the shield, SEM tilt 40°, paratype, 15H-7, 25-27 cm (136.05 mbsf), 84166, 30000×, 300nm.

fig. 9. *R. alis* n. sp. type 2, distal view. The arches are asymmetric along the coccolith side, paratype, 16H-1, 5-7 cm (136.35 mbsf), 83319, 20000×, 1 µm.

fig. 10. *R. alis* n. sp. type 2, distal-oblique view. One arch develops asymmetrically along the coccolith side and it is continuous with the second symmetric arch, paratype, 16H-1, 35-37 cm (136.65 mbsf), 82702, 20000×, 1 µm.

fig. 11. *R. alis* n. sp. type 4, distal-oblique view. On the opposite side of the arch, the inner tube elements slightly extend above the shield level. The rim is slightly wider with respect to that of *R. alis* n. sp. type 1. The central area is covered by bars enlarged inward., paratype, 15H-7, 63-65 cm (136.43 mbsf), 83005, 20000×, 1 µm. Lower left side of the image, *R. premoliae* n. sp.

fig. 12. *R. alis* n. sp. type 4, distal view. Note incipient hammer-like morphology of elements terminations, paratype, 15H-7, 25-27 cm (136.05 mbsf), 86594, 20000×,1 µm.

fig. 13. *R. alis* n. sp. type 5, distal view. Two arches develop asymmetrically along the sides, paratype, 15H-7, 15-17 cm (135.95 mbsf), 83264, 20000×, 1 µm.

fig. 14. *R. alis* n. sp. type 5, distal view. Note the upward vertical orientation of the outer arch-elements (right side of the form), paratype, 15H-7, 55-57 cm (136.35 mbsf), 86124, 20000×, 1 µm.

fig. 15. *R. alis* n. sp. type 5, distal-oblique view. Arch-shaped structure viewed from the inside and outside, paratype, 15H-7, 63-65 cm (136.43 mbsf), 83313, 20000×, 1 µm.

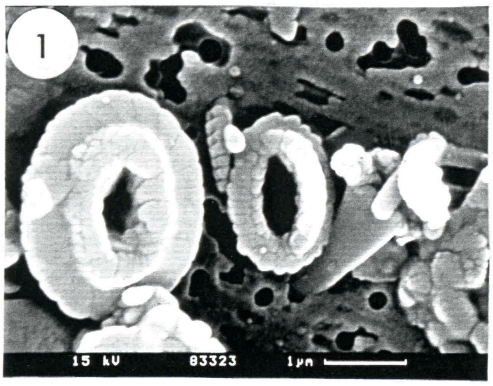
1
15 kV 83323 1µm

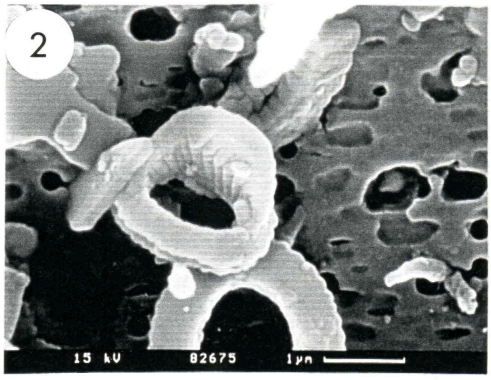
2
15 kV 82675 1µm

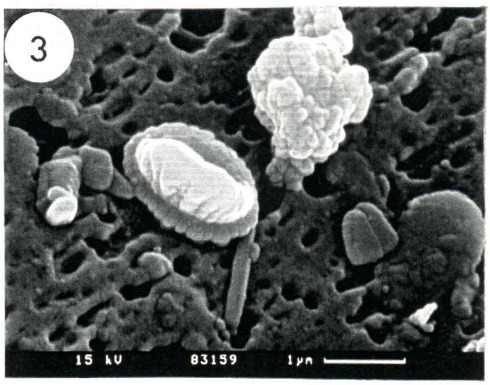
3
15 kV 83159 1µm

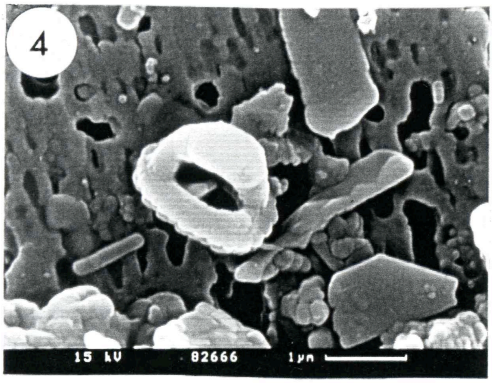
4
15 kV 82666 1µm

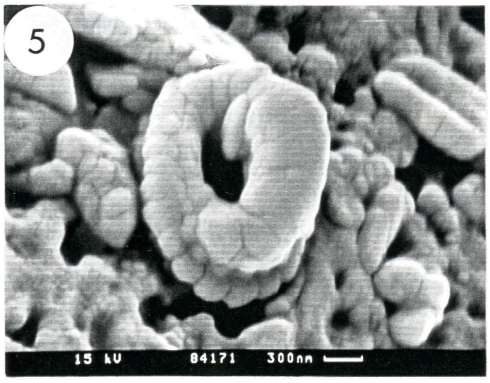
5
15 kV 84171 300nm

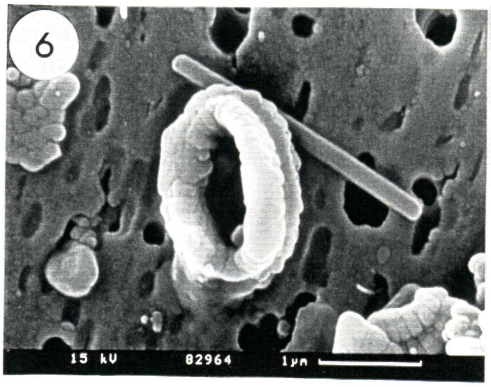
6
15 kV 82964 1µm

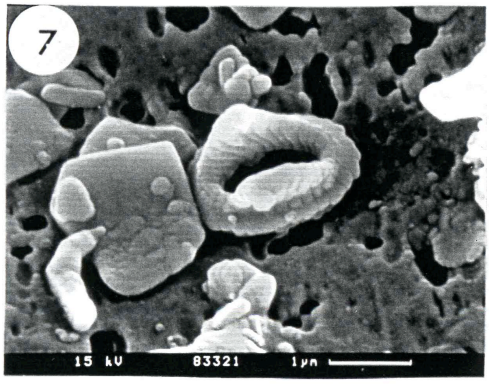
7
15 kV 83321 1µm

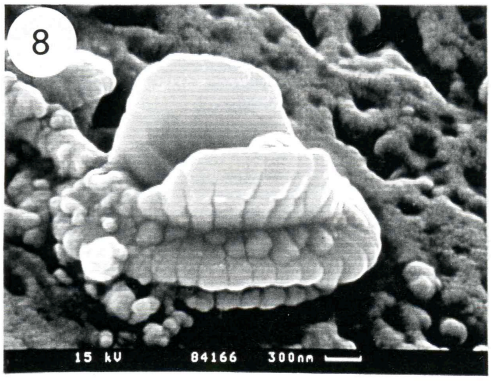
8
15 kV 84166 300nm

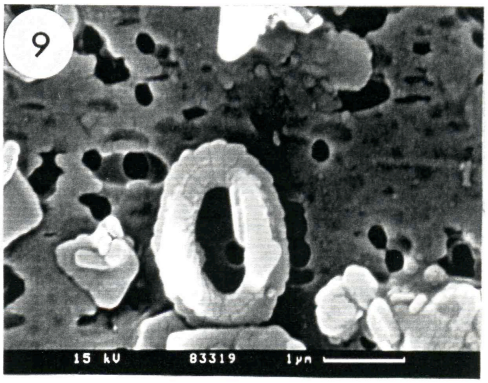
9
15 kV 83319 1µm

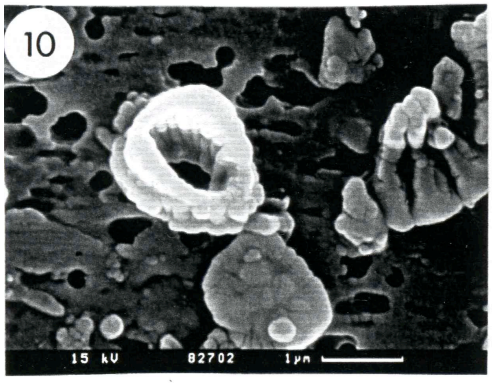
10
15 kV 82702 1µm

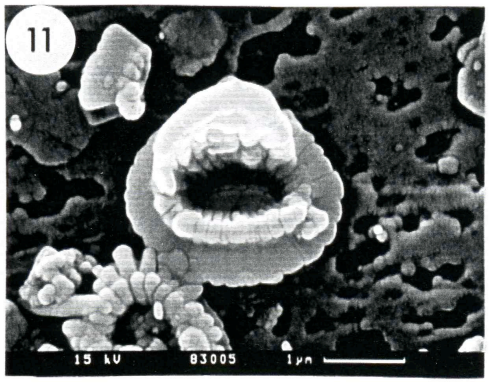
11
15 kV 83005 1µm

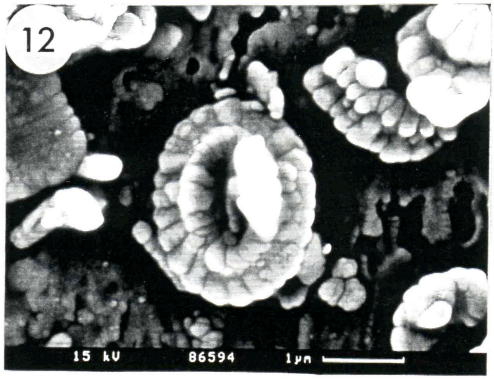
12
15 kV 86594 1µm

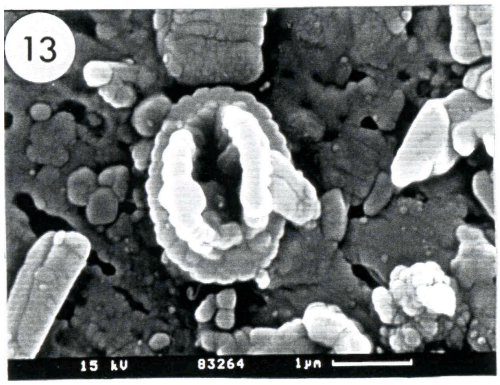
13
15 kV 83264 1µm

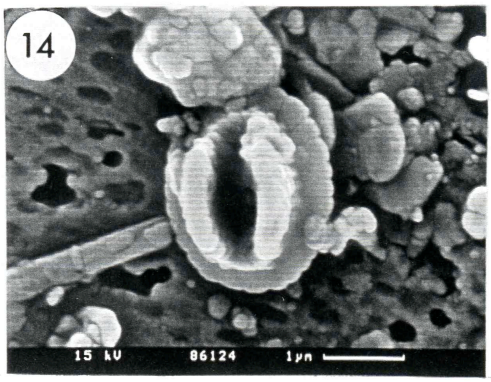
14
15 kV 86124 1µm

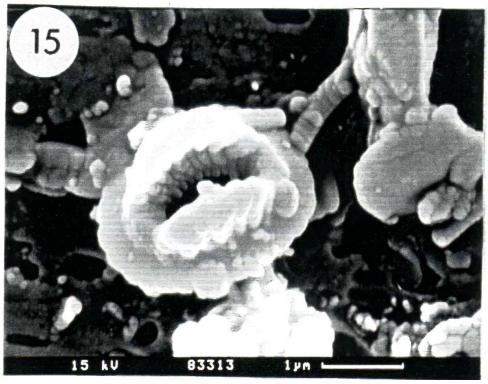
15
15 kV 83313 1µm

Explanation of Plate 2. New very small reticulofenestrids from the early Pliocene of the Caribbean Sea. See caption to Plate 1 for details on entries.

fig. 1. *R. alis* n. sp. type 3, distal view. The elements that extend above the distal shield level do not show imbrication, are massive and variably extend inwards closing the central area, paratype, 15H-7, 25-27 cm (136.05 mbsf), 83164, 20000×, 1 µm.

fig. 2. *R. alis* n. sp. type 3, distal view, paratype, 15H-2, 125-127 cm (129.55 mbsf) 82922, 20000×, 1 µm.

fig. 3. *R. alis* n. sp. type 3, distal-oblique view (left side of the illustration), paratype, 15H-2, 105-107 cm (129.35 mbsf), 81929, 20000×, 1 µm. On the right side, *R. premoliae* n. sp. in side view.

fig. 4. Three *R. alis* n. sp. type 3 specimens, distal view, paratypes, 15H-2, 105-107 cm (129.35 mbsf), 81930, 20000×, 1 µm.

fig. 5. Two *R. alis* n. sp. type 3 specimens, distal view. The specimens show a wider central area and the extension are moderately massive, paratypes, 15H-1, 45-47 cm (127.25 mbsf), 85452, 20000×, 1 µm.

fig. 6. *Reticulofenestra. pujosiae* n. sp., distal view. A few inner tube elements, close to the longitudinal poles show low extension, paratype, 16H-2, 25-27 cm (138.45 mbsf), 85443, 20000×, 1 µm.

fig. 7. *R. pujosiae* n. sp., distal view. The rim is particularly narrow and discontinuous, dissolution may have occurred, paratype, 16H-2, 25-27 cm (138.45 mbsf), 85960, 20000×, 1 µm.

fig. 8. *R. pujosiae* n. sp., distal view. The NE low extensions show an arch-like morphology, paratype, 16H-1, 85-87 cm (137.15 mbsf), 84335, 20000×, 1 µm.

fig. 9. *R. pujosiae* n. sp., distal view. Few elements (SW position) are slightly shorter, paratype, 16H-1, 5-7 cm (136.35 mbsf), 84550, 20000×, 1 µm.

fig. 10. *R. pujosiae* n. sp., distal view. A few inner tube elements, after the longitudinal pole (NE-SW), weakly extend, paratype, 16H-2, 25-27 cm (138.45 mbsf), 85962, 20000×, 1 µm.

fig. 11. *R. pujosiae* n. sp., distal view. The low extensions show an arch-like morphology. A few elements are weakly slitted with incipient hammer-like terminations, holotype, 16H-2, 25-27 cm (138.45 mbsf), 85444, 20000×, 1 µm.

fig. 12. *Gephyrocapsa theyeri,* distal view, 16H-1, 75-77 cm (137.05 mbsf), 82970, 25000×, 1 µm.

fig. 13. *G. theyeri,* distal view, 16H-1, 35-37 cm (136.65 mbsf), 82699, 30000×, 300nm.

fig. 14. *G. theyeri,* distal view. Note the crystal face of the elements terminations of the bridge and vertical orientation from the shield, 15H-7, 55-57 cm (136.35 mbsf), 83314, 20000×, 1 µm.

fig. 15. *G. theyeri,* distal-oblique view, 15H-7, 55-57 cm (136.35 mbsf), 83316, 25000×, 1 µm.

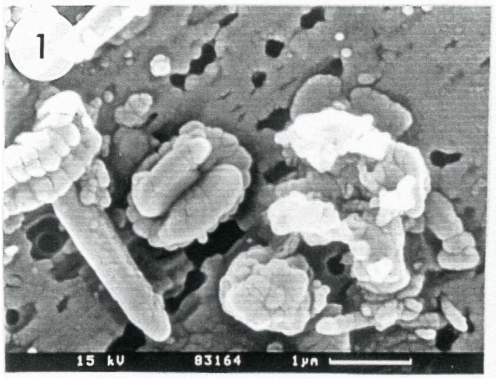
1
15 kV 83164 1µm

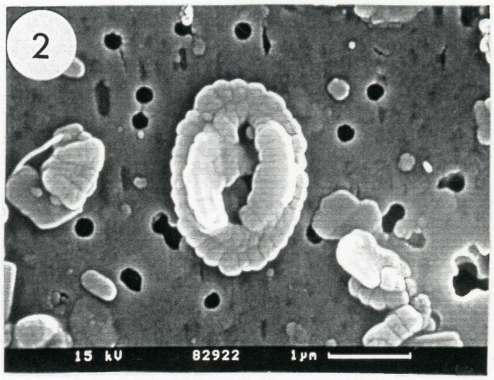
2
15 kV 82922 1µm

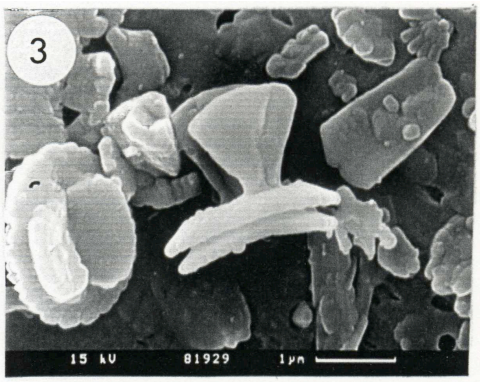
3
15 kV 81929 1µm

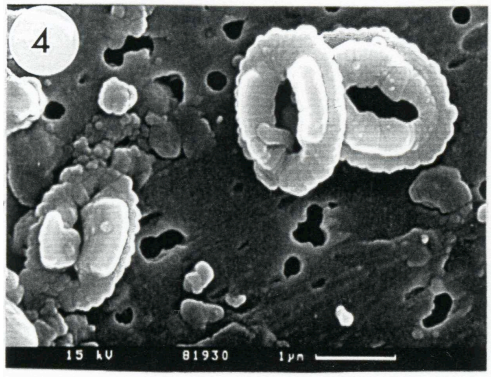
4
15 kV 81930 1µm

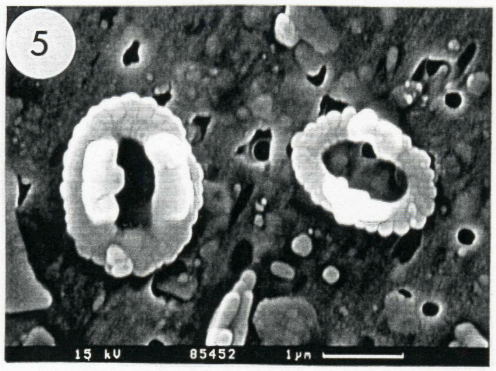
5
15 kV 85452 1µm

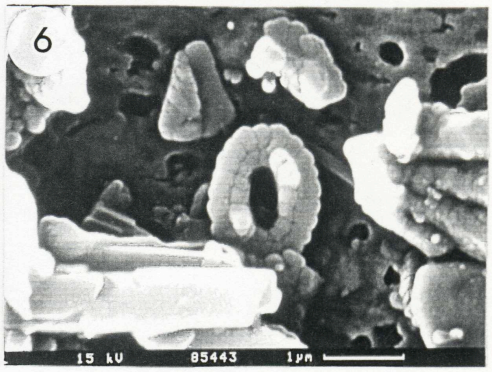
6
15 kV 85443 1µm

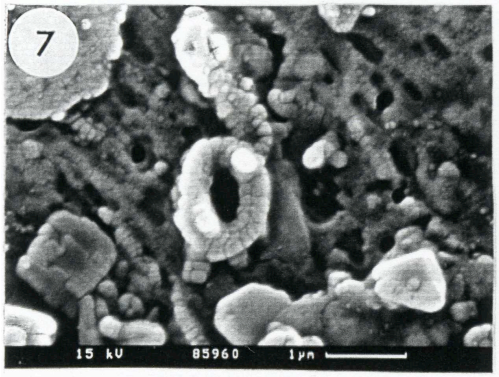
7
15 kV 85960 1µm

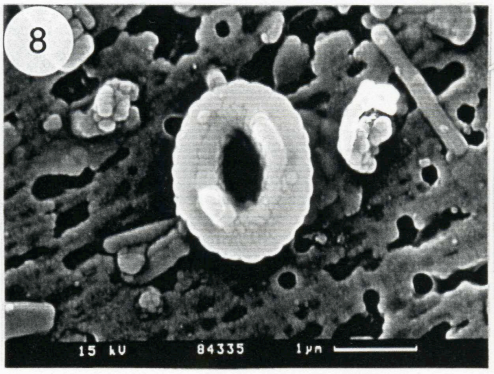
8
15 kV 84335 1µm

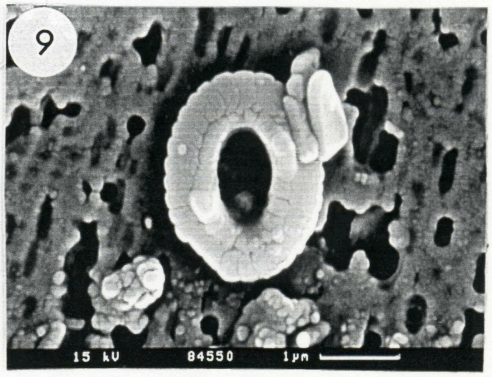
9
15 kV 84550 1µm

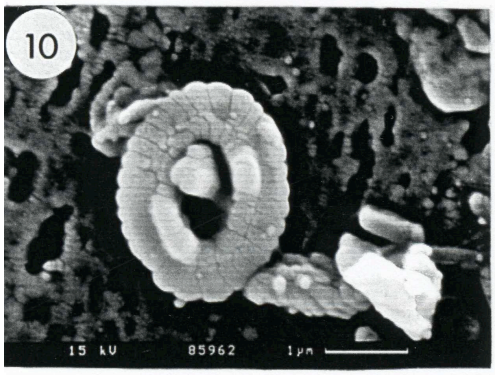
10
15 kV 85962 1µm

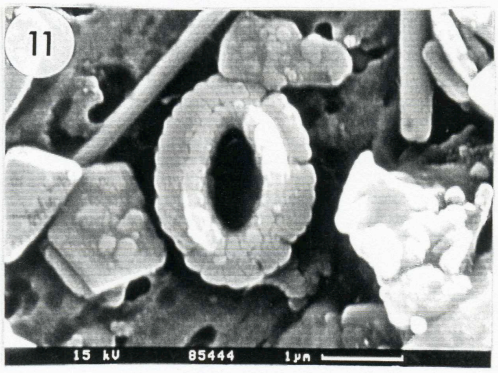
11
15 kV 85444 1µm

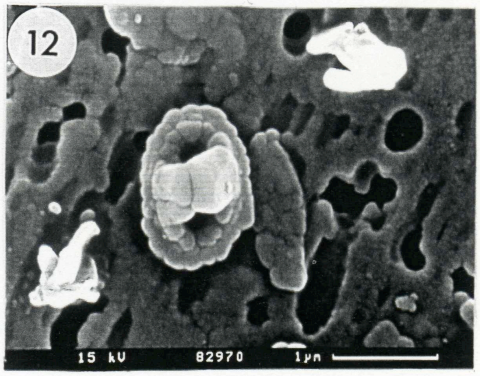
12
15 kV 82970 1µm

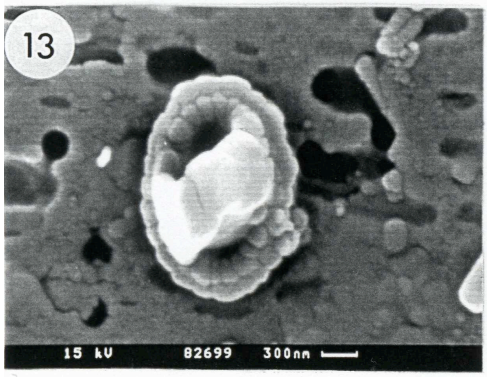
13
15 kV 82699 300nm

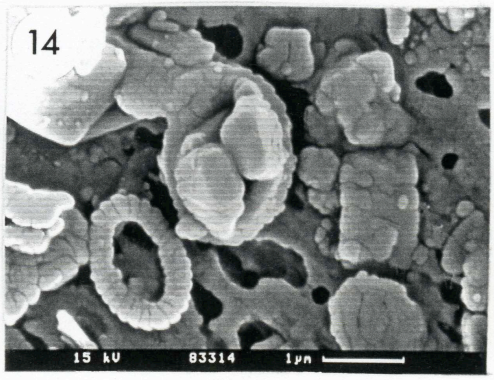
14
15 kV 83314 1µm

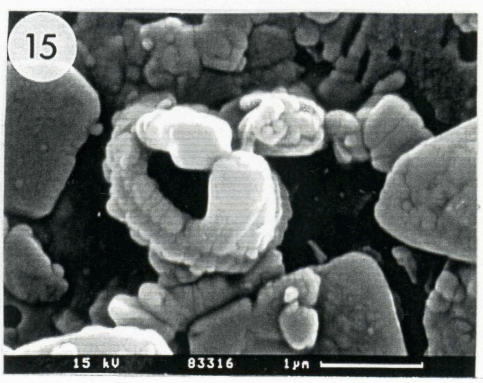
15
15 kV 83316 1µm

Explanation of Plate 3. New very small reticulofenestrids from the early Pliocene of the Caribbean Sea. See caption to Plate 1 for details on entries.

fig. 1. *Reticulofenestra. premoliae* n. sp. type 1, distal-oblique view. The extensions on one side of the shield (upper side) are very likely remains of spines, grill elements conjunct forming a median suture, holotype, 15H-4, 5-7 cm (131.35 mbsf), 82557, 20000×, 1 µm.

fig. 2. *R. premoliae* n. sp. type 1, distal view. Spines develop at/close to the transversal pole, he central area bars give rise to a prominent calcification, paratype, 16H-1, 85-87 cm (137.15 mbsf), 82663, 20000×, 1 µm.

fig. 3. *R. premoliae* n. sp. type 1, proximal-oblique view. The central area elements are conjunct with the distal shield elements. Tooth like protrusions are present around the central area, paratype, 15H-5, 15-17 cm (132.95 mbsf), 83122, 20000×, 1 µm.

fig. 4. *R. premoliae* n. sp. type 1, distal-oblique view, SEM tilt 30°, paratype, 15H-4, 95-97 cm (132.25 mbsf), 83144, 20000×, 1 µm.

fig. 5. *R. premoliae* n. sp. type 2, distal-oblique view. The extensions on the sides of the shield are very likely remains of spines, calcified central area median suture, paratype, 15H-2, 95-97 cm (129.25 mbsf), 81949, 19300×, 1 µm.

fig. 6. *R. premoliae* n. sp. type 2, distal view. Few inner tube elements close to and at the transverse pole show a slightly higher degree of extension above the distal shield level with respect to the other, these are likely remain of spines, paratype, 15H-4, 95-97 cm (132.25 mbsf), 83140, 20000×, 1 µm.

fig. 7. Three specimens of *R. premoliae* n. sp. type 2 in distal view. Upper side, type 2A, right side, type2B, lower left side, intermediate specimens. Paratypes, 15H-3, 5-7 cm (129.85 mbsf), 81866, 8300×, 3 µm.

fig. 8. Transitional form between *R. premoliae* n. sp. type 1-2 and *R. premoliae* n. sp. type 3-4, distal view, paratype, 15H-7, 63-65 cm (136.43 mbsf), 86591, 20000×, 1 µm.

fig. 9. *R. premoliae* n. sp. type 3, distal view, paratype, 15H-6, 135-137 cm (135.65 mbsf), 83112, 20000×, 1 µm.

fig. 10. *R. premoliae* n. sp. type 3, distal-oblique view. SEM tilt 38°, paratype, 15H-0, 5-7 cm (136.43 mbsf), 84174, 20000×, 1 µm.

fig. 11. *R. premoliae* n. sp. type 3, distal-oblique view. Note the highly calcified spines, paratype, 15H-6, 115-117 cm (135.45 mbsf), 84564, 20000×, 1 µm.

fig. 12. *R. premoliae* n. sp. type 4, distal view, paratype, 16H-1, 85-87 cm (137.15 mbsf), 84336, 25000×,1 µm.

fig. 13. *R. premoliae* n. sp. type 4, distal view, paratype, 15H-0, 5-7 cm (136.43 mbsf), 85439, 20000×, 1 µm.

fig. 14. *R. premoliae* n. sp. type 4, distal view. A single inner tube element close to the transverse pole (right side) weakly extends. The distal shield elements along the ends show a higher degree of slitting and have incipient hammer-like terminations. Those along the side have a less pronounced degree of slitting and show sub-rounded terminations. The inner tube elements are not imbricated, paratype, 15H-6, 115-117 cm (135.45 mbsf), 83266, 20000×, 1 µm.

fig. 15. *R. premoliae* n. sp. type 5, distal view, paratype, 16H-1, 85-87 cm (137.15 mbsf), 84334, 20000×, 1 µm.

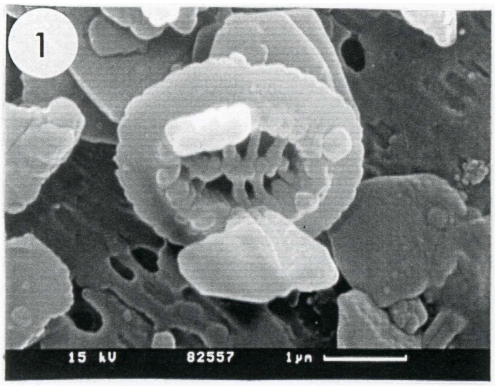
1
15 kV 82557 1µm

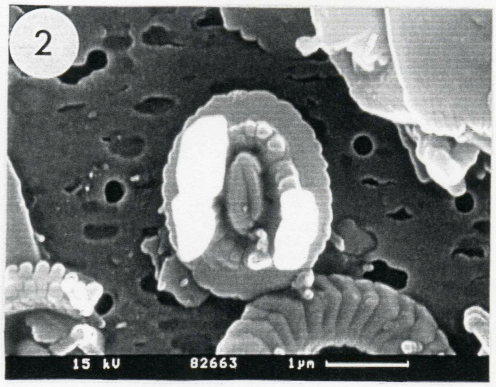
2
15 kV 82663 1µm

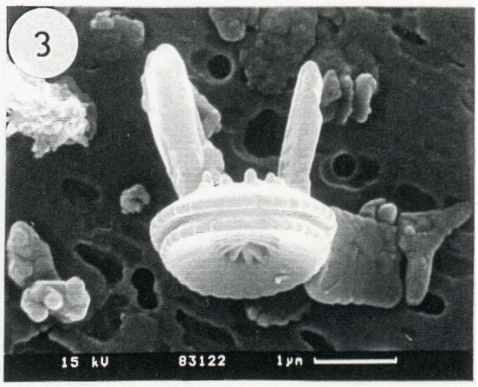
3
15 kV 83122 1µm

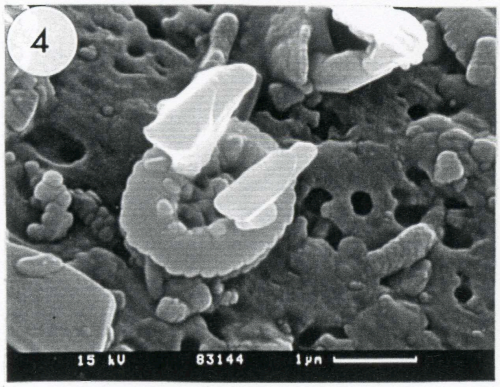
4
15 kV 83144 1µm

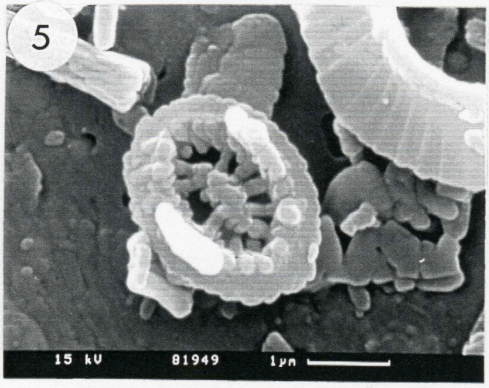
5
15 kV 81949 1µm

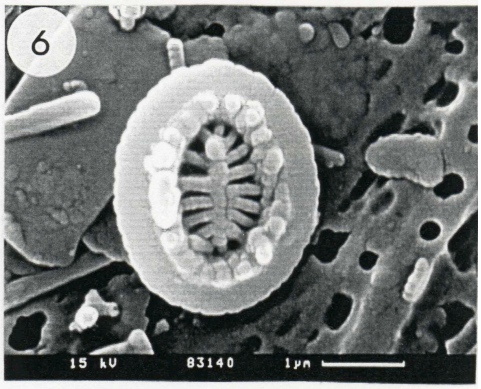
6
15 kV 83140 1µm

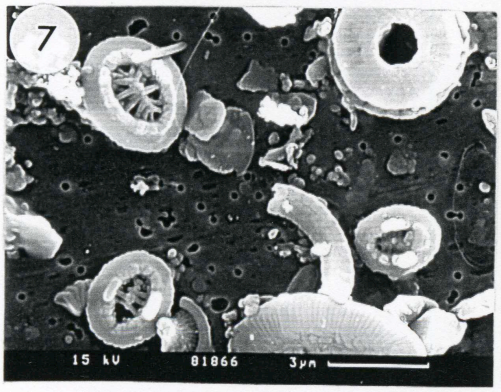
7
15 kV 81866 3µm

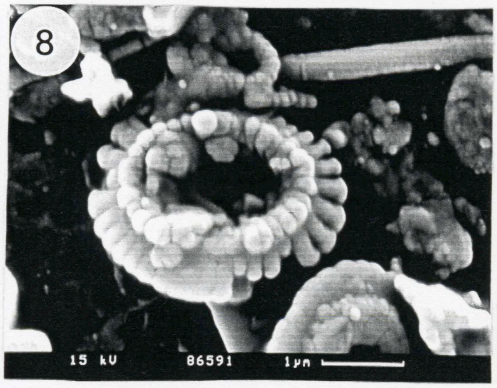
8
15 kV 86591 1µm

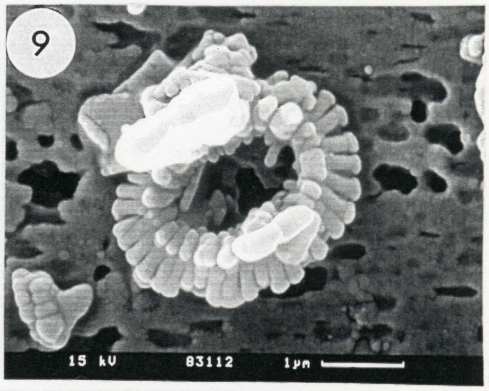
9
15 kV 83112 1µm

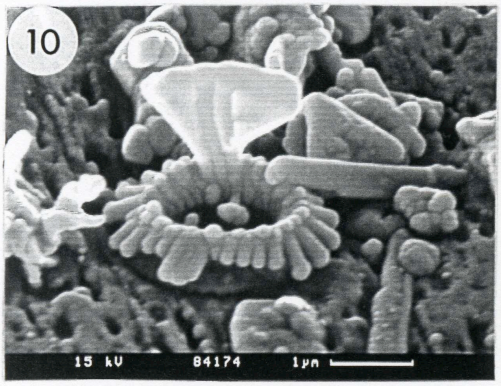
10
15 kV 84174 1µm

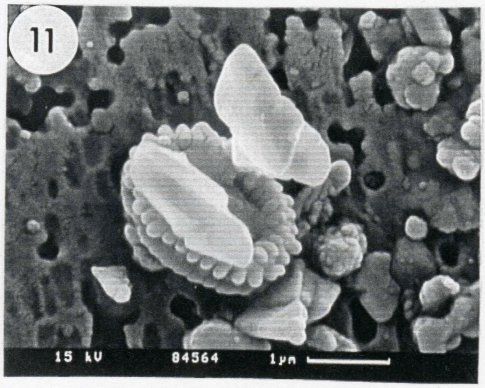
11
15 kV 84564 1µm

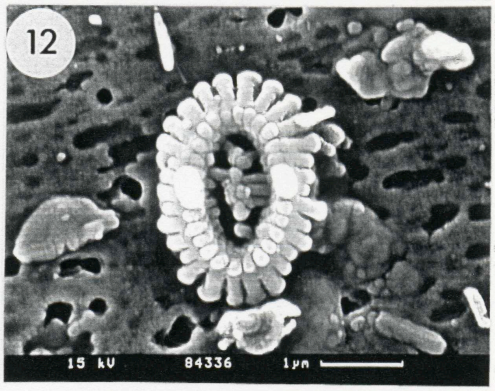
12
15 kV 84336 1µm

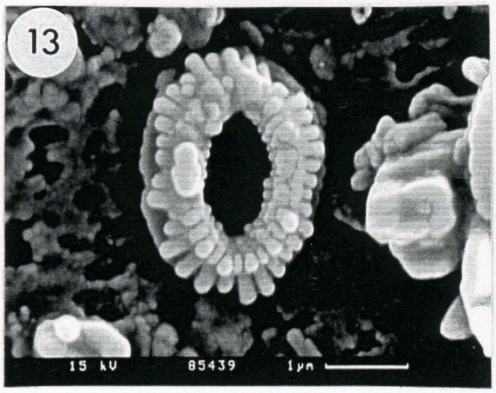
13
15 kV 85439 1µm

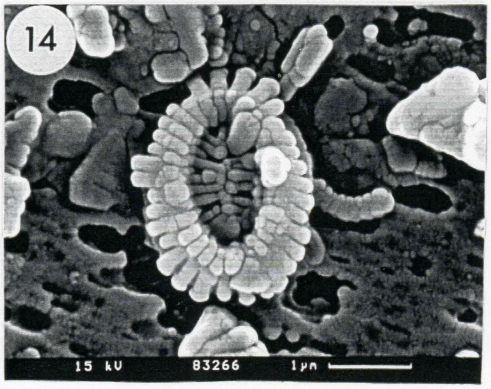
14
15 kV 83266 1µm

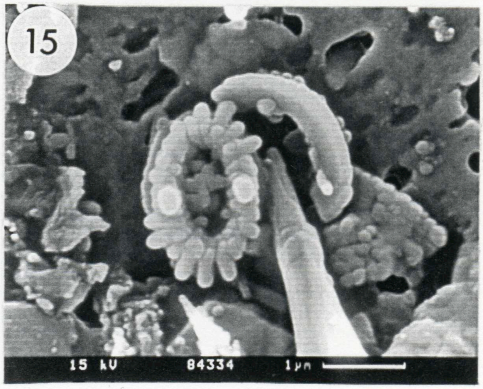
15
15 kV 84334 1µm

CHAPTER 4

Behind the increase in size of small *Gephyrocapsa*: the earliest adaptive radiation of the populations (early Pliocene, South Caribbean Sea)

Daniela Crudeli[1], Jeremy R. Young[2], Hanno Kinkel[1]

[1]Institute for Geosciences, Christian-Albrechts-Universität Kiel, Ludewig-Meyn-Str.10, 24118 Kiel, Germany.

[2]Palaeontology Dept., Cromwell Road, The Natural History Museum, London SW7 5BD, UK.

Manuscript to be submitted to Marine Micropaleontology

CHAPTER 4

Behind the increase in size of small *Gephyrocapsa*: the earliest adaptive radiation of the populations (early Pliocene, South Caribbean Sea)

Daniela Crudeli[1], Jeremy R. Young[2], Hanno Kinkel[1]
[1]Institute for Geosciences, Christian-Albrechts-Universität Kiel, Ludewig-Meyn-Str.10, 24118 Kiel, Germany.
[2]Palaeontology Dept., Cromwell Road, The Natural History Museum, London SW7 5BD, UK.

Abstract

We documented, for the first time, a high-resolution pattern of size variation of small *Gephyrocapsa* from the first consistent occurrence (FCO) of *G. theyeri* until 3.8 Ma (early Pliocene, Hole 1000A). Morphometry and qualitative scanning electron microscope observations allow us to recognise five new, phylogenetically related *Gephyrocapsa* species, which may have evolved from *G. theyeri*. Taxonomic description includes morphometry on the types of the species. Quantitative and qualitative data are used to qualitatively trace the occurrence of the species in the cores.

Two new species occurred soon after the FCO of G. *theyeri*, nearly synchronously with the first occurrence (FO) of *R. calicis,* this is associated with phenetic variation among *G. theyeri* and indicates a strong evolutionary pressure on populations. The time-progressive size increase of small *Gephyrocapsa* was associated with further evolutionary events. These correlate at basin-wide scale, suggesting a continuous and complex pattern of radiation. Documented biodiversity is in agreement with ample genetic-phenetic variability of these coccolithophores.

Size variations closely follow changes in paleofluxes and suggest an ecology control. Abundance changes correlate with the light microscope (LM) pattern on small *Gephyrocapsa* and suggest that evolution may have been triggered by basin wide variation in the ecological conditions of the water column.

Patterns in size variation are surprisingly similar to those of the Quaternary and suggest that the latter are also evolutionary. Thus, widely documented cyclic size variation in reticulofenestrids are likely evolutionary.

The light microscope FCO of small *Gephyrocapsa* and acme are evolutionary and are reliable biostratigraphic events.

Major changes in surface water circulation in the Caribbean area and in the Equatorial Pacific linked to the closure of the Isthmus of Panama likely played an important role in the evolutionary radiation of *Gephyrocapsa.*.

Keywords: *Gephyrocapsa*; microevolution; early Pliocene; Caribbean

1. Introduction

After *Emiliania huxleyi*, *Gephyrocapsa* species are by far the most common coccolithophores in modern oceans. They often replace *Emiliania huxleyi* as the dominant forms.

Gephyrocapsa was initially thought to be a post Pliocene genus (Gartner, 1972; Gartner, 1977) but it is now well established that the global first common occurrence (FCO) took place in the early Pliocene, within the *R. pseudoumbilicus* Zone. The early population was composed by specimens often < 2 μm in size (Okada, 2000) and it is commonly referred to as "small *Gephyrocapsa*", a term introduced by Gartner (1977) to include very small Quaternary gephyrocapsids not easily identifiable at species level by light microscopy (LM). From the FCO, small *Gephyrocapsa* showed a worldwide increase in abundance, defined as the small *Gephyrocapsa* acme interval (Marino and Flores, 2002). During the late Pliocene it disappeared, or strongly decreased in abundance (Rio, 1982; Okada, 2000; Marino and Flores, 2002). *Gephyrocapsa* became firmly established in the late Pliocene nannofossil associations, dominated most Quaternary assemblages and decreased only close the top of the Pleistocene, due to the increased dominance of *E. huxleyi* appeared at 270 kyr (Thierstein et al., 1977). This group of coccoliths has a predominant role in Quaternary biostratigraphy (Gartner, 1977; Rio, 1982; Perch-Nielsen, 1985) and is very useful for paleoceanographic reconstructions (Bollmann, 1997; Bollmann, et al., 1998; Bollmann, et al., 2002).

Relatively few studies have focused on the evolutionary dynamics of the *Gephyrocapsa* plexus in the Quaternary. Matsuoka and Okada (1989) first studied morphometric changes of *Gephyrocapsa* from the subtropical Pacific during the last 1.3 Ma. Matsuoka and Okada (1990), extended this work to the tropical Indian Ocean (Site 709) and identified size variation cycles in *Gephyrocapsa* of a duration of about 500 ky), which were thought to represent separate phyletic lineages. Matsuoka and Fujioka (1992) further showed the repetition of this size change cycles characterized by the successive occurrence of a wide range of *Gephyrocapsa* populations.

By contrast, the early Pliocene *Gephyrocapsa* has received little attention. Driever (1988) conducted a pioneer low-resolution morphometric study by LM on the plexus from Pliocene Mediterranean land sections. At his n2 biohorizon (appearance of rare *Gephyrocapsa* spp.) in the early Pliocene, the author observed the dominance of ≈2 μm long specimens and the presence of a larger population (>3.5 μm) upwards. Other authors have qualitatively observed a time-progressive size increase (up to 3.5 μm) after the FCO, of small *Gephyrocapsa* (e.g. Okada, 2000; Marino and Flores, 2002). Excluding the work by Driever (1988), no detailed studies on small *Gephyrocapsa* size variation have been carried out to date.

However, the reasons for the observed size increase in the early Pliocene are unknown. In particular, it is an open question whether the size increase reflects increase in size of a single species or it is due to successive evolution of larger species within a radiating plexus. A few scanning electron microscopy (SEM) studies have focused on the species-level composition of the early Pliocene *Gephyrocapsa*. These have shown a quite scattered biodiversity (Pirini-Raddrizzani, 1977; Samtleben, 1980; Driever, 1988). Pirini-Raddrizzani (1977) and Lohman and Ellis (1981) described two ornate forms, *G. mediterranea* and *G. florencia*, respectively. Neither species has been reported since, jet suggest significant biodiversity of the Pliocene group.

Recently, based on a high-resolution SEM study of exceptionally well-preserved samples from the Caribbean early Pliocene (Leg 165, Hole 1000A), Crudeli et al. (in prep. 3) recognised *G. theyeri* as the first species occurring in the record and established its first occurrence (FO) at 137.15 mbsf and its FCO at 136.43 mbsf dated at 4.45 Ma and 4.35 Ma, respectively, according to Steph et al. (in revision). In that work, the authors reconstructed the phylogeny of various *Reticulofenestra* species, including *Reticulofenestra calicis,* a species recently described from the same sediments sections (Crudeli and Kinkel, 2004).

In order to constrain the evolutionary pattern of *Gephyrocapsa* we:

1 - quantitatively investigated at high-resolution time progressive size variation of the *Gephyrocapsa* population from the FCO of *G. theyeri* till 3.8Ma,
2 – observed at high-resolution the phenetic variability of the coccoliths composing the association and consistently recognise species
3 – calculated the paleofluxes of small *Gephyrocapsa* by high-resolution SEM

1.2. Taxonomy of *Gephyrocapsa*

Many extant and fossil *Gephyrocapsa* species have been described by LM or SEM. The taxonomy of the group is in a state of confusion. Species names are commonly applied to meet Quaternary biostratigraphy. As a consequence, there is very little reliable stratigraphic documentation for the overall genus (e.g. Gartner, 1991, for discussion). For example, the LM size-definition of Pliocene small *Gephyrocapsa* varies among authors (e.g. <3.5 µm, Rio, 1982; <2.5 µm, Matsuoka and Okada, 1989 and Okada, 2000). This "confusion" is mainly the result of the intergradational and complex morphological variability of these coccoliths and in the difficulties to decipher them by LM. As outlined below, a response to the question why this important group is taxonomically so problematic came from recent molecular genetic results.

1.2.1. Modern *Emiliania* and *Gephyrocapsa*, and their biodiversity

Molecular genetic studies have shown that *Emiliania* is the result of a recent divergence in the *Gephyrocapsa* clade (Sáez et al., 2004, and references therein). Thierstein et al. (1977) established the FO of *E. huxleyi* at 270 kyr. The species became dominant in the last 85 kyr mostly replacing *Gephyrocapsa* (Thierstein et al., 1977). *E. huxleyi* has been considered a single species with worldwide distribution. Nonetheless, recent studies have shown that *E. huxleyi* consists of at least three genotypically distinct types or species (Young and Westbroek, 1991; Medlin et al. 1996; Bleiswijk et al. 1991) and probably even five or more (Findlay and Giraudeau, 2000; Paasche et al., 2002; Iglesias-Rodriguez et al., 2002; Young et al. 2003). These types are differentiated by subtle morphological differences. The biodiversity of the modern gephyrocapsid (>2.5 µm long) is wide and there is some consensus on taxonomy (Young et al., 2003). However, recent research suggests that an ample morphological-genetic biodiversity probably characterised modern *G. oceanica* and *G. muellerae* (Bollmann 1997; Geisen et al., 2004; Young et al., 2005, and references therein), the most commonly recognised species.

The *Gephyrocapsa* with <2.5 µm long coccoliths are morphologically diverse. Specimens are usually referred to either *G. ericsonii* McIntyre and Be 1967 or *G. ornata* Heimadal 1973, but other very small species may be present (Young et al., 2003).

1.3. Approach

Morphometry is an important tool for the analyses the evolutionary dynamics of populations and in species recognition. Common parameters measured on *Gephyrocapsa* are size, central area diameter, and bridge angle relative to long or short axis. In their SEM study on the evolutionary dynamics of Quaternary gephyrocapsids, Matsuoka and Okada (1990) measured these parameters on two-hundred specimens, which allowed for an extremely good recognition of the phenetic variability of the group through time. Species, however, in addition, often differ in subtle morphological features that cannot be resolved by morphometry.

It was a priority of our study to recognise the species-level composition of the population from the FO of *G. theyeri*. We did this on the base of a consistent recognition of phenotypes and then erect them as species and described.

We initially carried out a high-resolution study on size variation of the population (50 specimens each 10 centimetres) then performed more detailed morphometry on 10-15 specimens per sample. These data plus qualitative and quantitative SEM observations allow us to consistently recognise five new *Gephyrocapsa* species and get consistent data on the species-level evolutionary dynamics of the early Pliocene population.

2. Materials and Methods

Two-hundred three samples at 10 cm intervals (138.45 mbsf to 118.25 mbsf) from cores from the South Caribbean Basin (ODP Leg 165, Hole 1000A, latitude 16°33.223´N longitude 79°52.044´W, 916m water depth) (Sigurdsson et al., 1997) were analysed. The interval investigated corresponds to Zone CN11 of Okada and Bukry (1980) (Kameo and Bralower, 2000). The age model of the cores was developed by Steph et al. (in rev.) by orbital tuning of high-resolution stable oxygen isotope records of planktic and benthic foraminifera. The filtration method by Andruleit (1996) was used for sample preparation, where 0.1g of dry sediment was weighted with analytical precision of ± 0.0005 using an electronic precision balance. Carbonate saturated tap water was used to dilute the sediment. In order to disintegrate small lumps, samples were ultrasonically treated (1-3 cycle of 5-10 seconds). The suspension was split two times in 10 aliquots by an electrical rotary sample divider splitter (™Fritsch). One hundredth of the initial suspension was filtered with a low pressure vacuum pump onto a polycarbonate-membrane filter (50 mm diameter, 0.40 µm pore size) and successively dried for ≈24 hours at 45°C. A filter segment was fixed on an aluminium stub and coated with gold/palladium for subsequent quantification of the nannoflora on a CamScan 44 scanning electron microscope at 6.000x.

The number of coccoliths per gram of dry sediments was calculated by the formula given in Andruleit (1996). Calcareous nannofossil accumulation rates (number of specimens/cm^2/ky) were calculated using the dry bulk density (DBD) (Sigurdsson et al., 1997) and sedimentation rates (Steph et al., in revision) (e.g. Ziveri et al., 1999). The DBD was extrapolated by linear correlation between DBD and

GRAPE (Gamma Ray Attenuation Porosity Evaluation) from samples at 1 m resolution (Sigurdsson et al., 1997).

2.1. Morphometric measurements

Within the interval of initial occurrence of *Gephyrocapsa*, we measured the length and width of 10 (136.43-135.95 mbsf - meters below sea floor) and 30 (135.85-135.75 mbsf) specimens (10 cm resolution). From 135.65-118.25 mbsf we measured a standard of 50 specimens following Bollmann (1997). In total up to 8800 specimens were measured to within 0.1 µm. Dimensions of coccoliths encountered along a SEM (6.000×) transect were measured at 20000×, or at lower magnification (15000×) when forms large. The size of specimens not perfectly parallel to the horizontal plain was approximated, tilted or broken specimens were not considered. This was corrected measuring randomly selected coccoliths of similar size. Data are available in the PANGAEA database (www.pangaea.com). For each sample, the frequency distribution of the length (interval size, 0.2 µm) was obtained. In this work only selected plots are shown, all diagrams can be found in Crudeli (2005). A test on the significance of the size variation of 50 specimens was performed on 5 samples measuring further 50 specimens (data in Crudeli, 2005). For each sample, we calculated the average length of the 50 specimens population.

From the same sediment sections, the length and width of further 10 to 15 specimens were measured from samples at 10-20 cm resolution (up to 1200 coccoliths). The bridge angle, measured clockwise from the long axis, the central-area (CA) width and number of distal shield elements were measured on corresponding video-prints. The rim width was calculated by the coccolith width and CA width. Length and CA width data from 5 to 10 stratigraphically continuous samples have been combined and plots are reported in this work. All scatter plots of width, bridge angle and CA width vs. length can be found in Crudeli (2005).

2.2. Taxonomic study

Morphological observations of the new *Gephyrocapsa* species described here were conducted by SEM at 20000× magnification. For each species, 15 to 49 specimens were observed in detail from a selected sample, or from two closely spaced samples. Parameters measured, live on the SEM image (20000×) were: distal shield and central area length and width and the rim width. The number of distal shield elements and the bridge angle measured clockwise from the long axis, as reported in the descriptions, were obtained from micrographs or video prints of the specimens. The descriptions follow the nomenclature of Young et al. (1997).

2.3. Paleofluxes - taxonomic remarks

Given the absence of comparable studies and the morphological variability of the population, we applied an informal taxonomy to *Gephyrocapsa* specimens. Specimens with tooth-like protrusions around the central area were separately counted and are here named *G. bollmannii* spp. The other forms were qualitatively separated into small and large specimens. Small *Gephyrocapsa* refers to all the *Gephyrocapsa* specimens recorded in each sample by SEM counting.

3. Results and discussion

3.1. Biodiversity among the small *Gephyrocapsa* population

The SEM examination of *Gephyrocapsa* specimens, during the quantification of the nannoflora, morphometric analyses and successive extensive re-examination of selected samples, up to 1000 video prints and up to 230 micrographs allow us to recognise 5 new *Gephyrocapsa* species among the early Pliocene small *Gephyrocapsa* population. Moreover, a species similar to *G. theyeri* is observed and described but we reserve to apply a name since variation is likely intraspecific. In this work we extend the description of *G. theyeri*. The new species are described in the following and illustrated in Plates 1-2. For each species, the number of specimens and the ODP Sample/s of the taxonomic description are reported in table 1. Morphometric values are reported in table 1 and plotted in figure 2. The average length and average bridge angle of the species are plotted in figure 6 and compared with morohlogical variability of Holocene *Gephyrocapsa*. Depth-age correspondence can be found in appendix.

The type locality and type horizon coincide: South Caribbean Sea, ODP Hole 1000A (16°33.223´N 79°52.044´W), early Pliocene, *R. pseudoumbilicus* Zone, Zone CN11 of Okada and Bukry (1980) (Zone NN15 of Martini, 1971) (Kameo and Bralower, 2000).

The types of the new species, SEM stubs and accompanying sub-samples of the topotype material are deposited at the Department of Palaeontology, The Natural History Museum, London.

3.1.1. Systematic descriptions

Family Noelaerhabdaceae Jerkovic, 1970 emend. Young and Bown, 1997

Genus *Gephyrocapsa* Kamptner, 1943

Type species *Gephyrocapsa oceanica* Kamptner, 1943

Gephyrocapsa theyeri Pujos, 1987 (Pl. 1, figs. 1-2)

Gephyrocapsa sp. 1 Samtleben, 1980, Pl. 12, fig. 23

Gephyrocapsa theyeri n. sp. Pujos, 1987, Pl. 3, figs. 1, 4

Between the FO (4.45 Ma) to the FCO (4.35 Ma), *G. theyeri* specimens (16 specimens) are 1.4-2 µm long with an average length of 1.6 µm which corresponds to the holotype description (1.6 µm, length, 1.1 µm width) and all have a narrow rim (Plate 1, fig. 1; Fig. 1a). Among these, 14 have a low bridge angle (35°) which is the value of the holotype, two specimens have a higher bridge angle (65°) (Fig. 1b). There are no differences in rim morphology, size and central-area, so the variation is likely intraspecific. The bridge of *G. theyeri* is commonly formed by 3-5 elements, rarely by 7 elements. The holotype bridge is formed by 6 elements. These, from the ends, progressively meet each other in clockwise direction so that, the element closer to the transversal pole is the one that meet the elements from the opposite side to form the bridge. When the elements are few, this pattern is less clear. Very commonly the bridge-elements meet with an offset and show crystal faces, but specimens with no clear offset occur and occasionally the one overlap at length the other. The bridge is commonly massive, particularly in the earliest specimens and it became slightly more regular in later forms. Selected species appear to have a thinner rim outward to the bridge but this may be due to dissolution.

New *Gephyrocapsa* species

The new *Gephyrocapsa* species show very similar basic morphology. This is described first, the phenetic peculiarity of each new species is detailed thereafter. The species are composed by two shields of similar size and are broadly too normally elliptical. They have a narrow rim and a wide central-area that lacks central-area structures. The distal shield elements are of similar petaloid shape. Occasionally, a few randomly distributed distal shield elements are thinner. The outwards terminations of the distal shield elements vary. These are all sub-straight or straight and with a dextrally oriented tip. Close to the ends, the distal shield elements show weak to pronounced sinistral obliquity. Those at the sides show weakly dextral or radial obliquity. *G. samtlebenii* n. sp. has closed central-area and may have a grill. The inner tube elements of the species are weakly to non imbricated and extend towards or weakly above the distal shield level often giving rise to a low collar.

From the inward portion of the distal shield elements, outward and on the distal shield elements, a few (1-7) randomly disposed overgrowths occur. Commonly these have no particular shape, i.e. they are simply elongated outward (≈0.1-0.3 µm) with sub-rounded terminations and do not reach the outward terminations of the shield elements. Elongated overgrowth has sinistral orientation. The overgrowth can be micrometric. Commonly, the overgrowth occurs outwards from the bridge. These have rounded or incipient hammer-like-morphology. This last morphology is observed even when overgrowth is micrometric.

Gephyrocapsa sp. cf. *theyeri* (Pl. 1, figs. 3-6)

Gephyrocapsa "*margereli/aperta*-Type" Samtleben, 1980, Plate 12, figs. 23, 26-27.

Differential diagnosis. The species differs from *G. theyeri* in having a slightly wider rim.

Remarks. From Zone NN15 (North Atlantic) Samtleben (1980) described *G.* sp. 1. The author did not assigned a holotype and this *G.* sp. 1 was included in *G. theyeri* by Pujos (1987). The first specimens occurring in the record at Site 1000A are identical to the holotype of *G. theyeri* (Crudeli et al. in prep. 3; this work). In the description of *G.* sp. 1, Samtleben (1980) distinguished between forms with high and low bridge referred as "*margereli/aperta*-Type" (his Plate 12, figs. 23, 26-27) and "*sinuosa*-Type" (his Plate 12, figs. 24-25) respectively. The *margereli/aperta*-Type forms are very similar to our *G.* sp. cf. *theyeri* specimens and indicate a wide distribution of these forms.

Gephyrocapsa drieveri n. sp. Crudeli and Young (Pl. 1, figs. 7-10)

Etymology: dedicated to B.W.M. Driever, who worked on *Gephyrocapsa*.

Diagnosis: very small placolith with narrow rim with non-uniform length of distal shield elements, wide central-area lacking central-area structures and bridge at intermediate to high angle to the long axis.

Holotype: SEM micrograph 86787, Pl. 1, fig. 8

Paratypes: SEM micrographs 86893, 86561, 86778, Pl. 1, figs. 7, 9-10

Type material: ODP Sample 1000A-15H-5, 105-107cm (133.85 mbsf).

Phenetic peculiarity: the distal shield elements of *G. drieveri* n. sp. are of varying length around the central-area. Commonly, the distal shield elements close to the NE (SW) position or to the NE and

SW positions are about 0.1-0.2 µm narrower then the other elements that are on average 0.4 µm wide. Specimens with shorter elements close to the NW (SE) or NW and SE positions also occur but more sporadically.
Differential diagnosis: the species differs from *G.* sp. cf. *theyeri* only by the irregular length of the distal shield elements.

Gephyrocapsa samtlebenii n. sp. Crudeli and Young (Pl. 2, figs. 1-4)

Etymology: dedicated to C. Samtleben, who worked on *Gephyrocapsa*.

Diagnosis: very small placolith with narrow central-area, wide rim and bridge at intermediate to high angle to long axis.

Holotype: SEM micrograph 86470, Pl. 2, fig. 1.
Paratypes: SEM micrographs 86480, 86885, Pl. 2, figs. 2-3.
Type material: ODP Sample 1000A-15H-5, 115-117cm (133.95 mbsf).
Phenetic peculiarity: The species shows consistently a smaller central area. A central area grill has not been observed, however, it may have been present since in few specimens, remain of grill bars appear to be present. The inner tube elements extend to or very weakly below the distal shield level. The bridge is formed by 2-4 elements. The elements meet over the central-area with no to weak off set. The connection commonly shows an I-shaped morphology. The crystal faces are almost totally fused, there are only very few free crystal surfaces.
Differential diagnosis. The species differs from the previously described species by the closed central-area.

Gephyrocapsa bollmannii n. sp. Crudeli and Young (Pl. 2, figs. 5-6)

Etymology: dedicated to J. Bollmann, who worked on *Gephyrocapsa*.

Diagnosis: very small to small placolith with narrow rim, wide central-area lacking central-area structures, distal tooth-like protrusions around the central-area and bridge at high to intermediate angle to long axis.

Holotype: SEM micrographs 83039, 83040, Pl. 2, figs. 5-6.
Type material: ODP Sample 1000A-14H-2, 24-26cm (119.04 mbsf).
Phenetic peculiarity: *G. bollmannii* n. sp. is characterised by distal tooth-like protrusions around the central-area. These are continuous with the inner tube elements, are vertically oriented and low to 0.5 µm high.
Differential diagnosis: *G. bollmannii* n. sp. differs from *G. matsuokae* n. sp. because it posses tooth-like protrusions around the central-area. The species differs from modern *G. ornata* Heimdal, 1973 because the bridge is variably massive. The bridge of *G. ornata* is formed from thin plates. In contrast to *G. ornata*, *G. bollmannii* n. sp. lacks central-area structures. The size and rim morphology of *G. bollmannii* n. sp. are identical to that of *G. matsuokae* n. sp. The overgrowth does not fuse with the distal shield elements outwards terminations as observed in *G. matsuokae* n. sp.

Remarks: A specimen with tooth-like protrusions and a bridge morphologically very similar to that of *G. ornata* (paddle-like) was observed by us. Detailed observations reveal that this was formed by arched elements.

Gephyrocapsa matsuokae n. sp. Crudeli and Young (Pl. 2, figs. 10-12)

G. margereli Bréhéret, 1978, Samtleben, 1980, Pl. 12, fig. 20

Etymology: dedicated to H. Matsuoka, who worked on *Gephyrocapsa*.
Diagnosis: very small placolith with narrow rim, wide central-area lacking central-area structures, moderate to weak rising collar and bridge at high to intermediate angle to long axis.

Holotype: SEM micrograph 86756, Pl. 2, fig. 10.

Paratypes: SEM micrographs 82205, 82168, Pl. 2, figs. 11-12.
Type material: ODP Sample 1000A-14H-2, 24-26cm (119.04 mbsf).
Differential diagnosis: the species differs from *G. bollmannii* n. sp. because of the absence of tooth-like protrusions. A part from size, *G. matsuokae* n. sp. is similar to *G.* sp. cf. *theyeri*.

Gephyrocapsa jerkovicii n. sp. Crudeli and Young (Pl. 2, figs. 13-15)

Etymology: dedicated to M.L. Jerkovic, micropaleontologist

Diagnosis: very small to small placolith with moderately narrow rim, wide central-area lacking central-area structures, distinct collar, and bridge at intermediate angle to long axis.

Holotype: SEM micrograph 86795, Pl. 2, fig. 15.
Paratypes: SEM micrographs 86520, 86789, Pl. 2, figs. 13-14.
Differential diagnosis: the species is similar to *G. margereli* which was described from the Pleistocene by Bréhéret (1978). The two distinguished varieties (Bréhéret 1978, his Plate 2, figs. 1-2) are 2.7-4.8 μm in size. Despite specimens of *G. jerkovicii* n. sp. larger then 3.2 μm occur in the record (up to 3.7 μm, our pers. obs.), *G. jerkovicii* n. sp. is smaller (2.4-3.2 μm). *G. jerkovicii* n. sp. is similar to *G. matsuokae* n. sp. and *G.* sp. cf. *theyeri* but is larger and has a wider rim.

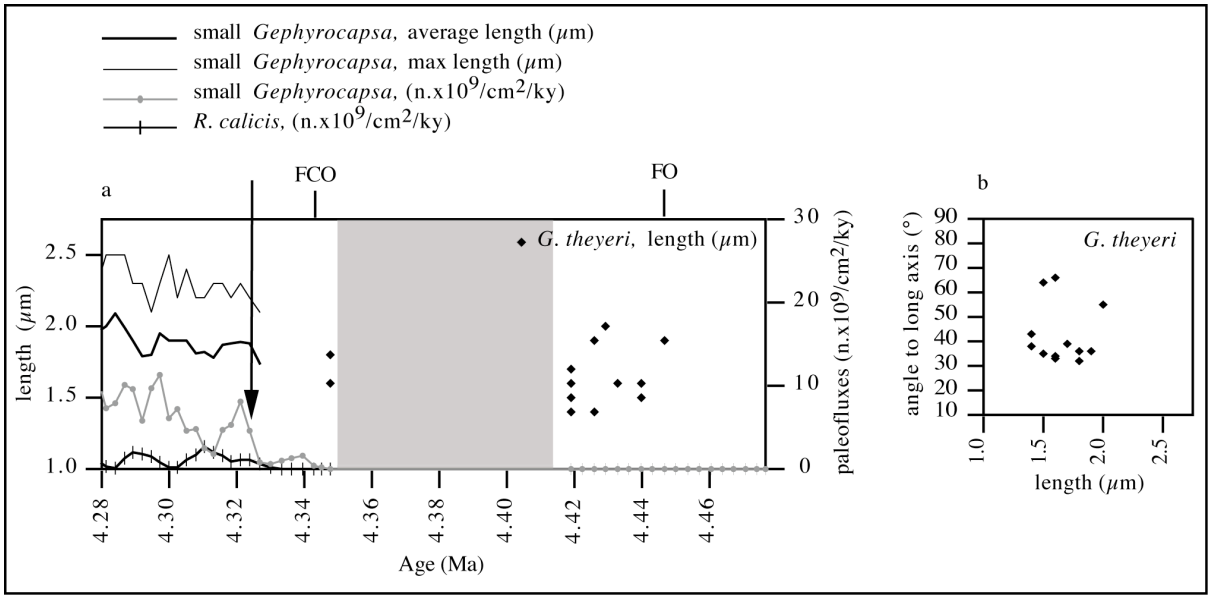

Fig. 1. a - Length of *G. theyeri* specimens (black dots) from the FO (137.15 mbsf, 4.45 Ma) to the FCO (136.43 mbsf, 4.35 Ma), compared with the average length, maximum length and paleofluxes (n.x10^9/cm2/ky) of small *Gephyrocapsa* and with the paleofluxes *R. calicis*. Till sample 135.75mbsf (4.33 Ma) (black arrow), the small *Gephyrocapsa* population is almost exclusively composed by *G. theyeri*. b - plot of the bridge angle (to long axis) vs. length of *G. theyeri* specimens from the FO to the FCO.

species	ODP Sample	maximum length (μm)	minimum length (μm)	average length (μm)	maximum width (μm)	minimum width (μm)	average width (μm)	maximum ellipticity	minimum ellipticity	average ellipticity	CA maximum length (μm)	CA minimum length (μm)	CA average length(μm)	CA maximum width (μm)	CA minimum width (μm)	CA average width (μm)	rim maximum width (μm)	rim minimum width (μm)	rim average width (μm)	n. DS elements	average n. DS elements	bridge angle (°)	average bridge angle (°)
G. sp. cf. *theyeri*	(11) 15H-6, 5-7 cm - (15) 15H-5, 105-107 cm	2.4	1.7	2.1	2.0	1.4	1.7	1.3	1.1	1.2	1.6	0.7	1.2	1.2	0.6	0.8	1.1	0.4	0.9	28-38	31	29-59	39
G. drieveri n. sp.	(29) 15H-6, 5-7 cm - (20) 15H-5, 105-107 cm	2.5	1.8	2.1	2.0	1.4	1.7	1.4	1.2	1.2	1.4	0.9	1.2	1.0	0.6	0.8	1.2	0.6	0.9	26-36	31	28-54	40
G. samtlebenii n. sp.	(15) 15H-5, 115-117 cm	2.1	1.6	1.9	1.8	1.3	1.6	1.3	1.1	1.2	1.7	0.7	1.0	0.8	0.4	0.6	1.2	0.8	1.0	20-30	24.5	40-90	61.7
G. bollmannii n. sp.	(23) 14H-2, 24-26 cm	3.2	1.9	2.5	2.7	1.4	2.1	1.4	1.1	1.2	2.1	1.1	1.5	1.5	0.7	1.0	1.3	0.7	1.0	28-42	34	20-38	28
G. matsuokae n. sp.	(23) 14H-2, 24-26 cm	3.0	2.2	2.4	2.4	1.7	2.0	1.3	1.2	1.2	1.7	1.1	1.4	1.1	0.6	0.9	1.4	0.8	1.0	28-38	32.9	23-45	33
G. jerkovicii n. sp.	(28) 14H-5, 75-77 cm	3.2	2.4	2.9	2.8	2.2	2.5	1.2	1.1	1.2	1.7	1.2	1.5	1.1	0.8	1.0	1.7	1.2	1.5	30-50	37.7	28-48	38.1

Tab. 1. Morphological details of *G.* sp. cf. *theyeri*, *G. drieveri* n. sp., *G. samtlebenii* n. sp., *G. bollmannii* n. sp., *G. matsuokae* n. sp. and *G. jerkovicii* n. sp., number of specimens on which the taxonomic description is based and ODP Sample. DS, distal shield elements, CA, central area.

3.1.2. Discussion - taxonomy

3.1.2.1. Morphology based phylogeny

The new species are referred to *Gephyrocapsa* Kamptner 1943 since they are elliptical placoliths with distal diametrically opposed elements that arch obliquely across the central-area forming a bridge. The morphological continuity among *G.* sp. cf. *theyeri*, *G. drieveri* n. sp., *G. bollmannii* n. sp., *G. matsuokae* n. sp. and *G. jerkovicii* n. sp. suggests that these species are phylogenetically related and probably evolved from *G. theyeri*. By contrast, *G. samtlebenii* n. sp. is morphologically different from the previous species and may represent a separate lineage.

Most modern *Gephyrocapsa* species, even the smallest, have a central area grill. This also includes the type species *G. oceanica* (Young et al. 2003 and references therein). Among the new species, only in *G. samtlebenii* n. sp. a grill may have been present. The species is among the smallest and would

support the inference that the absence of central-area grill in the other species is a primary phenetic character and not due to preservation. Moreover, other reticulofenestrids like *R. premoliae* n. sp. often have a preserved grill (Crudeli et al., in prep. 3).

3.1.2.2. *G. drieveri* n. sp. and *G.* sp. cf. *theyeri*

The rim width around the central-area of reticulofenestrids is usually very stable (Young, 1989) as it results from uniform growth outward of the distal and proximal shield elements during coccolithogenesis (Young et al., 1999). Variation in length of the distal shield elements of *G. drieveri* n. sp. appears to be different from the normal biomineralization model. The variation in rim width can be very subtle, it is however consistent and thus not due to dissolution. This makes it very unlikely that *G. drieveri* n. sp. represents an intraspecific variation among the *G.* sp. cf. *theyeri* population. It is also unlikely that dissolution or overgrowth is the primary cause of this morphology since it is consistently observed. Dissolution would have been expected to preferentially affect the elements along the side (Young, 1989). It is possible that this rim morphology occurred more frequently among reticulofenestrids but that, because of the dominance of LM studies, it has not been previously described. In modern *Gephyrocapsa*, this variation is not observed and, therefore, may be characteristic of fossil Neogene forms only.

Except from the rim morphology, *G. drieveri* n. sp. is identical to *G.* sp. cf. *theyeri*. This indicates that size alone can not detect species.

3.1.2.3. Overgrowth

Overgrowth on the distal shield of most of the new *Gephyrocapsa* species varies between species and among specimens from micrometric to overgrowth elements. This kind of overgrowth was observed in e.g. *R. alis* n. sp. specimens on the side with no arch, and similar overgrowth is observed on other small reticulofenestrids (our pers. obs.). The outer tube elements show strong modification in coccoliths of *R. calicis* (Crudeli and Kinkel, 2004). It is possible that the overgrowth observed in the new *Gephyrocapsa* species is due to modification of the outer tube. However, at the base of the outer arch-elements of *R. alis* n. sp., overgrowth is occasionally observed. But these elements are the prolongation of the outer tube elements (Crudeli et al., in prep. 3). Thus, a double modification of the outer tubes occurs or the overgrowth is a modification of the surface of the distal shield elements. Overgrowth without particular shape could be simply inorganic precipitation, overgrowth elements are likely biologically formed. Overgrowth is asymmetric around the central area and, from the same samples, the same species may or may not be characterised by such variation. This suggests that this morphology is intraspecific, possibly ecologically controlled.

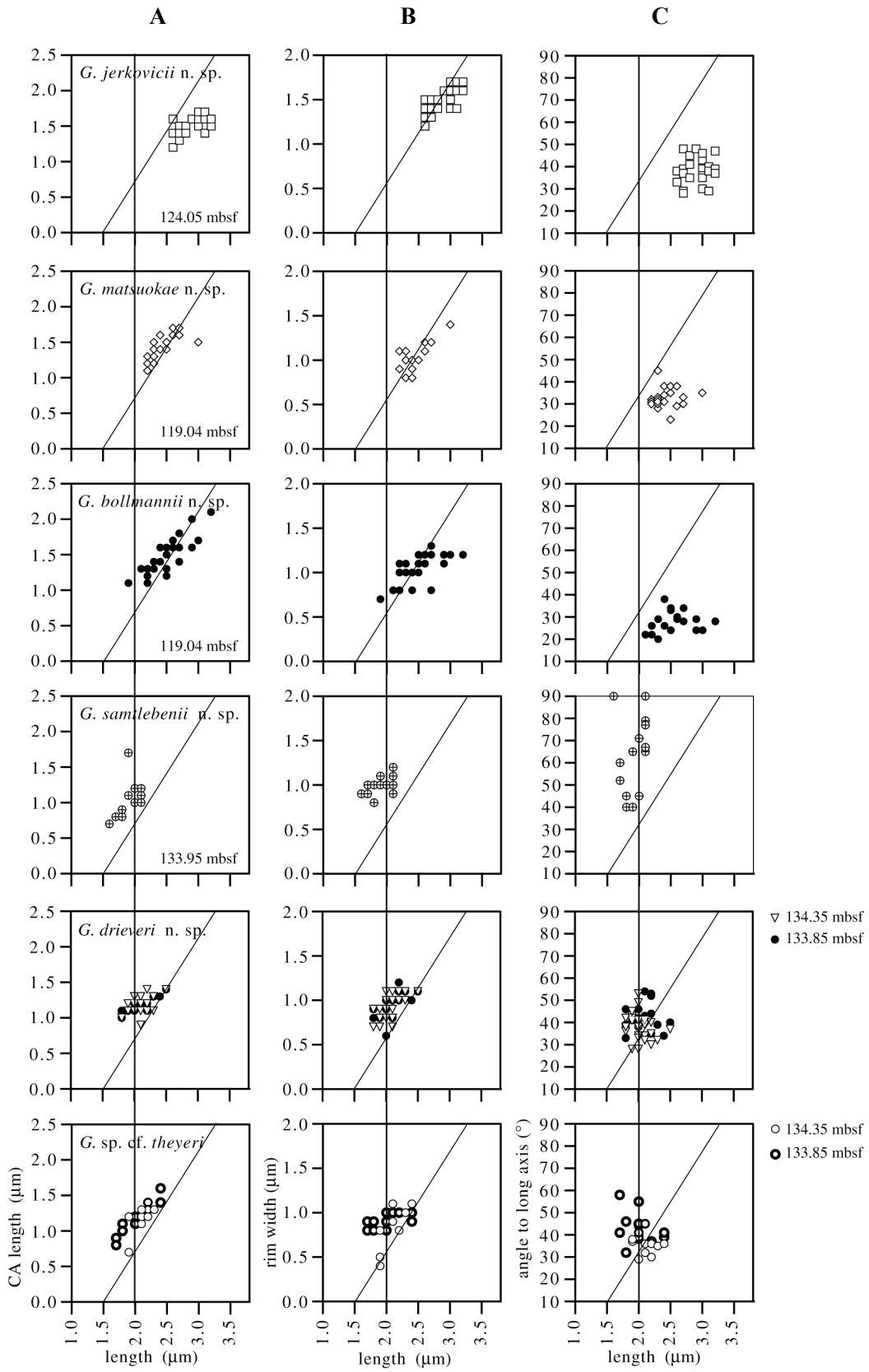

Fig. 2. *G.* sp. cf. *theyeri*, *G. drieveri* n. sp., *G. samtlebenii* n. sp., *G. bollmannii* n. sp., *G. matsuokae* n. sp. and *G. jerkovicii* n. sp., plots of the central-area length (A), rim width (B), and bridge angle to long axis (C) vs. length of the specimens (holotype and paratypes) on which the description is based. The depth of the ODP sample/s is reported on the left side of each plot. The vertical line at 2 µm and oblique line, as in Matsuokae and Okada (1990), evidence that the new species cluster with the small Quaternary gephyrocapsids.

3.2. Occurrence of the new *Gephyrocapsa* species

Quantification data coupled with re-examination of selected samples, micrographs and video prints acquired during study are used here to qualitatively trace the occurrence of the described species (Fig. 3). *G. samtlebenii* n. sp. is a rare, but likely long ranging species. The species occur already at 135.85 mbsf, the holotype is described from sample at 133.95 mbsf (4.28 Ma) and the specimens illustrated in plate 2 (fig. 4) (126.88 mbsf) is likely *G. samtlebenii* n. sp. *G.* sp. cf. *theyeri* and *G. drieveri* n. sp. are recognisable in sample at 135.75 mbsf (4.32 Ma) but whereas *G.* sp. cf. *theyeri* has likely a continuous record, *G. drieveri* n. sp. specimens appears not to be present longer. The paleofluxes of *G. bollmannii* spp. qualitatively trace the occurrence of *G. bollmannii* n. sp. (Fig. 3). This is certainly true for sediments younger than 4 Ma and for the interval between 4.07-4.13 Ma (Fig. 3) as resulted from our re-examination of samples. Nonetheless, specimens similar to *G. bollmannii* n. sp. are present at sample 128.25 mbsf (4.17 Ma) and a few, smaller forms were observed in older sediments. It is questionable if that older population correspond to the same species. *G. jerkovicii* n. sp. is likely the youngest species. It is described from sample at 124.05 mbsf (3.95 Ma). A bimodality in the frequency distribution of length (2.2 μm and 2.8 μm) is clear at 123.65 mbsf but larger specimens occur earlier (Fig. 5), e.g. at 125.25 mbsf (4.0 Ma).

The samples from which the holotypes of *G. drieveri* n. sp. and *G. samtlebenii* n. sp. have been described, represent the FO of the species. No FO is established for the other species.

3.3. Evolutionary development of *Gephyrocapsa* - morphometry

3.3.1. Statistical significance of size variation

The size of the small *Gephyrocapsa* shows significant variation during the investigated interval (Fig. 4). Given the small size of specimens, a low SEM magnification would have probably resulted in underestimation of small forms. Analyses therefore were conducted along a fixed transect at 6000x magnification which was ideal to examine a relatively large area of the SEM stub and allowed detection of the smallest forms (e.g. 0.8 μm long).

3.3.2. Variation in size

Three cycles in increase in average size of small *Gephyrocapsa* occur from 4.33 to 4.15 Ma (Fig. 3). The first cycle takes place in about 60 kyr, with fine oscillations, successive increases and decreases in size occur during 30 to 20 kyr. Average size fluctuations are paralleled by similar variation in the maximum length. By contrast, coccoliths minimum size shows a time-progressive decrease from 1.4 μm to 1.0 μm at 4.16 Ma. The frequency distribution of length is unimodal and maximum length oscillating between 1.8 μm and 2.2 μm (Crudeli, 2005) and is plotted here for a selected interval of size increase (134.65-132.85 mbsf, 4.30-4.25 Ma, Fig. 5). The length was obtained on an equal number of specimens (50) recorded along a fixed SEM transect therefore the frequency plots give a qualitative estimation of the contribution, in abundance, of the very small specimens over larger ones in the samples.

G. sp. cf. *theyeri* is closely similar to *G. theyeri*. Just after its FCO, a weak variation in rim width of *G. theyeri* is observed by SEM and, in this interval that was re-checked by SEM, it is somewhat difficult to distinguish between *G. theyeri* and *G.* sp. cf. *theyeri.* Given the high evolutionary pressure indicated by the occurrence of *G. drieveri* n. sp., *G. samtlebenii* n. sp. and *R. calicis* here (Figs. 1, 3),

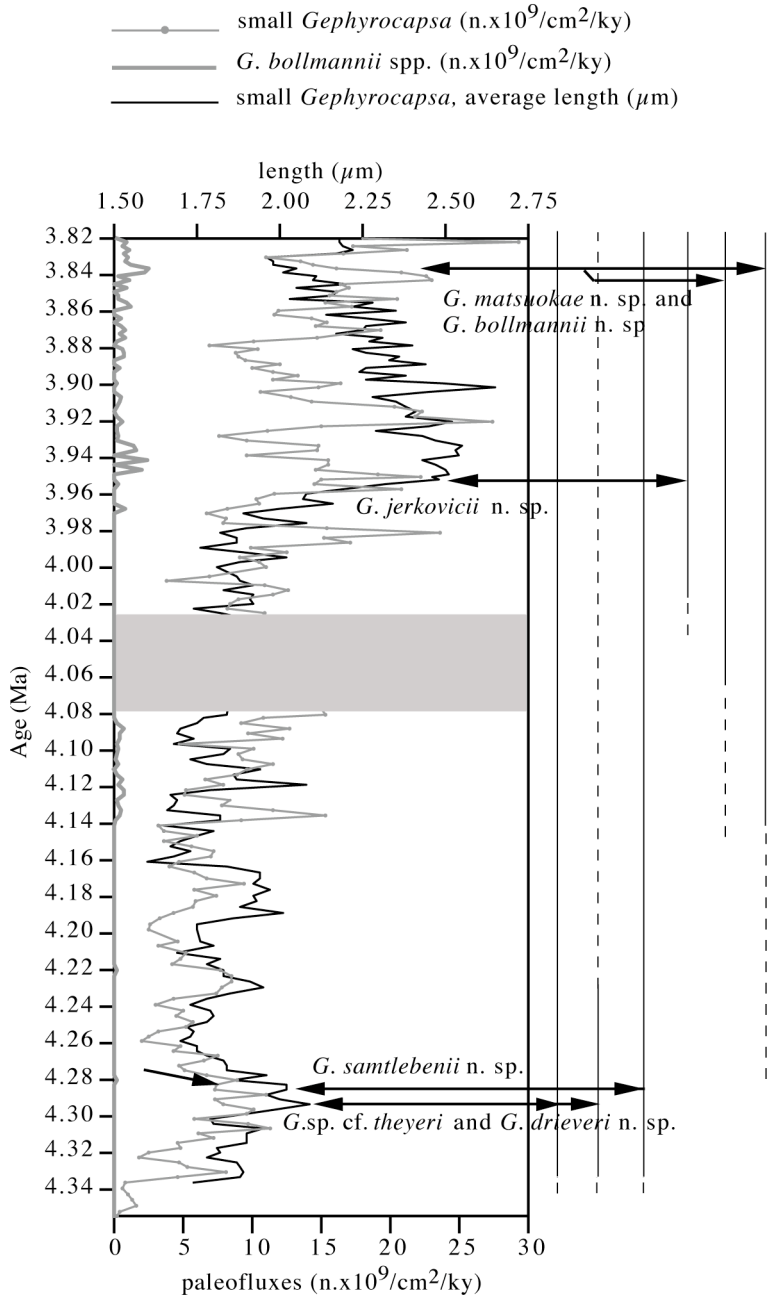

Fig. 3. Paleofluxes (n.x10^9/cm/ky) of small *Gephyrocapsa* and *G. bollmannii* spp. compared with the average length of small *Gephyrocapsa*. The samples from which the holotypes of the new species are described is indicate by the arrows. Vertical lines (right side of the panel) trace the range of the new species in the cores. The gray box indicates a gap in the age model (Steph et al., in press).

it may be possible that *G.* sp. cf. *theyeri* represents a separate species. A few *G. drieveri* n. sp. specimens are present in those samples. The initial increase in size obtained by morphometry (Fig. 4) is therefore in part due to a variable presence of these larger species (*G.* sp. cf. *theyeri* and *G. drieveri* n. sp.). SEM observations and a few measurements on *G. theyeri* specimens compared with the morphometry on *G.* sp. cf. *theyeri*, indicate that increase in rim width corresponds to increase of other parameters and suggests that *G.* sp. cf. *theyeri* may represent intraspecific variation among *G. theyeri*.

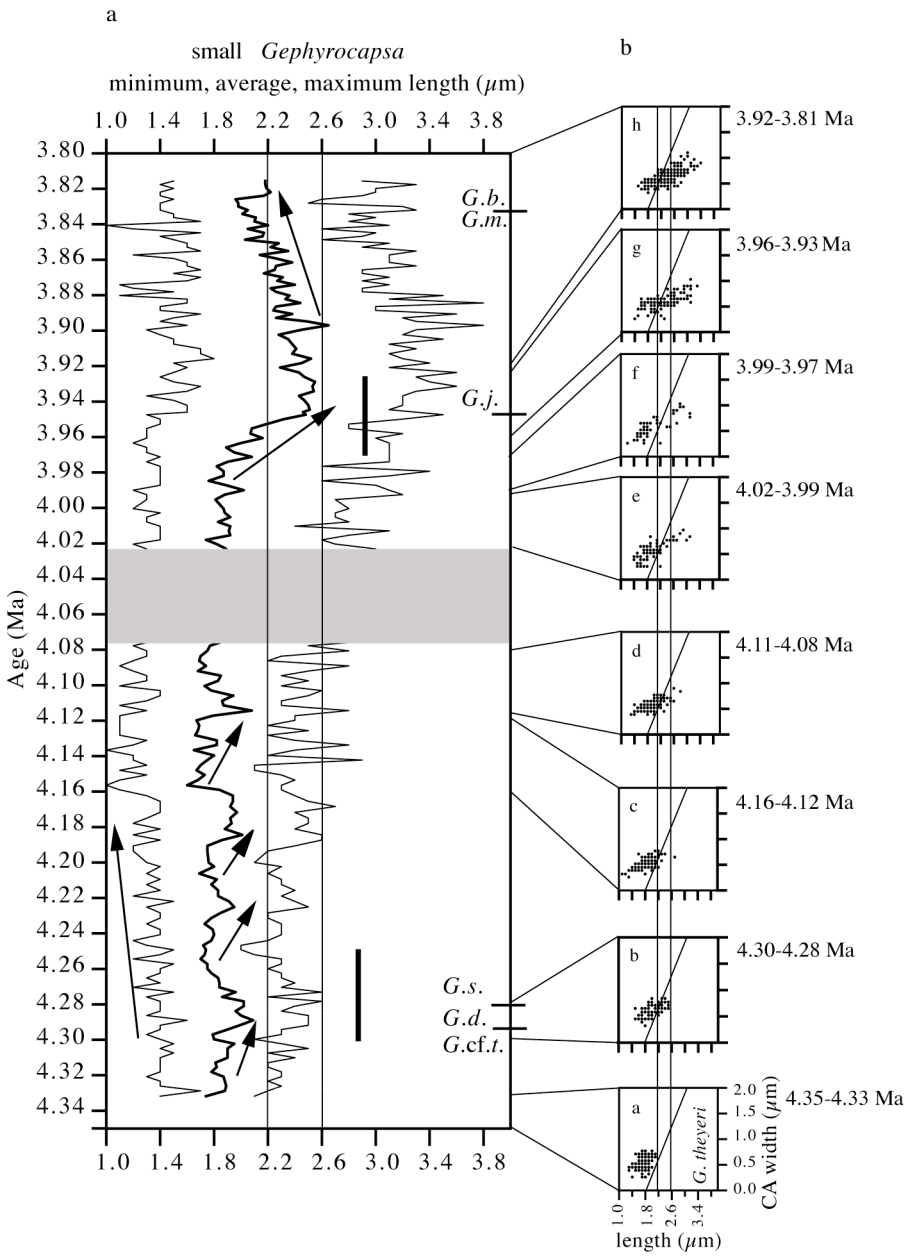

Fig. 4. Morphometry of small *Gephyrocapsa.* a - , minimum, average and maximum length of the population. 10 to 50 specimens measured at 10 centimetres resolution, see methods for details. The age of samples on which the taxonomic description of the new species (*G.* cf. *t., G.* sp. cf. *theyeri*; *G.d*., *G. drieveri* n. sp.; *G.s., G. samtlebenii* n. sp.; *G.b., G. bollmannii* n. sp.; *G.m., G. matsuokae* n. sp.; *G.j., G. jerkovicii* n. sp.) is based is indicated by short horizontal lines (right side of the panel). The depth–age correspondence can be found in Appendix 1. b- plots of the central area width vs. length of small *Gephyrocapsa*: 10 to 15 specimens were measured for each sample. Data from samples covering selected time-interval are here combined. The gray box indicates a gap in the age model (Steph et al., in press).
Vertical black lines correspond to intervals of figure 5 where the frequency distribution of the length is shown.

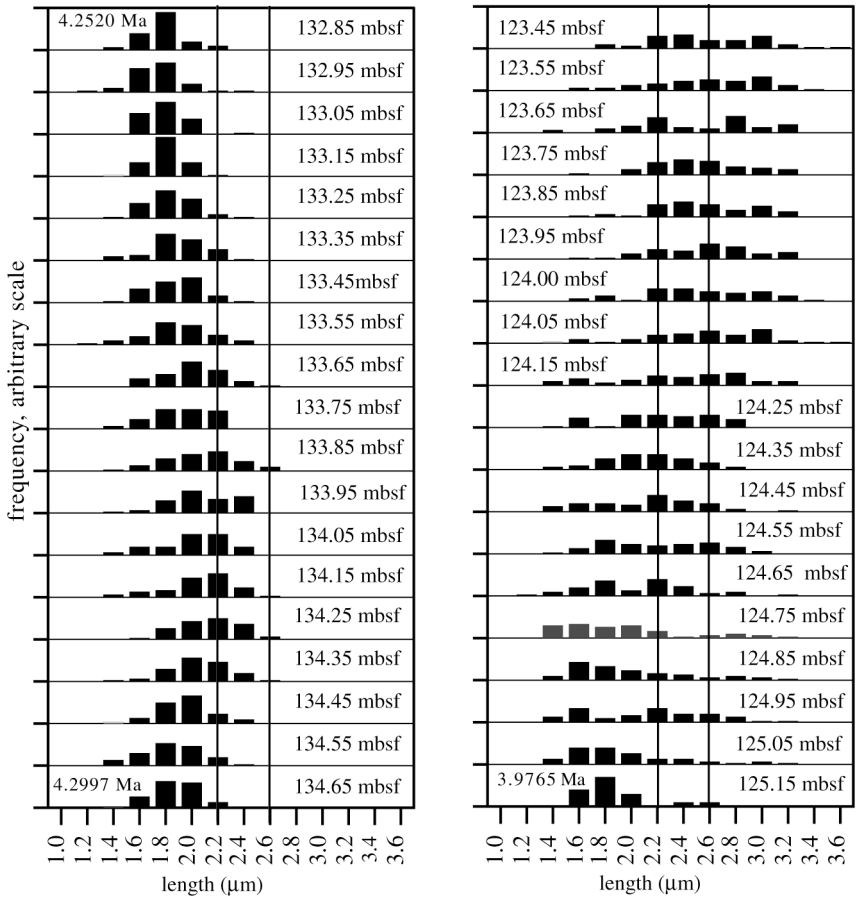

Fig. 5. Frequency distribution of the length (size interval, 0.2 μm) (50 specimens per sample) against depth (mbsf) from two selected intervals of size increase (a - 4.2997 Ma to 4.2520 Ma, b - 3.9765 Ma to 3.9314 Ma) of small *Gephyrocapsa*. Intervals are indicated in figure 4 by black vertical lines.

The plots of the CA width vs. length of *G. theyeri* specimens (4.35-4.33 Ma, Fig. 4a) and those of the successive population (Fig. 4b) show that a population of smaller specimens is time-progressively followed by a larger population. The first cycle of size increases, with the occurrence of *G. samtlebenii* n. sp. and *G. drieveri* n. sp. therefore represents an evolutionary event. A similar pattern occurs during the two successive cycles of size increase, i.e. when larger specimens compose the population and the smaller forms are minor components. This is also shown by the frequency distribution of length (Fig. 5).

As discussed later, the main size increase of the population (after about 4 Ma, Fig 4) is evolutionary. The second and third cycles of increase in size (Fig. 4) may be due to paleoecology or may be evolutionary. Here, based on SEM observations, most specimens are referable to *G. theyeri* and *G.* sp. cf. *theyeri* and a few to *G. drieveri* n. sp. (Fig. 3). Therefore, these cycles are evolutionary only if sibling species (Knowlton, 1993) originate, which appear unlikely. Thus paleoecology appears to be more significant in forcing these size variations. The pattern in average size of the small *Gephyrocapsa* populations is closely coupled to variation in paleofluxes (Fig. 3). This suggests that the two size increases are due to favourable paleoecological conditions for the large *G.* sp. cf. *theyeri* and *G. drieveri* n. sp. population and of disadvantage for the smaller *G. theyeri.*

The abundance profile of small *Gephyrocapsa* is roughly opposite to that of *R. calicis* (Crudeli et al., in prep. 3; this work, Fig. 1), a likely oligotrophic species (Crudeli et al., in prep. 3) and suggests that

the smaller *G. theyeri* are oligotrophic. This is apparently ambiguous since, among placoliths, the smaller morphotypes are commonly thought to be the more eutrophic (e.g Okada, 2000). Possible implications are discussed below.

From about 4.15 Ma to 4.11 Ma, the average size of small *Gephyrocapsa* increases but a similar variation in maximum size does not occur (Fig. 4). This variation possibly records the presence of *G. bollmannii* n. sp. which presence is suggested by the paleofluxes of *G. bollmannii* spp. (Fig. 3). The speciation event of *G. bollmannii* n. sp. may have occurred around this time interval. The species is very similar to *G. matsuokae* n. sp. which also may have occurred already here. Nonetheless, specimens larger then 2.6 µm occur occasionally in the lower record, but more commonly after 4.14 Ma.

After 4.11 Ma, the average size is constant and increases from 3.98 Ma on (3.98-3.94 Ma) indicating the presence of a large-size *Gephyrocapsa* population. Whereas the average and maximum differs by ≈0.4 µm in the lower record, after about 4.10 Ma the difference is higher and often larger than 1 µm. This gives a visual idea of the contribution of the smaller forms to the total assemblages.

The record of the minimum size of small *Gephyrocapsa,* shows a strong size reduction around 4.16-4.12 Ma. This reduction is likely due to paleoecology since *R. alis* n. sp. shows a marked increase (Crudeli et al., in prep. 3) and suggests changes in ecological conditions. From about 3.87 Ma upward, size decreases and likely record the disappearance of the larger species.

3.3.3. Complementary studies - implications

The distribution of *G. theyeri* and *G.* sp. cf. *G. theyeri* appears global (Crudeli et al., in prep. 3 and this work). Moreover, *G. theyeri* is clearly the single *Gephyrocapsa* species composing the small *Gephyrocapsa* population in the early Pliocene of the Pacific (Crudeli, unpublished) with a FCO synchronous to Caribbean Site 1000A based on high-resolution stable isotope stratigraphy (Tiedemann et al., submitted). The size increase of small *Gephyrocapsa* after about 4 Ma (Fig. 4) correlates well with that documented by Driever (1988) and there is very good correspondence between qualitative observations by previous authors (e.g. Marino and Flores, 2002) and suggests basin-wide distribution of the larger species (e.g. *G. jerkovicii* n. sp.). In addition, a similar size reduction of the plexus, documented here at about 3.8 Ma on, was documented by Driever (1988). This suggests a basin-wide and likely synchronous evolutionary event in the early Pliocene population.

Variations in abundance of coccolithophores reflect changes in optimal ecological conditions. Subsequently, known ecological preferences of species are useful proxies for paleoenvironmental-paleoecological reconstructions. If the increase in paleofluxes of small *Gephyrocapsa*, after the FCO (Fig. 3), would have been detected only at Site 1000A, this could have been interpreted as changes in local paleoecological conditions. However, the pattern in paleofluxes is very similar to that recorded from other areas (Driever, 1988; Marino and Flores, 2002; Okada, 2000; Kameo and Sato, 2000; Gibbs et al., 2005) suggesting that identical ecological conditions have occurred at different sites to support these new evolved populations. This suggests that the increase in abundance of small *Gephyrocapsa* is due to widespread variation in the characters of the water masses that supported ocean-wide proliferation of the species and likely their evolutionary radiation. However, the increase in abundance of small *Gephyrocapsa* is widespread in the Atlantic but not in the Pacific (Kameo and

Sato, 2000). Since it is evolutionary, the difference could be only explained by different ecological conditions occurred in the two basins.
Marino and Flores (2002) suggested the use of the LM acme interval of small *Gephyrocapsa* as a biostratigraphic marker. This work supports this suggestion, since the acme is associated with evolutionary events. The FCO of small *Gephyrocapsa*, with the FO of *R. calicis* represent an important instrument for fine-scale biostratigraphy. Driever (1988) already used the appearance or rare *Gephyrocapsa* spp. as a datum for his biohorizont n2.

3.3.4. Comparison with the evolutionary model of protists

Recent molecular genetic studies, carried out on key coccolithophores species, have shown that many coccolithophores conventionally regarded as single species represent assemblages of sibling species of monophyletic origin (Sáez et al., 2003). For many species tested by molecular genetic, the molecular clock estimates suggest that sibling species have deep divergences close to the origin of the broader morphotypes (Sáez et al., 2003). This has lead to the suggestions that microevolution in coccolithophores may follow a pattern of initial radiation and subsequent stasis rather than complex reticulate evolution (de Vargas et al., 2004). For many coccolithophores, even those tested by molecular genetics, the level of phenetic variation indicative of cryptic or pseudo cryptic species is however poor (de Vargas et al., 2004; Young et al., 2005). The recent divergence of *E. huxleyi*, supported by the fossil record and molecular genetic studies (Thierstein et al., 1977; Sáez et al., 2004) and the high-level of phenetic-genetic differentiation among coccolithophores (e.g. Young and Westbroek, 1991) suggests that fast morphological-genetic evolution is a common pattern among reticulofenestrid coccolithophores. As suggested by morphological continuity, the species described here, *R. calicis* and other new very small reticulofenestrid species represent a monophyletic group (Crudeli et al., in prep. 3; this work). The FO of *G. theyeri* at 4.45Ma as well as the FO occurrence of *G. samtlebenii* n. sp., *G. drieveri* n. sp. and *R. calicis* around 4.3 Ma demonstrate an exceptional increase in speciation rates among this group in the early Pliocene. As discussed, there is no definitive evidence that *G.* sp. cf. *theyeri* represents a discrete species from *G. theyeri*. If the opposite is true, the evolutionary radiation would have even been more pronounced. Evolution follows a pattern of short-term initial radiation. Speciation is not concentrated in a single main initial radiation, as suggested by the successive occurrence of e.g. *G. jerkovicii* n. sp. and *G. bollmannii* n. sp, but occurs in a stepwise pattern. These last however, occur within few thousand years. As discussed by Crudeli et al. (in prep. 3), the short duration of *R. calicis* may support fast evolution among the group. *G. drieveri* n. sp. appears not to be present longer in the fossil record, and may have a short duration supporting a pattern of fast evolution. Evolution may be very short and species of the population may easily undergone extinction. Our study is however not conclusive since it is based on a single core and the discontinuous occurrence of these recently described species may be simply related to local paleoecology. Globally distributed species like *E. huxleyi* should be regarded as complexes composed of locally adapted population (Geisen et al., 2004, for discussion). In this respect, *G. drieveri* n. sp. may represent a locally adapted population. By contrast, *G. samtlebenii* n. sp. and *G.* sp. cf. *theyeri* appear long ranging species (at least 500 kyr) and may suggest differential environmental-evolutionary selection on different phenotypes.
High genetic differentiation without phenetic variation has also been proposed. Our result support that, in reticulofenestrids, genetic differentiation is coupled with phenetic variation as predicted by

preliminary molecular genetic studies on reticulofenestrids coccolithophores (Geisen et al., 2004 and references therein). However, as shown by the very small *R. alis* n. sp. (Crudeli et al., in prep. 3) morphological plasticity may be high.

Given the recent divergence of *E. huxleyi* and its genetic variability (Geisen et al., 2004; Young et al., 2005) we expect that, from fossil record species-level studies (e.g. *Emiliania*) on evolutionary patterns similar to those documented here will be available in the future. The fact that the initial evolutionary radiation agrees with the predicted evolutionary model, supports the idea, that our fine-scale morphological differentiation of species is in agreement to a genetic species concept that can be aplied to fossil species and morphospecies.

3.3.5. *Gephyrocapsa* in the late Pliocene

After the initial radiation and the evolution of larger species (e.g. *G. jerkovicii* n. sp.), only the small *Gephyrocapsa* specimens seem to survive (Fig. 4). After the maximum in abundance, small *Gephyrocapsa* disappear from oceanic settings (Okada, 2000; Marino and Flores, 2002; Gibbs et al., 2005) or become rare (e.g. Kameo and Sato, 2000). The decrease in abundance of small *Gephyrocapsa* is not synchronous (Gibbs et al., 2005) and the group shows a longer record entering NN16 Zone (e.g. Okada, 2000). This is likely due to different paleoecological conditions at different sites which variably supported the populations. In the Mediterranean, during the Pliocene, small *Gephyrocapsa* decreases but has a continuous record to the late Pliocene (Driever, 1988). Small *Gephyrocapsa* species appear to have an affinity to hemipelagic environments (Okada, 1993), whereas larger species reveal an oceanic preference. *Gephyrocapsa* minute (GM, Bollmann, 1997) have widespread distribution and suggests broad ecological adaptation, by contrast, larger types have more restricted ecology (Bollmann, 1997; Bollmann et al., 2002). It may be possible that some small of the new species survived in restricted areas (e.g. Mediterranean) and successively increase again. Further studies are needed in order to understand the mechanism of evolution of the Gephyrocapsa group from its earliest early Pliocene radiation (Fig. 6). It is interesting to observe that the smaller forms, as previously discussed, appear to have an oligotrophic adaptation. Proliferation in the Mediterranean area of those species may be possible. Nonetheless, this would be in agreement which the supposed phyletic relation *G. theyeri*, possibly the stem species of the plexus and *R. alis* n. sp., a ornamented more oligotrophic very small reticulofenestrid species (Crudeli et al., in prep.3).

3.3.6. The cyclic variation of *Gephyrocapsa* in the Quaternary

Size increase cycles, accompanied by morphological variation of *Gephyrocapsa* specimens, occur in the Quaternary and cycles (about 500 kyr) have been predicted to represent evolutionary lineages (Matsuoka and Okada, 1990; Matsuoka and Fujoka, 1992). At the beginning of each cycle, the assemblage is commonly characterised by small forms of an average of 3 μm in size that diverge upward giving rise to larger forms that disappear thereafter. The larger forms of each cycle (large *Gephyrocapsa*) differ in morphology and these have been typified as *Gephyrocapsa* sp. A, *Gephyrocapsa* sp. B, *Gephyrocapsa* sp. D, and *Gephyrocapsa* sp. C (Matsuoka and Okada, 1990).

The pattern of size variation of small *Gephyrocapsa* documented here (500 kyr, Fig. 4) records the evolution of different species and is closely similar to the Quaternary cycles. Our analyses were conducted at much higher resolution and from cores with higher sedimentation rate (about 3 kyr,

Steph et al., in rev.). This similarity, suggests that each Quaternary cycle is in fact evolutionary as already predicted by Matsuoka and Okada (1990). The difference in morphology between *Gephyrocapsa* (separation in sp. A, sp. B, sp. C, and sp. D) also support that different species evolved from each cycle.

Reticulofenestrids also show strong size variation in the Neogene. In the Miocene, Young (1990) recognised a widespread size reduction of forms and defined a new biostratigraphic event, the small *Reticulofenestra* horizon. The author discussed the possibility that this was in fact evolutionary in contrast to simple ecological induced size variation. A similar decrease was observed by Takayama (1993) in addition to a second size reduction in correspondence to zone NN15-NN13. Kameo and Bralower (2000) showed various cycles in size variation of reticulofenestrids including a drastic decrease in size in the early Pliocene of the cores analysed here. Other authors have documented cyclic size variations of reticulofenestrids and discussed that these were possibly evolutionary (e.g. Kameo and Takayama, 1999).

The size increase of small *Gephyrocapsa* is evolutionary and supports the inference that the *Gephyrocapsa* Quaternary cycles are evolutionary. Crudeli et al., in prep. 3 showed species-level phylogenetic relation between the very small reticulofenestrids and *Gephyrocapsa*. Since these forms are closely related, it is possible that the various size variations of *Reticulofenestra* are in fact evolutionary controlled.

3.3.7. Some open questions

Still the question remains. What caused the radiation of *Gephyrocapsa* in the early Pliocene?, why there is surprising similarity with the cyclicity in Quaternary *Gephyrocapsa* and Neogene *Reticulofenestra*, why there is cyclicity?. One hypothesis is that the evolutionary pattern, with a variable number of species evolving from a smaller population, is intrinsic in the development of these coccolithophores. On the contrary a second hypothesis would suggest, that these cyclic patterns are controlled by ecological or paleoceanographic changes in the ocean, but it is hard to envisage, which mechanism would be responsible throughout the entire Neogene. Nonetheless, as previously discussed, the pattern of radiation of *Gephyrocapsa* appears related to ecology.

3.3.8. Models of evolution

As far as classical evolutionary models are concerned, the evolution of *G. samtlebenii* n. sp., *G. drieveri* n. sp. and *G. theyeri* agree with the model of punctuated equilibrium. On the contrary, the evolution of *G. bollmanni* n. sp. and the other species of similar size would agree with the model of phyletic evolution.

In general, from biostratigraphic data, the model of sympatric evolution seems applicable due to the wide documented synchronous LM occurrence of coccoliths in the fossil record. Diachronic occurrences, however have been documented as well (Gibbs et al., 2005). Focusing on the initial divergence of the plexus, sympatric speciation appears likely. Allopatry would be supported by very diachronous evolution of *G. theyeri* in the Pacific, but the occurrence is highly synchronous.

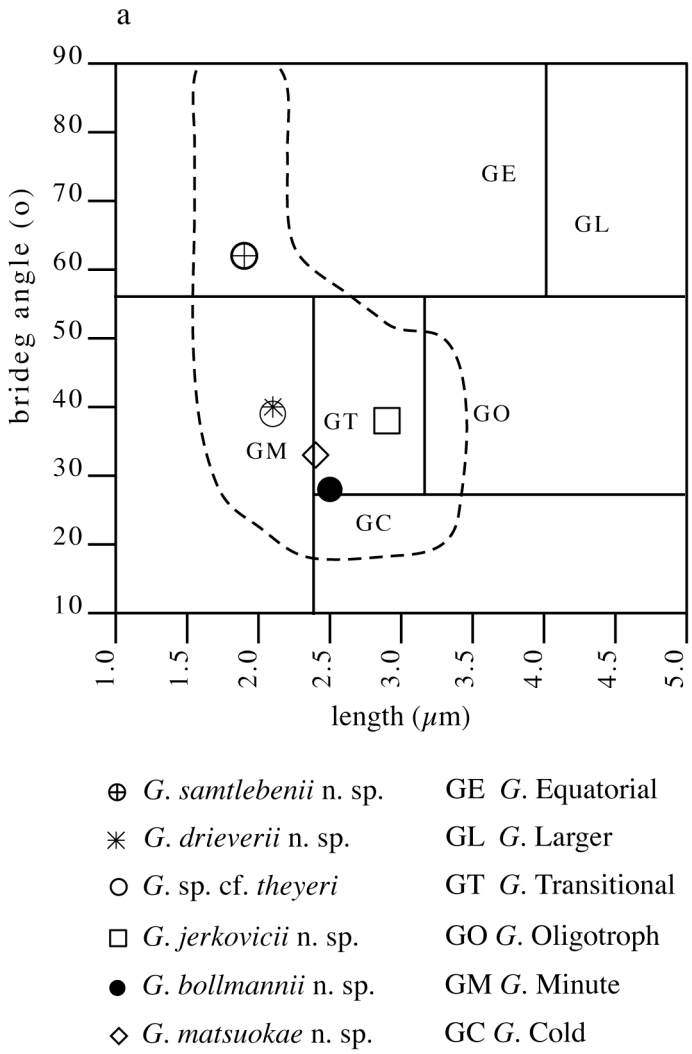

Fig. 6. Plot of the average bridge angle vs. average length (holotype and paratypes) of *Gephyrocapsa* sp. cf. *theyeri*, *G. drieveri* n. sp., *G. samtlebenii* n. sp., *G. bollmannii* n. sp., *G. matsuokae* n. sp. and *G. jerkovicii* n. sp. (symbols) compared to the frequency maxima of the average bridge angle vs. average length of *Gephyrocapsa* morphotype from the Holocene (cap letters) from Bollmann (1997). The dash line indicates the total morphospace of the new species (see table 1 for morphometric details) – redrawn from Bollmann (1997).

3.3.9. The closure of the Panama Isthmus

Diversity curves are commonly used to constrain the evolutionary development of coccolithophore. These, often show pronounced variation in correspondence of major environmental changes (Bown et al., 2004). However, diversity data may be biased by several factors and caution must be taken in their interpretation (Young et al., 2005). Samples preservation and LM vs. SEM study are among the most significant factors that can bias such estimations (Gartner, 1988; Young et al., 2005). Our study, revealed a higher biodiversity among reticulofenestrids. The evolutionary radiation of *Gephyrocapsa* and *Pseudoemiliania,* documented by the basin-wide LM FCO and FO respectivally, are thought to be triggered by the significant paleoceanographic changes related to the North Hemisphere Glaciations.

Major changes in surface water circulation in the Caribbean area and Equatorial Pacific and related changes in salinity and temperature of the water masses occurred during the closure of the Isthmus of Panama (e.g. Haug et al., 2001; Steph et al., in rev.; Groeneveld et al., submitted). From the Caribbean Sea, significant evolutionary events are documented for planktonic and benthic foraminifera, corals,

molluscs (e.g. Jackson et al., 1993; Collins et al., 1996). Likely, the significant changes in paleoceanography related to the final steps of the closure of the Isthmus are responsible for such evolutionary radiation. Further detailed comparison between the radiation of *Gephyrocapsa* and paleoceanographic reconstructions are therefore necessary.

The causes of plankton evolution still remain elusive (Norris, 2000). Viral infection, have been proposed as a major cause for plankton extinction (Emiliani, 1993). Few studies have investigated causes related to coccolithphores evolution (e.g. Gibbs et al., 2005 and references therein). A number of extinction events characterise the nannoflora in the early to middle Pliocene. It is expected that the different *Gephyrocapsa* species evolved in order to occupy peculiar ecological niches possibly caused by significant changes in the water system circulation related to the closure or major gateways in the Pliocene. Loss of niches by means of niches competition and changes in the character of the ecological niches may have likely favoured the extinction of other forms.

4. Conclusions

Modern reticulofenestrids generally express a wide higher biodiversity than their fossil record, which is most likely due to selective preservation and to the dominance of LM studies which can not resolve their fine-scale morphological variation.

The early Pliocene record of small *Gephyrocapsa* was previously documented only by LM studies which showed a word-wide FCO in the *R. pseudoumbelicus* Zone and few reports of size variation. These studies could not resolve aspects related to the evolutionary radiation of this important group of coccolithophores in the Pliocene. The occurrence was supposed to be related with the onset of the Northern Hemisphere Glaciation. An intriguing coincidence between the LM FCO of small *Gephyrocapsa* at about 4.0 Ma documented by biostratigraphy and significant paleoceanographic changes in the Panama Isthmus (Haug et al., 2001) suggested to analyse the radiation in this area where an amount of evolutionary events have been previously documented.

By high-resolution SEM analyses of well-preserved samples from cores from the Caribbean Sea we documented for the first time a high-resolution pattern of size variation of small *Gephyrocapsa* from the FO of *G. theyeri* until 3.8Ma. On the base of this results and qualitative-extensive SEM observations on the morphological variability of forms, we describe five new *Gephyrocapsa* species and document phenetic variation of *G. theyeri*.

1 - The LM pattern of small *Gephyrocapsa* is related to an exceptional evolutionary radiation of the group. Initial radiation is followed by other speciations suggesting a complex pattern of evolution. Evolution, in this group of coccolithophore may be very fast and species may have undergone frequent extinction.

2 - The new species suggest a strong evolutionary pressure among reticulofenestrids and we predict that comparable morphological evolution will be shown by other coccolithophore genera e.g. *Pseudoemiliania*.

3 - The first size increase cycle of small *Gephyrocapsa* is evolutionary, the two successive are likely ecologically controlled. The younger increase in size is evolutionary. The pattern of size variation is

recorded in the Atlantic and Mediterranean and likely record the occurrence of the species described. The paleofluxes of small *Gephyrocapsa* observed here are comparable to the abundance patterns of previous works and suggests a strong link between paleoecology and species-level evolution. Important variation of the paleoecological condition of the water column related to the phases of the closure of the Panama Isthmus may have played a significant role in the radiation of coccolithophores.

4 - The early Pliocene size increase of small *Gephyrocapsa* has been qualitatively and quantitatively observed by LM by different authors. This is the result of the evolution of different *Gephyrocapsa* species. It is expected that a similar diversification will be recognised in other areas.

5 - The continuous record in the Pliocene Mediterranean suggests that some smaller species survived and may have successively undergone similar radiation.

6 - Our study supports that both, the FCO of the LM small *Gephyrocapsa* (in LM) and successive development of an acme are valid biostratigraphic events.

7 - Comparison with the evolutionary model of planktic organism developed from molecular genetic studies indicate that our morphospecies may be more closely related to genetically distinct populations than expected from classical morphospecies concept.

8 - The pattern of the evolutionary development of the small *Gephyrocapsa* population is closely similar to that observed in *Gephyrocapsa* during the Quaternary, and in *Reticulofenestra* during the Miocene and Pliocene. This suggests that these cycles may be also evolutionary which needs to be tested.

This study demonstrates that more information on plankton evolution can be recorded from the fossil archive than previously thought. Species-level evolutionary studies are possible from the fossil record but well-preserved samples are a key prerequisite for such studies.
The early Pliocene size increase of small *Gephyrocapsa* has been qualitatively and quantitatively observed by LM by different authors. Behind this, is the evolution of different *Gephyrocapsa* species.

Our study, that is not by any maen a complete study on the species-level variation of *Gephyrocaspa*, provides a framework for the study of evolutionary developments of reticulofenestrids from the fossil record. Moreover, the recent result from molecular genetic studies can now be tested in the fossil record.

Acknowledgements
This research used samples provided by the Ocean Drilling Program. Funding for this research was provided by Deutsche Forschungsgemeinschaft (DFG) Gateways Research Unit (Impact of Gateways on ocean circulation, climate, and evolution), Kiel University. U. Schuldt and B. Bader, C. Jones and A. Ball are warmly thanked for SEM assistance at Kiel University and at the NHM, London, respectively.

This work represents part of the Doctor of Natural Science thesis at The University of Kiel for D.C.

References

Andruleit, H., 1996. A filtration technique for quantitative studies of coccoliths. Micropaleontology, 42, 4, 403-406.

Bollmann, J., 1997. Morphology and biogeography of *Gephyrocapsa* coccoliths in Holocene sediments. Mar. Micropaleontol., 29, 319-350.

Bollmann, J., Baumann, K.-H., Thierstein, H.R., 1998. Global dominance of *Gephyrocapsa* coccoliths in the late Pleistocene: selective dissolution, evolution, or global environmental change? Paleoceanography 13, 5, 517-529.

Bollmann, J., Henderiks, J., Brabec, B., 2002. Global calibration of *Gephyrocapsa* coccolith abundance in Holocene sediments for paleotemperature assessment. Paleoceanography, 17, 7-1-9, doi: 10.1029/2001PA000742.

Bown, P.R., Lees, J.A., Young, J.R., 2004. Calcareous nannoplankton evolution and diversity through time. In: Thierstein, H.R. and Young, J.R. (Eds), Coccolithophores - From molecular processes to global impact. Springer, pp. 481-506.

Bréhéret, J.G., 1978. Formes nouvelles quaternaires et actuelles de la famille des Gephyrocapsaceae (Coccolithophorides). C.R. Acad. Sc. Paris 287, D, 447-449.

Bleijswijk, J.V., Wal, P.V.D., Kempers, R., Veldhuis, M.J.W., 1991. Distribution of two types of *Emiliania huxleyi* (Prymnesiophyceae) in the northeast Atlantic region as determined by immunofluorescence and coccolith morphology. J. Phycol., 27, 566-570.

Collins, L.S., Budd, A.F., Coates, A.G., 1996. Earliest evolution associated with closure of the Tropical American Seaway. Proc. Natl. Acad. Sci. USA, 93, 6069-6072.

Crudeli, D., Kinkel, H., 2004. *Reticulofenestra calicis* n. sp., an unusual small reticulofenestrid coccolith from the Lower Pliocene of the South Caribbean Sea. Micropaleontology, 50, 4, 369-379.

Crudeli, D., 2005. Early Pliocene evolution of coccolithophores in the Caribbean Sea: taxonomy, biostratigraphy, paleoecology and paleoceanography PhD thesis, Kiel University.

Crudeli, D., Young, J.R., Kinkel, H., (in prep. 3). *Reticulofenestra alis* n. sp., *R. pujosiae* n. sp. and *R. premoliae* n. sp., key-species in the reconstruction of the phylogeny of *Gephyrocapsa theyeri* and *R. calicis* (Coccolithophore, early Pliocene, South Caribbean).

de Vargas, C., Sáez, A.G., Medlin, L.K., Thierstein, H.R., 2004. Super-species in the calcareous plankton. In: Thierstein, H.R. and Young, J.R. (Eds.). Coccolithophores - From Molecular Processes to Global Impact. Springer, pp. 271-298.

Driever, B.W.M., 1988. Calcareous nannofossils biostratigraphy and paleoenvironmental interpretation of the Mediterranean Pliocene. Utrecht Micropaleontol. Bull. 36, 1-245.

Findlay, C.S., Giraudeau, J., 2001. Extant calcareous nannoplankton in the Australian sector of the Southern Ocean (austral summers 1994 and 1995). Mar. Micropaleontol., 40, 4, 417-439.

Gartner, S., 1972. Late Pleistocene calcareous nannofossils in the Caribbean and their interoceanic correlation. Palaeogeogr. Palaeoclimatol. Palaeoecol. 12, 169-191.

Gartner, S., 1977. Calcareous nannofossil biostratigraphy and revised zonation of the Pleistocene. Mar. Micropaleontol. 2, 1-25.

Gartner, S., 1988. Paleoceanography of the Mid-Pleistocene. Mar. Micropaleontol., 13, 23-46.

Gartner, S., 1991. A note on Gephyrocapsa Caribbeanica and Amphosphaera-shaped Schyphoshaera. INA Newsletter 13/3, 103-104.

Geisen, M., Billard, C., Broerse, A.T.C., Cros, L., Probert, I., Young, J.R., 2002. Life-cycle associations involving pairs of holococcolithophorid species: intraspecific variation or cryptic speciation? Eur. J. Phycol. 37, 531-550.

Geisen, M., Young, J.R., Probert, I., Sáez, A.G., Baumann, K.-H., Bollmann, J., Cros, L., Devargas, C., Medlin, L.K., Sprengel, C., 2004. Species level variation in coccolithophores. In: Thierstein, H.R. and Young, J.R. (Eds.), Coccolithophores - From molecular processes to global impact. Springer, pp. 327-366.

Gibbs, S.J., Young, J.R., Bralower, T.J., Shackleton, N.J., 2005. Nannofossil evolutionary events in the mid-Pliocene: an assessment of the degree of synchrony in the extinctions of *Reticulofenestra pseudoumbilicus* and *Sphenolithus abies*. Palaeogeogr. Palaeoclimatol. Palaeoecol. 217, 155-172.

Groeneveld, J., Nürnberg, D., Steph, S., Tiedemann, R., Reichart, G.J., Reuning, L., Crudeli, D., (submitted). Increasing Mg/Ca SSTs for the Pliocene Caribbean: Western Atlantic Warm Pool formation, salinity influence or diagenetical overprint? Geochem. Geophys. Geosyst.

Heimdal, B.R., 1973. Two new taxa of recent coccolithophorids. "Meteor" Forschungsergebnisse, Reihe D, Biologie, 13, 70-75.

Iglesias-Rodríguez, M.D., Sáez, A.G., Groben, R., Edwards, K.J., Batley, J., Medlin, L.K., Hayes, P.K., 2002. Polymorphic microsatellite loci in global populations of the marine coccolithophorid *Emiliania huxleyi*. Molecular Ecol. Notes 2, 495-497.

Jerkovic, M.L., 1970. *Noëlaerhabdus* nov. gen. type d'une nouvelle famille de Coccolithophoridés fossiles: Noëlaerhabdus du Miocêne supérieur de Yougoslavie. Compt. Rend. Ac. Sci. Paris D, 270, 468-470.

Kameo, K., Bralower, T.J., 2000. Neogene calcareous nannofossil biostratigraphy of Sites 998, 999, and 1000, Caribbean Sea. In: Leckie, R.M., Sigurdsson, H. et al. (Eds), Proc. ODP Sci. Results 165, 3-17.

Kameo, K., 2002. Late Pliocene Caribbean surface water dynamics and climatic changes based on calcareous nannofossil records. Palaeogeogr. Palaeoclimatol. Palaeoecol. 2791.P

Kameo, K., Takayama, T., 1999. Biostratigraphic significance of sequential size variations of the calcareous nannofossil genus *Reticulofenestra* in the Upper Pliocene of the North Atlantic. Mar. Micropaleontol. 37, 41-52.

Kameo, K., Sato, T., 2000. Biogeography of Neogene calcareous nannofossils in the Caribbean and the eastern equatorial Pacific-floral response to the emergence of the Isthmus of Panama. Mar. Micropaleontol. 39, 201-218.

Kameo, K. and Bralower, T.J. 2000. Neogene calcareous nannofossil biostratigraphy of Sites 998, 999, and 1000, Caribbean Sea. Proceedings of the Ocean Drilling Program, Scientific Results 165, 3-17.

Kamptner, E., 1943. Zur Revision der Coccolithineen-Spezies *Pontosphaera huxleyi* Lohmann. Anz. Akad. Wiss. Wien 80, 43-49.

Knowlton, N. 1993. Sibling species in the sea. Annual Reviews of Ecology and Systematics, 24, 189-216.

Lohman, W.H., Ellis, C.H., 1981. A new species and new fossil occurences of calcareous nannoplankton in Eastern Mediterranean. J. Paleontol. 55, 2, 389-394.

Matsuoka, H., Okada, H., 1989. Quantitative analysis of Quaternary nannoplankton in the subtropical northwestern Pacific Ocean. Mar. Micropaleontol. 14, 97-118.

Matsuoka, H., Okada, H., 1990. Time-progressive morphometric changes of the genus *Gephyrocapsa* in the Quaternary sequence of the tropical Indian Ocean, Site 709. In: Duncan, R.A., Backman, J. et al (Eds.), Proc. ODP Sci. Results 115, 255-270.

Matsuoka, H., Fujioka, K., 1992. Morphometric changes of the genus *Gephyrocapsa* at Site 790, subtropical Pacific Ocean. In: Taylor, B., Fujioka, K. et al. (Eds.), Proc. ODP Sci. Results 126, 263-269.

Marino, M., Flores, J.A., 2002. Miocene to Pliocene calcareous nannofossil biostratigraphy at ODP Leg 177 Sites 1088 and 1090. Mar. Micropaleontol. 45, 291-307.

Martini, E., 1971. Standard Tertiary and Quaternary calcareous nannoplankton zonation. In: Farinacci, A. (Ed.), Proc. 2nd Planktonic Conf., Tecnoscienza, Roma, pp. 738-785.

Medlin, L.K., Barker, G.L.A., Campbell, L., Green, J.C., Hayes, P.K., Marie, D., Wrieden, S., Vaulot, D., 1996. Genetic characterisation of Emiliania huxleyi (Haptophyta). J. Mar. Systems, 9, 13-32.

Okada, H., 1983. Modern nannofossil assemblages in sediments of coastal and marginal seas along the western Pacific Ocean. Utrecht Micropaleontolog. Bull., 30, 171-187.

Okada, H., Honjo, S., 1973. The distribution of oceanic coccolithophorids in the Pacific. Deep Sea Res. 20, 355-374. (1339)

Okada, H., Honko, S., 1975. Distribution of coccolithophores in marginal seas along the western Pacific Ocean and in the Red Sea. Marine Biology, 31, 271-285. (584) & (846)

Okada, H., Bukry, D., 1980. Supplementary modification and introduction of code numbers to the low-latitude coccolith biostratigraphic zonation (Bukry, 1973; 1975). Mar. Micropaleontol. 5, 321-325.

Okada, H., 2000. Neogene and Quaternary Calcareous Nannofossils from the Blake Ridge, Sites 994, 995, and 997. In: Paull, C.K., Matsumoto, R. et al. (Eds), Proc. ODP Sci. Results 164, 331-341.

Paasche, E., 2002. A review of the coccolithophorid *Emiliania huxleyi* (Prymnesiophyceae), with particular reference to growth, coccolith formation, and calcification-photosynthesis interactions. Phycologia 40, 6, 503-529.

Perch-Nielsen, K., 1985. Cenozoic calcareous nannofossils. In: Bolli, H.M., Saunders, J.B., Perch-Nielsen, K. (Eds), Plankton Stratigraphy. Cambridge University Press, Cambridge, pp. 427-554.

Pirini Radrizzani, C., Valleri, G., 1977. New data on calcareous nannofossils from the Pliocene of the Tyrrhenian basin Site 132 DSDP, Leg 13. Riv. Ital. Paleontol. Stratigr. 83, 4, 897-924.

Pujos, A., 1987. Late Eocene to Pleistocene medium-sized and small-sized "Reticulofenestrids". Abh. Geol. Bundesanst. 39, 239-277.

Rio, D., 1982. The fossil distribution of coccolithophore genus *Gephyrocapsa* Kamptner and related Plio-Pleistocene chronostratigraphic problems. In: Prell, W.L., Gardner, J.V. et al. (Eds), Init. Rep. DSDP 68, 325-343.

Sáez, A.G., Probert, I., Geisen, M., Quinn, P., Young, J.R., Medlin, L.K., 2003. Pseudo-cryptic speciation in coccolithophores. Proc. Nat. Ac. Sci. 100, 12, 7163-7168.

Sáez, A.G., Probert, I., Young, J.R., Medlin, L.K., 2004. A review of the phylogeny of the Haptophyta. In: Thierstein, H.R. and Young, J.R. (Eds.), Coccolithophores - From molecular processes to global impact. Springer, 251-270.

Sato, T., Kameo, K., Takayama, T., 1991. Coccolith biostratigraphy of the Arabian Sea. In: Prell, W.L., Niitsuma, N. et al. (Eds), Proc. ODP Sci. Results 117, 37-54.

Samtleben, C., 1980. Die Evolution der Coccolithophoriden-Gattung *Gephyrocapsa* nach Befunden im Atlantik. Paläontol. Z. 54, 91-127.

Sigurdsson, H., Leckie, R.M., Acton, G.D. et al. 1997. Proc. ODP Initial Reports, 165.

Steph, S., Tiedemann, R., Groenevel, J., Nürnberg, D., Reuning, R., Haug, G., (in revision.). Changes in Caribbean surface hydrography during the Pliocene shoaling of the Central American Seaway. Paleoceanography.

Takayama, T., 1993. Notes on Neogene calcareous nannofossil biostratigraphy of the Ontong Java Plateau and size variations of *Reticulofenestra* Coccoliths. Proc. ODP Sci. Results 130, 179-229.

Thierstein, H.R., Geitzenauer, K.R., Molfino, B., Shackleton, N.J., 1977. Global synchroneity of late Quaternary coccolith datum levels; validation by oxygen isotopes. Geology 5, 4000-4004.

Westbroek, P., Brown, C.W., van Bleijswijk, J., Brownlee, C., Brummer, G.J., Conte, M., Egge, J., Fernandez, E., Jordan, R., Knappertsbusch, M., Stefels, J., Veldhuis, M., van der Wal, P., Young, J.R., 1993. A model system approach to biological climate forcing. The example of *Emiliania huxleyi*. Glob. Planet. Change, 8, 27-46.

Young, J.R., 1989. Observations on heterococcolith rim structure and its relationship to developmental processes. In: Crux, J., van Heck, S.E. (Eds), Nannofossils and their applications. Ellis Horwood Limited, Chichester, pp. 1-20.

Young, J.R., 1990. Size variation of Neogene *Reticulofenestra* coccoliths from Indian Ocean DSDP cores. J. Micropalaeontol. 9, 1, 71-86.

Young, J.R., 1998. Neogene. In: Bown, P.R. (Ed), Calcareous Nannofossil Biostratigraphy. Br. Micropaleontol. Soc. Publ. London, pp. 225-265.

Young, J.R., Westbroek, P., 1991. Genotypic variation in the coccolithophorid species *Emiliania huxleyi*. Mar. Micropaleontol. 18, 5-23.

Young, J.R., Bown, P.R., 1997. Cenozoic calcareous nannoplankton classification. J. Nannoplankton Res. 19, 36-47.

Young, J.R., Bown, P.R., Burnett, A., 1994. Palaeontological perspectives. In: Green, J.C., Leadbeater, B.S.C. (Eds), The Haptophyte Algae. Clarendon Press, Oxford, pp. 379-392.

Young, J.R., Bergen, J.A., Bown, P.R., Burnett, J.A., Fiorentino, A., Jordan, R.W., Kleijne, A., van Niel, B.E., Romein, A.J.T., von Salis, K., 1997. Guidelines for coccolith and calcareous nannofossil terminology. Palaeontology 40, 875-912.

Young, J.R., Davis, S.A., Bown, P.R., Mann, S., 1999. Coccolith ultrastructure and biomineralisation. J. Struct. Biol. 126, 195-215.

Young, J.R., Geisen, M., Cros, L., Kleijne, A., Sprengel, C., Probert, J., Østergaard, J., 2003. A guide to extant coccolithophore taxonomy. J. Nannoplankton Res. 1, 1-125.

Young, J.R., Geisen, M., Probert, J., (in press). A review of selected aspects of coccolithophore biology with implications for palaeobiodiversity estimation. Micropaleontology.

Ziveri, P., Young, J.R., van Hinte, J.E., 1999. Coccolithophore Export Production and Accumulation Rates. In: On determination of sediment accumulation rates. GeoResearch Forum, Trans Tech Publications LTD, Switzerland, 5, 41-56.

Plate 1. SEM of *Gephyrocaps theyeri, G.* sp. cf. *theyeri* and *G. drieveri* n. sp. from cores from ODP Hole 1000A. For each illustration, the ODP Sample, micrograph code, SEM magnification and scale bar are given.

fig. 1. *G. theyeri*, distal view, 16H-1, 5-7 cm (136.35 mbsf), 83324, 20000×, 1 μm.

fig. 2. *G. theyeri*, distal view, 15H-6, 105-107cm (135.35 mbsf), 86820, 20000×, 1 μm.

fig. 3. *G.* sp. cf. *theyeri*, distal view, 15H-5, 105-107 cm (133.85 mbsf), 86786, 20000×, 1 μm.

fig. 4. *G.* sp. cf. *theyeri*, distal view, 15H-5, 105-107 cm (133.85 mbsf), 86884, 20000×, 1 μm.

fig. 5. *G.* sp. cf. *theyeri*, distal view, 15H-6, 15-17 cm (134.45 mbsf), 86563, 20000×, 1 μm.

fig. 6. *G.* sp. cf. *theyeri*, distal view, 15H-5, 105-107 cm (133.85 mbsf), 86890, 20000×, 1μm.

fig. 7. *G. drieveri* n. sp., distal view, paratype, 15H-5, 105-107 cm (133.85 mbsf), 86893, 20000×, 1μm.

fig. 8. *G. drieveri* n. sp., distal view, holotype, 15H-5, 105-107 cm (133.85 mbsf), 86787, 20000×, 1 μm.

fig. 9. *G. drieveri* n. sp., distal view, paratype, 15H-6, 25-27 cm (134.55 mbsf), 86561, 20000×, 1 μm.

fig. 10. *G. drieveri* n. sp., distal view, paratype, 15H-6, 5-7 cm (134.35 mbsf), 86778, 20000×, 1 μm.

fig. 11. *G. drieveri* n. sp. or *G.* sp. cf. *theyeri*? in distal view, 15H-5, 105-107 cm (133.85 mbsf), 84572, 20000×, 1 μm.

fig. 12. *G. drieveri* n. sp. or *G.* sp. cf. *theyeri* in side view, 15H-5, 105-107 cm (133.85 mbsf), 86886, 20000×, 1 μm.

fig. 13. *G.* sp. cf. *theyeri*, distal view, 15H-1, 8-10 cm (126.88 mbsf), 86833, 20000×, 1 μm.

fig. 14. Two specimens of *G.* sp. cf. *theyeri* and one specimen of *R. alis* type 3 in distal view, 15H-2, 115-117 cm (129.45 mbsf), 86576, 17000×, 1 μm.

fig. 15. A slightly overgrown specimen of *G.* sp. cf. *theyeri*, distal view, 14H-4, 85-87 cm (122.65 mbsf), 86806, 20000×, 1 μm.

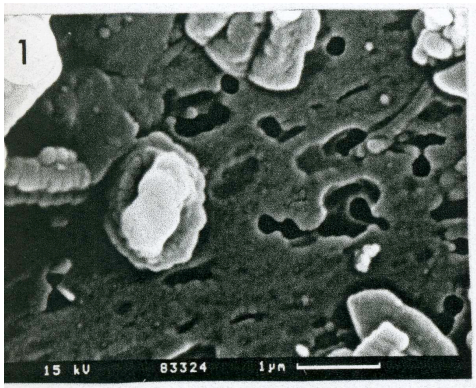
1
15 kV 83324 1µm

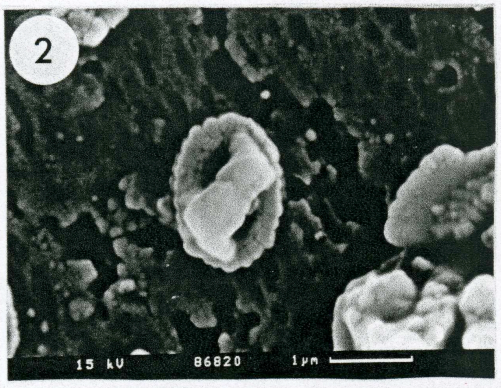
2
15 kV 86820 1µm

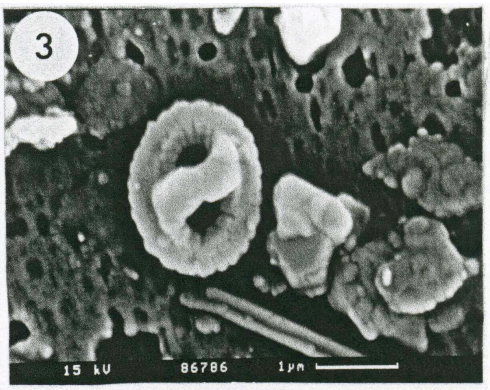
3
15 kV 86786 1µm

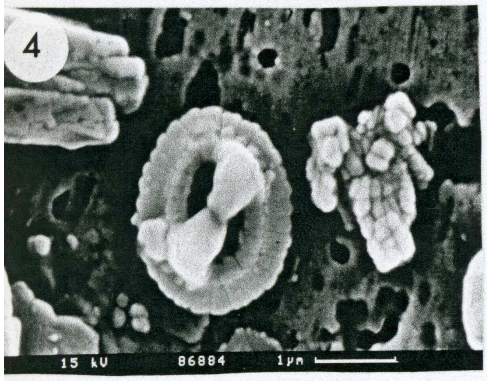
4
15 kV 86884 1µm

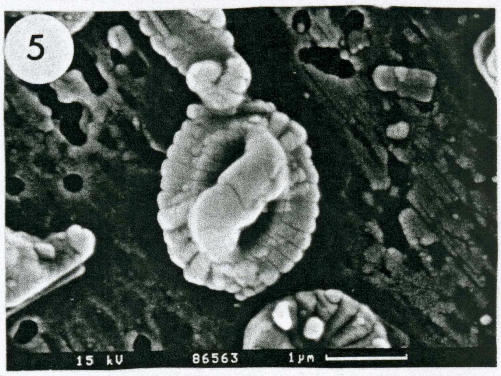
5
15 kV 86563 1µm

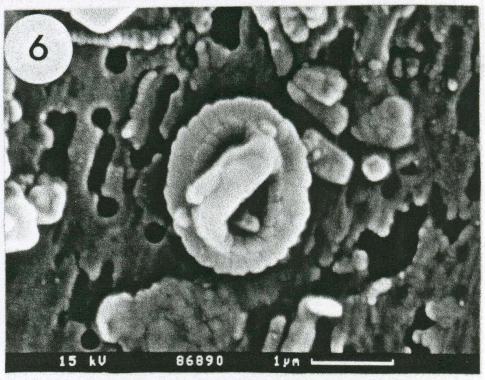
6
15 kV 86890 1µm

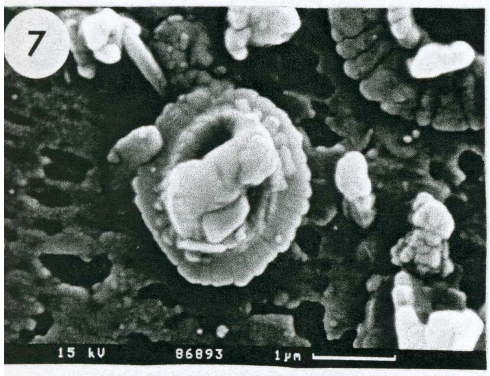
7
15 kV 86893 1µm

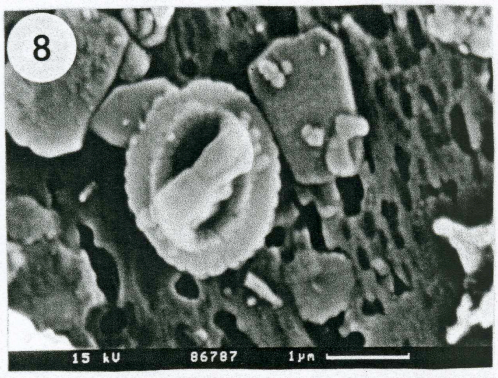
8
15 kV 86787 1µm

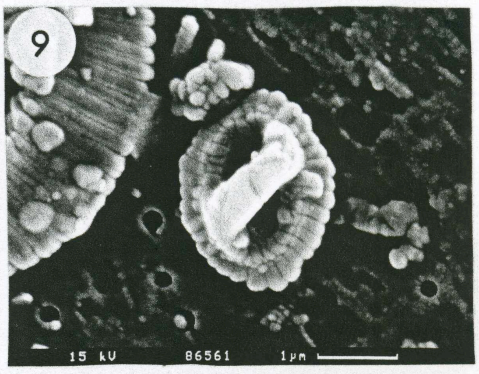
9
15 kV 86561 1µm

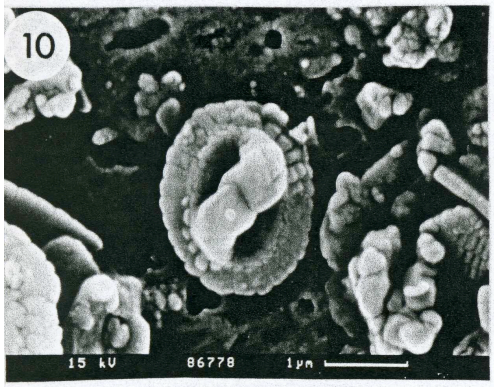
10
15 kV 86778 1µm

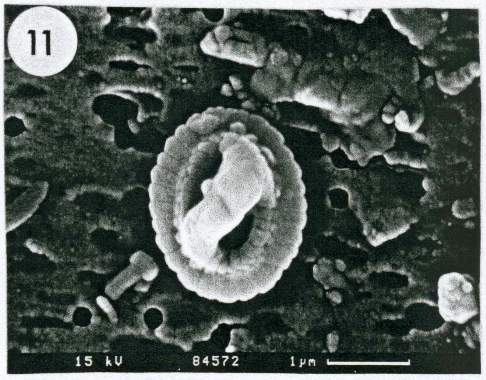
11
15 kV 84572 1µm

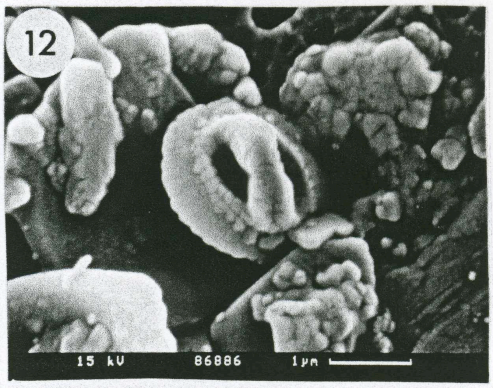
12
15 kV 86886 1µm

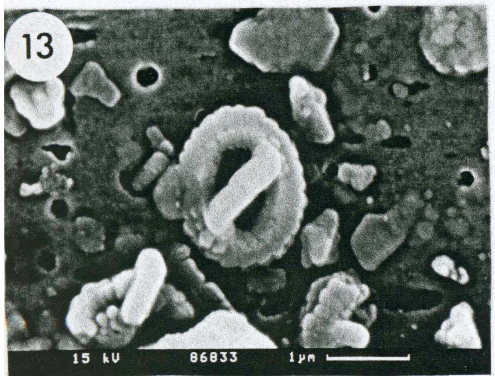
13
15 kV 86833 1µm

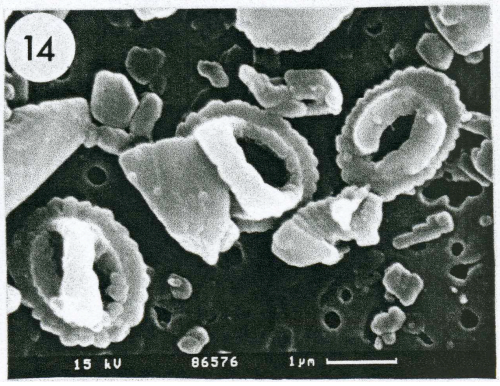
14
15 kV 86576 1µm

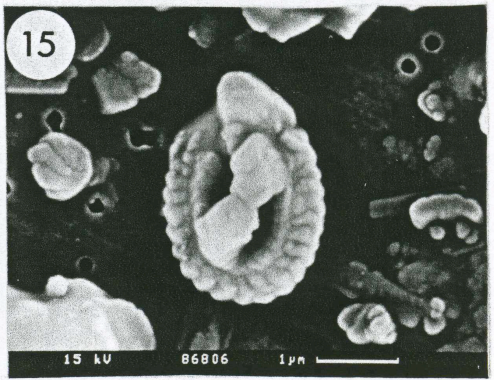
15
15 kV 86806 1µm

Plate 2. SEM of *G. samtlebenii* n. sp., *G. bollmannii* n. sp., *G. matsuokae* n. sp. and *G. jerkovicii* n. sp. from cores from ODP Hole 1000A. For each illustration, the ODP Sample, micrograph code, SEM magnification, scale bar are given.

fig. 1. *G. samtlebenii* n. sp., distal view, holotype, 15H-5, 115-117 cm (133.95 mbsf), 86470, 20000×, 1 μm.
fig. 2. *G. samtlebenii* n. sp., distal view, paratype, 15H-5, 115-117 cm (133.95 mbsf) 86480, 25000×, 1 μm.
fig. 3. *G. samtlebenii* n. sp., distal view, paratype, 15H-5, 105-107 cm (133.85 mbsf), 86885, 20000×, 1 μm.
fig. 4. *G. samtlebenii* n. sp., distal view, 15H-1, 8-10 cm (126.88 mbsf), 86827, 20000×, 1 μm.
fig. 5. *G. bollmannii* n. sp., distal view, holotype, 14H-2, 24-26 cm (119.04 mbsf), 83039, 20000×, 1 μm.
fig. 6. *G. bollmannii* n. sp., side view, same specimens of figure 5, this plate, SEM tilt 31°, 83040, 20000×, 1 μm.
fig. 7. *G. bollmannii* n. sp., distal view, 14H-4, 145-147 cm (123.25 mbsf), 83033, 20000×, 1 μm.
fig. 8. *G. bollmannii* n. sp., side view, 14H-5, 5-7 cm (123.35 mbsf), 83059, 20000*x*, 1 μm.
fig. 9. A slightly overgrown *G. bollmannii* n. sp. specimens, distal view, 15H-1, 135-137 cm (128.15 mbsf), 83643, 20000×, 1 μm.
fig. 10. *G. matsuokae* n. sp., distal view, holotype, 14H-2, 24-26cm (119.04 mbsf), 86756, 20000×, 1 μm.
fig. 11. *G. matsuokae* n. sp., distal view, paratype, 14H-2, 24-26 cm (119.04 mbsf), 82205, 18000×, 1 μm.
fig. 12. *G. matsuokae* n. sp., distal view, paratype, 14H-2, 85-87 cm (119.65 mbsf), 82168, 20000×, 1 μm.
fig. 13. *G. jerkovicii* n. sp., distal view, paratype, 14H-5, 85-87 cm (124.15 mbsf), 86520, 20000×, 1μm.
fig. 14. *G. jerkovicii* n. sp., distal view, paratype, 14H-5, 75-77 cm (124.05 mbsf), 86789, 20000×, 1 μm.
fig. 15. *G. jerkovicii* n. sp., distal view, holotype, 14H-5, 75-77 cm (124.05 mbsf), 86795, 20000×, 1 μm.

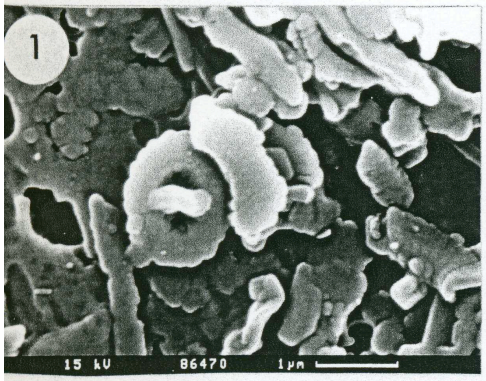
1
15 kV 86470 1µm

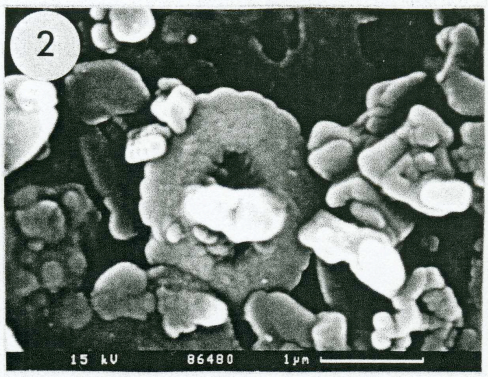
2
15 kV 86480 1µm

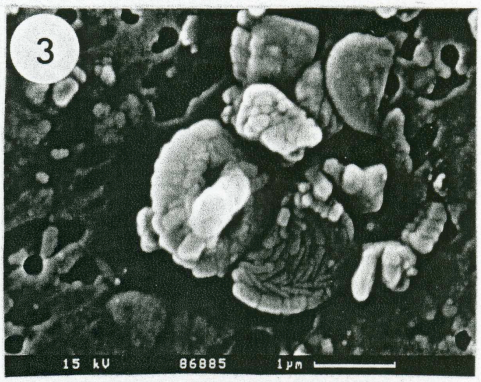
3
15 kV 86885 1µm

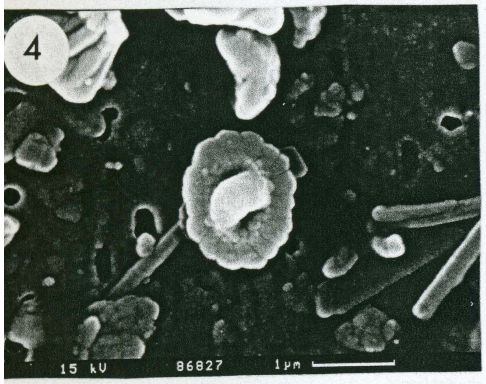
4
15 kV 86827 1µm

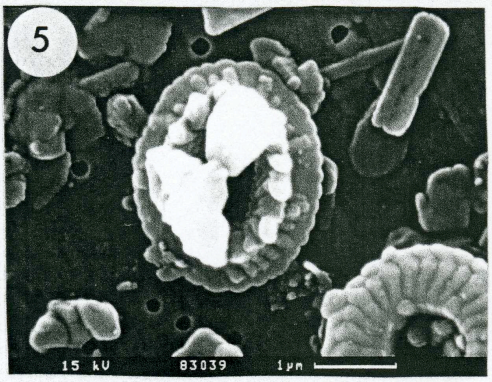
5
15 kV 83039 1µm

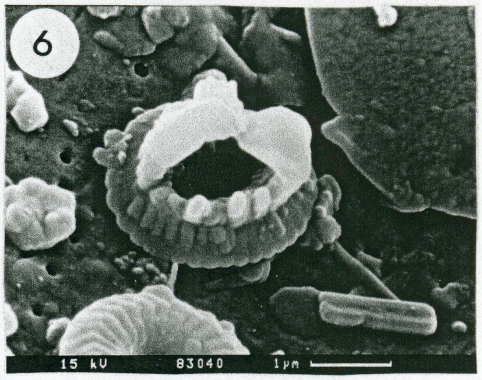
6
15 kV 83040 1µm

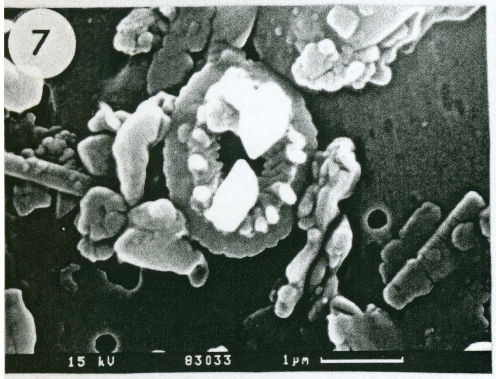
7
15 kV 83033 1µm

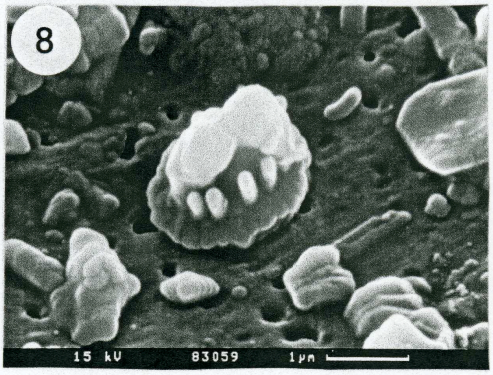
8
15 kV 83059 1µm

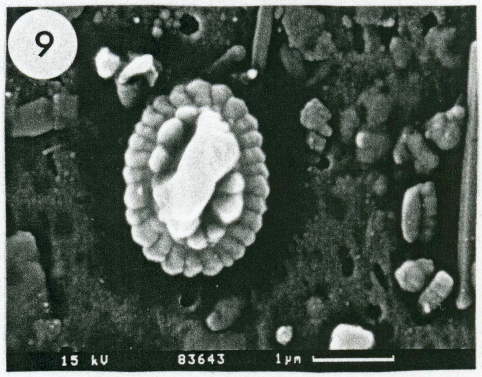
9
15 kV 83643 1µm

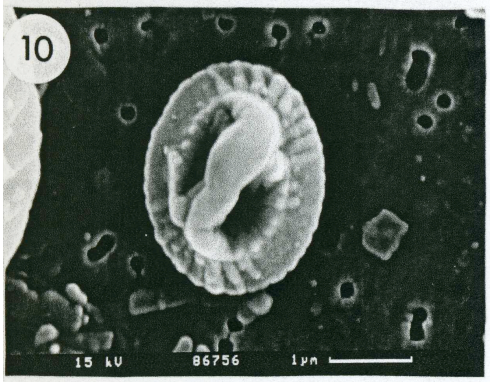
10
15 kV 86756 1µm

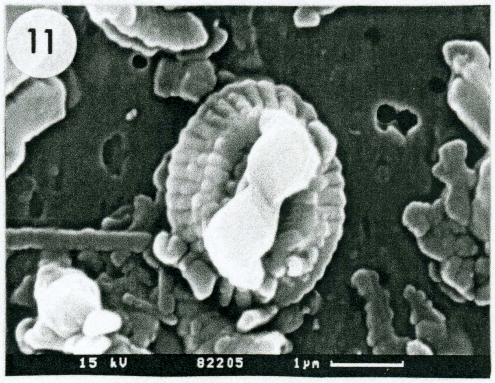
11
15 kV 82205 1µm

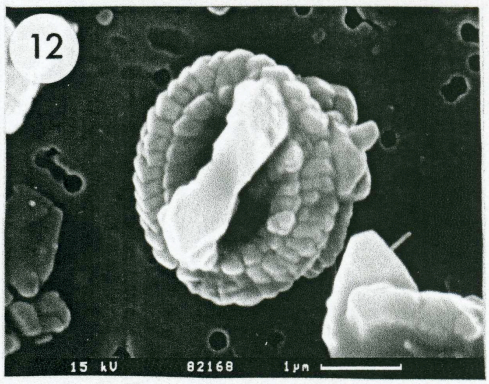
12
15 kV 82168 1µm

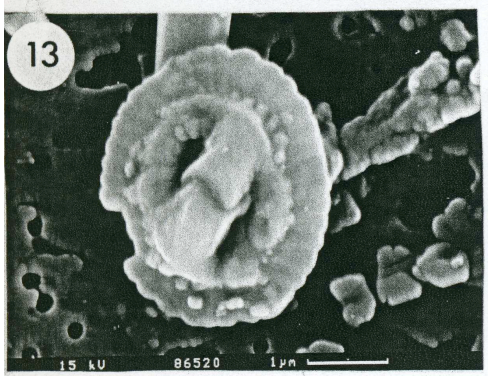
13
15 kV 86520 1µm

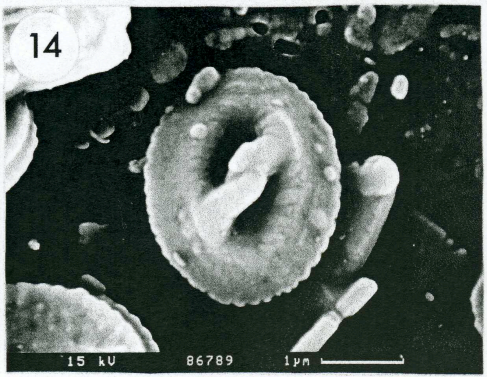
14
15 kV 86789 1µm

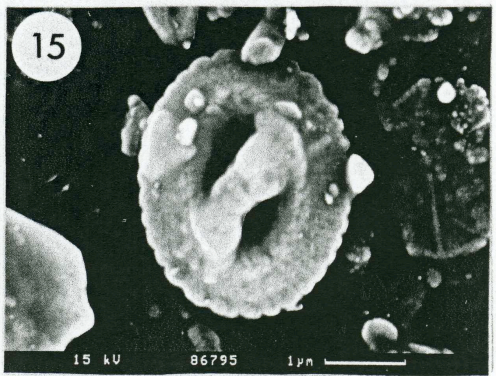
15
15 kV 86795 1µm

Core	Type	Section	Top (cm)	Botton (cm)	depth (mbsf)	Age (Ma)
14	H	1	95	97	118,25	3,8156
14	H	1	104	106	118,34	3,8176
14	H	1	115	117	118,45	3,8198
14	H	1	126	128	118,56	3,8219
14	H	1	135	137	118,65	3,8239
14	H	1	144	146	118,74	3,8259
14	H	2	5	7	118,85	3,8281
14	H	2	15	17	118,95	3,8300
14	H	2	24	26	119,04	3,8320
14	H	2	35	37	119,15	3,8342
14	H	2	44	46	119,24	3,8362
14	H	2	55	56	119,35	3,8384
14	H	2	65	67	119,45	3,8406
14	H	2	75	77	119,55	3,8426
14	H	2	85	87	119,65	3,8448
14	H	2	95	97	119,75	3,8468
14	H	2	104	106	119,84	3,8487
14	H	2	114	116	119,94	3,8507
14	H	2	124	126	120,04	3,8529
14	H	2	135	137	120,15	3,8551
14	H	2	145	147	120,25	3,8573
14	H	3	5	7	120,35	3,8593
14	H	3	15	17	120,45	3,8615
14	H	3	25	27	120,55	3,8635
14	H	3	35	37	120,65	3,8657
14	H	3	45	47	120,75	3,8677
14	H	3	55	56	120,85	3,8699
14	H	3	65	67	120,95	3,8719
14	H	3	75	77	121,05	3,8741
14	H	3	85	87	121,15	3,8761
14	H	3	94	96	121,24	3,8781
14	H	3	105	107	121,35	3,8802
14	H	3	115	117	121,45	3,8822
14	H	3	125	127	121,55	3,8844
14	H	3	135	137	121,65	3,8864
14	H	3	145	147	121,75	3,8886
14	H	4	5	7	121,85	3,8906
14	H	4	15	17	121,95	3,8928
14	H	4	25	27	122,05	3,8948
14	H	4	35	37	122,15	3,8970
14	H	4	45	47	122,25	3,8995
14	H	4	55	56	122,35	3,9023
14	H	4	65	67	122,45	3,9048
14	H	4	75	77	122,55	3,9076
14	H	4	85	87	122,65	3,9102
14	H	4	95	97	122,75	3,9130
14	H	4	106	108	122,86	3,9158
14	H	4	115	117	122,95	3,9183
14	H	4	125	127	123,05	3,9208
14	H	4	135	137	123,15	3,9236
14	H	4	145	147	123,25	3,9261
14	H	5	5	7	123,35	3,9289
14	H	5	15	17	123,45	3,9314
14	H	5	25	27	123,55	3,9342
14	H	5	35	37	123,65	3,9368
14	H	5	45	47	123,75	3,9393
14	H	5	55	56	123,85	3,9421
14	H	5	65	67	123,95	3,9446
14	H	5	70	72	124,00	3,9460
14	H	5	75	77	124,05	3,9474
14	H	5	85	87	124,15	3,9499
14	H	5	95	97	124,25	3,9527
14	H	5	105	107	124,35	3,9552
14	H	5	115	117	124,45	3,9581
14	H	5	125	127	124,55	3,9606
14	H	5	135	137	124,65	3,9634
14	H	5	145	147	124,75	3,9659
14	H	6	5	7	124,85	3,9687
14	H	6	15	17	124,95	3,9712
14	H	6	25	27	125,05	3,9740
14	H	6	35	37	125,15	3,9765
14	H	6	45	47	125,25	3,9793
14	H	6	55	57	125,35	3,9819
14	H	6	65	67	125,45	3,9847
14	H	6	75	77	125,55	3,9872
14	H	6	85	87	125,65	3,9900
14	H	6	95	97	125,75	3,9925
14	H	6	105	107	125,85	3,9953
14	H	6	125	127	126,05	4,0004
14	H	6	135	137	126,15	4,0028
14	H	6	145	147	126,25	4,0052
14	H	7	5	7	126,35	4,0079
14	H	7	15	17	126,45	4,0103
14	H	7	25	27	126,55	4,0129
14	H	7	35	37	126,65	4,0154
14	H	7	45	47	126,75	4,0180
14	H	7	55	56	126,85	4,0204
14	H	7	65	67	126,95	4,0231
15	H	1	8	10	126,88	4,0760
15	H	1	15	17	126,95	4,0777
15	H	1	25	27	127,05	4,0806
15	H	1	35	37	127,15	4,0836
15	H	1	45	47	127,25	4,0862
15	H	1	55	57	127,35	4,0891
15	H	1	65	67	127,45	4,0920
15	H	1	75	77	127,55	4,0946
15	H	1	85	87	127,65	4,0975
15	H	1	95	97	127,75	4,1004
15	H	1	105	107	127,85	4,1030
15	H	1	115	117	127,95	4,1059
15	H	1	125	127	128,05	4,1088
15	H	1	135	137	128,15	4,1114
15	H	1	145	147	128,25	4,1143
15	H	2	5	7	128,35	4,1172
15	H	2	15	17	128,45	4,1198
15	H	2	25	27	128,55	4,1227
15	H	2	35	37	128,65	4,1256
15	H	2	45	47	128,75	4,1282

Core	Type	Section	Top (cm)	Botton (cm)	depth (mbsf)	Age (Ma)
15	H	2	55	57	128,85	4,1311
15	H	2	65	67	128,95	4,1337
15	H	2	75	77	129,05	4,1366
15	H	2	85	87	129,15	4,1396
15	H	2	95	97	129,25	4,1422
15	H	2	105	107	129,35	4,1451
15	H	2	115	117	129,45	4,1480
15	H	2	125	127	129,55	4,1506
15	H	2	135	137	129,65	4,1535
15	H	2	145	147	129,75	4,1564
15	H	3	5	7	129,85	4,1590
15	H	3	15	17	129,95	4,1623
15	H	3	25	27	130,05	4,1655
15	H	3	35	37	130,15	4,1684
15	H	3	45	47	130,25	4,1717
15	H	3	55	56	130,35	4,1750
15	H	3	65	67	130,45	4,1779
15	H	3	75	77	130,55	4,1811
15	H	3	85	87	130,65	4,1844
15	H	3	95	96	130,75	4,1873
15	H	3	105	107	130,85	4,1906
15	H	3	115	117	130,95	4,1935
15	H	3	135	137	131,15	4,2000
15	H	3	143	145	131,23	4,2023
15	H	4	5	7	131,35	4,2062
15	H	4	15	17	131,45	4,2095
15	H	4	25	27	131,55	4,2124
15	H	4	35	37	131,65	4,2157
15	H	4	45	47	131,75	4,2189
15	H	4	55	57	131,85	4,2219
15	H	4	65	67	131,95	4,2251
15	H	4	75	77	132,05	4,2284
15	H	4	85	87	132,15	4,2313
15	H	4	95	97	132,25	4,2346
15	H	4	105	107	132,35	4,2378
15	H	4	115	117	132,45	4,2407
15	H	4	125	127	132,55	4,2440
15	H	4	135	137	132,65	4,2467
15	H	4	145	147	132,75	4,2492
15	H	5	5	7	132,85	4,2520
15	H	5	15	17	132,95	4,2544
15	H	5	25	27	133,05	4,2572
15	H	5	35	37	133,15	4,2599
15	H	5	45	47	133,25	4,2624
15	H	5	55	57	133,35	4,2651
15	H	5	65	67	133,45	4,2679
15	H	5	75	77	133,55	4,2704
15	H	5	85	87	133,65	4,2731
15	H	5	95	97	133,75	4,2758
15	H	5	105	107	133,85	4,2783
15	H	5	115	117	133,95	4,2810
15	H	5	125	127	134,05	4,2838
15	H	5	135	137	134,15	4,2863
15	H	5	145	147	134,25	4,2890
15	H	6	5	7	134,35	4,2918
15	H	6	15	17	134,45	4,2942
15	H	6	25	27	134,55	4,2970
15	H	6	35	37	134,65	4,2997
15	H	6	45	47	134,75	4,3022
15	H	6	55	57	134,85	4,3049
15	H	6	65	67	134,95	4,3074
15	H	6	75	77	135,05	4,3101
15	H	6	85	87	135,15	4,3129
15	H	6	95	97	135,25	4,3154
15	H	6	105	107	135,35	4,3181
15	H	6	115	117	135,45	4,3208
15	H	6	125	127	135,55	4,3233
15	H	6	135	137	135,65	4,3261
15	H	6	145	147	135,75	4,3288
15	H	7	5	7	135,85	4,3318
15	H	7	15	17	135,95	4,3350
15	H	7	25	27	136,05	4,3383
15	H	7	35	37	136,15	4,3412
15	H	7	45	47	136,25	4,3445
15	H	7	55	57	136,35	4,3478
15	H	7	63	65	136,43	4,3501
15	H	0	5	7	136,43	4,3527
16	H	1	5	7	136,35	4,4240
16	H	1	15	17	136,45	4,4273
16	H	1	25	27	136,55	4,4309
16	H	1	35	37	136,65	4,4342
16	H	1	45	47	136,75	4,4378
16	H	1	55	57	136,85	4,4411
16	H	1	65	67	136,95	4,4448
16	H	1	75	77	137,05	4,4480
16	H	1	85	87	137,15	4,4517
16	H	1	95	97	137,25	4,4550
16	H	1	105	107	137,35	4,4586
16	H	1	115	117	137,45	4,4619
16	H	1	125	127	137,55	4,4655
16	H	1	135	137	137,65	4,4688
16	H	1	145	147	137,75	4,4721
16	H	2	5	7	138,25	4,4757
16	H	2	15	17	138,35	4,4790
16	H	2	25	27	138,45	4,4816

CHAPTER 5

The Pliocene Mg/Ca SST increase in the Caribbean: Western Atlantic Warm Pool formation, salinity influence or diagenetic overprint?

Jeroen Groeneveld[1], Dirk Nürnberg[1], Silke Steph[1], Ralf Tiedemann[1], Gert-Jan Reichart[2], Lars Reuning[1] and Daniela Crudeli[3]

[1]IFM-Geomar, Leibniz Institute of Marine Sciences, Kiel, Germany
[2]Faculty of Earth Sciences, Utrecht University, The Netherlands, and, AWI, Institute for Polar and Marine Research, Bremerhaven, Germany
[3]Institute of Geosciences, University of Kiel, Germany

Manuscript submitted to Geochemistry, Geophysics, Geosystems

CHAPTER 5

The Pliocene Mg/Ca SST increase in the Caribbean: Western Atlantic Warm Pool formation, salinity influence or diagenetic overprint?

Jeroen Groeneveld (1), Dirk Nürnberg (1), Silke Steph (1), Ralf Tiedemann (1), Gert-Jan Reichart (2), Lars Reuning (1), Daniela Crudeli (3)

(1) IFM-Geomar, Leibniz Institute of Marine Sciences, Kiel, Germany
(2) Faculty of Earth Sciences, Utrecht University, The Netherlands, and, AWI, Institute for Polar and Marine Research, Bremerhaven, Germany
(3) Institute of Geosciences, University of Kiel, Germany

Abstract

We performed combined analyses of Mg/Ca and $\delta^{18}O$ on the planktonic foraminifer *Globigerinoides sacculifer* from Caribbean ODP Site 1000 in order to reconstruct the effect of the shoaling of the Isthmus of Panama on sea surface temperatures (SST) and salinities (SSS) for the early Pliocene. After 4.5 Ma, the positive, precessional correlation between Mg/Ca and $\delta^{18}O$ suggests that the $\delta^{18}O$ signal is mainly driven by salinity. During maximum SSS, Mg/Ca approaches ~7 mmol/mol (~34-35°C), implying that the large SSS variations exert a profound influence on Mg/Ca, overestimating Mg/Ca by 20-30% (~3-4°C). Foraminiferal Sr/Ca ratios, carbonate mineralogy, calcareous nannofossil analysis, and SEM suggest that diagenetically induced aragonite dissolution and reprecipitation caused crystalline overgrowths on foraminiferal tests with extremely high Mg/Ca-ratios. LA-ICP-MS measurements and pore water data exclude that the overgrowths significantly contributed to the high Mg/Ca ratios. After correcting the Mg/Ca ratios after 4.5 Ma for the salinity effect, the $SST_{Mg/Ca}$ record shows an increase by ~2°C due to the progressive shoaling of the Isthmus of Panama.

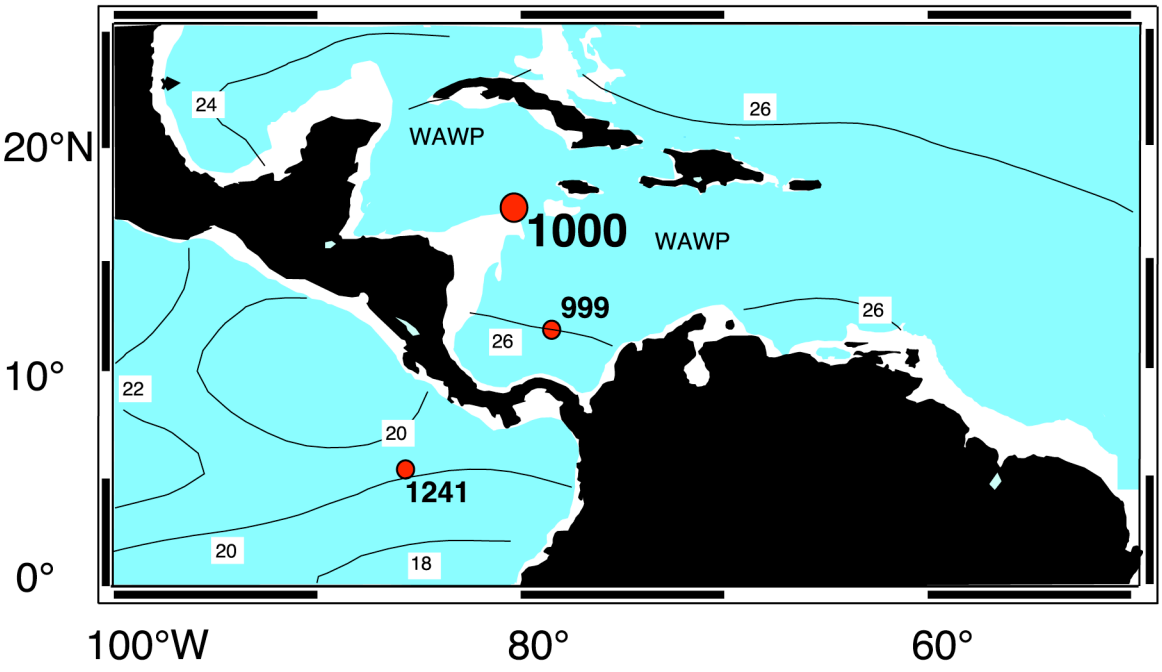

Figure 6.1 Present day configuration of the Caribbean Sea with the location of Site 1000 (16°33.222'N, 79°52.044'W, 916 m water depth). Also indicated are Sites 999 [*Haug et al.*, 2001] and 1241 (Groeneveld et al., submitted). WAWP is the Western Atlantic Warm Pool. Isolines indicate annual average temperatures at a water depth of ~50 m (Levitus and Boyer, 1994), the assumed habitat depth of *G. sacculifer*, showing a temperature difference of ~5°C between the Caribbean and the east Pacific.

Introduction

We present a high-resolution Mg/Ca record for ODP Site 1000 from the Caribbean for the time interval from 5.6 Ma to 3.9 Ma for the planktonic foraminifer *Globigerinoides sacculifer*. Main objective of the study was to investigate what the effect of the restriction of the exchange of upper ocean water masses between the Pacific and the Caribbean, due to the progressive closure of the Panamanian Gateway (Haug et al., 2001; Steph et al., submitted), was on the development of sea surface temperatures (SST) in the Caribbean. Comparison with the $\delta^{18}O$ record of *G. sacculifer* was used to determine the effect of salinity on the Mg/Ca record. To investigate the effect of carbonate diagenesis on the Mg/Ca reconstruction, we established additional records of Sr/Ca on *G. sacculifer*, calcareous nannofossil abundance (*Florisphaera profunda*) and carbonate mineralogy (aragonite), while scanning electron micoscope (SEM) and LA-ICP-MS analyses were performed to further quantify the effect of carbonate diagenesis.

Closure of the Panamanian Gateway

The late Miocene/early Pliocene gradual closure of the Panamanian Gateway effectively changed oceanographic patterns between the Pacific and Atlantic oceans, and thus led to profound changes in global atmospheric circulation and climate. The closure of the Panamanian Gateway was responsible for changing the Pacific, Caribbean, and Atlantic water mass signatures, generating the Western Atlantic Warm Pool (WAWP), and intensifying thermohaline circulation in the North Atlantic via increasing salt and heat transport to high northern latitudes (Maier-Reimer et al., 1990; Tiedemann and Franz, 1997; Haug and Tiedemann, 1998; Billups et al., 1999; Haug et al., 2001). As a consequence, the intensification of the Gulfstream system might have had an important role in the initiation of the northern hemisphere glaciation (NHG), which started during the mid Pliocene (Haug and Tiedemann, 1998; Driscoll and Haug, 1998).

Haug et al. (2001) interpreted the divergent pattern of planktonic $\delta^{18}O$ records from the Caribbean (Site 999) and the tropical Pacific (Site 851) at 4.6 Ma and the subsequent 0.5‰ increase in $\delta^{18}O$ in the Caribbean since ~4.2 Ma as the establishment of the salinity contrast between Pacific and Caribbean surface waters. This hydrographic change was caused by the plate tectonic shoaling of the Panamanian sill to less than 100 m, which effectively restricted the surface water exchange between the Pacific and the Atlantic, and therefore increased SSS in the Caribbean by 1-2 salinity units by means of an increased atmospheric transport of water vapor from the Caribbean into the Pacific. Recent results from Caribbean Site 1000 (Steph et al., submitted) show that, in accordance with this general increase in Caribbean SSS, salinity gradients within the Caribbean increased and varied on precessional timescales. Low SSS gradients occurred during minima in northern hemisphere summer insolation and were interpreted to reflect enhanced inflow of low salinity Pacific surface water into the Caribbean. During maxima in northern hemisphere summer insolation Pacific inflow of low salinity surface waters was reduced, resulting in higher SSS gradients between Sites 999 and 1000.

However, the final closure of the Panamanian Gateway was not established until ~2.7-2.2 Ma, when the major exchange of mammals via the Isthmus between North and South-America took place (Webb, 1997; Stehli and Webb, 1985), and nannofossil assemblages from the Caribbean and the eastern Pacific (Kameo and Sato, 2000), and $SSTs_{Mg/Ca}$ between the east Pacific (ODP Site 1241) and the Caribbean (ODP Site 999) permanently diverged (Groeneveld et al., manuscript in preparation).

Mg/Ca paleothermometry

The advantage of measuring Mg/Ca and $\delta^{18}O$ on the same biotic carrier is that synchronous estimates of SST and global ice volume can be determined and used to calculate $\delta^{18}O_{seawater}$ and SSS, thereby avoiding the bias of seasonality and/or habitat differences that occur when proxy data from different faunal groups are used. The paired analysis of $\delta^{18}O$ and Mg/Ca on the mixed layer dwelling planktonic foraminifer *G. sacculifer* from ODP Site 1000 provides new insights on the oceanographic evolution of the Caribbean during the shoaling of the Isthmus of Panama as well as clear evidence for complications which may arise when applying Mg/Ca paleothermometry. Our studies concentrate on the late Miocene/early Pliocene time interval between 5.6 Ma and 3.9 Ma.

Commonly, the $\delta^{18}O$ signal of planktonic foraminifers records the combined effects of global ice volume, sea surface temperature, and local salinity. The Mg content of foraminifers is mainly dependant on the temperature of the water in which the foraminifer calcifies as deduced from cultivating work and field studies (Nürnberg, 1995, 2000; Nürnberg et al., 1996, 2000; Lea et al., 1999; Mashiotta et al., 1999; Elderfield and Ganssen, 2000; Dekens et al., 2002). Therefore, the Mg/Ca paleothermometry has become an accepted, powerful tool in paleoceanography for the reconstruction of SSTs. Other factors like salinity (Nürnberg, 1996; Lea et al., 1999) and pH (Lea et al., 1999) additionally affect foraminiferal Mg/Ca, but were hitherto considered to play minor roles since their opposite effects on Mg/Ca would cancel each other and absolute changes are considered to have been small (Lea et al., 2000; Nürnberg et al., 2000). Although the effects of dissolution within the water column have been studied extensively (Dekens et al., 2002; Rosenthal and Lohmann, 2002; de Villiers, 2003; Regenberg et al., manuscript in preparation), the effects of diagenetic processes on Mg/Ca ratios have only recently become under attention (Reuning et al., in press; Pena et al., submitted).

First efforts to determine high-resolution element ratio profiles through single foraminiferal test chambers were performed by means of microprobe (Nürnberg et al., 1996; McKenna and Prell, 2004), who showed the heterogeneity of Mg/Ca ratios within single foraminiferal tests. Recent studies have used Laser Ablation Inductively Coupled Mass Spectrometry (LA-ICP-MS) to further investigate inter- and intra-test variability showing the good spatial resolution of this method in determining contaminant phases on foraminiferal tests (Reichart et al., 2003; Hathorne et al., 2003; Eggins et al., 2003; Pena et al., submitted). Here we used LA-ICP-MS to determine the chemistry of the crystal overgrowth which was evident from SEM on the foraminiferal tests after the cleaning process and to investigate to what extent the bulk test chemistry was influenced.

Materials and Methods

ODP Site 1000 was cored during Leg 165 on the Nicaraguan Rise (Pedro Channel) in the Caribbean (16°33.222'N, 79°52.044'W, Fig 6.1). The shallow site location of 916 m in comparison with the depth of the Caribbean lysocline at 4000 m (Archer, 1996) implies that carbonate dissolution is negligible. Samples were taken every 10 cm, reflecting a temporal resolution of ~3 kyr per sample. 20-25 specimens of *Globigerinoides sacculifer* were selected from the 315-400 µm size fraction. Specimens visibly contaminated by ferromanganese oxides and specimens with a final sac-like chamber were not selected for analysis. The age model for Site 1000 was based on the $\delta^{18}O$ record of the benthic foraminifer *C. wuellerstorfi* (Steph et al., submitted). Since no composite depth exists for Site 1000, a preliminary age model was constructed by identifying major isotopic stages according to the nomenclature of Shackleton et al. (1995). The preliminary age model was then correlated to the orbitally tuned age model of ODP Site 925/926 from Ceara Rise (Bickert et al., 1997; Tiedemann and

Franz, 1997; Shackleton and Hall, 1997). The final age model revealed the presence of dominant precession cycles in the planktonic $\delta^{18}O$ record, which were then used to further tune the age model (Steph et al., submitted).

Mg/Ca-analysis

After gentle crushing, the samples were cleaned according to the cleaning protocol of Barker et al. (2003). To remove clays, the samples were rinsed 4-6 times with distilled deionized water and twice with methanol (suprapure) with ultrasonical cleaning steps (2-3 minutes) after each rinse. Subsequently, samples were treated with a hot (97°C) oxidizing 1% NaOH/ H_2O_2 solution (10 mL 0.1 *N* NaOH (analytical grade); 100 µL 30% H_2O_2 (suprapur)) for 10 minutes to remove organic matter. Every 2.5 minutes, the vials were rapped on the bench top to release any gaseous build-up. After 5 minutes, the samples were placed in an ultrasonic bath for a few seconds in order to maintain contact between reagent and sample. This treatment was repeated after refreshment of the oxidizing solution. Any remaining oxidizing solution was removed by three rinsing steps with distilled deionized water. After transferring the samples into clean vials, a weak acid leach with 250 µL 0.001 M HNO_3 (subboiled distilled) was applied with 30 seconds ultrasonic treatment and subsequent two rinses with distilled deionized water. After cleaning, the samples were dissolved in 0.075 M nitric acid (HNO_3) (subboiled distilled) and diluted with distilled deionized water up to 3 mL containing 10 ppm of yttrium as an internal standard.

Analyses were run on an ICP-OES (ISA Jobin Yvon, Spex Instruments S.A. GmbH) with polychromator applying yttrium as an internal standard. We selected element lines for analyses which were most intensive and undisturbed (Ca: 317.93 nm; Mg: 279.55 nm; Sr: 407.77 nm; Fe: 238.21 nm; Mn: 257.61 nm; and Y: 371.03 nm). Element detection was performed with photomultipliers, the high-tension of which was adapted to each element concentration range. The relative standard deviation is 0.45% for magnesium and 0.15% for calcium. The Mg/Ca reproducibility of replicate samples of *G. sacculifer* is good (r^2 = 0.8), giving a temperature error of $\pm$ 0.7°C. The analytical error in temperature is $\pm$ 0.12°C. Fe/Ca and Mn/Ca analyses indicated that contamination with clays or Mn-carbonates after the cleaning procedure was not an issue. The conversion of foraminiferal Mg/Ca ratios into SST was carried out by applying the equation of Nürnberg et al. (2000) (SST = (Log(Mg/Ca)-Log 0.491)/0.033).

LA-ICP-MS

Laser Ablation Inductively Coupled Mass Spectrometry (LA-ICP-MS) (ICP-MS, Micromass Platform) was used to measure Mg, Sr and Ca chamber profiles of selected cleaned foraminiferal tests. Craters of 80 µm were ablated using an Excimer 193 nm deep ultra violet laser (Lambda Physik) with Geolas optics (Günther et al., 1997). Energy density at the sample surface was kept at 2 mJ/cm^2, shot repetition rate at 8 Hz. Laser ablation of calcite requires ablation at ultra violet wave lengths since higher wave lengths result in uncontrolled cleavage. The ablated material was transported by a continuous He flow and mixed with an Ar make up gas before injection into the Ar plasma of the quadropole ICP-MS instrument (Micromass Platform). A collision and reaction cell was used to give improved results by reducing spectral interferences on the minor isotopes of Ca (^{42}Ca, ^{43}Ca and ^{44}Ca). Interelemental fractionation was insignificant due to the relative low depth to width ratio of the ablation craters produced. Calibration was performed against U.S. National Institute of Standards and Technology SRM 612 glass using the concentration data of Pearce et al. (1997), with Ca as an internal standard. Calcium carbonate is well suited for LA-ICP-MS because Ca can be used as an internal standard at 40 wt%. For

quantifying Ca we used mass 44, monitoring masses 42 and 43 as an internal check. Using Ca as an internal standard allows direct comparison to trace metal to Ca ratios from traditional wet-chemical studies. Magnesium concentrations were calculated using masses 24 and 26. Although the accuracy for mass 24 is higher, both isotopes agree within a few percent. For strontium concentrations mass 88 was used. Analyses were performed at the Faculty of Earth Sciences, University of Utrecht, The Netherlands.

For the laser ablation measurements we selected cleaned *G. sacculifer* fragments from four different samples, two contaminated samples, i.e. with crystalline overgrowths (sample 14-5-115 and sample 14-5-125) and two uncontaminated samples, i.e. without crystalline overgrowths (sample 14-5-95 and sample 14-5-145) (Table 6.1). On each fragment multiple transects were ablated to certify that in-test heterogeneities were avoided and an average signal was produced. In total, 25 profiles were ablated, 11 through the uncontaminated samples, i.e. without crystalline overgrowths, and 14 through the contaminated samples, i.e. with crystalline overgrowths (Fig 6.6)

Carbonate mineralogy

Carbonate mineralogy was determined using a Philips PW1710 diffractometer (IFM-Geomar, Kiel) with a cobalt Kσ tube at 40 KV and 35 mA. The samples were scanned from 25°-40° at a scanning speed of 0.01 steps per second to cover the significant peaks of the various carbonate minerals. The percentage of aragonite and calcite, dolomite was not present in significant amounts, relative to total carbonate content was calculated from peak area ratios using in-house calibration curves. Peak areas were measured using the computer based integration program MacDiff (Petschick, 1999). The non-linear relationship between calcite and aragonite was calculated from ratios calibrated from standards measured on the diffractometer.

Calcareous nannofossil analysis

The relative abundance record of F. profunda was obtained by high-resolution scanning electron microscope (SEM) analysis of calcareous nannofossil assemblages (Crudeli et al., manuscript in preparation). Analyses were conducted at a magnification of 6000X using a CamScan 44-Serie-2-CS-44 SEM (University of Kiel). Methods on sample preparation were reported in Crudeli and Kinkel (2004). An amount of 0.1 g of dry sediment was diluted with carbonate-saturated tap water. The solution was then divided with a rotary splitter device. A final solution with 0.001 g of sediment was filtered with a low-pressure vacuum pump onto a polycarbonate-membrane filter (pore size, 0.40 μm; diameter, 50 mm). A segment of filter was then mounted on a scanning electron microscope (SEM) stub.

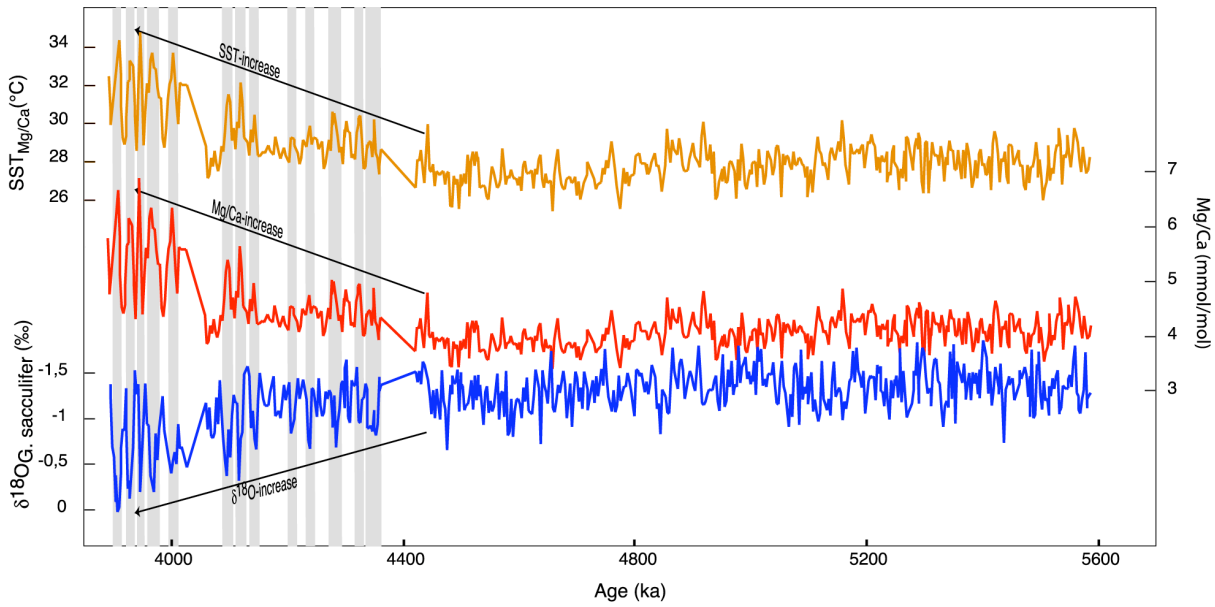

Figure 6.2 Results for Site 1000 for the time interval 5.6 Ma to 3.9 Ma. Arrows indicate trends associated with the restriction of upper ocean water masses between the Pacific and the Caribbean since 4.5 Ma. Mg/Ca ratios are measured on tests of the planktonic foraminifer *G. sacculifer*. Mg/Ca ratios are converted into SSTs using the formula of Nürnberg et al. (2000). $\delta^{18}O$ was measured on tests of the planktonic foraminifer *G. sacculifer* (Steph et al., submitted). Bars show the positive correlation between Mg/Ca and $\delta^{18}O$. Note that $\delta^{18}O$ is plotted reversely.

Results and discussion

The total range of Mg/Ca ratios can be divided into two time intervals, before and after 4.5 Ma. Values before 4.5 Ma are relatively stable and range between 3.5 and 4.5 mmol/mol, translating into $SSTs_{Mg/Ca}$ between 26.5°C and 29°C. The range of Mg/Ca ratios after 4.5 Ma increases to values between 4 and 7 mmol/mol, providing $SSTs_{Mg/Ca}$ between 28°C and 35°C (Fig 6.2).

The late Miocene to earliest Pliocene Mg/Ca record (5.6-5.0 Ma) implies a relatively uniform $SST_{Mg/Ca}$ pattern of 26.5-29°C (Fig 6.2). This time interval is characterized by a typical negative correlation between Mg/Ca and $\delta^{18}O$, e.g. high SSTs and low $\delta^{18}O$ values. Here, the $\delta^{18}O$ fluctuations, ranging between –1.05‰ and –1.7‰, are mainly related to changes in temperature, because the effects of ice volume and local salinity on the planktonic $\delta^{18}O$ signal are assumed to have remained small during the late Miocene/early Pliocene. Orbital-scale changes in global ice volume affected the late Miocene/early Pliocene $\delta^{18}O$ signal by less than 0.15‰ (Tiedemann et al., 1994). Large changes in salinity affecting planktonic $\delta^{18}O$ can be largely excluded for this time interval, as the free exchange between Pacific and Caribbean surface water masses prohibited the establishment of salinity gradients (Haug et al., 2001). Hence, we translated the late Miocene/early Pliocene $\delta^{18}O$ amplitude fluctuations of ~0.65 ‰ directly into temperature, providing isotopic SST changes of ~2°C. Such amplitude corresponds to those calculated from the Mg/Ca signal.

The time interval from 5.0-4.5 Ma (Fig 6.2) is characterized by both positive and negative correlations between $SST_{Mg/Ca}$ and $\delta^{18}O$. A positive correlation between $\delta^{18}O$ and Mg/Ca, e.g. high $SSTs_{Mg/Ca}$ are paralleled by high $\delta^{18}O$ values, was not reported before and we interpret such a scenario in the way that $\delta^{18}O$ is no longer solely reflecting changes in temperature, but is becoming dominated by salinity. Since a synchronous increase in SST and SSS influences the $\delta^{18}O$ signal in opposite directions, the effect of temperature on $\delta^{18}O$ appears to be fully compensated and even overprinted by the strong SSS signal. The onset of the positive correlation between $SST_{Mg/Ca}$ and $\delta^{18}O$ suggests that the shoaling of the Isthmus of Panama started to affect the continuous

throughflow of low salinity waters from the Pacific into the Caribbean, leading to increased influence of higher saline Atlantic/Caribbean waters.

After the critical threshold at ~4.5 Ma, when the salinity contrast between Pacific and Caribbean became established (Haug et al., 2001) and salinity gradients between the southern and central Caribbean increased (Steph et al., submitted), we observe a nearly perfect positive correlation in the paired Mg/Ca and $\delta^{18}O$ records of *G. sacculifer* (r = 0.71) (Fig 6.2). Maximum $SSTs_{Mg/Ca}$ and maximum SSSs are occurring at the same time. Starting at 4.5 Ma, the $SSTs_{Mg/Ca}$ imply a warming of ~4°C until 3.9 Ma, an increase in $SST_{Mg/Ca}$ amplitudes up to 5°C, and $SST_{Mg/Ca}$ maxima of up to 35°C (Fig 6.2).

The extreme $SST_{Mg/Ca}$ maxima of up to 35°C and amplitudes of up to 5°C appear to be very unlikely for the early Pliocene. Firstly, modern SSTs at ~30-50 m water depth, the assumed habitat depth of *G. sacculifer* (Fairbanks et al., 1982), do not exceed 30-31°C in open ocean conditions (Levitus and Boyer, 1994), and it is unreasonable to expect significantly higher SSTs during the early Pliocene. Secondly, this time interval is known to represent a globally warm and stable climate of unipolar glaciation with a pole-equator temperature gradient, which was smaller than today. Hence, amplitudes in $SST_{Mg/Ca}$ as large as 5°C appear to be rather unlikely. Recently, Molnar and Cane (2002) suggested permanent El Niño-like conditions throughout the early Pliocene. In addition, studies in the high-latitudinal Atlantic indicated that SSTs might have been warmer by up to 8°C than today, while the tropical SSTs remained the same or were, due to increased heat transport to higher latitudes, even slightly cooler than today (Cronin et al., 1993; Crowley, 1996; Dowsett et al., 1996; Billups et al., 1998; Groeneveld et al., submitted).

How do we explain the extremely high $SSTs_{Mg/Ca,}$ the large $SST_{Mg/Ca}$ amplitude variations and the positive correlation to $\delta^{18}O$ during the time interval 4.5-3.9 Ma? Factors potentially affecting the Mg/Ca-signal will be discussed below.

Impact of Pliocene salinity changes on foraminiferal Mg/Ca and $\delta^{18}O$

Both the positive relationship between the Mg/Ca and $\delta^{18}O_{G.\ sacculifer}$ records (Fig 6.2), and the suggested increase in Caribbean SSS after 4.5 Ma (Haug et al., 2001; Steph et al., submitted) basically suggest that the planktonic $\delta^{18}O$ record is dominated by variations in SSS. In a first approach we simply assumed that the $\delta^{18}O$ fluctuations of up to 1.3‰ for the time interval 4.5-3.9 Ma (Fig 6.2), only reflect salinity variations, on the order of three salinity units, when applying Broeckers (1989) rule of thumb; 1‰ $\delta^{18}O$ = 2 salinity units (Fig 6.3b). By doing so, possible temperature and ice effects on $\delta^{18}O_{G.\ sacculifer}$ are ignored. On average, the corresponding SSS record would thus imply an increase of 1.5 salinity units in the Caribbean since 4.5 Ma. Subsequently, we corrected the Mg/Ca record for the effect of these potential salinity changes. Cultivating experiments with *G. sacculifer* revealed a positive relationship between foraminiferal Mg/Ca and salinity (Nürnberg et al., 1996) ($Mg/Ca = 0.248*10^{(0.031*Sal)}$, $R^2 = 0.994$), suggesting a 7% to 10% increase in Mg/Ca per salinity unit. Similar results were found by Lea et al. (1999), who concluded from cultivating experiments with *Globigerina bulloides* that a salinity change of 1 salinity unit results in a 4 $\pm$ 3% increase in Mg/Ca. Salinity variations of ~3 salinity units deduced from the planktonic $\delta^{18}O$ record would therefore result in a $SST_{Mg/Ca}$ overestimation of 3.0-3.6°C (7% increase in Mg/Ca per one unit salinity increase). After correcting the Mg/Ca record for changes in salinity $SST_{Mg/Ca}$ shows maximum amplitudes of ~4.5°C, and maximum $SST_{Mg/Ca}$ estimates up to 32°C. The average $SST_{Mg/Ca}$ increase from 4.5-3.9 Ma is ~3°C (Fig 6.3c).

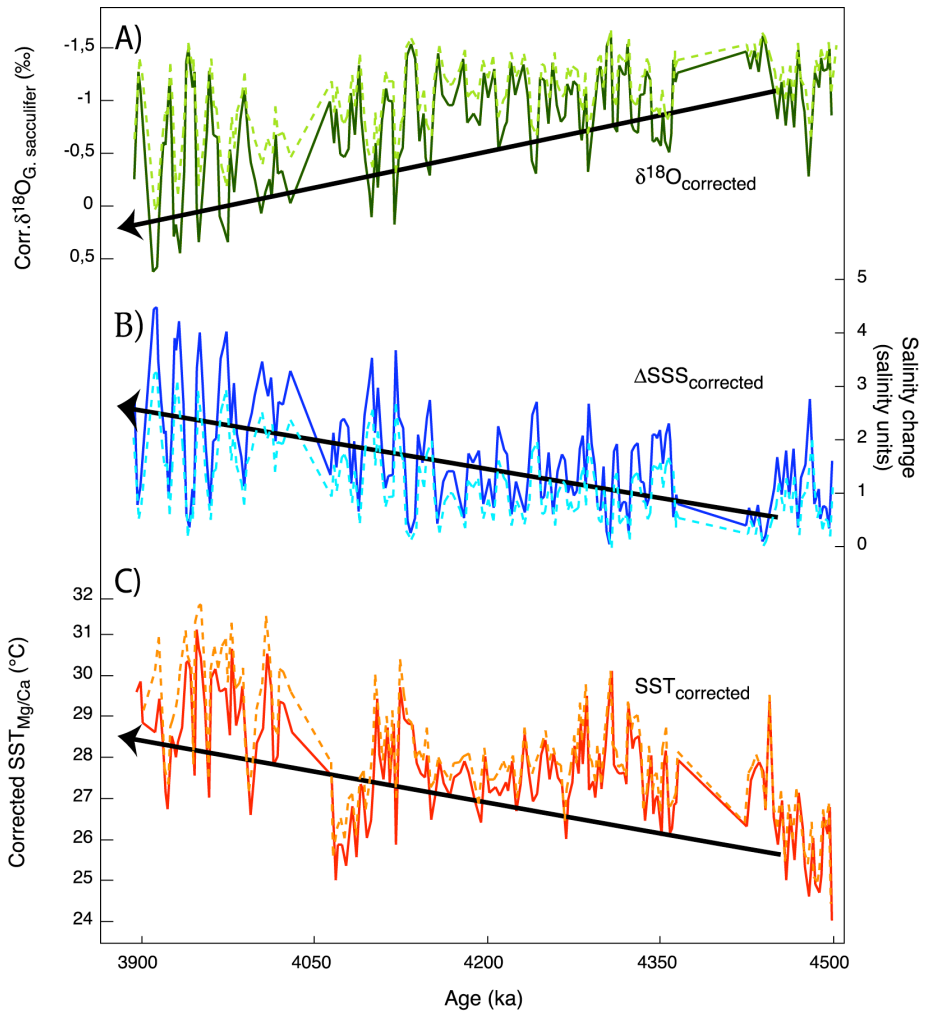

Figure 6.3 Correction of the $SST_{Mg/Ca}$ record for the influence of salinity. Arrows indicate trends associated with the restriction of upper ocean water masses between the Pacific and the Caribbean since 4.5 Ma. **A.** $\delta^{18}O$ of *G. sacculifer*, corrected for a temperature cyclicity of 2.5°C. Dotted line shows the original $\delta^{18}O$ record. **B.** Change in salinity, calculated using the basic rule that $\Delta 1‰\ \delta^{18}O = \Delta 2$ salinity units salinity (Broecker, 1989). Dotted line shows the result from the first approach. **C.** Corrected $SST_{Mg/Ca}$ record. Mg/Ca ratios were corrected by using a 7% increase in Mg/Ca per 1 unit increase in salinity. Dotted line shows the result from the first approach.

In a second approach, we additionally consider potential temperature and ice effects on the $\delta^{18}O_{G.\ sacculifer}$ signal. Furtermore we assume $SST_{Mg/Ca}$ fluctuations of ~2.5°C during the earlier part of the record (5.6-5.0 Ma) persisting to 3.9 Ma. Such an assumption is reasonable because large glacial-interglacial temperature amplitudes did not occur before the intensification of the Northern Hemisphere Glaciation. To subtract the 2.5°C temperature cyclicity from the $\delta^{18}O_{G.\ sacculifer}$ record, we interprete the positive correlation between the two proxies (4.5-3.9 Ma) in such a way that the highest $\delta^{18}O$ values represent both highest salinity and highest temperatures. The temperature effect on $\delta^{18}O$ can then be assessed for each data point, using the value in individual data points relative to the maximum value and using the (fundamental) relationship that a shift of 1‰ $\delta^{18}O$ represents 4°C. This value is subsequently subtracted from the $\delta^{18}O_{G.\ sacculifer}$ record, resulting in larger $\delta^{18}O$ amplitudes.

As a next step, we correcte the $\delta^{18}O_{G.\ sacculifer}$ record for the global ice volume effect. From terrestrial settings it is known that an ice cap of limited extend existed on Antarctica during the early Pliocene (Webb and Harwood, 1991), and minor ice sheets existed on Greenland (Jansen et al., 1990). Glacial to interglacial variations in global

ice volume during the Pliocene, nevertheless, were only on the order of 0.15-0.25‰ (Hodell and Warnke, 1991; Kennett and Hodell, 1993; Shackleton et al., 1995; Mix et al., 1995; Tiedemann et al., submitted) with average values of about 0.6-0.7‰ lower than present day values (Shackleton et al., 1995). Such a shift in isotopic values was explained by a deep water warming of ~1°C and a global ice volume effect equivalent to 20-25 m sea level change (Kennett and Hodell, 1993; Shackleton et al., 1995). We use the benthic $\delta^{18}O$ record of ODP Site 1241 from the east Pacific to estimate early Pliocene changes in global ice volume, thereby assuming that Marine Isotope Stage (MIS) 100 represents two-third of the change in global ice volume between the Last Glacial Maximum and the Holocene (Raymo et al., 1989; Tiedemann et al., submitted; Groeneveld et al., submitted). The resulting sea level record is then normalized and subtracted from the $\delta^{18}O_{G.\ sacculifer}$ record of Site 1000 (Groeneveld et al., submitted). However, precession dominated periodicities in planktonic Mg/Ca and $\delta^{18}O$ are not significantly influenced by the obliquity dominated Pliocene glacial to interglacial sea level changes. Sea level changes can, therefore, be ignored in our further calculations.

The resulting temperature corrected $\delta^{18}O_{G.\ sacculifer}$ record for the time interval 4.5-3.9 Ma the amplitude in $\delta^{18}O_{G.\ sacculifer}$ now is ~2‰, equivalent to 4 salinity units (Fig 6.3a, b). As a final step, we correct the $SST_{Mg/Ca}$ record for these salinity effects, similar as in the first approach. The maximum Mg/Ca ratios were corrected by as much as 20-30%, which corresponds to temperature corrections of 3-4°C. The corrected $SST_{Mg/Ca}$ record now shows reduced amplitude fluctuations of ~3°C, absolute values ranging from 25-31°C, and a general warming trend of ~2°C since 4.5 Ma (Fig 6.3c). These results provide the first evidence that the restricted exchange of surface water between the east Pacific and the Caribbean due to the progressive shoaling of the Isthmus of Panama led to a considerable warming of Caribbean surface waters, and hence to the initiation of the Western Atlantic Warm Pool. Because the Caribbean is the source region of the Gulf Stream, the resulting northward transport of warmer and saltier water masses increased, which might have contributed to an intensified formation of North Atlantic Deep Water.

Diagenetic alteration of the foraminiferal tests

Sediments with high calcium carbonate contents are prone to diagenetic overprinting, dissolution and reprecipitation, especially when the carbonate is present as metastable aragonite or high-Mg calcite (Swart and Guzikowski, 1988; Malone et al., 1990; Munnecke et al., 1997; Melim et al., 2002). Site 1000 is surrounded by carbonate platforms, which supply high amounts of aragonite to the core location (Sigurdsson et al., 1997). Aragonite in sediments is susceptible to dissolution, which subsequently can result in reprecipitation as inorganic calcite. Aragonite is not present in the studied samples before 4.5 Ma, i.e. the interval with normal Mg/Ca ratios (Fig 6.4). However, after 4.5 Ma alternations between aragonite-rich (up to 60%) and cemented aragonite-poor layers (<30%) occur, showing precessional cyclicity (Fig 6.4). This precessional variation in aragonite negatively correlated with the foraminiferal Mg/Ca record ($r = -0.80$, <4.05 Ma), which points into the direction of a diagenetic imprint, related to carbonate chemistry. Periods of aragonite dissolution, reprecipitation of inorganic calcite could have resulted in diagenetic Mg-rich overgrowth on the foraminiferal tests, resulting in abnormally high foraminiferal Mg/Ca ratios (up to ~7 mmol/mol) (Fig 6.2).

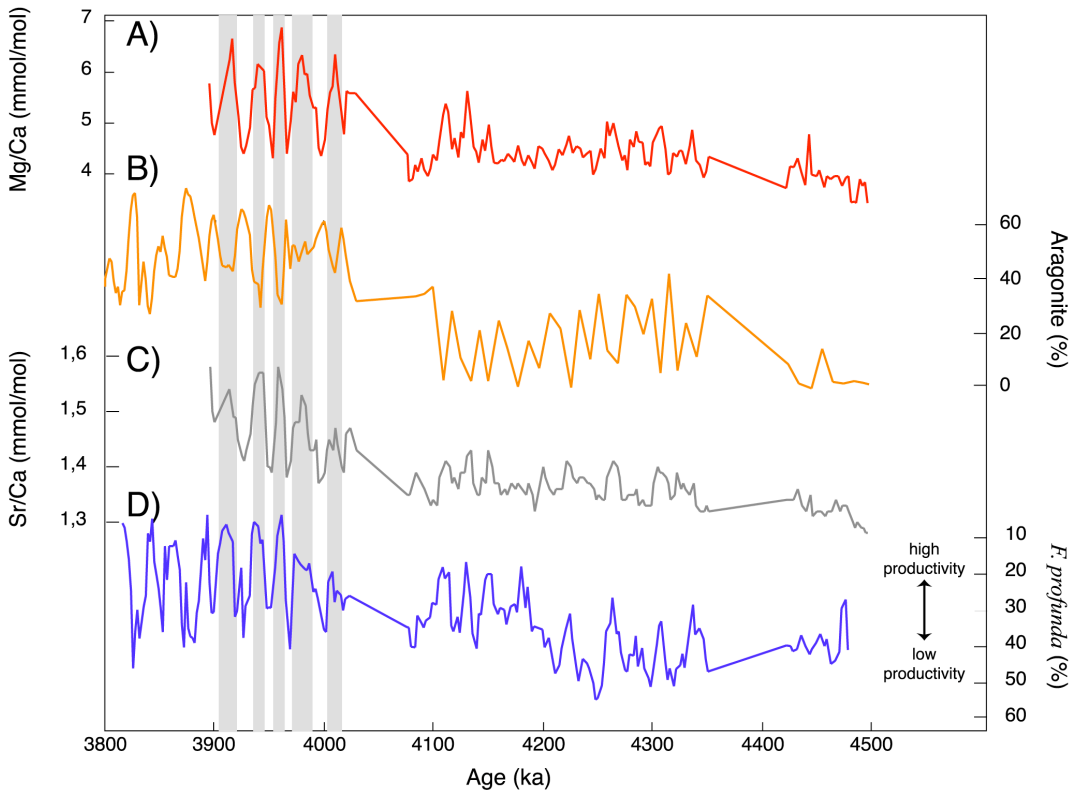

Figure 6.4 Mg/Ca results in comparison with $Sr/Ca_{G.\ sacculifer}$, aragonite content, and relative abundance of *F. profunda* for the time interval from 4.5 Ma to 3.9 Ma. Bars show the correlation between the individual records. **A.** Mg/Ca ratios, measured on tests of the planktonic foraminifer *G. sacculifer.* **B.** Aragonite content, measured on bulk sediment by XRD analysis. **C.** Sr/Ca ratios, measured on tests of the planktonic foraminifer *G. sacculifer,* indicative of diagenetic alteration. **D.** Relative abundance (plotted reversely) of *F. profunda*, indicative of variation in primary productivity.

SEM studies indeed show that crystalline overgrowths are present on the inner surfaces of foraminiferal tests after 4.5 Ma (Fig 6.5), corresponding to the high Mg/Ca ratios (Fig 6.2). These crystals resilient to the cleaning procedures normally applied before Mg/Ca analyses. Foraminiferal tests with low Mg/Ca ratios after 4.5 Ma, as well as tests from the older part of the core (>4.5 Ma), do not show these crystalline overgrowths (Fig 6.5). Together this strongly suggests that diagenetic overgrowth, originating from partial dissolution of aragonite which contributed to the unusually elevated foraminiferal Mg/Ca ratios.

Previously, Sr/Ca of bulk sediment has been used as an indicator of sediment diagenesis (Baker et al., 1982; Swart and Guzikowski, 1988; Hampt and Delaney, 1997). Since in the record of Site 1000 foraminiferal Sr/Ca and Mg/Ca ratios are positively correlated after 4.5 Ma (r = 0.76, <4.05 Ma), we exploited the possibility to use foraminiferal Sr/Ca as an indication for diagenetic overprinting via aragonite dissolution. Maximum values of foraminiferal Mg/Ca and lower sedimentary aragonite correspond to foraminiferal Sr/Ca increasing to values between 1.35-1.58 mmol/mol. Typical Sr/Ca ratios for foraminiferal tests are generally lower, ranging from 1.25-1.40 mmol/mol, similar to the older part of the record. This suggests dissolution of Sr-rich aragonite and subsequent carbonate reprecipitation from pore waters with elevated Sr/Ca ratios.

Temporal variations in aragonite diagenesis are closely related to changes in marine productivity, which are reflected in the relative abundance of the coccolithophorid *Florisphaera profunda*, which lives at the bottom of the photic zone (Molfino and McIntyre, 1990; Beaufort et al., 1997; de Garidel-Thoron et al., 2001) (Fig 6.4). Variations in the coccolithophorid *F. profunda* at Site 1000 are positively correlated with the aragonite record (r = 0.71), showing that at times of enhanced aragonite dissolution reflected by high Sr/Ca ratios, relative abundances of *F. profunda* are low (Fig 6.4). These low relative abundances reflect high marine productivity at

the surface of the mixed layer, which enhances nutrient utilization and relatively reduces nutrient flux to the bottom of the photic zone, hence, resulting in decreased relative abundances of *F. profunda* (Crudeli et al., manuscript in preparation).

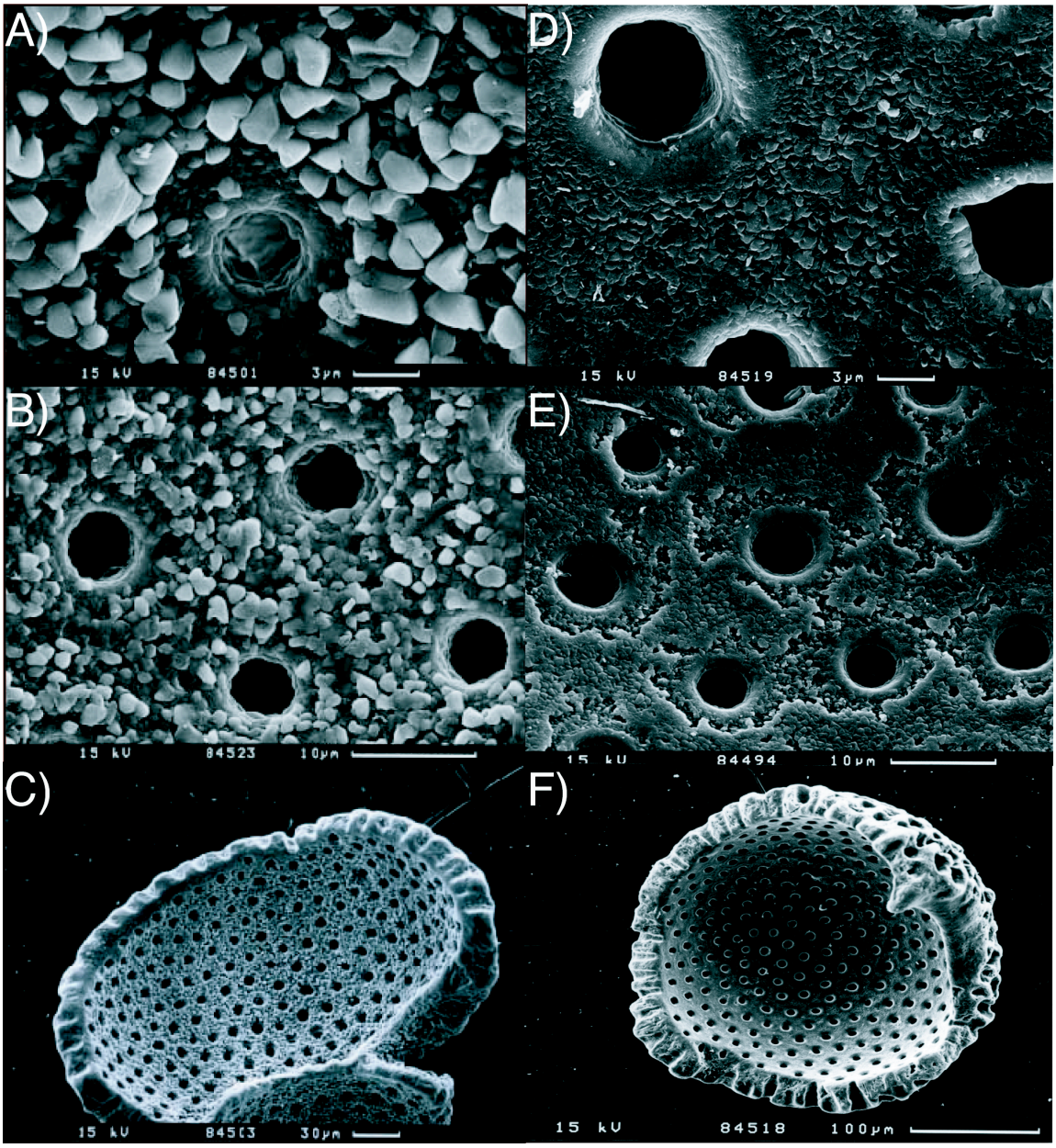

Figure 6.5 Scanning electron microscope images (CAMSCAN-Serie-2-CS-44, Univ. of Kiel, Germany) of cleaned tests of the planktonic foraminifer *G. sacculifer*. Bars indicate the scale of the images. For comparison, couples of two photos of about the same size scale are plotted together, one from a contaminated test and one from an uncontaminated test. **A-C.** Foraminiferal tests containing an overgrowth of diagenetic crystals. **D-F.** Cleaned foraminiferal tests without the presence of diagenetic crystals. Slight indications of dissolution are visible, most likely caused by the intense cleaning procedure.

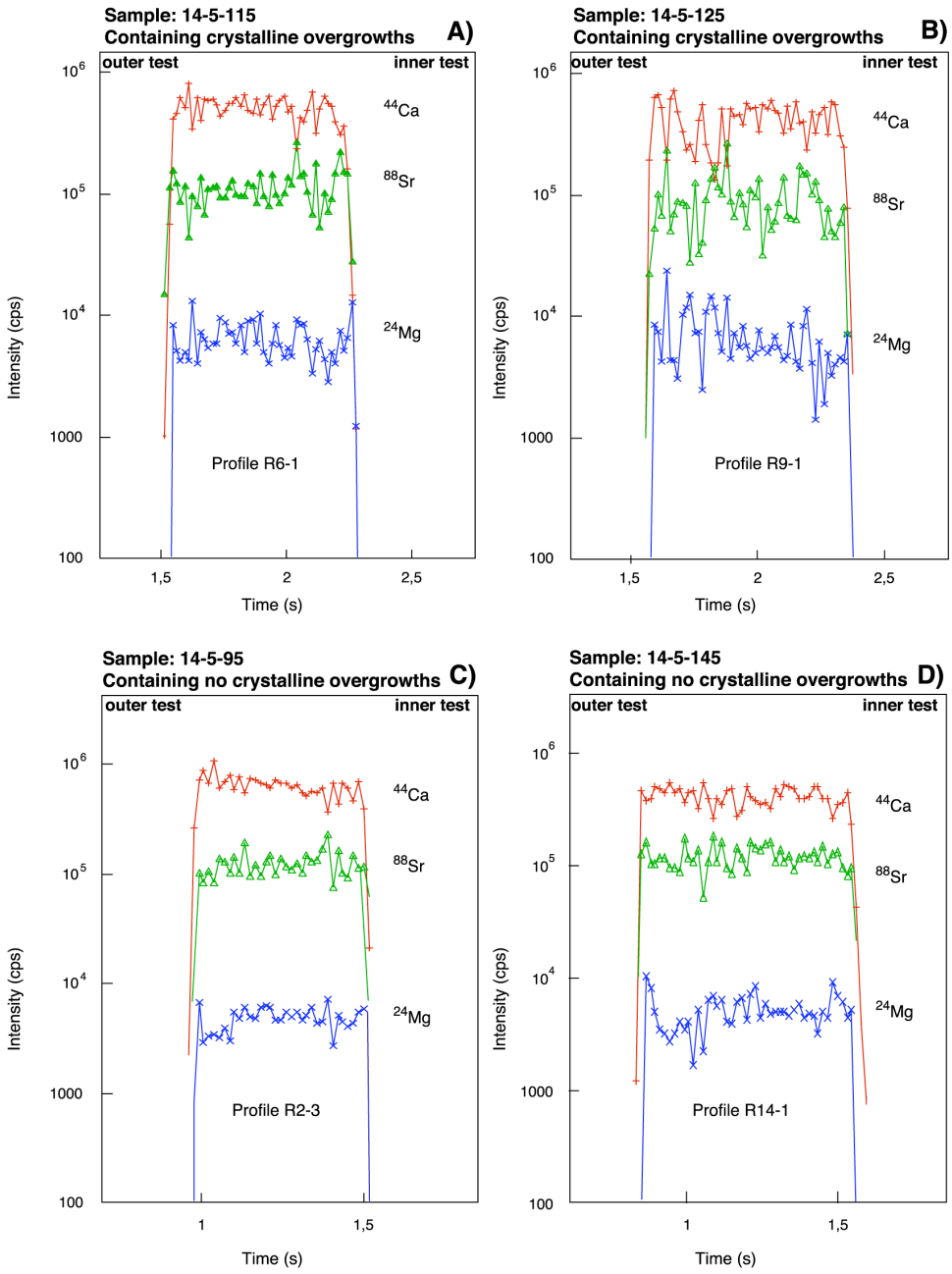

Figure 6.6 Results from LA-ICP-MS for selected contaminated, i.e. with crystalline overgrowths, and uncontaminated, i.e. without crystalline overgrowths, samples. Measurements performed on tests of the planktonic foraminifer *G. sacculifer*. All profiles are ablated from the outer side of the test toward the inner site. **A-B.** Typical ablation profiles for Mg and Sr through the contaminated, i.e. with crystalline overgrowths, samples 14-5-115 and 14-5-125. All intensities are normalized to ^{44}Ca. Time (s) represents the duration of the measurement. **C-D.** Typical ablation profiles for Mg and Sr through the uncontaminated, i.e. without crystalline overgrowths, samples 14-5-95 and 14-5-145. All intensities are normalized to ^{44}Ca. Time (s) represents the duration of the measurement.

How is marine productivity affecting aragonite dissolution? During microbial sulphate reduction reactive organic material becomes oxidized, reducing interstitial sulphate concentration and releasing CO_2 and H_2S to the pore water. The concomitant pH lowering leads to the undersaturation of the pore water with respect to metastable carbonate phases and hence, to carbonate dissolution, which increases alkalinity. Continuing sulphate reduction eventually causes an increase in the ion activity product of $CaCO_3$ (Ben-Yaakov, 1973) and subsequently leads to the precipitation of inorganic calcite. This inorganic calcite primarily reflects porewater chemistry and can, therefore, deviate considerably from the biogenic calcite. Alkalinity increases during the initial stage of sulphate

reduction due to the dissolution of carbonate, whereas in a later phase further alkalinity increase is reduced by the precipitation of inorganic calcite (Morse and Mackenzie, 1990) (Fig 6.7). This means that during periods with relatively high productivity, more organic matter is decomposed, thereby lowering the pH of the pore water, favoring aragonite dissolution, and subsequently reprecipitation as inorganic calcite (Reuning et al., submitted).

Whether such diagenetic processes affect the $\delta^{18}O$ composition of foraminiferal tests needs to be considered (Killingley, 1983; Schrag et al., 1995). In fact, the positive correlation between Mg/Ca and $\delta^{18}O$ after 4.5 Ma (see chapter 3.2), and the fact that $\delta^{18}O$ exhibits the same precessional variations as the diagenetically induced oscillations in aragonite and Sr/Ca, might imply that $\delta^{18}O$ is potentially also affected by carbonate diagenesis. However, as the benthic $\delta^{18}O$ record of Site 1000 closely matches those of ODP Site 925 (Ceara Rise) and 999 (Caribbean) (Steph et al., submitted), we suspect that the primary signal of the planktonic $\delta^{18}O$ record is preserved. If the $\delta^{18}O$ record would contain a diagenetic component, such an effect would increase the $\delta^{18}O$ signal of the diagenetically affected samples, resulting in increased $\delta^{18}O$ amplitudes (Killingley, 1983; Schrag et al., 1995). Further work needs to be done to decipher the diagenetic effect on $\delta^{18}O$.

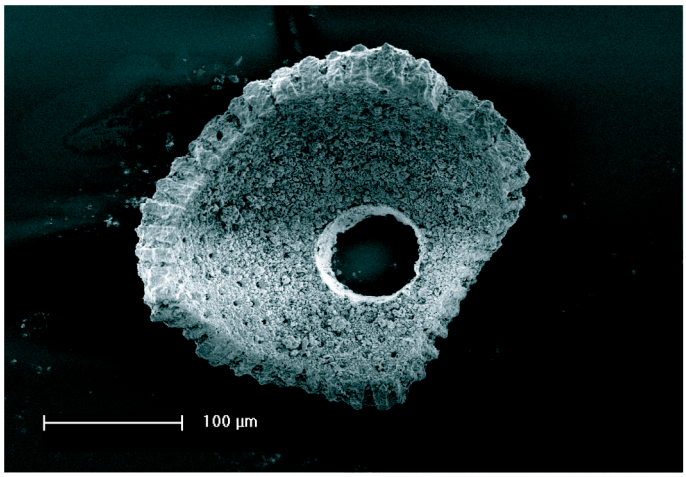

Figure 6.7E. *G. sacculifer* test, showing an ablation crater formed by LA-ICP-MS analysis (Photo taken at Utrecht Univ., The Netherlands).

Quantifying the effect of carbonate diagenesis by LA-ICP-MS

To quantify the Mg content of these diagenetic crystalline overgrowths, Laser Ablation Inductively Coupled Plasma Mass Spectrometry (LA-ICP-MS) (Eggins et al., 2003; Reichart et al., 2003; Hathorne et al., 2003) was applied. A laser ablation profile through a foraminiferal chamber wall allows the investigation of both internal heterogeneities of element-incorporation and concentration anomalies related to possible crystalline overgrowths. Since SEM showed the size of the single crystals to be 2-3 µm (Fig 6.5), they are within the spatial depth resolution of LA-ICP-MS, in view of the laser pulse rate (6 pulses per second) and the ICP-MS quadropole mass scanning rate. Energy density at the sediment surface was set at 2 J/cm^2, resulting in less than 200 nm of material in depth removed per pulse.

Laser ablation measurements of profiles across the foraminiferal tests with/without crystalline overgrowths show relatively similar Ca-normalized Mg distribution patterns (Fig 6.6). It is important to note that the calculated Mg/Ca ratios derived from the LA-ICP-MS measurements agree, within the method standard deviation of 5-10%, to the traditional whole test ICP-OES measurements performed on the same samples (Table 6.1). There is no significant change in the LA-ICP-MS Mg signal of the chamber walls with depth, although these profiles include measurements directly performed within the crystalline overgrowths. In view of the ablation rate and the

ICP-MS mass scanning it is reasonable to assume that the innermost 2 to 3 datapoints represent the crystalline overgrowths. When average test Mg concentrations are calculated excluding these data points no significant different values are obtained for Mg/Ca ratios. Evidently, the crystalline overgrowths do not contribute significantly to the high Mg/Ca ratios. Still, foraminiferal tests after 4.5 Ma and most prominent after 4.05 Ma, for samples with the maxima in $\delta^{18}O$, are enriched in Mg. These Mg/Ca ratios, remaining high throughout the entire test, cannot be explained by partial (or total) recrystallization of the foraminiferal tests, as diagenetic overgrowths at the test surfaces and slight dissolution signs (Fig 6.5), most likely caused by the rigorous cleaning procedure, were the only visible disturbances.

Similar to the laser ablation Mg-profiles, Sr is not showing any significant concentration changes within the chamber walls, although one would expect higher Sr/Ca levels in the inorganic crystalline overgrowths (see Chapter 3.3) (Fig 6.6). However, the relatively high standard deviation of the laser ablation Sr measurements (5-10%) is of the same order as the absolute increase in foraminiferal Sr/Ca (~8%) after 4.05 Ma in comparison with the older samples.

Table 6.1 Comparison between bulk ICP-OES measurements and LA-ICP-MS analyses for Mg/Ca and Sr/Ca. Shown are average results from multiple ablation profiles through cleaned *G. sacculifer* tests from two contaminated, i.e. with crystalline overgrowths, samples (14-5-115 and 14-5-125) and two uncontaminated, i.e. without crystalline overgrowths, samples (14-5-95 and 14-5-145).

Sample	Age (ka)	State	Number of profiles (analyses/profile)	Mg/Ca (mmol/mol) ICP-OES	Mg/Ca-uncont.interval (mmol/mol) LA-ICP-MS*
1000,14-5-95	3952	no crystalline overgrowth	4 (37)	4.30	3.84
1000,14-5-145	3965	no crystalline overgrowth	4 (38)	4.39	4.29
1000,14-5-115	3958	crystalline overgrowth	5 (45)	6.57	6.89
1000,14-5-125	3960	crystalline overgrowth	4 (47)	6.87	6.23

* relative standard deviation is 5-10%

Sample	Age (ka)	State	Number of profiles (analyses/profile)	Sr/Ca (mmol/mol) ICP-OES	Sr/Ca-uncont.interval (mmol/mol) LA-ICP-MS*
1000,14-5-95	3952	no crystalline overgrowth	4 (37)	1.39	1.45
1000,14-5-145	3965	no crystalline overgrowth	4 (38)	1.38	1.44
1000,14-5-115	3958	crystalline overgrowth	5 (45)	1.58	1.66
1000,14-5-125	3960	crystalline overgrowth	4 (47)	1.54	1.55

* relative standard deviation is 5-10%

Quantifying the impact of pore water chemistry on foraminiferal Mg/Ca and Sr/Ca

We used pore water data of Site 1000 (Fig 6.7, (Lyons et al., 2000)) to calculate the potential Mg/Ca and Sr/Ca ratios of precipitated inorganic calcite. The elemental composition of a diagenetic phase precipitating from pore water is dependent on the pore water element composition and the inorganic distribution coefficient. In fact, the calculation of the Mg/Ca ratio in the inorganically precipitated crystalline overgrowths is dependant on the distribution coefficient used for Mg (Tripati et al., 2003; Reuning et al., in press; Table 6.2b). There is a large variety of Mg distribution coefficients either assessed from sediments or experimentally derived ranging between

Table 6.2 Measured properties of Site 1000, possible distribution coefficients for Mg and Sr and calculated compositions of the inorganic calcite. **A.** Pore water data (Sample 15-3-145, 4.202 Ma) are from *Lyons et al.* (2000) and are used to calculate the composition of the inorganic calcite. ‚Average maximum of the contaminated Sr/Ca_{foram}' refers to the average Sr/Ca ratio of those samples which show the diagenetic overprint. ‚Average maximum of the uncontaminated Sr/Ca_{foram}' refers to the average Sr/Ca ratio of the samples from the older, uncontaminated part of the record, but only those from the maximum values. ‚Average maximum of the contaminated Mg/Ca_{foram}' refers to the average Mg/Ca ratio of those samples which show the diagenetic overprint. **B.** By using different distribution coefficients for Mg and the pore water composition, the possible Mg/Ca ratios of the inorganic calcite are calculated. **C.** By using different distribution coefficients for Sr and the pore water composition, the possible Sr/Ca ratios of the inorganic calcite are calculated. Using these compositions in combination with the measured Sr/Ca_{foram}, the mass percentage of the diagenetic overprint of the bulk analysed foraminifer is calculated (Mc = ((Cb* Mb) - (Mp* Cp))/ Cc, see text for explanation; *Lohmann*, 1995). **D.** Original Mg/Ca ratios of the contaminated foraminiferal tests. Combining the mass percentage of the diagenetic overprint with the calculated Mg/Ca ratios of the overgrowth, the Mg/Ca ratios of the original contaminated foraminiferal tests are calculated (Cp = ((Cb*Mb)-(Cc*Mc))/Mp, see text for explanation, *Lohmann*, 1995). Shaded area shows the range of values which are considered to be realistic estimates. These values result in SSTs between 32.4°C and 33.9°C, indicating that the carbonate diagenesis is not able to explain the extreme measured Mg/Ca ratios.

a)

Specifications Site 1000:	**Value**	**Reference**
Sr pore water	1771 µM	Lyons et al. 2000
Ca pore water	10.5 mM	Lyons et al. 2000
Mg pore water	33.9 mM	Lyons et al. 2000
Sr/Ca pore water	168.7 mmol/mol	Lyons et al. 2000
Mg/Ca pore water	3230 mmol/mol	Lyons et al. 2000
averaged maximum Sr/Ca_{foram} <4.05 Ma	1.55 mmol/mol	this study
averaged maximum Sr/Ca_{foram} >4.5 Ma	1.36 mmol/mol	this study
averaged maximum Mg/Ca_{foram} <4.05 Ma	6.33 mmol/mol	this study

b)

Distribution coefficient Mg (1) (inorganic calcite)	**Reference**	**$Mg/Ca_{crystal}$ mmol/mol**
0.0008	Baker et al., 1982	2.58
0.004	Delaney, 1989	12.92
0.012	Mucci and Morse, 1983	38.76

(1) $D = Mg/Ca_{mineral} / Mg/Ca_{solution}$

c)

Distribution coefficient Sr (2) (inorganic calcite)	**Reference**	**$Sr/Ca_{crystal}$ mmol/mol**	**Mass percentage crystal (%)**
0.015	Delaney, 1989	2.53	16.1
0.040	Baker et al., 1982	6.75	3.4
0.050	Delaney, 1989	8.43	2.7
0.060	Katz et al., 1972	10.12	2.1

(2) $D = Sr/Ca_{mineral} / Sr/Ca_{solution}$

d)

	Mass percentage of the crystals (%)				
		16.1	**3.4**	**2.7**	**2.1**
Mg/Ca of the	**2.58**	7.05	6.46	6.43	6.41
crystals (mmol/mol)	**12.92**	5.06	6.10	6.15	6.19
	38.76	0.11	5.18	5.43	5.63

$0.8 * 10^{-3}$ and $12.3 * 10^{-3}$ (Baker et al., 1982; Mucci and Morse, 1983; Delaney, 1989; Morse and Bender, 1990; Andreasen and Delaney, 2000) (Table 6.2b). Morse and Bender (1990) and Delaney (1989) demonstrated that such variability can be explained by changing element concentrations in pore water during the recrystallization process.

There are several arguments for using Sr/Ca for our calculations instead of Mg/Ca. Firstly, the pore water composition for the studied interval of Site 1000 is mainly determined by selective dissolution of aragonite, which is relatively enriched in Sr (1000-10,000 ppm) (Fig 6.7). Secondly, the distribution coefficient of Sr is much better constrained (0.015-0.06) than the distribution coefficient of Mg (Baker et al., 1982; Delaney, 1989; Morse and Bender, 1990; Table 6.2c). Thirdly, the range of Sr/Ca ratios in modern planktonic foraminifers is moderate (1.25-1.40 mmol/mol). Such a range in Sr/Ca is typically found in samples >4.5 Ma having no crystalline overgrowths. We therefore assume that excess Sr in the samples <4.05 Ma showing crystalline

overgrowths (~1.55 mmol/mol) is due to aragonite dissolution and subsequent reprecipitation. In this way the significant increase in foraminiferal Sr/Ca ratios is considered to indicate diagenetic overprinting. The averaged maximum Sr/Ca ratio in the aragonite-free interval >4.5 Ma is 1.36 mmol/mol. The interval <4.05 Ma, instead, shows an increase in Sr/Ca of 12% to an averaged maximum of 1.55 mmol/mol. The assumption that this increase is solely due to diagenesis allows us to estimate the portion of diagenetic calcite with respect to the initial foraminiferal calcite (Reuning et al., in press).

First, we calculated the potential Sr/Ca ratio of the diagenetically precipitated inorganic calcite by using the pore water Sr- and Ca-concentrations (Fig 6.7; Table 6.2; Lyons et al. (2000)). Depending on the existing Sr-distribution coefficients, the expected Sr/Ca ratios of the inorganically precipitated overgrowths vary between 2.5-10.1 mmol/mol (Table 6.2). Subsequently, we used the Lohmann (1995) equation to calculate the mass percentage of the inorganic diagenetic calcite:

$$Mc = ((Cb* Mb) - (Mp* Cp))/ Cc \qquad (1)$$

with Cp = averaged maximum Sr/Ca_{foram} >4.5 Ma (1.36 mmol/mol), Cb = averaged maximum Sr/Ca_{foram} <4.05 Ma (1.55 mmol/mol), Cc = the calculated $Sr/Ca_{crystal}$ (2.5-10.1 mmol/mol), Mb = the mass percentage of the analysed foraminifer (1), Mp = the mass percentage of the original foraminiferal test (Mb-Mc), and Mc = the mass percentage of the inorganic, diagenetic calcite. Accordingly, the amount of diagenetically precipitated calcite is 2.1-3.4% of the entire foraminiferal sample, with a maximum value of >16% when applying the lowest Sr-distribution coefficient (Table 6.2c). This extreme value clearly does not correspond to the distribution pattern of the diagenetic overgrowths, consisting of small crystals (~2-3 µm) mainly attached to the inner test surfaces (Fig 6.5).

Knowing both the amount of diagenetically precipitated calcite and the expected Mg/Ca ratios of these overgrowths (Table 6.2b), we are able to correct the measured Mg/Ca ratios for the diagenetic effect. Table 6.2d combines the different assumptions on the portion (2.1-16.1%) and on the Mg/Ca ratios of the diagenetic overgrowths (2.58-38.76 mmol/mol) in dependance of the different distribution coefficients, and provides Mg/Ca ratios of the diagenetically unaffected foraminiferal tests. These Mg/Ca ratios range from unrealistically low 0.11 mmol/mol (16.1% diagenetic overprint with Mg/Ca = 38.76 mmol/mol) to maximum 7.05 mmol/mol (16.1% diagenetic overprint with Mg/Ca = 2.58 mmol/mol) (Table 6.2d).

As the distribution coefficients for naturally precipitated inorganic calcite tend to be lower than those for experimentally precipitated calcite (Baker et al., 1982; Delaney, 1989), we conclude that the Mg/Ca ratios for the unaffected foraminiferal calcite most likely range between 6.10 and 6.46 mmol/mol. These calculated Mg/Ca ratios, corrected for the diagenetic imprint, are similar to the measured averaged maximum value of 6.33 mmol/mol after 4.05 Ma, and convert into $SSTs_{Mg/Ca}$ of 33.2-33.9°C still being unrealistically high. We conclude that the observed crystalline overgrowths do not provide enough Mg to shift the foraminiferal Mg/Ca ratios to high values.

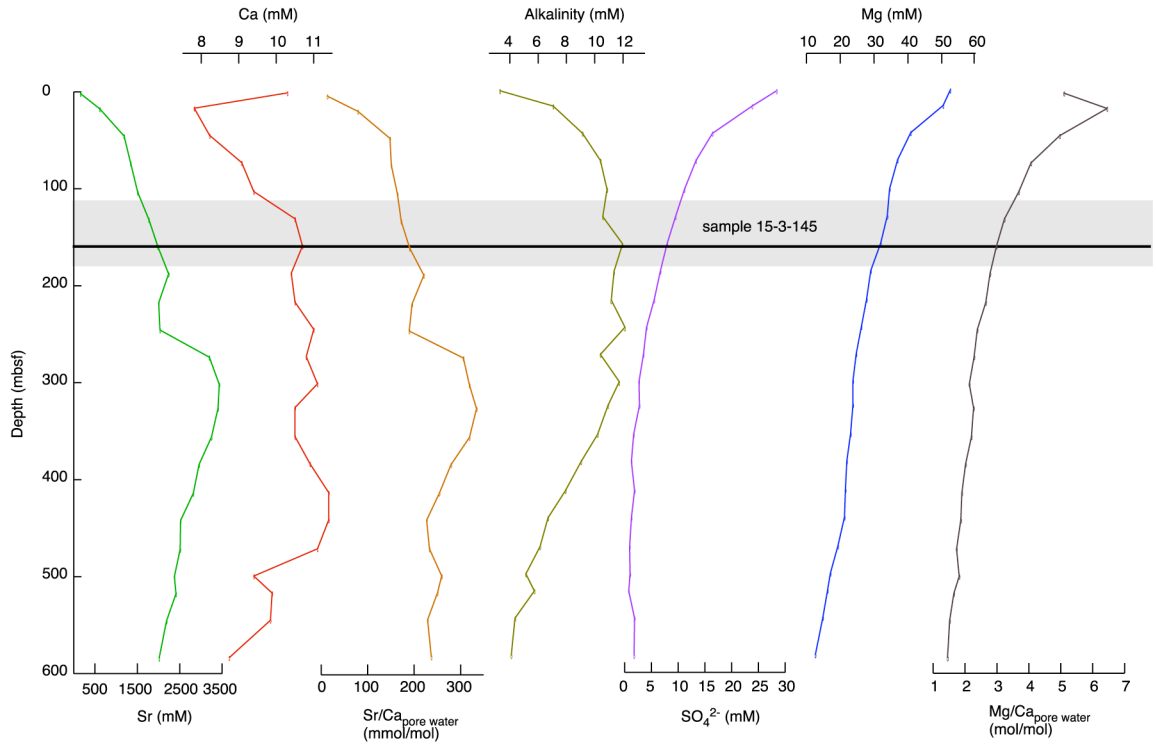

Figure 6.7 Pore water profiles of Site 1000 for magnesium (Mg), strontium (Sr), calcium (Ca), sulfate (SO_4^{2-}), alkalinity, and Mg/Ca and Sr/Ca of the pore water, reflecting shallow burial diagenetic reactions. Data are from Lyons et al. (2000). Shaded interval indicates the interval which provided samples for this study. Solid black line shows the position of the pore water sample (15-3-145) which was used for the calculation of the inorganic calcite Mg/Ca and Sr/Ca ratios.

Pliocene change in seawater Mg/Ca

The application of Mg/Ca paleothermometry to sample material from older time slices, for example in this study the Pliocene, requires to consider possible changes in $Mg/Ca_{seawater}$ (Lear et al., 2000; Billups and Schrag, 2003; Tripati et al., 2003). From cultivating experiments Brown (1996) concluded that Mg/Ca_{foram} is linearly dependent on $Mg/Ca_{solution}$ (0.1 mol/mol change in $Mg/Ca_{seawater}$ leads to 0.059 mmol/mol change in Mg/Ca_{foram}). Recently, Ries (2004) showed that several carbonate building organisms exhibit an exponential relationship between Mg/Ca_{foram} and $Mg/Ca_{solution}$. The residence time of Mg in seawater is ~13 m.y. (Broecker and Peng, 1982), which basically suggests that paleo sea surface temperature reconstructions on much shorter time scales would not be affected by a change in $Mg/Ca_{seawater}$. However, on long time scales Mg and Ca in seawater might have changed due to varying continental weathering rates (Berner et al., 1983; Wilkinson and Algeo, 1989), hydrothermal alteration of basalt at mid ocean ridges (Mottle and Wheat, 1994; Elderfield and Schulz, 1996), carbonate deposition (Wilkinson and Algeo, 1989), and ion exchange reactions of Mg with clays (Gieskes and Lawrence, 1981). Based on the models of Wilkinson and Algeo (1989) and Stanley and Hardie (1998), $Mg/Ca_{seawater}$ was lowered by maximum 0.4 mol/mol during the early Pliocene. When applying the calibration formula introduced by Lear et al. (2000) to correct for this change in $Mg/Ca_{seawater}$, the resulting $SST_{Mg/Ca}$ record is offset to even higher $SST_{Mg/Ca}$ by maximum 1°C in comparison to the original $SST_{Mg/Ca}$ dataset.

This consideration, in combination with the relatively short time interval of our record which excludes large variations in $Mg/Ca_{seawater}$, and the resemblance of the $SSTs_{Mg/Ca}$ >4.5 Ma with modern Caribbean SSTs, suggests that the Pliocene drop in $Mg/Ca_{seawater}$ cannot explain the extreme $SSTs_{Mg/Ca}$ observed after 4.05 Ma and therefore, made us decide not to apply a correction for changed $Mg/Ca_{seawater}$.

Conclusions

Combined analyses of Mg/Ca and $\delta^{18}O$ on the planktonic foraminifer *G. sacculifer* from ODP Site 1000 allowed to study changes in Caribbean surface hydrography during the effective restriction of surface throughflow through the Panamanian Gateway between 5.6-3.9 Ma. The reconstruction of $SST_{Mg/Ca}$ and SSS from combined foraminiferal Mg/Ca and $\delta^{18}O$ measurements implies a relatively uniform $SST_{Mg/Ca}$ pattern of 26.5°C-29°C for the time interval 5.6-5.0 Ma. This period is characterized by the typical negative correlation between Mg/Ca and $\delta^{18}O$. This pattern changes after 5.0 Ma, when both positive and negative correlations between $SST_{Mg/Ca}$ and $\delta^{18}O$ occur.

After 4.5 Ma, we show a nearly perfect positive correlation between Mg/Ca and $\delta^{18}O$, i.e. high $SST_{Mg/Ca}$ are paralleled by high $\delta^{18}O$ values, on a precessional timescale. Such a positive correlation was not reported before. We interpret such a positive relationship between $SST_{Mg/Ca}$ and $\delta^{18}O$ the way that the salinity effect on the $\delta^{18}O$ signal dominates those of global ice volume and temperature. Converting the $\delta^{18}O$ record into SSS yields salinity amplitudes of up to 4 salinity units. At times of peak SSS, foraminiferal Mg/Ca increase to up to ~7 mmol/mol, transferring to unrealistically high $SST_{Mg/Ca}$ of up to 35°C with amplitudes of up to 5°C. We suspect that the large variations in SSS have a profound influence on the Mg/Ca record overestimating Mg/Ca ratios by 20-30% and $SST_{Mg/Ca}$ by 3-4°C.

SEM analyses of foraminiferal tests of *G. sacculifer* showing anomalously high Mg/Ca ratios reveal crystalline overgrowths. Foraminiferal Sr/Ca ratios, carbonate mineralogy, and calcareous nannofossil analysis suggest that diagenetically induced aragonite dissolution and reprecipitation caused these overgrowths. LA-ICP-MS measurements and pore water data, however, exclude the possibility that the diagenetic overgrowths provide enough Mg to generate the extremely high foraminiferal Mg/Ca ratios observed after 4.5 Ma. According to our estimation, the diagenetic overprint may account for a potential error on Mg/Ca of maximum -0.1 to 0.3 mmol/mol (-0.3°C to 1°C in temperature).

After correcting the foraminiferal Mg/Ca ratios after 4.5 Ma for the salinity effect, the reconstructed $SST_{Mg/Ca}$ record shows an increase in Caribbean SST by ~2°C due to the progressive shoaling of the Isthmus of Panama, possibly indicating the initiation of the Western Atlantic Warm Pool.

Acknowledgements

This research used samples and data provided by the Ocean Drilling Program, which is sponsored by the U.S. National Science Foundation and participating countries under management of Joint Oceanographic Institutions. This study was performed within DFG-Research Unit „Impact of Gateways on Ocean Circulation, Climate, and Evolution“ (FOR451/1-1 TP B2). We like to thank Silvia Koch, Kerrin Wittmaack, Nicole Gau, Jutta Heintze, Kristin Nass, Beate Bader, Ute Schuldt, Paul Mason, and Gijs Nobbe for sample preparation and laboratory assistence. We gratefully thank Marcus Regenberg, Joachim Schönfeld, Martin Ziegler, and ... anonymous reviewers for their useful comments and the improvement of the manuscript.

References

Andreasen, G. H., and M. L. Delaney (2000), Lithologic controls on calcite recrystallizations in Cenozoic deep-sea sediments, *Mar. Geol., 163,* 109-124.

Archer, D. E. (1996), An atlas of the distribution of calcium carbonate in sediments of the deep sea. *Global Biogeochem. Cycles, 10,* 159-174.

Baker, P., J. M. Gieskes, and H. Elderfield (1982), Diagenesis of carbonates in deep-sea sediments evidence from Sr/Ca ratios and interstitial dissolved Sr^{2+} data, *J. Sediment. Petrol., 52,* 71-82.

Barker, S., M. Greaves, and H. Elderfield (2003), A study of cleaning procedures used for foraminiferal Mg/Ca paleothermometry, *Geochem. Geophys. Geosyst., 4(9),* 8407, doi:10.1029/2003GC000559.

Beaufort, L., Y. Lancelot, P. Camberlin, O. Cayre, E. Vincent, F. Bassinot, and L. Labeyrie (1997), Insolation cycles as a major control of equatorial Indian Ocean primary production, *Science, 278,* 1451-1454.

Ben-Yaakov, S. (1973), pH Buffering of pore water of recent anoxic marine sediments, *Limnology and Oceanography, 18,* 86-94.

Berner, R. A. (1971), *Principles of chemical sedimentology,* 240 pp, McGraw-Hill Book Co., International Series in the Earth and Planetary Sciences.

Berner, R. A., A. C. Lasaga, and R. M. Garrels (1983), The carbonate-silicate geochemical cycle and its effect on atmospheric carbon dioxide over the past 100 million years, *Am. J. Sci., 283,* 641-683.

Bickert, T., W. B. Curry, and G. Wefer (1997), Late Pliocene to Holocene (2.6-0 Ma) western equatorial Atlantic deep-water circulation: Inferences from benthic stable isotopes, Leg 154, *Proc. Ocean Drill. Program, Sci. Results, 154,* 239-254.

Billups, K., and D. P. Schrag (2003), Application of benthic foraminiferal Mg/Ca ratios to questions of Cenozoic climate change. *Earth Planet. Sci. Lett., 209,* 181-195.

Billups, K., A. C. Ravelo, and J. C. Zachos (1998), Early Pliocene climate: A perspective from the western equatorial Atlantic warm pool, *Paleoceanography, 13,* 459-470.

Billups, K., A. C. Ravelo, J. C. Zachos, and R. D. Norris (1999), Link between oceanic heat transport, thermohaline circulation, and the Intertropical Convergence Zone in the early Pliocene Atlantic, *Geology, 27,* 319-322.

Broecker, W. S. (1989), The salinity contrast between the Atlantic and Pacific oceans during glacial time, *Paleoceanography, 4,* 207-212.

Broecker, W. S., and T. H. Peng (Eds.) (1982), *Tracers in the Sea,* 690 pp, Palisades, New York.

Brown, S. J. (1996), Controls on the trace metal chemistry of foraminiferal calcite and aragonite, 231 pp, Ph.D. thesis, Univ. Cambridge, Cambridge, UK.

Cronin, T. M., R. Whatley, A. Wood, A. Tsukagoshi, N. Ikeya, E. M. Brouwers, and W. M. Briggs Jr. (1993), Microfaunal evidence for elevated Pliocene temperatures in the Arctic Ocean, *Paleoceanography, 8,* 161-173.

Crowley, T. J. (1996), Pliocene climates: the nature of the problem, *Mar. Micropaleontology, 27,* 3-12.

Crudeli, D., and H. Kinkel (2004), *Reticulofenestra calicis n. sp.*, an unusual small reticulofenestrid coccolith from the Lower Pliocene of the South Caribbean Sea, *Micropaleontology, 50(4),* 369-379.

Dekens, P. S., D. W. Lea, D. K. Pak, and H. J. Spero (2002), Core top calibration of Mg/Ca in tropical foraminifera: Refining paleotemperature estimation, *Geochem. Geophys. Geosyst., 3(4),* 1022, doi:10.1029/2001GC000200.

Delaney, M. L. (1989), Temporal changes in interstitial water chemistry and calcite recrystallization in marine sediments, *Earth Planet. Sci. Lett, 95,* 23-37.

Dowsett, H. J., J. Barron, and R. Poore (1996), Middle Pliocene sea surface temperatures: a global reconstruction, *Mar. Micropaleontology, 27,* 13-25.

Driscoll, N. W., and G. H. Haug (1998), A short circuit in thermohaline circulation: A cause for Northern Hemisphere Glaciation? *Science, 282,* 436-438.

Eggins, S., P. de Deckker, and J. Marshall (2003), Mg/Ca variation in planktonic foraminifera shells: Implications for reconstruction of paleoseawater temperature and habitat migration, *Earth Planet. Sci. Lett. 212(3-4),* 291-306.

Elderfield, H., and A. Schultz (1996), Mid-ocean ridge hydrothermal fluxes and the chemical composition of the ocean, *Annual Reviews of Earth and Planetary Sciences, 24,* 191-224.

Elderfield, H., and G. Ganssen (2000), Past temperature and $\delta^{18}O$ of surface ocean waters inferred from foraminiferal Mg/Ca ratios, *Nature, 405,* 442-445. Fairbanks, R. G., M. Sverdlove, R. Free, P. H. Wiebe, and A. W. H. Be (1982), Vertical distribution and isotopic fractionation of living planktonic foraminifera from the Panama Basin, *Nature, 298,* 841-844.

de Garidel-Thoron, T., L. Beaufort, B. K. Linsley, and S. Dannenmann (2001), Millennial- scale dynamics of the East Asian winter monsoon during the last 200,000 years, *Paleoceanography, 16,* 1-12.

Gieskes, J. M., and J. R. Lawrence (1981), Alteration of volcanic matter in deep sea sediments, evidence from the chemical composition of interstitial waters from deep sea drilling cores, *Geochim. Cosmochim. Acta, 45,* 1687-1703.

Given, R. K., and B. H. Wilkinson (1985), Kinetic control of morphology, composition, and mineralogy of abiotic sedimentary carbonates, *J. Sediment. Petrol., 55,* 109-119.

Günther, D., R. Frischknecht, C. A. Heinrich, and H. J. Kahlert (1997), Capabilities of a 193 nm ArF excimer laser for LA-ICP-MS micro analysis of geological materials, *J. Anal. At. Spectrom., 12,* 939 944.

Hampt, G., and M. L. Delaney (1997), Influences of calcite Sr/Ca records from Ceara Rise and other regions: Distinguishing ocean history and calcite recrystallization, *Proc. Ocean Drill. Program, Sci. Results, 154,* 491-500.

Hathorne, E. C., O. Alard, R. H. James, and N. W. Rogers (2003), Determination of intratest variability of trace elements in foraminifera by Laser Ablation ICP-MS, *Geochem. Geophys. Geosyst., 4(12),* 8408, doi:10.1029/2003GC000539.

Haug, G. H., and R. Tiedemann (1998), Effect of the formation of the Isthmus of Panama on Atlantic Ocean thermohaline circulation, *Nature, 393,* 673-676.

Haug, G. H., R. Tiedemann, R. Zahn, and A. C. Ravelo (2001), Role of Panama uplift on oceanic freshwater balance, *Geology, 29,* 207-210.

Hodell, D. A., and D. A. Warnke (1991), Climate evolution of the Southern Ocean during the Pliocene epoch from 4.8 to 2.6 million years ago, *Quat. Sci. Rev., 10,* 205-214.

Jansen, E., S. Sjoholm, U. Bleil, and J. A. Erichsen (1990), Neogene and Pleistocene glaciations in the northern hemisphere and late Miocene-Pliocene global ice volume fluctuations: Evidence from the Norwegian Sea. in *Geological history of the polar oceans: Arctic versus Antarctic,* edited by U. Bleil, and J. Thiede, 677-5, Kluwer Acad. Norwell. Mass.

Kameo, K., and T. Sato (2000), Biogeography of Neogene calcareous nannofossils in the Caribbean and the eastern equatorial Pacific – floral response to the emergence of the Isthmus of Panama, *Mar. Micropaleontology, 39,* 201-218.

Katz, A., E. Sass, A. Starinsky, and H. D. Holland (1972), Strontium behavior in the aragonite-calcite transformation: an experimental study at 40-98°C, *Geochim. Cosmochim. Acta, 36,* 481-496.

Kennett, J. P., and D. A. Hodell (1993), Evidence for relative climate stability of Antarctica during the early Pliocene: A marine perspective, *Geograph. Ann., 75,* 205-220.

Killingley, J. S. (1983), Effects of diagenetic recrystallization on $^{18}O/^{16}O$ values of deep-sea Sediments, *Nature, 301,* 594-597.

Lea, D. W., T. A. Mashiotta, and H. J. Spero (1999), Controls on magnesium and strontium uptake in planktonic foraminifera determined by live culturing, *Geochim. Cosmochim. Acta, 63,* 2369-2379.

Lear, C. H., H. Elderfield, and P. A. Wilson (2000), Cenozoic deep-sea temperatures and global ice volumes from Mg/Ca in benthic foraminiferal calcite, *Science, 287,* 269-272.

Levitus, S., and T. Boyer (1994), *World ocean atlas 1994, Vol.4, Temperature,* NOAA Atlas NESDIS, 4, U.S. Dept. of Commerce, Washington, D.C.

Lohmann, G. P. (1995), A model for variation in the chemistry of planktonic foraminifera due to secondary calcification and selective dissolution, *Paleoceanography, 10,* 445-457.

Lyons, T. W., R. W. Murray, and D. G. Pearson (2000), A comparative study of diagenetic pathways in sediments of the Caribbean Sea: Highlights from pore-water results, *Proc. Ocean Drill. Program, Sci. Results, 165,* 287-298.

Maier-Reimer, E., U. Mikolajewicz, and T. Crowley (1990), Ocean general circulation model sensitivity experiment with an open central american isthmus, *Paleoceanography, 5,* 349-366.

Malone, M. J., P. Baker, S. Burns, and P. Swart (1990), Geochemistry of periplatform carbonate sediments, Ocean Drilling Progran Site 716 (Maldives Archipelago, Indian Ocean). *Proc. Ocean Drill. Program, Sci. Results, 115,* 647-659.

McKenna, V. S., and W. L. Prell (2004), Calibration of the Mg/Ca of *Globorotalia truncatulinoides* (right) for the reconstruction of marine temperature gradients, *Paleoceanography, 19,* PA2006, doi:10.1029/2000PA000604.

Melim, L. A., H. Westphal, P. K. Swart, G. P. Eberli, and A. Munnecke (2002), Questioning carbonate diagenetic paradigms: evidence from the Neogene of the Bahamas, *Mar. Geol., 185,* 27-53.

Mix, A. C., N. G. Pisias, W. Rugh, J. Wilson, A. Morey, and T. K. Hagelberg (1995), Benthic foraminifer stable isotope record from Site 849 (0-5 Ma): Local and global climate changes, *Proc. Ocean Drill. Program, Sci. Results, 138,* 371-412.

Molfino, B., and A. McIntyre (1990), Precessional forcing of nutricline dynamics in the equatorial Atlantic, *Science, 249,* 766-769.

Molnar, P., and M. A. Cane (2002), El Nino's tropical climate and teleconnections as a blueprint for pre-Ice Age climates, *Paleoceanography, 17,* 1021, doi:10.1029/2001PA000663.

Morse, J. W., and M. L. Bender (1990), Partition coefficients in calcite: Examination of factors influencing the validity of experimental results and their application to natural systems, *Chem. Geol., 82,* 265-277.

Morse, J. W., and F. T. Mackenzie (1990), *Geochemistry of Sedimentary Carbonates,* 707 pp., New York, Elsevier.

Mottle, M. J., and G. Wheat (1994), Hydrothermal circulation through mid-ocean ridge flanks: Fluxes of heat and magnesium, *Geochim. Cosmochim. Acta, 58,* 2225-2237.

Mucci, A., and J. W. Morse (1983), The incorporation of Mg^{2+} and Sr^{2+} into calcite overgrowths: influences of growth rate and solution composition, *Geochim. Cosmochim. Acta, 47,* 217-233.

Munnecke, A., H. Westphal, J. J. G. Reijmer, and C. Samtleben (1997), Microspar development during early marine burial diagenesis: a comparison of Pliocene carbonates from the Bahamas with Silurian limestones from Gotland (Sweden), *Sedimentology, 44,* 977-990.

Nürnberg, D. (1995), Magnesium in tests of *Neogloboquadrina Pachyderma sinistral* from high northern and southern latitudes, *J. Foraminiferal Res., 25,* 350-368.

Nürnberg, D. (2000), Taking the temperature of past ocean surfaces, *Science, 289,* 1698-1699.

Nürnberg, D., J. Bijma, and C. Hemleben (1996), Assessing the reliability of magnesium in foraminiferal calcite as a proxy for water mass temperatures, *Geochim. Cosmochim. Acta, 60,* 803-814.

Nürnberg, D., A. Müller, and R. R. Schneider (2000), Paleo-sea surface temperature calculations in the equatorial east Atlantic from Mg/Ca ratios in planktic foraminifera: A comparison to sea surface temperature estimates from U^k 37, oxygen isotopes, and foraminiferal transfer function, *Paleoceanography, 15,* 124-134.

Pearce, N. J. G., W. T. Perkins, J. A. Westgate, M. P. Gorton, S. E. Jackson, C. R. Neal, and S. P. Chenery (1997), A compilation of new and published major and trace element data for NIST SRM 610 and NIST SRM 612 glass reference materials, *Geostandards Newsletter, 21,* 115-144

Pena, L. D., E. Calvo, I. Cacho, S. Eggins, and C. Pelejero (submitted), Identification and removal of Mn-Mg-rich contaminant phases in foraminiferal tests: Implications for Mg/Ca past temperature reconstructions, *Geochem. Geophys. Geosyst.,* 2005GC000930.

Raymo, M. E., W. F. Ruddiman, J. Backman, B. M. Clement, and D. G. Martinson (1989), Late Pliocene variation in Northern Hemisphere ice sheets and North Atlantic deep water circulation, *Paleoceanography, 4,* 413-446.

Reichart, G. J., F. Jorissen, P. Anschutz, and P. R. D. Mason (2003), Single foraminiferal test chemistry records the marine environment, *Geology, 31,* 355-358.

Reuning, L., J. J. G. Reijmer, C. Betzler, P. Swart, and T. Bauch (2005), The use of paleoceanographic proxies in carbonate periplatform settings – opportunities and pitfalls, *Sed. Geol.,* in press.

Ries, J. B. (2004), Effect of ambient Mg/Ca ratio on Mg fractionation in calcareous marine invertebrates: A record of the oceanic Mg/Ca ratio over the Phanerozoic, *Geology, 32,* 981-984.

Rosenthal, Y., and G. P. Lohmann (2002), Accurate estimation of sea surface temperatures using dissolution-corrected calibrations for Mg/Ca paleothermometry, *Paleoceanography, 17,* 1044, doi:10.1029/2001PA000749.

Schrag, D. P., D. J. DePaolo, and F. M. Richter (1995), Reconstructing past sea surface temperatures: Correcting for diagenesis of bulk marine carbonate, *Geochim. Cosmochim. Acta, 59,* 2265-2278.

Shackleton, N. J., M. A. Hall, and D. Pate (1995), Pliocene stable isotope stratigraphy of Site 846, *Proc. Ocean Drill. Program, Sci. Results, 138,* 337-353.

Shackleton, N. J., and M. A. Hall (1997), The Late Miocene stable isotope record, site 926, *Proc. Ocean Drill. Program, Sci. Results, 154,* 367-373.

Sigurdsson, H., R. M. Leckie, G. D. Acton, et al. (1997), *Proc. ODP, In. Repts, 165,* College Station, TX (Ocean Drilling Program).

Stanley, S. M., and L. A. Hardie (1998). Secular oscillations in the carbonate mineralogy of reef-building and sediment-producing organisms driven by tectonically forced shifts in seawater chemistry, *Palaeogeogr. Palaeoclimatol. Palaeoecol., 144,* 3-19.

Stehli, F. G., and S. D. Webb (Eds.) (1985), *The Great American Biotic Interchange,* 523 pp., Plenum Press, New York.

Steph, S., Tiedemann, R., Groenevel, J., Nürnberg, D., Reuning, R. & Haug, G. in revision. Changes in Caribbean surface hydrography during the Pliocene shoaling of the Central American Seaway. *Paleoceanography*.

Swart, P. K., and M. Guzikowski (1988), Interstitial water chemistry and diagenesis of

periplatform sediments from the Bahamas, ODP Leg 101, *Proc. Ocean Drill. Program, Sci. Results, 101,* 363-380.

Tiedemann, R., and S.O. Franz (1997), Water circulation, chemistry, and terrigenous sediment supply in the Equatorial Atlantic during the Pliocene, 3.3-2.6 Ma and 5-4.5 Ma, *Proc. ODP, Sci. Results, 154,* 299-318.

Tiedemann, R., M. Sarnthein, and N. J. Shackleton (1994), Astronomic timescale for the Pliocene Atlantic $\delta^{18}O$ and dust flux records of Ocean Drilling Program Site 659, *Paleoceanography, 9,* 619-638

Tripati, A. K., M. L. Delaney, J. C. Zachos, L. D. Anderson, D. C. Kelly, and H. Elderfield (2003), Tropical sea-surface temperature reconstruction for the early Paleogene using Mg/Ca ratios of planktonic foraminifera, *Paleoceanography, 18(4),* 1101, doi:10.1029/2003PA000937

Webb, S. D. (1997), *The great american faunal interchange in Central America: A natural and cultural history,* edited by Coates, A.G., 97-122, New Haven, Connecticut, Yale Univ.

Webb, P. N., and D. M. Harwood (1991), Late Cenozoic glacial history of the Ross Embayment, Antarctica, *Quat. Sci. Rev., 10,* 215-223.

Wilkinson, B. H., and T. J. Algeo (1989), Sedimentary carbonate record of calcium- magnesium Cycling, *Am. J. Sci., 289,* 1158-1194.

CHAPTER 6

CHAPTER 6

6.1. Summary and conclusions

Coccolithophores have an extended fossil record. As such, they represent an invaluable archive for changes in biological complexity through time. This can be studied in detail to reveal relations between the evolutionary dynamics of populations and environmental changes in the Earth's history. Nonetheless, to date only very few evolutionary studies on coccolithophores from the fossil record were carried out.

Recent molecular genetic works have shown that *Emiliania,* the most studied species*,* recently diverged from the *Gephyrocapsa* clade (Sáez et al., 2004). The species, considered a single taxon with worldwide distribution, consists of several genotypically distinct types or species, which differ by subtle morphological differences (Young et al., in press, and references therein). A high biodiversity likely characterise modern gephyrocapsid and many other coccolithophores (Young et al., in press; Geisen et al., 2004). Which are the evolutionary mechanisms and patterns that shape the recently discovered coccolithophores biodiversity? On one hand, available fossil record data support a simple pattern of evolution among coccolithophores, on the other, results from molecular genetic studies suggest that evolution may follow a much more complex pattern (de Vargas et al., 2004) (Fig. 1).

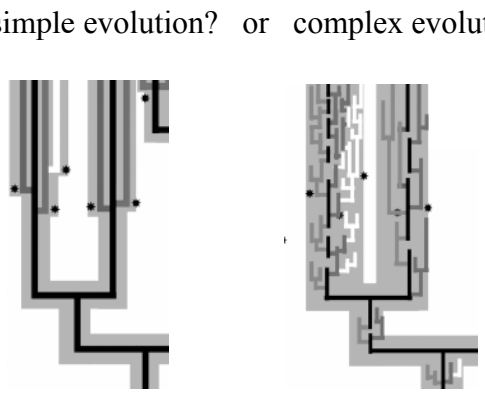

Fig. 1. Available fossil record data support simple evolution among coccolithophores. By contrast, results from molecular genetic studies suggest that evolution may follow a more complex pattern (redrawn from de Vargas et al., 2004).

The aim of this thesis was to test, what principal modes of evolution shaped coccolithophore populations in the past, and to what extend these evolutionary steps can be linked to changes in ocean's circulation. Therefore, two sediment cores recording the early Pliocene climate history and plankton evolution in the Caribbean Sea (Hole 1000A) and Eastern Equatorial Pacific (Site 1241) were chosen. Within this area, the geodynamic development led to the stepwise closure of the Isthmus of Panama with profound consequences on ocean circulation and marine biota. The backbone of this study was provided by high-resolution stable oxygen and carbon isotope measurements performed on planktic and benthic foraminifers. These records, in combination with the existing biostratigraphic and magnetostratigraphic control points were correlated with existing orbital tuned sediment cores (e.g. Tiedemann et al. 1994;

Tiedemann and Franz, 1997), providing a geochronological framework with a resolution of about 3 ky (Steph et al., in revision).

One of the major turnovers in Neogene coccolithophore evolution took place within the time interval (4.5-3.8 Ma): the rise of *Gephyrocapsa* from *Reticulofenestra*. This evolutionary event is mainly recognised as the first consistent occurrence (FCO) of small *Gephyorcapsa* defined by light microscopy (LM) (e.g. Okada 2000; Kameo and Sato 2000). Driever (1988) conducted a pioneer low-resolution morphometric study by LM on the small *Gephyorcapsa* (Mediterranean) from the FCO, in which he documented a time-progressive size increase (from 2 µm to 3.5 µm) of the plexus (Fig. 2). Other authors qualitatively observed this pattern (e.g. Marino and Flores, 2002). However, no high-resolution morphometric studies of the small *Gephyrocapsa* plexus have been carried. Moreover, the reasons for the observed size increase in the early Pliocene remained unknown. It was an open question whether the size increase reflects increase in size of a single species or it is due to successive evolution of larger species within a radiating plexus (Fig. 2).

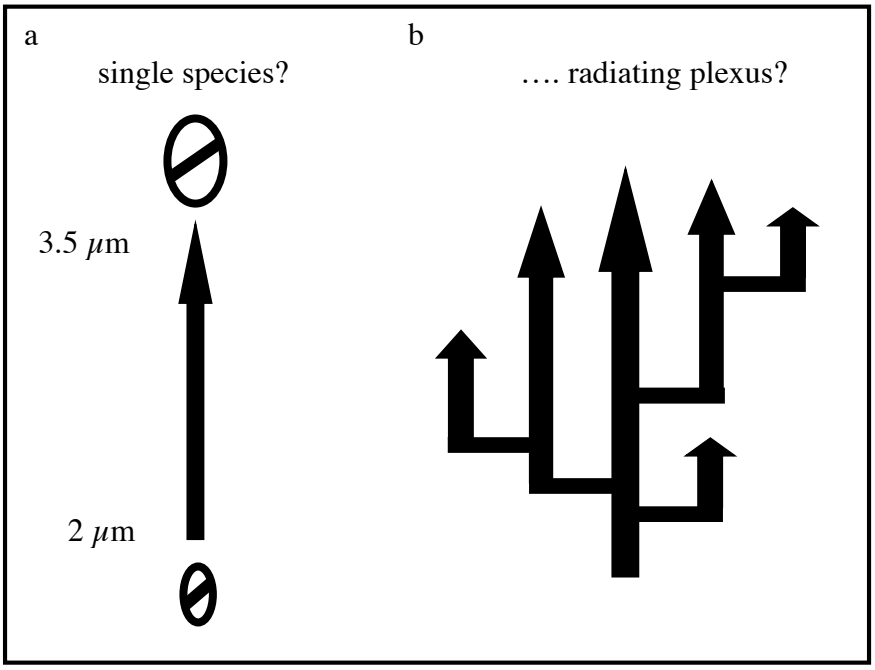

Fig. 2. a - Fossil record data of small *Gephyrocapsa* support the idea that the size increase (e.g. Driever, 1988) reflects evolution of a single species. This supports a simple pattern of evolution (i.e. phyletic gradualism). b - recent molecular genetic data have shown that species commonly considered long-ranging species with cosmopolitan distribution (e.g. *E. huxleyi*) are composed by several biologically distinct species. Mechanisms and patterns of evolution among the group may be thus much more complex.

Due to their small size, LM is not able to resolve single species in reticulofenestrid coccolithophores. In order to resolve the mechanisms of evolution, a study on the species-level variation of these coccolithophores has been carried out. In this thesis, scanning electron microscopy (SEM) was applied to document fine-scale phenetic variability between and within species. The SEM study of species-level

variation of very small reticulofenestrids allowed to recognize and depict, for the first time, and at species-level, the evolutionary radiation of *Gephyrocapsa* (Fig. 3).

This research has been carried out at the best possible temporal resolution using the orbital tuned chronostratigraphic framework of ODP Sites 1000A (Caribbean) and Site 1241 (Eastern Equatorial Pacific) (S. Steph et al., in revision). High-resolution SEM was used to decipher coccolithophore taxonomy at specific to intraspecific-level. Although the FCO of small *Gephyrocapsa* is well known from numerous biostratigraphic-paleoceanographic studies (e.g. Okada 2000; Kameo and Sato 2000), the exact timing of this event remained so far unclear since biostratigraphic studies are usually not carried out at such high chronostratigraphic resolution. Samples from the Caribbean Site 1000A and the east Pacific Site 1241 recording the FO and FCO of small *Gephyrocapsa* (*G. theyeri,* Chapters 3-4) were analysed. High-resolution stratigraphy (Steph et al., in revision; Tiedemann et al., submitted) indicates that both bioevents were synchronous in the two basins. Since the microevolutionary history of the plexus appeared very similar, the better preserved samples from the Caribbean Site 1000A compared to the east Pacific Site 1241 were chosen for the detailed taxonomic investigation.

A complex evolutionary history characterises *Reticulofenestra* and *Gephyrocapsa* coccolithophores during the early Pliocene (Caribbean Site 1000A). Fine-scale observations of very small reticulofenestrids allowed identification of stable morphotypes and the identification of different species. A major result was the recognition of four new *Reticulofenestra* species (*R. calicis, R. alis* n. sp., *R. pujosiae* n. sp. and *R. premoliae* n. sp.) (Chapters 2-3) and five new *Gephyrocapsa* species (*G. samtlebenii* n. sp., *G. drieveri* n. sp., *G. bollmannii* n. sp., *G. jerkovicii* n. sp., and *G. matsuokae* n. sp.) (Chapter 4). Despite clear evidence of morphological continuity, we do not refer the new very small reticulofenestrids to *Gephyrocapsa* because *Gephyrocapsa* is easily recognisable under LM. The first occurrence (FO) of *G. theyeri* (Chapter 3) at 4.45Ma was established, as dated by high-resolution isotope stratigraphy (Steph et al., in revision). This species was previously thought to have evolved in the Miocene, leaving an open question of the evolutionary mode of this important group of coccolithophores.
Morphological continuity allowed to infer phylogenetic relations among the new *Reticulofenestra* species and to trace the phylogeny of *Gephyrocapsa* (Fig 3). Our SEM study indicates that the single LM small *Gephyrocapsa* is indeed composed by several species populations. The widely documented LM FCO of small *Gephyrocapsa* is associated with the exceptional evolutionary radiation of *Gephyrocapsa* species. Results from this study also suggest that behind other LM reticulofenestrid size-defined group, many species may be hidden. This has significant implication for paleobiology-related studies.

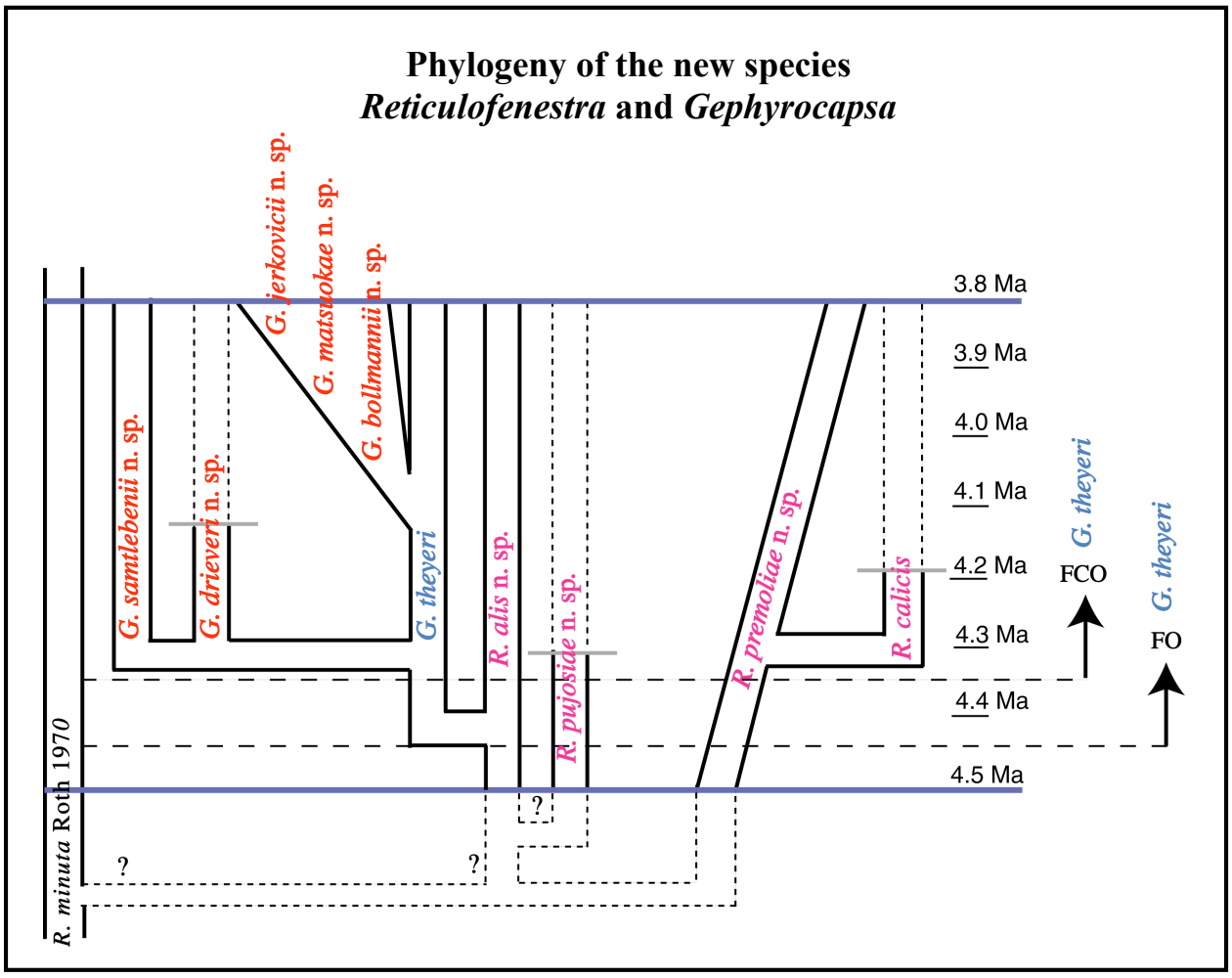

Fig. 3. Phylogeny of *Reticulofenesta* and *Gephyrocapsa* new species obtained by this thesis. The two lineages likely diverged from *R. minuta* (Roth, 1970). The range of species is indicated by solid bars. Dashed bars indicates possible range. This thesis focused on the last 4.5 Ma - 3.8 Ma, therefore further studies are needed in order to establish the exact range of the new species.

G. samtlebenii n. sp. and *G. drieveri* n. sp. evolved from *G. theyeri* at about 4.3 Ma, during an initial evolutionary radiation. Initial radiation is followed by other evolutionary events (e.g. occurrence of *G. bollmannii* n. sp., *G. matsuokae* n. sp.) suggesting a pattern of continuous morphological evolution of the plexus. Evolution in this group of coccolithophore appears to be very fast and species may suffer frequent extinction as suggested by the short occurrence of *R. calicis* (150 kys, Chapter 2 and Chapter 3), which first occurred close to the FCO of *G. theyeri* (4.33 Ma and 4.35 Ma, respectively, Chapter 3 and Chapter 4).

The fossil record of coccolithophores is characterised by a complex biodiversity (Chapters 2-4), which is closely similar to that of modern plankton discovered by molecular genetic studies (e.g. de Vargas et al. 2004). Thus, the model of complex evolution suggested by molecular genetic studies is confirmed by results of this thesis (Fig. 4).

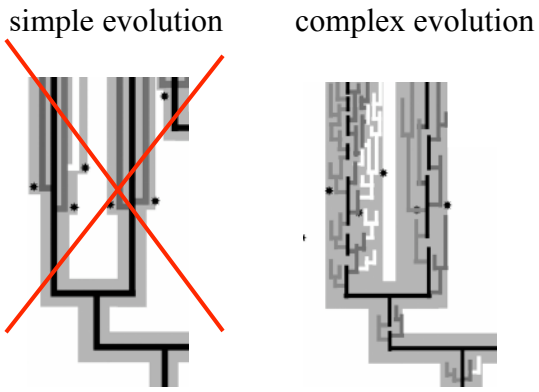

Fig. 4. The complex pattern of diversification of *Gephyrocapsa* species from the stem species *G. theyeri*, supports the model of complex evolution among coccolithophores (redrawn from de Vargas et al., 2004)

The pattern in size variation of small *Gephyrocapsa* is very similar to that recorded in the Atlantic and Mediterranean (by LM) by previous authors (e.g. Driever, 1988). This suggests basin-wide occurrence of the same populations and supports sympatry as an explanation of speciation. Paleofluxes patterns of small *Gephyrocapsa* closely resemble that recorded by low-resolution LM studies and suggest a link between paleoecology and species-level evolution.

The pattern of size variation of small *Gephyrocapsa* and the occurrence of larger populations close to the end of the radiative cycle (Fig. 5), matches the pattern of cyclic size variation of *Gephyrocapsa* in the Quaternary (Matsuoka and Okada, 1990; Matsuoka and Fujoka, 1992). This suggests that the latter reflects evolutionary events.

6.2. Abiotic forcing

The first diversification within *Reticulofenestra* was observed before 4.5 Ma. The presence of variable extensions along the central area of the coccoliths suggests the presence of different species (*R. alis* n. sp., *R. pujosiae* n. sp., and *R. premoliae* n. sp.) all descending from the ubiquitous long-ranging and widespread species *R. minuta* (Fig. 3). These species occurred in the Caribbean during a phase of very stable oceanographic conditions as indicated by the $\partial^{18}O$ and Mg/Ca-values of surface dwelling foraminifera (Steph et al., in revision; Groeneveld et al., submitted) and by high abundances of *F. profunda*, a well established proxy for overall productivity (Groeneveld et al., submitted), (Fig. 5). The evolutionary development became punctuated around 4.35 Ma when another new *Reticulofenestra* species (*R. calicis*) evolved (Crudeli and Kinkel, 2004). In the same interval, reticulofenestrid coccoliths occur with elements forming a bridge spanning the central area, the characteristic feature of the genus *Gephyrocapsa*. Successive to the first evolved *Gephyrocapsa* species *G. theyeri* (4.45 Ma), during an initial radiation, *G. samtlebenii* n. sp. and *G. drieveri* n. sp. (about 4.3 Ma) evolved. These events were followed by the evolution of *G. bollmannii* n. sp., *G. matsuokae* n. sp. and *G. jerkovicii* n. sp.

During the early phase of *Gephyrocapsa* evolution (4.35 to 4 Ma), primary productivity was low. The overall size in *Gephyrocapsa* markedly increased around 4 Ma in correspondence with an increase in

productivity. Morphometry and SEM observations support the evolution of *G. jerkovicii* n. sp. as an example of large-size *Gephyrocapsa* species. The size increase and origin of *G. jerkovicii* n. sp in the Caribbean is coeval with the pronounced increase in $\partial^{18}O$ and Mg/Ca-values of surface dwelling foraminifers and with the onset of the 23-kyr cyclicity documented by the relative abundance of *F. profunda* (Fig. 5). This observation points to an environmental forcing of this speciation event in the Caribbean, which was triggered by the paleoceanographic changes associated with the restriction in surface water circulation between the Pacific and Caribbean (Groeneveld et al., submitted; Steph et al., in revision). The initial radiation of the plexus occurred, however, during more stable oceanographic conditions. This suggests that intrinsic processes may trigger species evolution. We cannot exclude, however, that significant paleoceanographic changes occurred well before the investigated interval and possibly played a role on the earlier reticulofenestrid diversification.

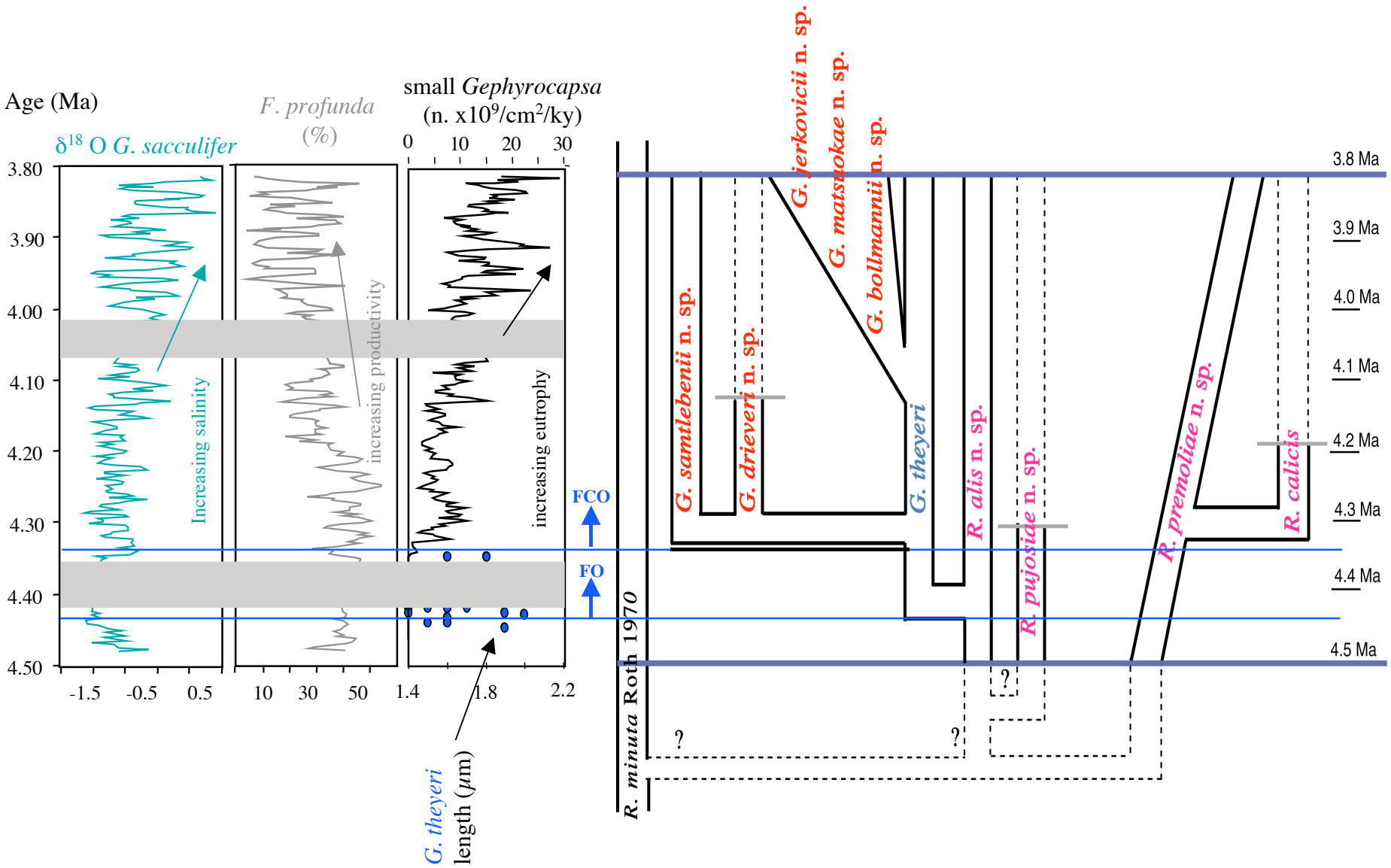

Fig. 5.Comparison between abiotic proxies and the evolutionary scheme of the new *Reticulofenestra* and *Gephyrocapsa* species. δ^{18}O *G. sacculifer* (Steph et al., in revision), % *F. profunda* (Groeneveld et al., submitted), (n. x10^9/cm^2/ky) small *Gephyrocapsa* (Crudeli et al., in prep.)

6.3. Comparison of Caribbean Site 1000A and Pacific Site 1241

Analysis was focused on samples recording the FCO of small *Gephyrocaps*a. Comparing Caribbean Site 1000A and Pacific Site 1241, we recognised *G. theyeri* as the single species occurring in the early record with a FO to be nearly synchronous on both side of the Central American Seaway (Steph et al., in revision; Tiedemann et al., submitted).

In particular, the highly synchronous FO of *R. calicis* and *G. theyeri,* within 20 kyrs in the Caribbean and Eastern Equatorial Pacific indicates that these are sympatric speciation events in the still well connected ocean basins. All new *Reticulofenestra* species evolved prior to the closure in both ocean basins. The syncronous disappearance of *R. calicis*, an extremely short-lived species, in both basins (as it is its FO) makes this new species an ideal biostratigraphic marker for the early Pliocene.

Short key intervals were investigated in detail by morphometry. *G. jerkovicii* n. sp. is mainly responsible for the size increase of the population after about 4 Ma (Hole 1000A). At Site 1241, the size increase occurs several ten thousand years later than in the Caribbean. It is not clear to what extend restriction of surface water exchange between the two ocean basins led to a hampered plankton dispersal, or whether the increasingly pronounced ecological differences between the two areas promoted the diachrony in the occurrence of the larger populations. It seems likely that the diachrony is related to ecophenotypic variation. So far there are no data available for allopatric and/or diachronous speciation events that took place after the final closure of the Gateway. It may be possible that these occurred during the final closure phases of the Late Pliocene and Quaternary. Moreover, it must be considered that ecological and preservational factors can complicate such studies. We cannot rule out, however, that the low diversity of *Gephyrocapsa* species in the Pacific is a result of reduced preservation of fine-scale morphological features in comparison with Caribbean coccoliths.

References

Crudeli, D. and Kinkel, H. 2004. *Reticulofenestra calicis* n. sp., an unusual small reticulofenestrid coccolith from the Lower Pliocene of the South Caribbean Sea. Micropaleontology, 50, 4, 369-379.

Driever, B.W.M. 1988. Calcareous nannofossils biostratigraphy and paleoenvironmental interpretation of the Mediterranean Pliocene. Utrecht Micropaleontol. Bull., 36, 1-245.

Geisen, M., Young, J.R., Probert, I., Sáez, A.G., Baumann, K.-H., Bollmann, J., Cros, L., Devargas, C., Medlin, L.K. and Sprengel, C. 2004. Species level variation in coccolithophores. In: Thierstein, H.R., Young, J.R. (Eds.), Coccolithophores - From molecular processes to global impact. Springer, 327-366.

Groeneveld, J., Nürnberg, D., Steph, S., Tiedemann, R., Reichart, G.J., Reuning, L. and Crudeli, D. (submitted). Increasing Mg/Ca SSTs for the Pliocene Caribbean: Western Atlantic Warm Pool formation, salinity influence or diagenetical overprint? Geochem. Geophys. Geosyst.

Kameo, K. and Sato, T. 2000. Biogeography of Neogene calcareous nannofossils in the Caribbean and the eastern equatorial Pacific-floral response to the emergence of the Isthmus of Panama. Mar.Micropaleontol., 39, 201-218.

Matsuoka, H., Okada, H. 1990. Time-progressive morphometric changes of the genus *Gephyrocapsa* in the Quaternary sequence of the tropical Indian Ocean, Site 709. In: Duncan, R.A., Backman, J. et al (Eds.), Proc. ODP Sci. Results, 115, 255-270.

Matsuoka, H., Fujioka, K. 1992. Morphometric changes of the genus *Gephyrocapsa* at Site 790, subtropical Pacific Ocean. In: Taylor, B., Fujioka, K. et al. (Eds.), Proc. ODP Sci. Results, 126, 263-269.

Okada, H. 2000. Neogene and Quaternary calcareous nannofossils from the Blake Ridge, Sites 994, 995, and 997. Proc. ODP Sci. Results, 164, 331-345.

Sáez, A.G., Probert, I., Young, J.R. and Medlin, L.K. 2004. A review of the phylogeny of the Haptophyta. In: Thierstein, H.R. and Young, J.R. (Eds.), Coccolithophores - From molecular processes to global impact. Springer, 251-270.

Steph, S., Tiedemann, R., Groeneveld, J., Nürnberg, D., Reuning, R. and Haug, G. (in revision). Changes in Caribbean surface hydrography during the Pliocene shoaling of the Central American Seaway. Paleoceanography.

Tiedemann, R., Sarnthein, M. and Shackleton, N. J. 1994. Astronomic timescale for the Pliocene Atlantic $\delta^{18}O$ and dust flux records of Ocean Drilling Program Site 659. Paleoceanography, 9, 619-638.

Tiedemann, R., and Franz, S.O. 1997. Water circulation, chemistry, and terrigenous sediment supply in the Equatorial Atlantic during the Pliocene, 3.3-2.6 Ma and 5-4.5 Ma. Proc. ODP Sci. Results, 154, 299-318.

Tiedemann, R., Sturm, A., Steph, S., Lund, S.P., and J. Stoner (submitted). Astronomically calibrated timescales from 6-2.5 Ma and benthic isotope stratigraphies of Sites 1236, 1237, 1239, and 1241. ODP Sci. Res. 202.

de Vargas, C., Sáez, A.G., Medlin, L.K. and Thierstein, H.R. 2004. Super-species in the calcareous plankton. In: Thierstein, H.R. and Young, J.R. (Eds.). Coccolithophores - From Molecular Processes to Global Impact. Springer, 271-298.

Young, J.R., Geisen, M. and Probert, I. (in press). A review of selected aspects of coccolithophore biology with implications for palaeobiodiversity estimation. Micropaleontology.

Publications

Crudeli, D., Young J.R. and Kinkel, H. (in preparation). Behind the increase in size of small *Gephyrocapsa*: the earliest adaptive radiation of the populations (early Pliocene, South Caribbean Sea).

Crudeli, D., Young J.R. and Kinkel, H. (in preparation). *Reticulofenestra alis* n. sp., *R. pujosiae* n. sp. and *R. premoliae* n. sp., key-species in the reconstruction of the phylogeny of *Gephyrocapsa theyeri* and *R. calicis* (Coccolithophore, early Pliocene, South Caribbean). Journal of Micropalaeontology.

Groeneveld, J., Nürnberg, D., Steph, S., Tiedemann, R., Reichart, G.J, Reuning, L. and **Crudeli, D.** (in revision). The Pliocene Mg/Ca SST increase in the Caribbean: Western Atlantic Warm Pool formation, salinity influence or diagenetic overprint? Geochemistry, Geophysics, and Geosystems.

Crudeli, D. and Kinkel, H. 2004. *Reticulofenestra calicis* n. sp., an unusual small reticulofenestrid coccolith from the Lower Pliocene of the South Caribbean Sea. Micropaleontology, 50, 4, 369-379.

Principato, M.S., **Crudeli, D.,** Ziveri, P., Slomp, C.P., Corselli, C., Erba, E. and de Lange, G.J. (in press). Phyto- and zooplankton paleofluxes during the deposition of sapropel S1 (eastern Mediterranean): biogenic carbonate preservation and paleoecological implications. Palaeogeography, Palaeoclimatology, Palaeoecology.

Crudeli, D., Young, J.R., Erba, E., Geisen, M., Ziveri, P., de Lange, G.J. and Slomp, C.P. (in press). Fossil record of holococcoliths and selected hetero-holococcolith associations from the Mediterranean (Holocene-late Pleistocene): evaluation of carbonate diagenesis and palaeoecological-palaeoceanographic implications. Palaeogeography, Palaeoclimatology, Palaeoecology.

Crudeli, D., Young, J.R., Erba, E., De Lange, G.J., Henriksen, K., Kinkel, H., Slomp, C.P. and Ziveri, P. 2004. Abnormal carbonate diagenesis in Holocene-Late Pleistocene sapropel - associated sediments from Eastern Mediterranean; evidence from *Emiliania huxleyi* coccolith morphology. In: G. Villa, J.A. Lees, P.R. Bown (Eds.), Calcareous nannofossil palaeoecology and palaeocenographic reconstructions. Marine Micropaleontology, 52/1-4, 217-240.

Thomson, J., **Crudeli, D.,** De Lange, G.J., Slomp, C.P., Erba, E., Corselli, C. and Calvert, S.E. 2004. *Florisphaera profunda* and the origin and diagenesis of carbonate phases in eastern Mediterranean sapropel units. Paleoceanography, 19, PA3003, 10.1029/2003PA000976.

Crudeli, D. and Young, J.R. 2003. SEM-LM study of holococcoliths preserved in eastern Mediterranean sediments (Holocene/Late Pleistocene). Journal of Nannoplankton Research, 25, 39-50.

Corselli, C., Principato, M. S., Maffioli, P., **Crudeli, D.** 2002. Changes in planktonic assemblages during sapropel S5 deposition: Evidence from Urania Basin area, eastern Mediterranean. Paleoceanography 17, 3, 1029, 10.1029/2000PA000536.

Curriculum vitae

Name and surname:	DANIELA CRUDELI
Place and date of birth:	Lugano, Switzerland, 1st April 1969
Nationality:	Italian
Permanent address:	Via Fusgine, 11 23030 S. Antonio Valfurva (Sondrio), Italy
Phone:	+39 02 66100770 – mobile phone: +39 340 2637902
Work address:	Inst. für Geowissenschaften, Christian Albrechts Universität Kiel, Ludewig-Meyn-str.10 D 24098, Kiel.
Phone:	++49 0431 8801628 Fax: ++49 0431 8805557
E-mail:	danielacrudeli@tiscali.it

Education: July 1988, scientific school leaving examination, Bormio, Sondrio, Italy

Studies: November 1988 - July 1996: master's degree in Geosciences, Dept. of Earth Sciences, University of Milan, Italy
Title of the thesis, Lithostratigraphy and biostratigraphy of the Cretaceous pelagic sedimentary record of the Gargano area (Southern Italy)
Title of practical apprenticeship thesis, Falda Ortles stratigraphy (Austroalpino superiore); M. Reit-Valle del Braulio (northern Italy)

Post-graduate research assistantat
October-December 1996, planktonic foraminifera analyses from ODP samples, Dept. of Earth Sciences, University of Milan

April-July 1997, planktonic foraminifera analyses from the Cismon core, Dept. of Earth Sciences, University of Milan

January 1998, assistant to Prof. T.D.Herbert (Brown University) on chemical-physical analysis of the Cismon core, Dept. of Earth Sciences, University of Milan

March 1998 – March 2001, fellowship within the S.A.P. (Sapropels And Paleoceanography) MAS3-CT97-0137 EU project, Dept. of Earth Sciences, University of Milan

Ph.D. studies
November 2000 - November 2001, Dept. of Earth Sciences, University of Milan
Title of the thesis, Mediterranean Pleistocene palaeoceanography based on calcareous nannofossils

November 2001 – July 2005, Institute of Geosciences, University of Kiel, Germany
Title of the thesis, Early Pliocene evolution of coccolithophores in the Caribbean Sea: Taxonomy, biostratigraphy, paleoecology and paleoceanography – supervisor, Prof. Dr. Priska Schäfer and PD Dr. Mara Weinelt

Studies abroad - June 2001, Taxonomic studies of Holocene calcareous nannofossils - Natural History Museum, London, UK - supervisor, Dr. J.R. Young - SYS-RESOURCE, an Access to Research Infrastructures project of the EU-IHP Program

Cruises, 1998 RV Urania Napoli-Bari (10-23/12/1998) - 1999 RV Logachev Antalya-Catania (18-08/16-09-1999), 2000 RV Pelagia El Cairo-Algeciras (06-05/01-06-2000)

Acknowledgements

I warmly thank my supervisor Prof. Dr. Priska Schäfer for the opportunity to carry out my thesis within the Paleontology Department. My gratitude goes to her and PD Dr. Mara Weinelt for their efforts in refereeing this thesis. Special thanks go to, PD. Dr. Dirk Nürnberg, Prof. Dr. Wolfgang Kuhnt, Prof. Dr. Ralph Schneider, Prof Dr. Karl Stattegger for being part of the disputation committee.

I specially thank Dr. Hanno Kinkel who gave me the opportunity to start PhD studies, that means to carry out fascinating scientific research. I thank Hanno for scientific discussion, but also for stopping me to look too long at small coccos at the scanning electron microscope and for the freedom he gave me in the choice of the approach used to explore aspects of coccolithophores evolution. My previous experience with coccolithophores research was mainly by light microscopy and I vividly recall the time Hanno spent on introducing me to the SEM and filtration techniques. I warmly thank Ute Schuldt of the SEM lab for the time she spent with me in trying to get better focused coccos images (at 20.000x, not really easy!) and in the development of hundred of micrographs. The micrographs in this thesis are a testimony of U. Schuldt and Dr. Beate Bader skills in taking care of the SEM. A special thank to Hauke Dibbern who coated samples for this thesis and to Wolfgang Reimers who taught me how to dry samples and for his help. Chris Jones and Alex Ball from the Electron Microscopy and Mineral Analysis (EMMA) at the Natural History Museum in London are thanked for teaching me (for the second time) how to independently use the field emission SEM. I was at the NHM in May 2001 (Sys Research project) using the FESEM for Holocene coccoliths studies. Dr. Jeremy Young was my mentor during this visit. I am especially grateful to Jeremy - since then he was always enthusiastic in discussing taxonomy and for his help when I get lost in the extreme phenetic variability of forms.
I would like to thank Harald, Jan, Ilka and Sonja for their help in samples filtration, mounting of micrographs, compilation of .xls tables and exotic literature searching. A warmly thank Prof. Dr. Wolfgang Kuhnt - I have stolen more then one time scientific journals from his private collection and Elisabetta Erba (Milano University) - for the time she spent in searching and sending me “old” papers from the University Library.

I thank Prof. Dr. Michael Sarnthein and Dr. Ralf Tiedemann and all the colleagues of the “Forschergruppe 451 - Ocean Gateways” Bettina Kaste, B. Bader, Gretta Bartoli, Jeroen Groeneveld, Jeannette Lezius, Andrea Lorenz, Christian Millo, Martina Blümel, Maia Zuvela, Dr. Andreas Schmittner, Claudia Sieler, Silke Steph, Frank Kösters and Lars Reuning - for the nice working atmosphere, scientific and private discussion and especially for the pizza-beer meeting at Oblomow. I specially thank Bettina and Claudia for help with various German language related problems and Hiroshi Kawamura who was so immediately friendly when I arrived in Kiel.
Ringrazio Stefania, Claudia e Filippo Crudeli per essere stati sempre vicini alla sorellona. Un grazie enorme a Max, mamma Sandra e papa Roberto per il supporto e incoraggiamento datomi in questi anni di studio.

Dedico questa tesi a tutti voi

APPENDICES

Hole 1000A - the appendices A and B contain:

A-(1-15) – From left to right: plots of the length vs. width, length vs. bridge angle, length vs. central area (CA) width per class of bridge angle (1-30°, 31°-60°, 61°-90°) of small *Gephyrocapsa* specimens from samples of cores 16H2 to 14H1 at 10-20 cm resolution (136.43 meters below sea floor (mbsf) to 118.34 mbsf). In plots of length vs. CA width per class of bridge angle, the different symbols represent class of bridge angle.

B-(1-3) – Frequency distribution of the length (interval size 0.2µm) of small *Gephyrocapsa* specimens from samples of cores 16H2 to 14H1 at 10-20 cm resolution (136.43 mbsf to 118.25 mbsf). The number of specimens measured per samples is detailed below.

- 136.43-135.95 mbsf, 10 specimens measured
- 135.85-135.75 mbsf, 30 specimens measured
- 135.65-118.25 mbsf, 50 specimens measured

The age, indicated near plots of selected samples, is from Steph et al. (in revision).

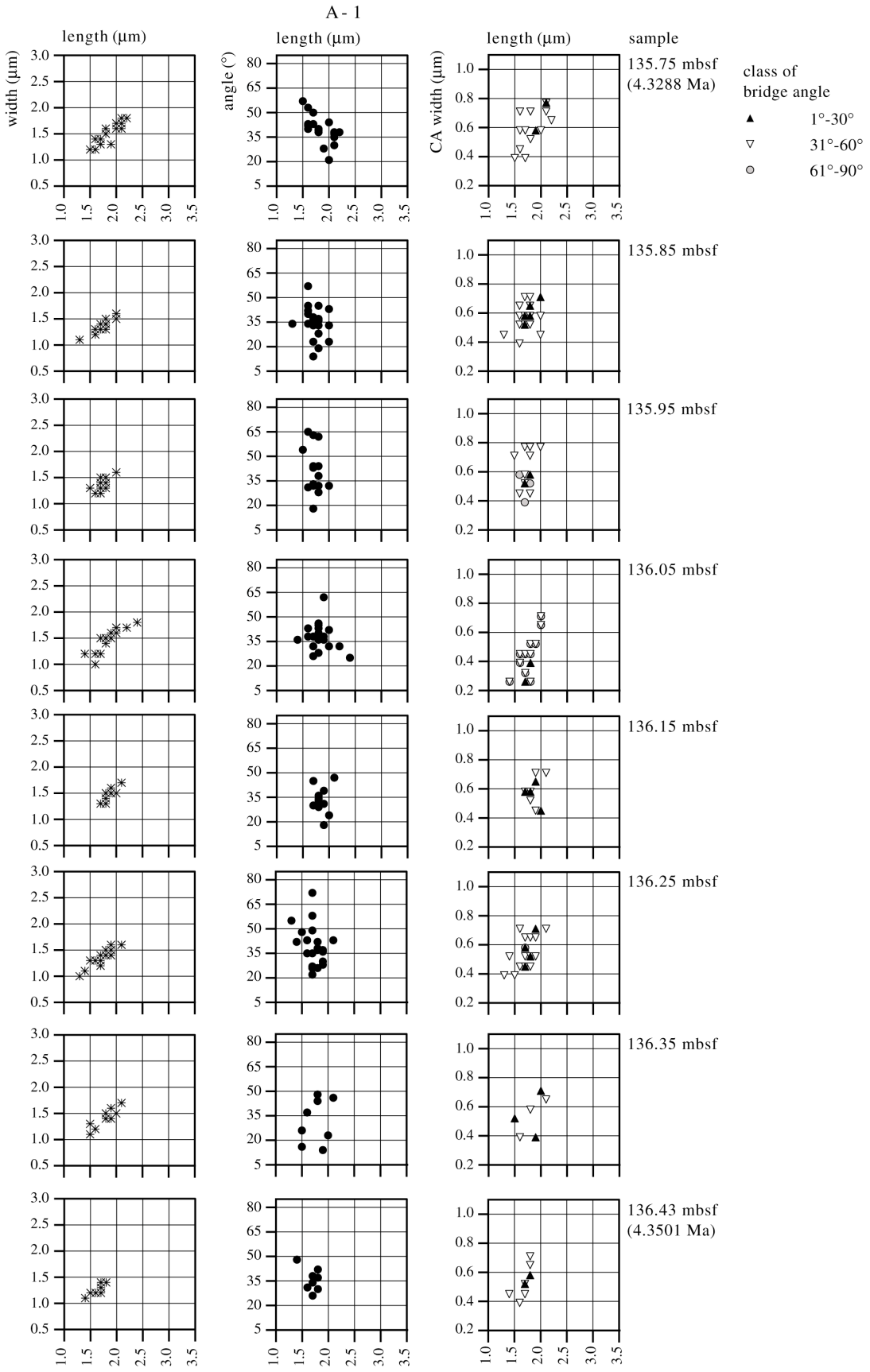
A - 1
length (µm)
width (µm)
length (µm)
angle (°)
length (µm)
CA width (µm)
sample
135.75 mbsf
(4.3288 Ma)
135.85 mbsf
135.95 mbsf
136.05 mbsf
136.15 mbsf
136.25 mbsf
136.35 mbsf
136.43 mbsf
(4.3501 Ma)
class of
bridge angle
1°-30°
31°-60°
61°-90°

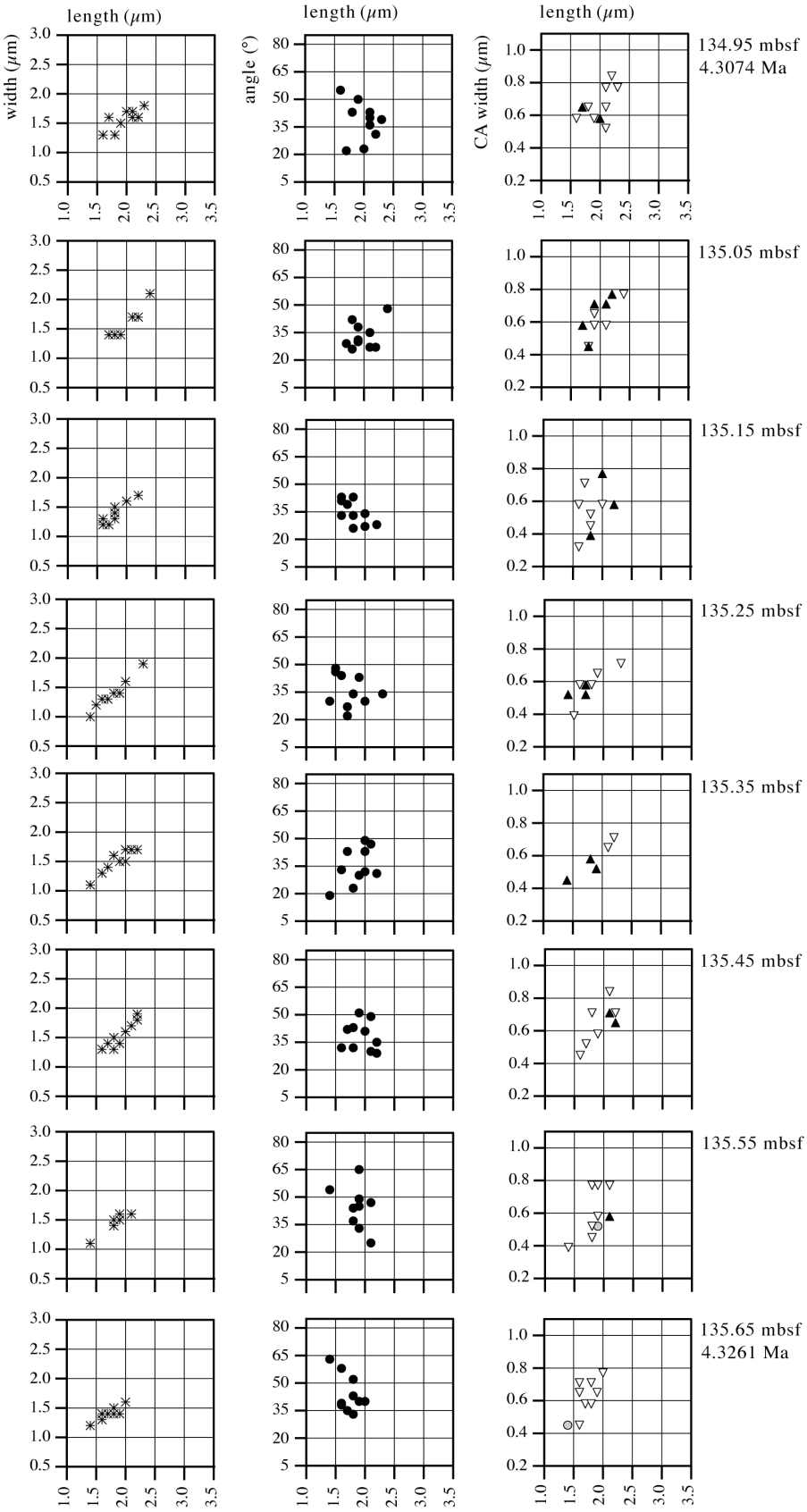
length (μm)
width (μm)
length (μm)
angle (°)
length (μm)
CA width (μm)
134.95 mbsf
4.3074 Ma
135.05 mbsf
135.15 mbsf
135.25 mbsf
135.35 mbsf
135.45 mbsf
135.55 mbsf
135.65 mbsf
4.3261 Ma

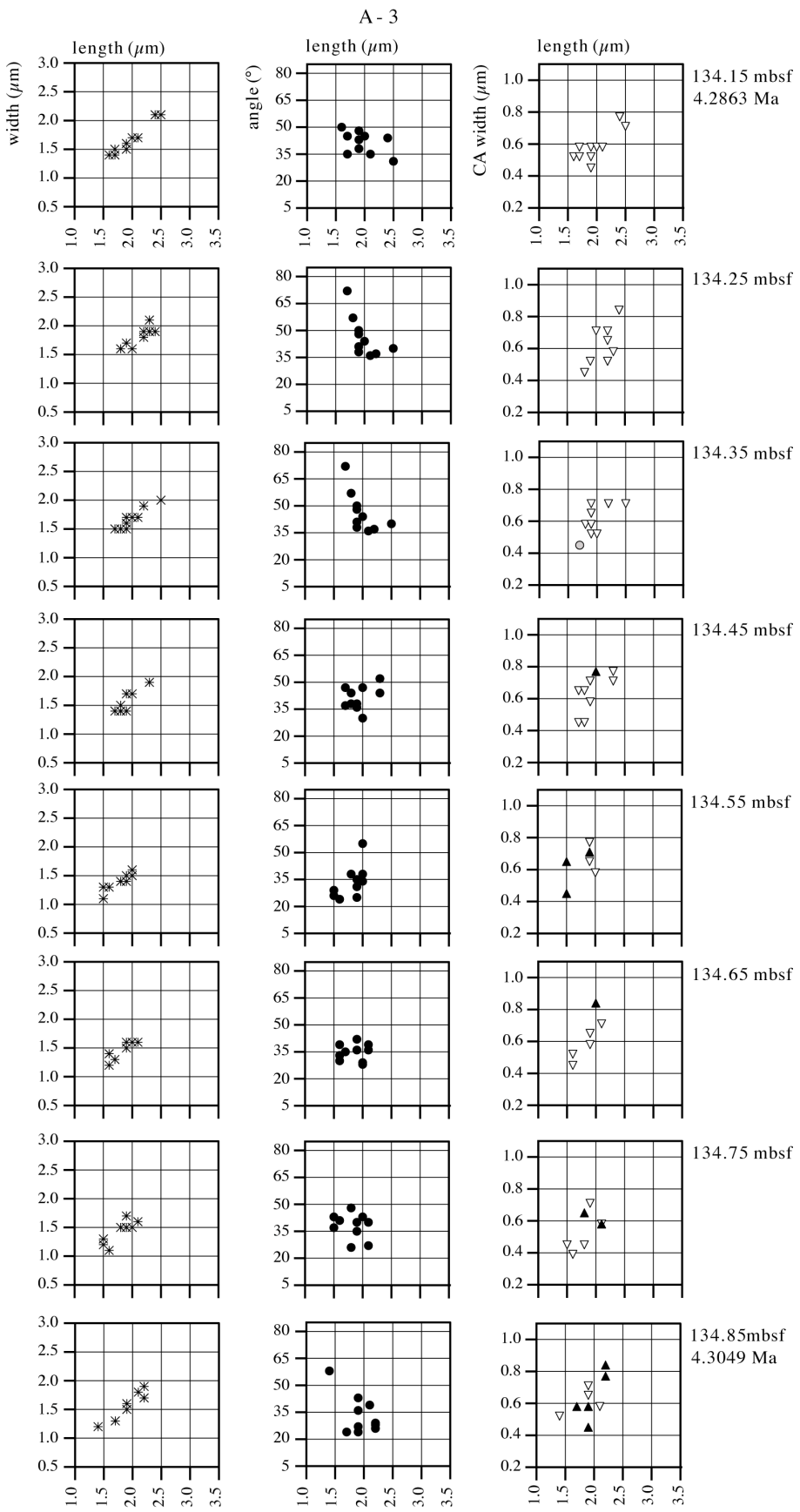
A - 3
length (μm)
width (μm)
length (μm)
angle (°)
length (μm)
CA width (μm)
134.15 mbsf
4.2863 Ma
134.25 mbsf
134.35 mbsf
134.45 mbsf
134.55 mbsf
134.65 mbsf
134.75 mbsf
134.85mbsf
4.3049 Ma

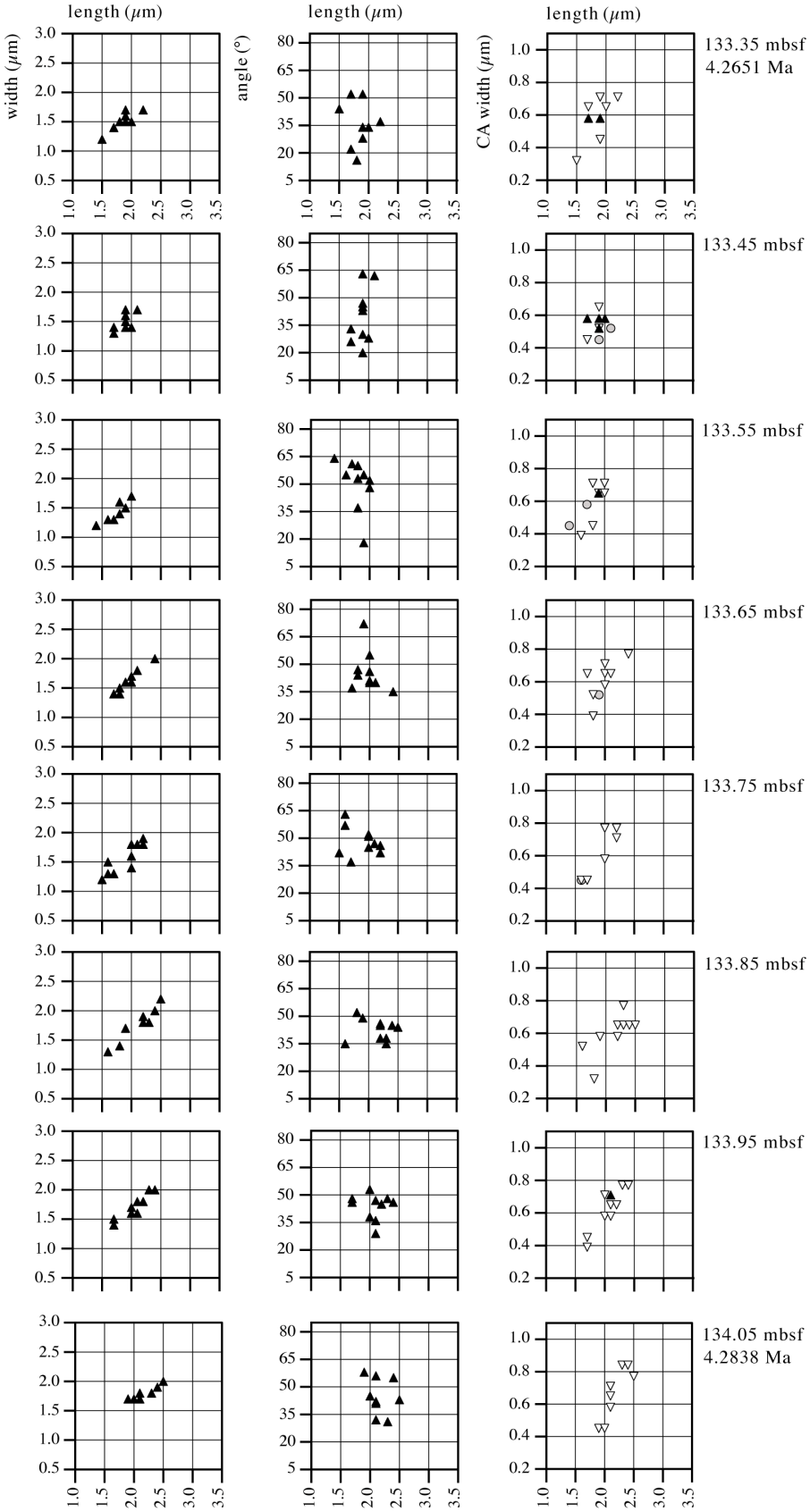
length (μm)
width (μm)
length (μm)
angle (°)
length (μm)
CA width (μm)
133.35 mbsf
4.2651 Ma
133.45 mbsf
133.55 mbsf
133.65 mbsf
133.75 mbsf
133.85 mbsf
133.95 mbsf
134.05 mbsf
4.2838 Ma

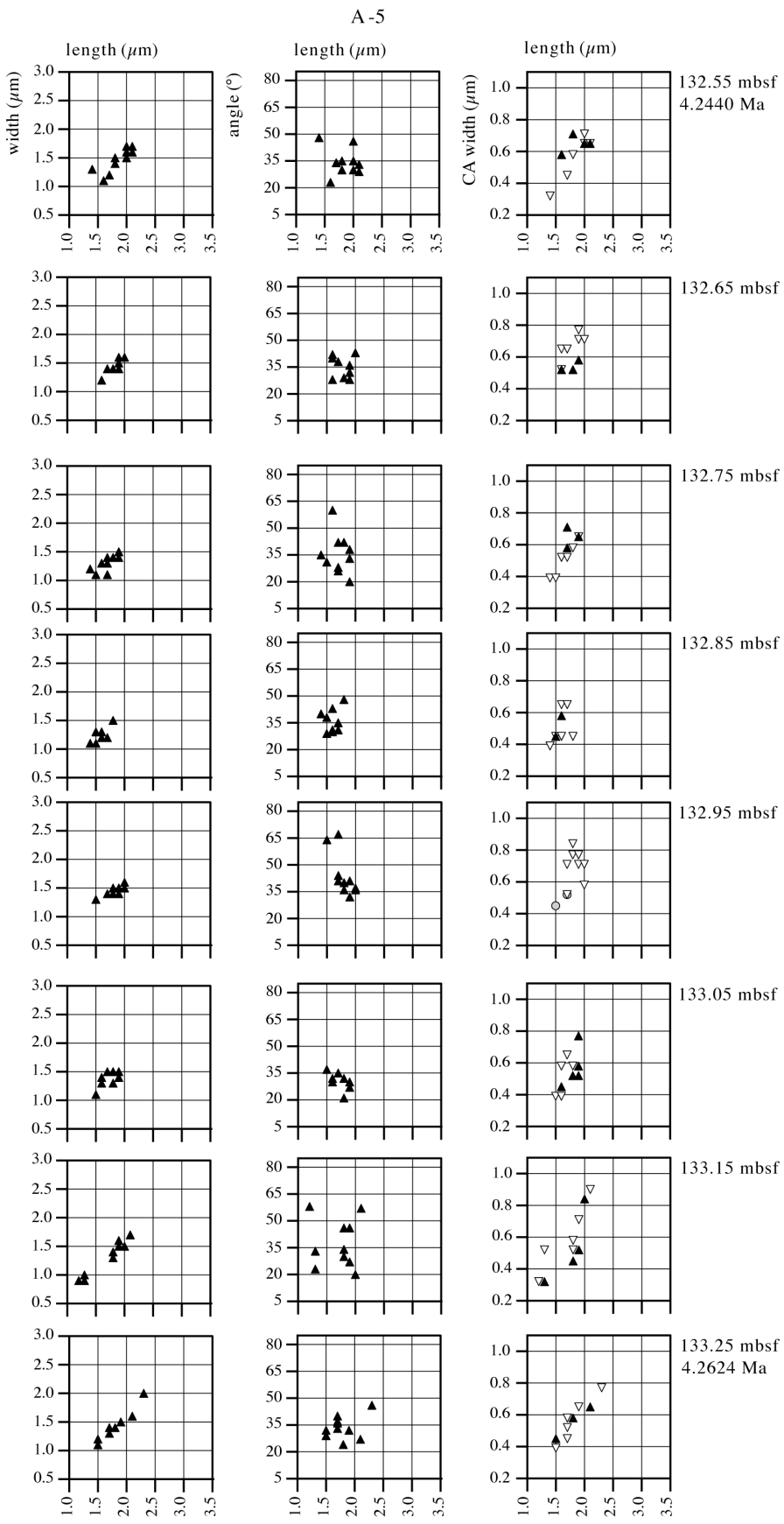
A -5
length (μm)
width (μm)
length (μm)
angle (°)
length (μm)
CA width (μm)
132.55 mbsf
4.2440 Ma
132.65 mbsf
132.75 mbsf
132.85 mbsf
132.95 mbsf
133.05 mbsf
133.15 mbsf
133.25 mbsf
4.2624 Ma

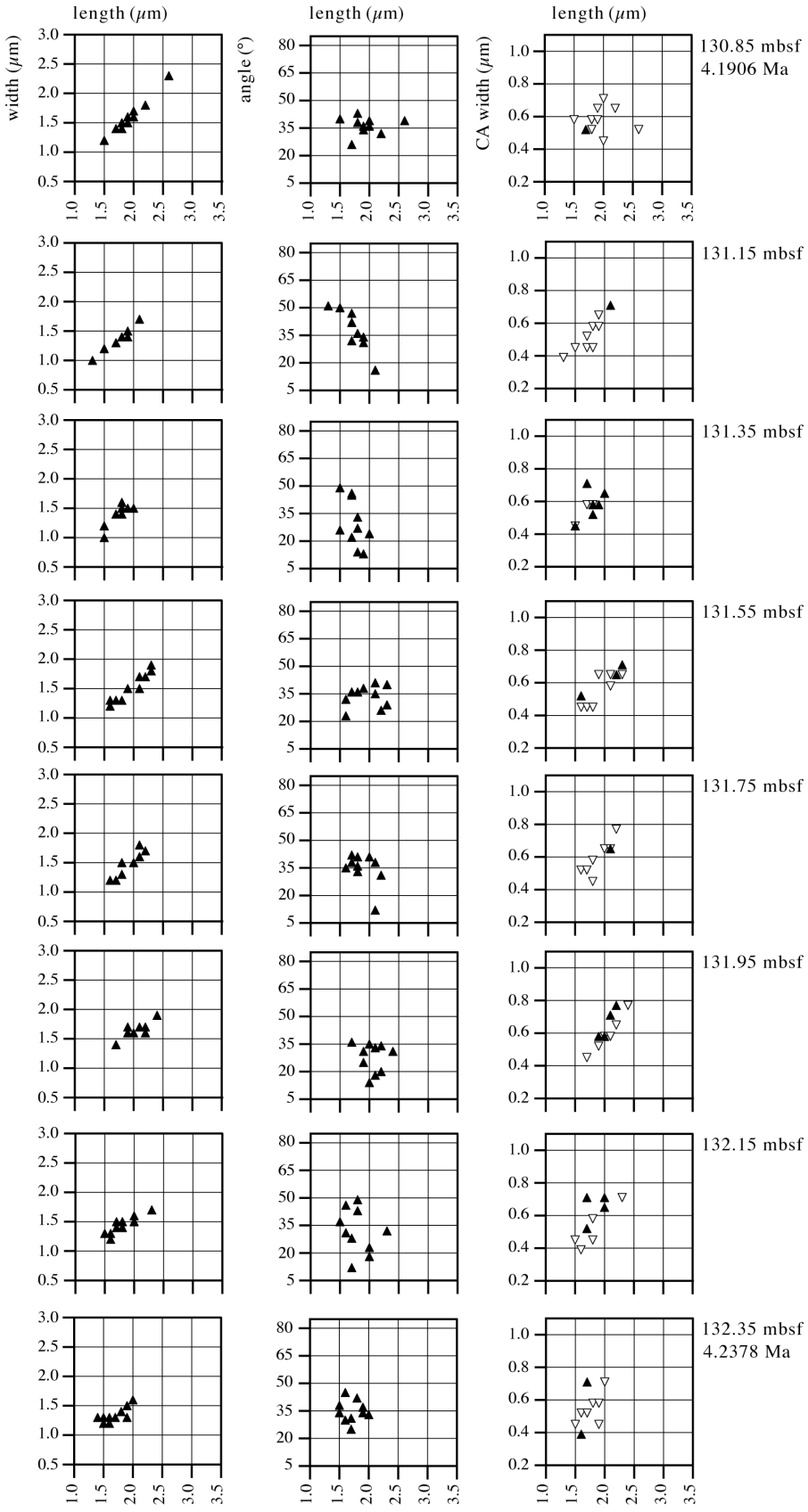
length (μm)
length (μm)
length (μm)
width (μm)
angle (°)
CA width (μm)
130.85 mbsf
4.1906 Ma
131.15 mbsf
131.35 mbsf
131.55 mbsf
131.75 mbsf
131.95 mbsf
132.15 mbsf
132.35 mbsf
4.2378 Ma

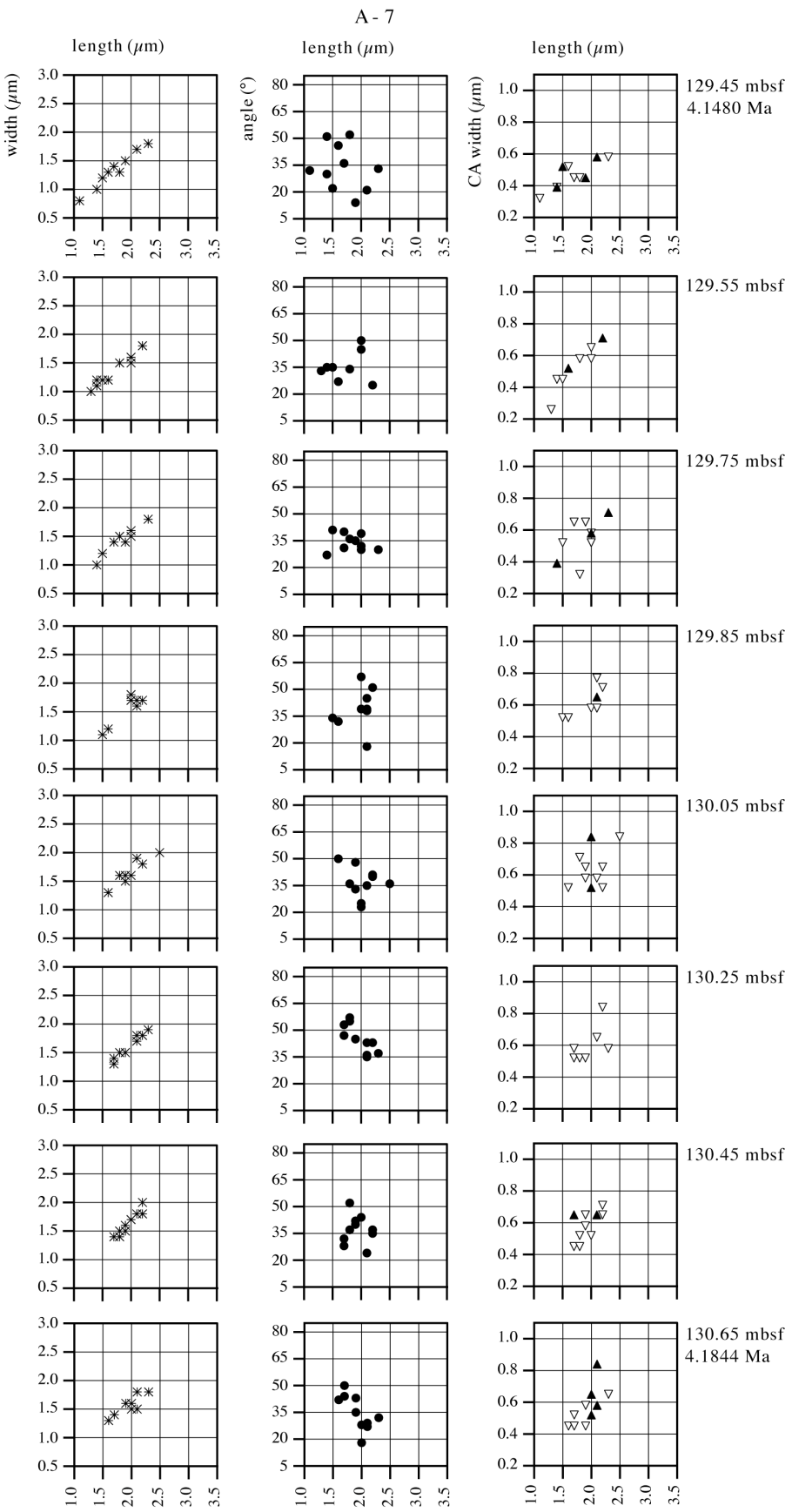
A - 7
length (μm)
length (μm)
length (μm)
width (μm)
angle (°)
CA width (μm)
129.45 mbsf
4.1480 Ma
129.55 mbsf
129.75 mbsf
129.85 mbsf
130.05 mbsf
130.25 mbsf
130.45 mbsf
130.65 mbsf
4.1844 Ma

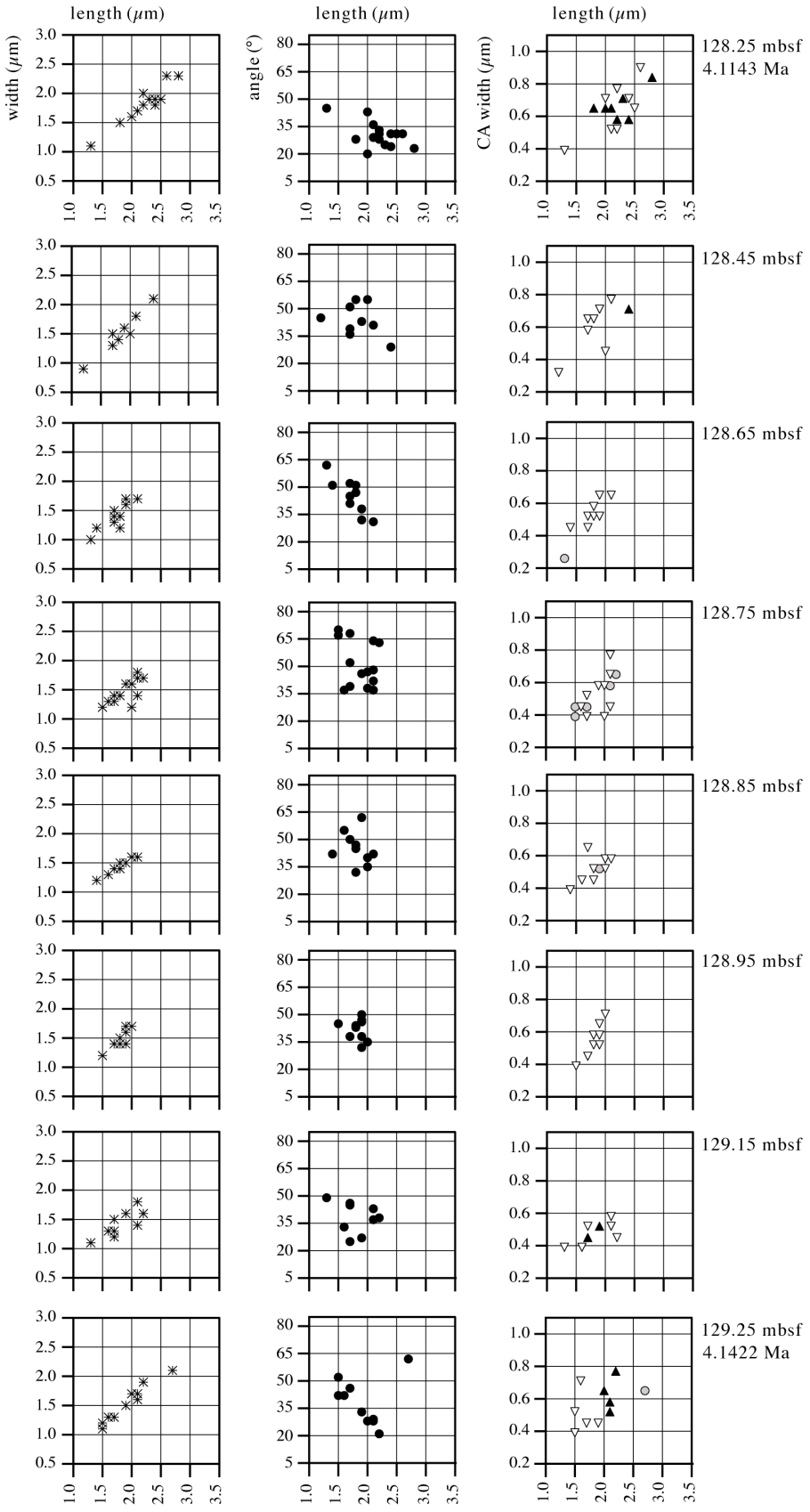
length (μm)
width (μm)
length (μm)
angle (°)
length (μm)
CA width (μm)
128.25 mbsf
4.1143 Ma
128.45 mbsf
128.65 mbsf
128.75 mbsf
128.85 mbsf
128.95 mbsf
129.15 mbsf
129.25 mbsf
4.1422 Ma

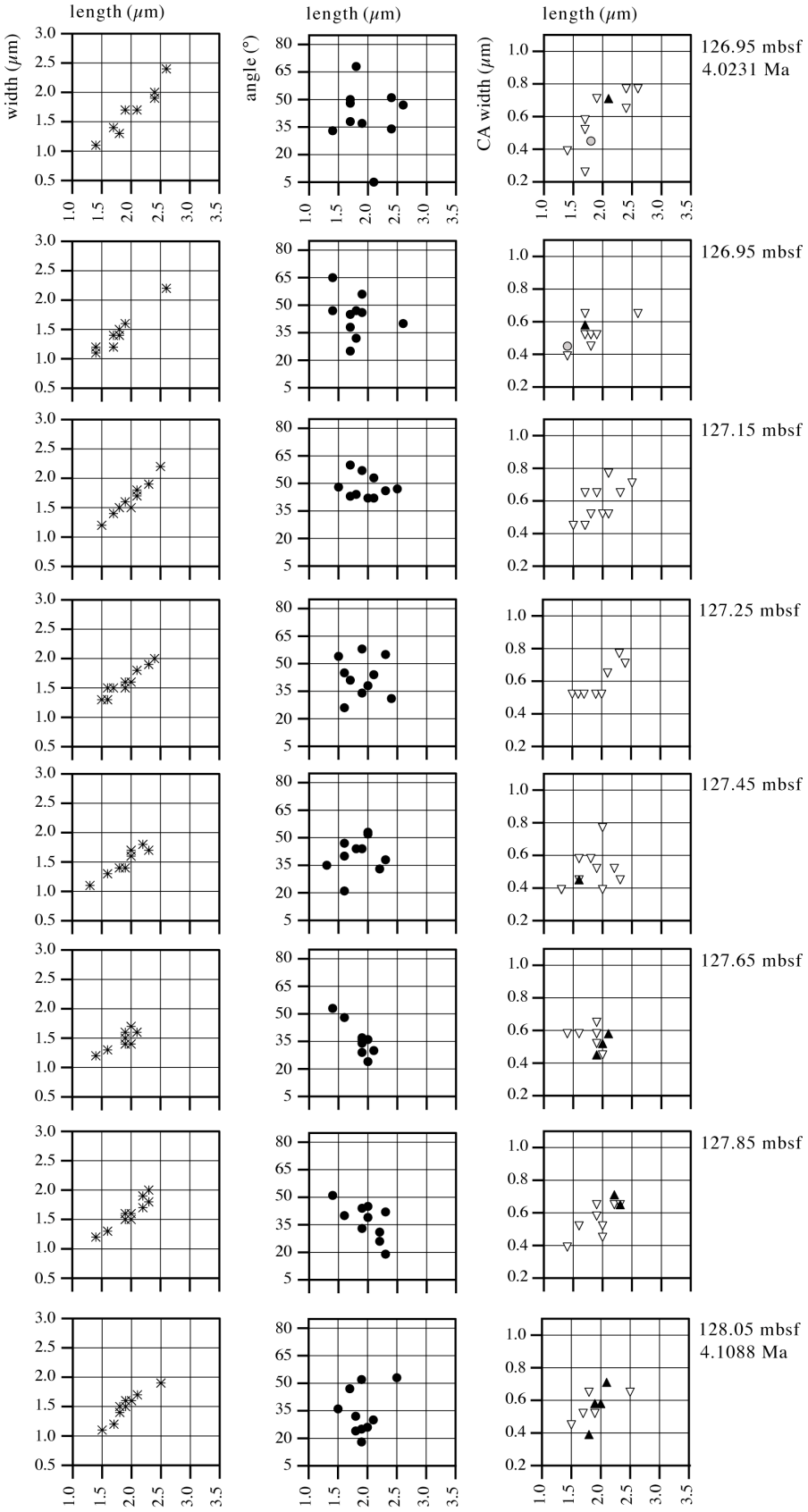
length (μm)
width (μm)
angle (°)
CA width (μm)
126.95 mbsf
4.0231 Ma
126.95 mbsf
127.15 mbsf
127.25 mbsf
127.45 mbsf
127.65 mbsf
127.85 mbsf
128.05 mbsf
4.1088 Ma

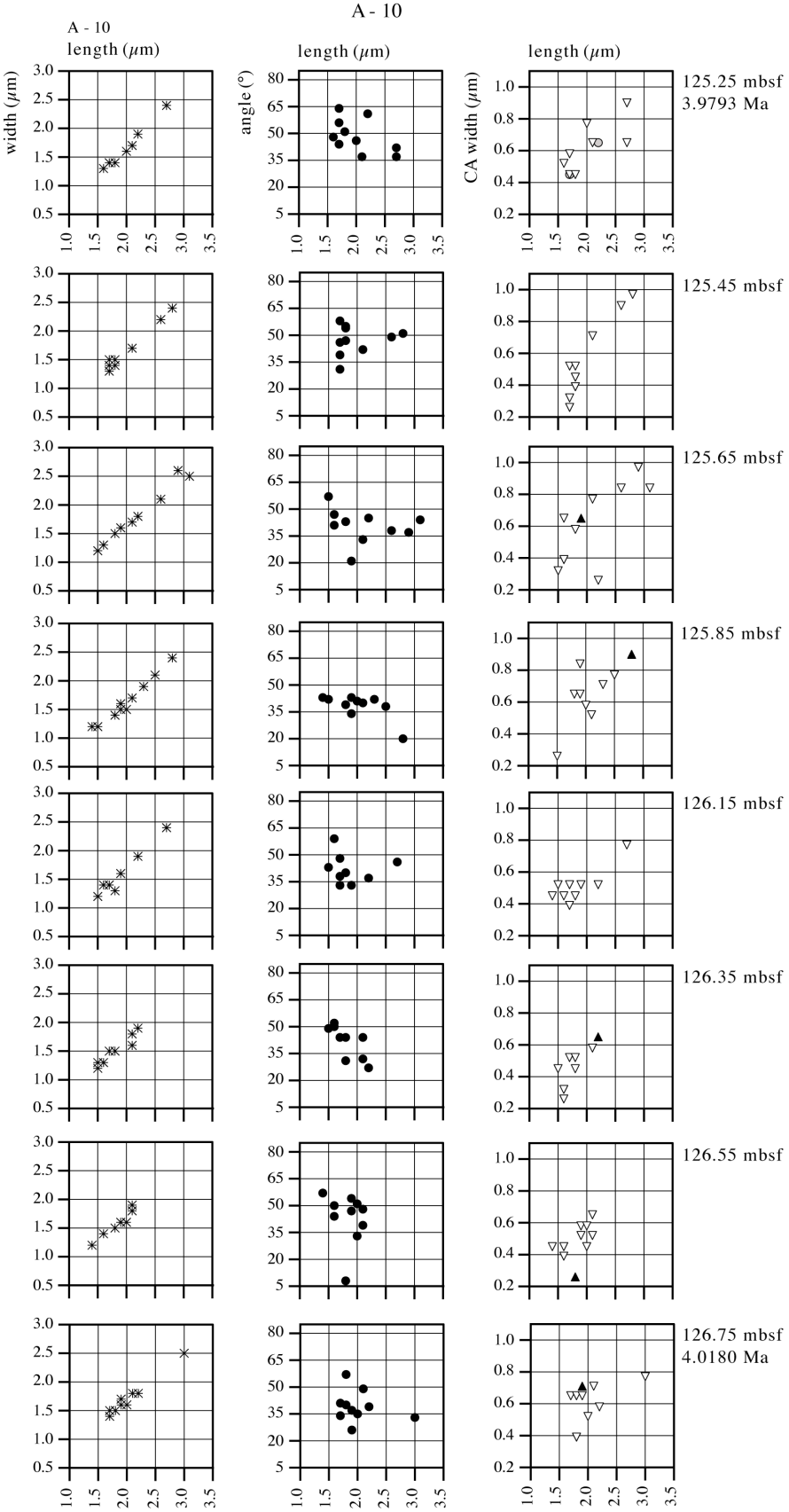
A - 10
A - 10
length (μm)
width (μm)
length (μm)
angle (°)
length (μm)
CA width (μm)
125.25 mbsf
3.9793 Ma
125.45 mbsf
125.65 mbsf
125.85 mbsf
126.15 mbsf
126.35 mbsf
126.55 mbsf
126.75 mbsf
4.0180 Ma

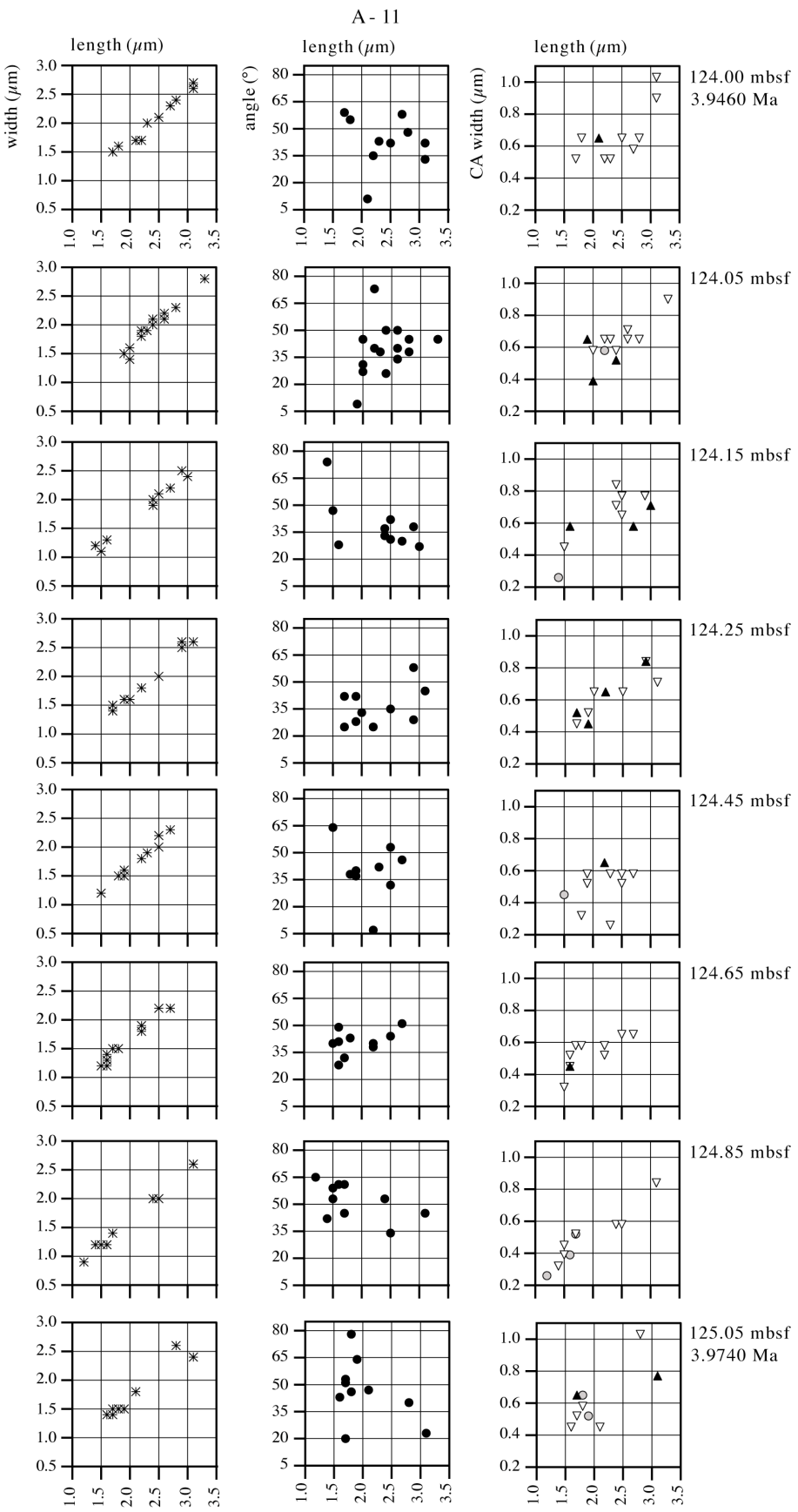
A - 11
length (μm)
length (μm)
length (μm)
width (μm)
angle (°)
CA width (μm)
124.00 mbsf
3.9460 Ma
124.05 mbsf
124.15 mbsf
124.25 mbsf
124.45 mbsf
124.65 mbsf
124.85 mbsf
125.05 mbsf
3.9740 Ma

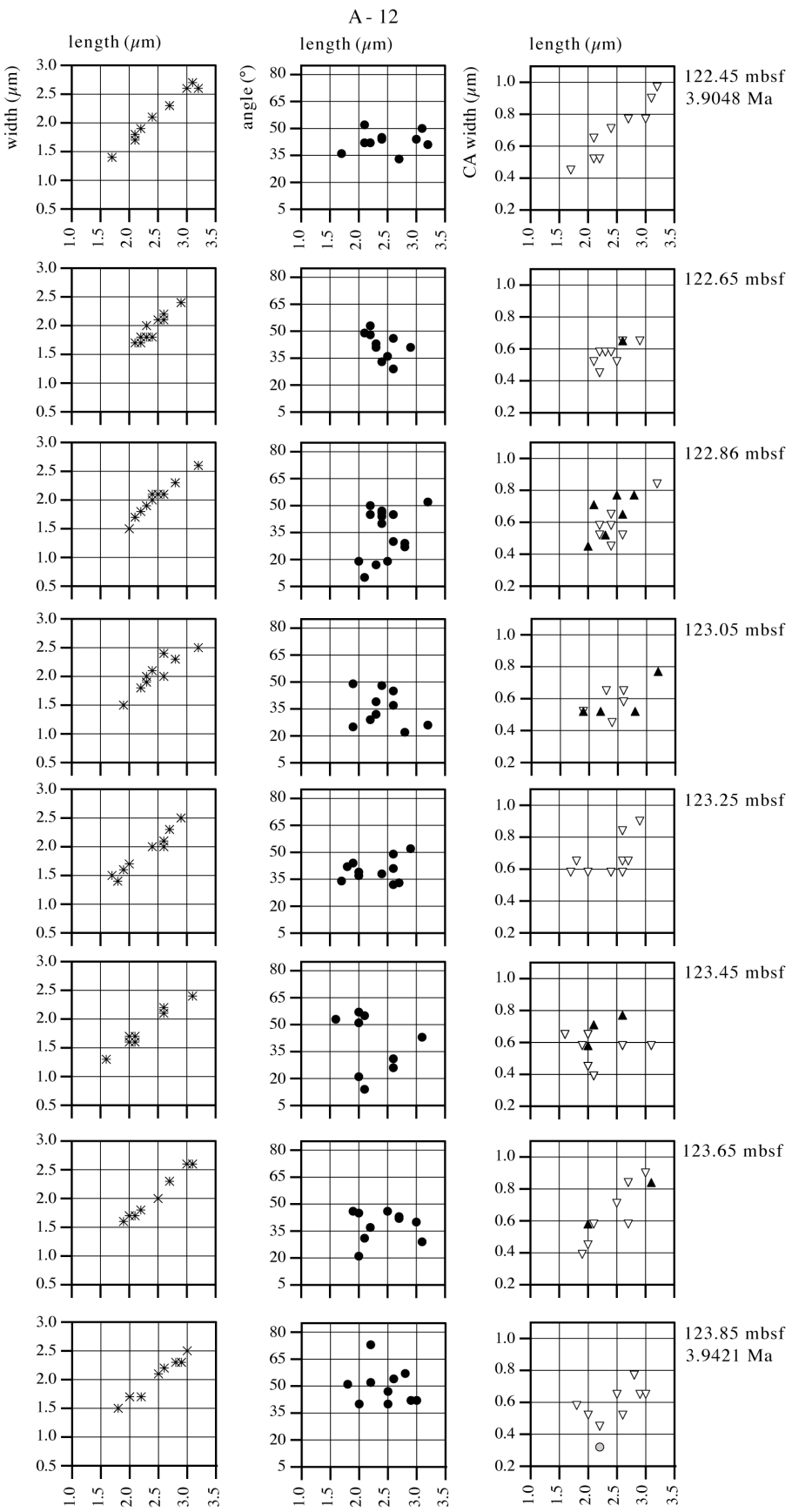
A - 12
length (μm)
width (μm)
length (μm)
angle (°)
length (μm)
CA width (μm)
122.45 mbsf
3.9048 Ma
122.65 mbsf
122.86 mbsf
123.05 mbsf
123.25 mbsf
123.45 mbsf
123.65 mbsf
123.85 mbsf
3.9421 Ma

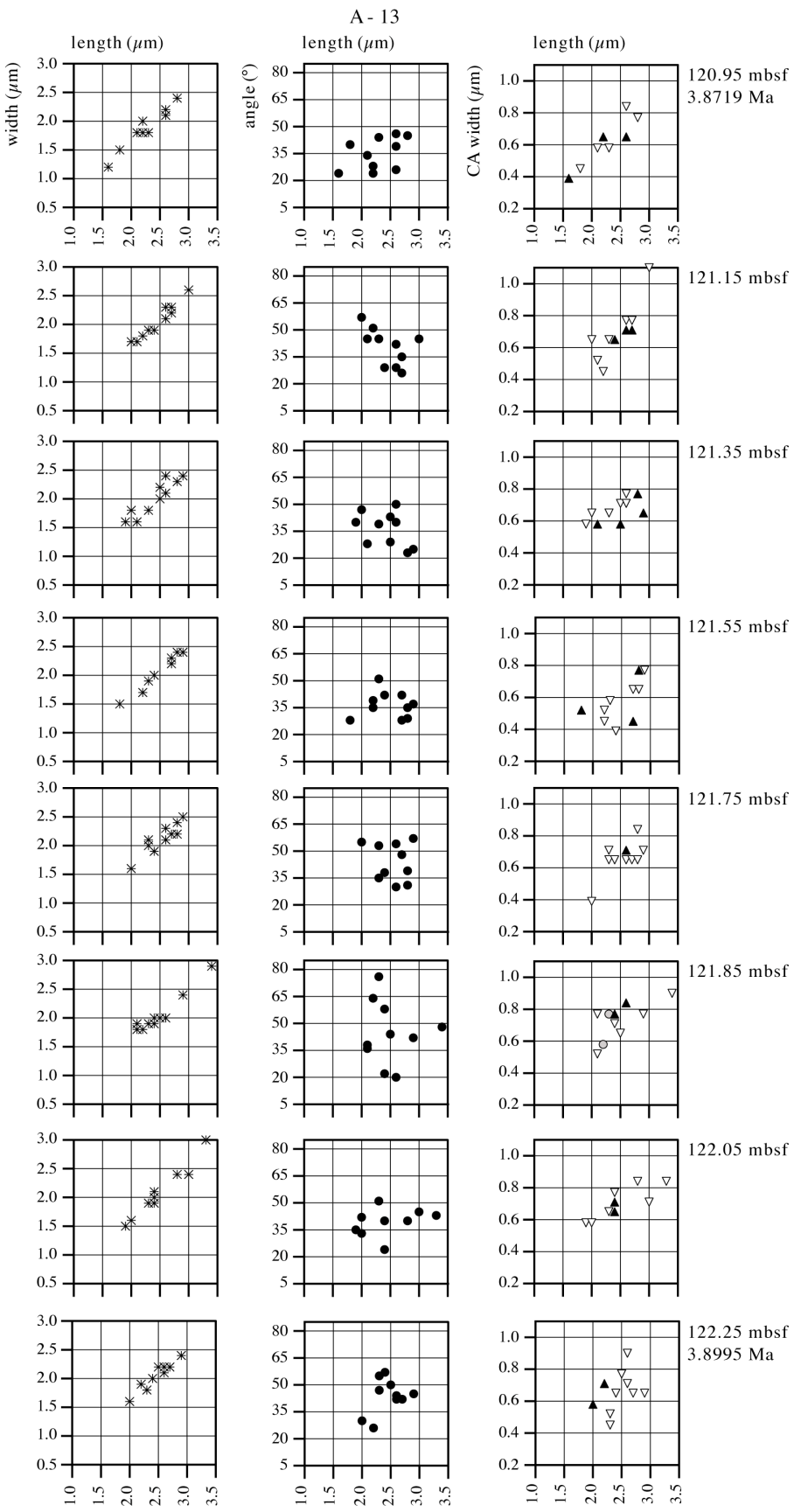
A - 13
length (μm)
width (μm)
angle (°)
CA width (μm)
120.95 mbsf
3.8719 Ma
121.15 mbsf
121.35 mbsf
121.55 mbsf
121.75 mbsf
121.85 mbsf
122.05 mbsf
122.25 mbsf
3.8995 Ma

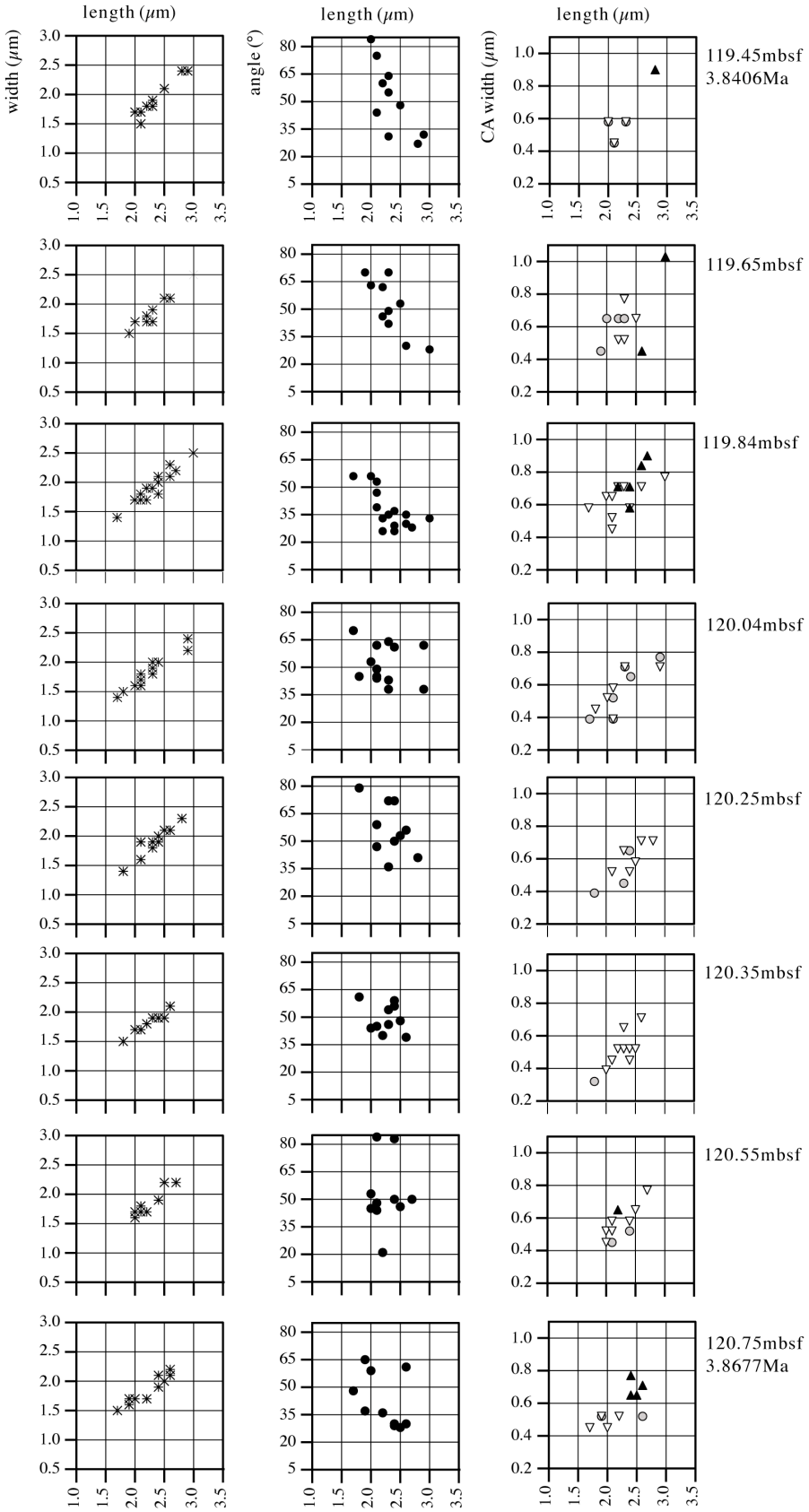
length (μm)
width (μm)
length (μm)
angle (°)
length (μm)
CA width (μm)
119.45mbsf
3.8406Ma
119.65mbsf
119.84mbsf
120.04mbsf
120.25mbsf
120.35mbsf
120.55mbsf
120.75mbsf
3.8677Ma

A - 15

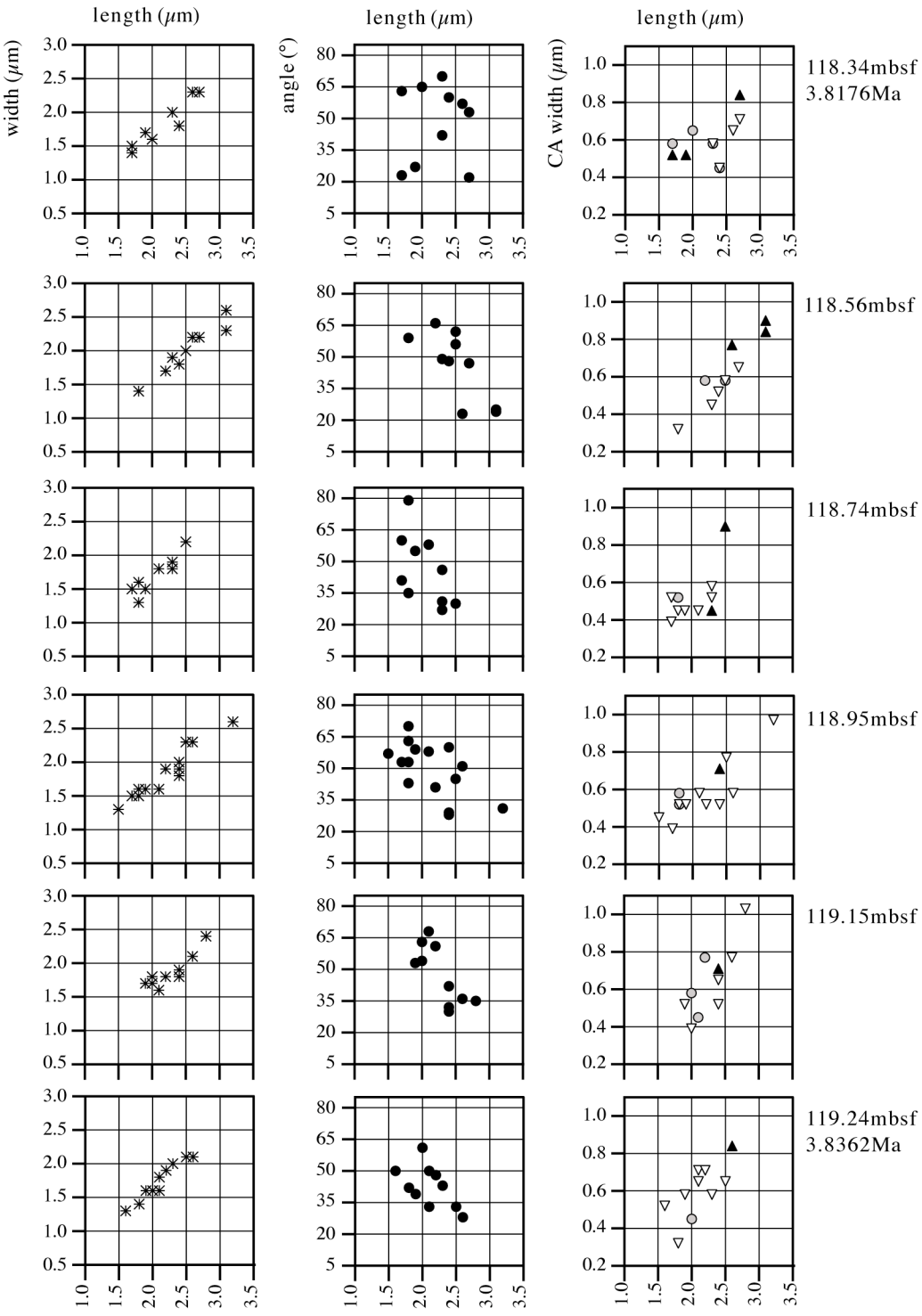
length (μm)
length (μm)
length (μm)
width (μm)
angle (°)
CA width (μm)
118.34mbsf
3.8176Ma
118.56mbsf
118.74mbsf
118.95mbsf
119.15mbsf
119.24mbsf
3.8362Ma

B- 1

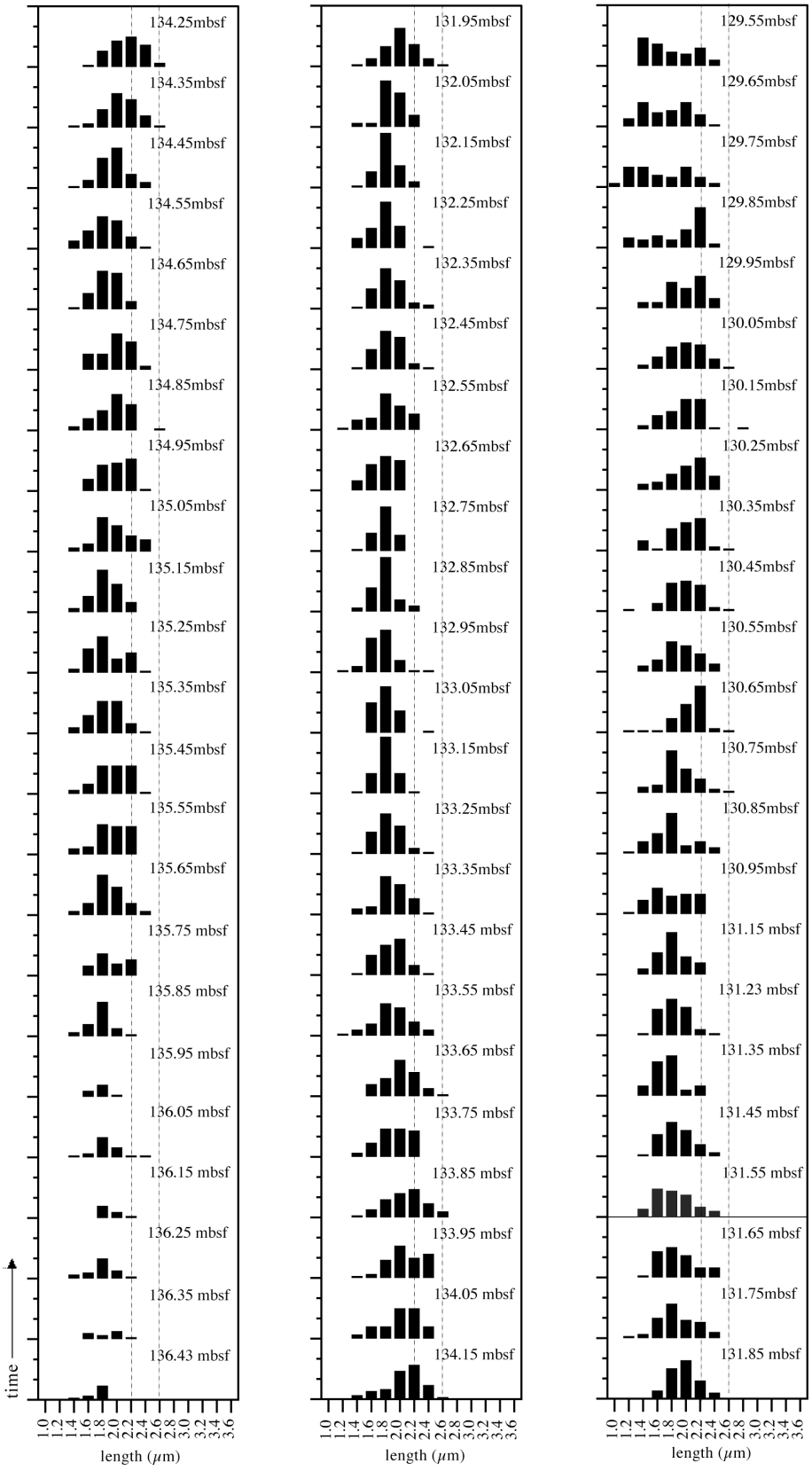
134.25mbsf
134.35mbsf
134.45mbsf
134.55mbsf
134.65mbsf
134.75mbsf
134.85mbsf
134.95mbsf
135.05mbsf
135.15mbsf
135.25mbsf
135.35mbsf
135.45mbsf
135.55mbsf
135.65mbsf
135.75 mbsf
135.85 mbsf
135.95 mbsf
136.05 mbsf
136.15 mbsf
136.25 mbsf
136.35 mbsf
136.43 mbsf
time
1.0 1.2 1.4 1.6 1.8 2.0 2.2 2.4 2.6 2.8 3.0 3.2 3.4 3.6
length (μm)
131.95mbsf
132.05mbsf
132.15mbsf
132.25mbsf
132.35mbsf
132.45mbsf
132.55mbsf
132.65mbsf
132.75mbsf
132.85mbsf
132.95mbsf
133.05mbsf
133.15mbsf
133.25mbsf
133.35mbsf
133.45 mbsf
133.55 mbsf
133.65 mbsf
133.75 mbsf
133.85 mbsf
133.95 mbsf
134.05 mbsf
134.15 mbsf
1.0 1.2 1.4 1.6 1.8 2.0 2.2 2.4 2.6 2.8 3.0 3.2 3.4 3.6
length (μm)
129.55mbsf
129.65mbsf
129.75mbsf
129.85mbsf
129.95mbsf
130.05mbsf
130.15mbsf
130.25mbsf
130.35mbsf
130.45mbsf
130.55mbsf
130.65mbsf
130.75mbsf
130.85mbsf
130.95mbsf
131.15 mbsf
131.23 mbsf
131.35 mbsf
131.45 mbsf
131.55 mbsf
131.65 mbsf
131.75mbsf
131.85 mbsf
1.0 1.2 1.4 1.6 1.8 2.0 2.2 2.4 2.6 2.8 3.0 3.2 3.4 3.6
length (μm)

B- 2

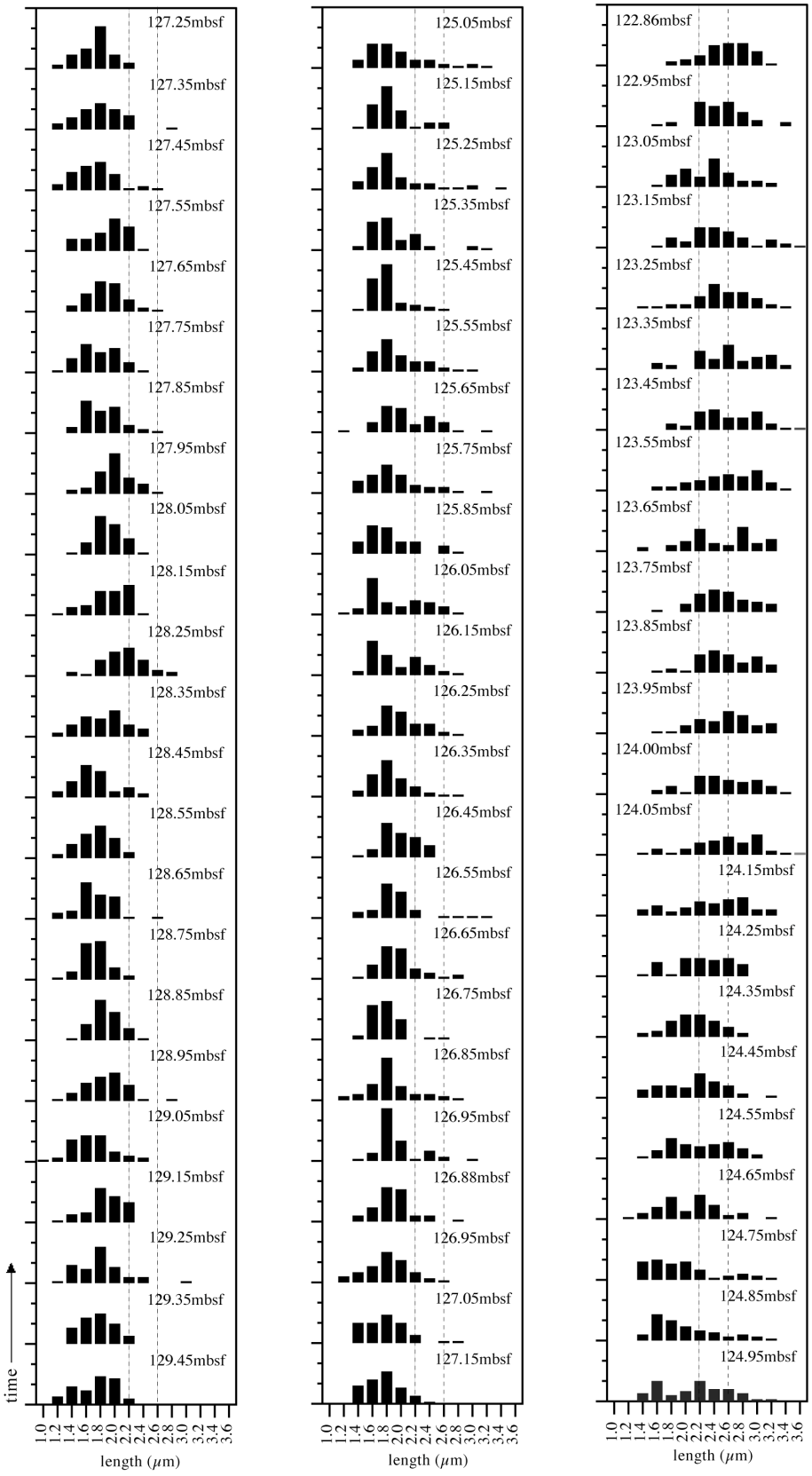
127.25mbsf
127.35mbsf
127.45mbsf
127.55mbsf
127.65mbsf
127.75mbsf
127.85mbsf
127.95mbsf
128.05mbsf
128.15mbsf
128.25mbsf
128.35mbsf
128.45mbsf
128.55mbsf
128.65mbsf
128.75mbsf
128.85mbsf
128.95mbsf
129.05mbsf
129.15mbsf
129.25mbsf
129.35mbsf
129.45mbsf
time
1.0 1.2 1.4 1.6 1.8 2.0 2.2 2.4 2.6 2.8 3.0 3.2 3.4 3.6
length (μm)
125.05mbsf
125.15mbsf
125.25mbsf
125.35mbsf
125.45mbsf
125.55mbsf
125.65mbsf
125.75mbsf
125.85mbsf
126.05mbsf
126.15mbsf
126.25mbsf
126.35mbsf
126.45mbsf
126.55mbsf
126.65mbsf
126.75mbsf
126.85mbsf
126.95mbsf
126.88mbsf
126.95mbsf
127.05mbsf
127.15mbsf
1.0 1.2 1.4 1.6 1.8 2.0 2.2 2.4 2.6 2.8 3.0 3.2 3.4 3.6
length (μm)
122.86mbsf
122.95mbsf
123.05mbsf
123.15mbsf
123.25mbsf
123.35mbsf
123.45mbsf
123.55mbsf
123.65mbsf
123.75mbsf
123.85mbsf
123.95mbsf
124.00mbsf
124.05mbsf
124.15mbsf
124.25mbsf
124.35mbsf
124.45mbsf
124.55mbsf
124.65mbsf
124.75mbsf
124.85mbsf
124.95mbsf
1.0 1.2 1.4 1.6 1.8 2.0 2.2 2.4 2.6 2.8 3.0 3.2 3.4 3.6
length (μm)

B - 3

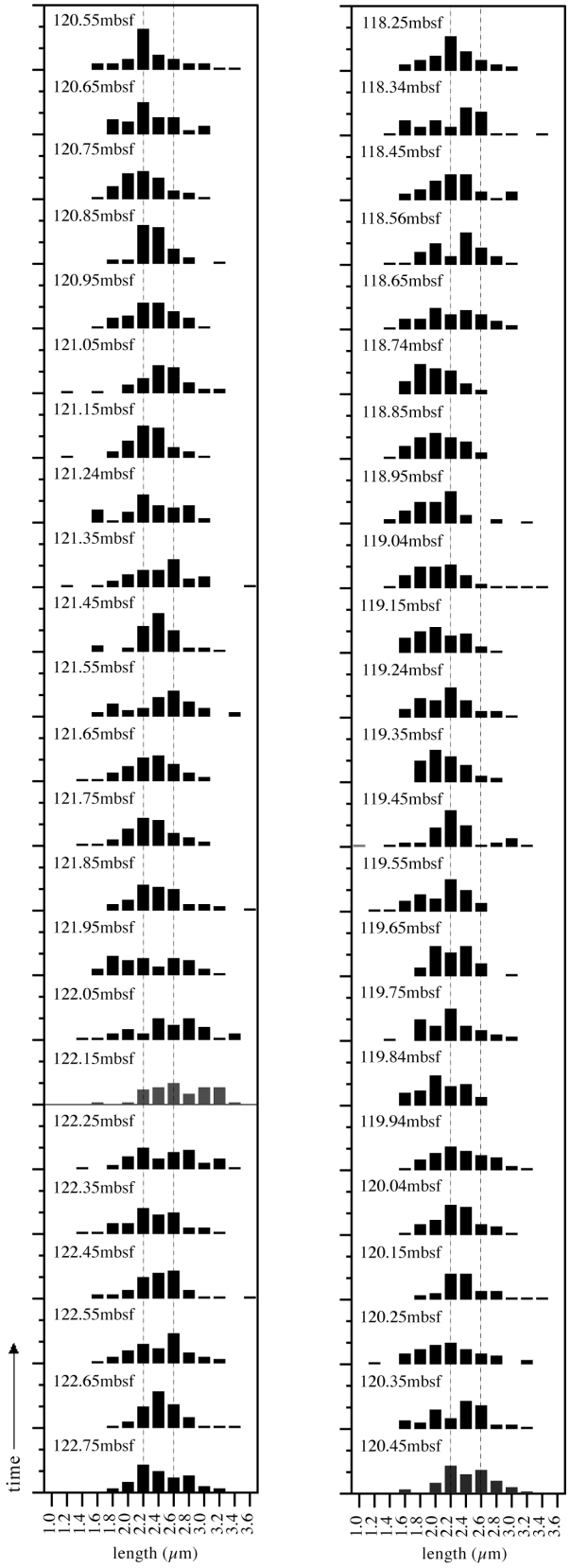
120.55mbsf
120.65mbsf
120.75mbsf
120.85mbsf
120.95mbsf
121.05mbsf
121.15mbsf
121.24mbsf
121.35mbsf
121.45mbsf
121.55mbsf
121.65mbsf
121.75mbsf
121.85mbsf
121.95mbsf
122.05mbsf
122.15mbsf
122.25mbsf
122.35mbsf
122.45mbsf
122.55mbsf
122.65mbsf
122.75mbsf
time
1.0 1.2 1.4 1.6 1.8 2.0 2.2 2.4 2.6 2.8 3.0 3.2 3.4 3.6
length (μm)
118.25mbsf
118.34mbsf
118.45mbsf
118.56mbsf
118.65mbsf
118.74mbsf
118.85mbsf
118.95mbsf
119.04mbsf
119.15mbsf
119.24mbsf
119.35mbsf
119.45mbsf
119.55mbsf
119.65mbsf
119.75mbsf
119.84mbsf
119.94mbsf
120.04mbsf
120.15mbsf
120.25mbsf
120.35mbsf
120.45mbsf
1.0 1.2 1.4 1.6 1.8 2.0 2.2 2.4 2.6 2.8 3.0 3.2 3.4 3.6
length (μm)

Erklärung

Hiermit erkläre ich, daß die Abhandlung – abgesehen von der Beratung durch meine Betreuer Prof. Dr. Priska Schäfer und Priv. Doz. Dr. Mara Weinelt – nach Inhalt und Form meine eigene Arbeit ist.

Ich habe diese Arbeit, ganz oder zum Teil, an keiner anderen Stelle im Rahmen eines Prüfungsverfahrens vorgelegt, veröffentlicht oder zur Veröffentlichung eingereicht.

Kiel, den 24 Mai 2005,

Crudeli Daniela